

Magnitudes and Mechanisms of Planar Restitution
in Motor Vehicle Collisions

Kenneth LaVaun Monson

Department of Mechanical Engineering

M.S. Degree, December 1997

ABSTRACT

The coefficient of restitution is an indicator of the level of elasticity in a collision. Restitution, or elastic rebound of a deformed surface, contributes to the change in velocity of collision partners, a common measure of injury severity in automobile collisions. Because of the complex nature of collisions between motor vehicles, the expected magnitude of the coefficient in such collisions is largely uncharacterized. Mechanisms influencing its value are not well understood. Using crash test data available in a database maintained by the National Highway Traffic Safety Administration (NHTSA), this research investigates the expected magnitude of the coefficient of restitution for a variety of collision types and geometries, including collisions with principal directions of force at the front, side, and rear of the vehicle. Vehicle-to-barrier and vehicle-to-vehicle collisions are considered. The influence of a variety of collision and vehicle parameters on restitution is also explored. Results show that one collision parameter, impact velocity, through its relationship with vehicle crush, is highly influential in determining the magnitude of restitution. Restitution generally decreases as impact velocity increases. In full-frontal barrier collisions involving vehicles with certain engine types, however, a contradiction of the trend occurs as the coefficient's value shifts upward before continuing to decrease with increasing velocity. Study of other parameters and collision types further clarifies restitution behavior.

COMMITTEE APPROVAL:

Geoffrey J. Germane, Committee Chair

Craig C. Smith, Committee Member

Kenneth W. Chase, Committee Member

Craig C. Smith, Graduate Coordinator

**Magnitudes and Mechanisms of Planar Restitution
in Motor Vehicle Collisions**

A Thesis Presented to the
Department of Mechanical Engineering
Brigham Young University

In Partial Fulfillment
of the Requirements for the Degree
Master of Science

by
Kenneth LaVaun Monson

December 1997

This thesis by Kenneth LaVaun Monson is accepted in its present form by the Department of Mechanical Engineering of Brigham Young University as satisfying the thesis requirement for the degree of Master of Science.

Geoffrey J. Germane, Committee Chair

Craig C. Smith, Committee Member

Kenneth W. Chase, Committee Member

Craig C. Smith, Graduate Coordinator

Date

Table of Contents

Table of Contents	iii
List of Tables.....	v
List of Figures.....	vii
Acknowledgements.....	xii
Nomenclature.....	xiii
Chapter 1: Introduction.....	1
1.1 BACKGROUND.....	1
1.1.1 Problem Description.....	1
1.1.2 Impact Direction and ΔV	3
1.2 OBJECTIVES AND SCOPE.....	6
1.2.1 Objectives.....	6
1.2.2 Delimitations.....	6
1.3 CONTRIBUTION OF THE THESIS.....	7
Chapter 2: Analysis And Review Of Previous Work.....	8
2.1 RESTITUTION AND IMPACT VELOCITY.....	8
2.2 RESTITUTION AND OTHER INFLUENTIAL PARAMETERS.....	12
2.3 IMPACT MODEL RE-DEFINING THE COEFFICIENT OF RESTITUTION.....	12
2.4 DERIVATION OF THE VEHICLE-TO-VEHICLE COEFFICIENT FROM BARRIER DATA.....	15
2.5 OTHER RESTITUTION RESEARCH.....	16
2.6 SUMMARY.....	16
Chapter 3: Theoretical Background.....	18
3.1 THE ANATOMY OF A COLLISION AND RESTITUTION.....	18
3.1.1 Vehicle Dynamics.....	18
3.1.2 Occupant Kinematics.....	20
3.2 AUTOMOBILE COLLISIONS AND RIGID BODY COLLISION MECHANICS.....	22
3.2.1 Rigid Body Assumptions.....	23
3.2.2 Conservation of Momentum and the Coefficient of Restitution.....	23
3.2.3 Conservation of Energy and the Coefficient of Restitution.....	23
3.3 APPLICATION OF CRASH TEST DATA.....	25
3.3.1 Derivation of the Coefficient of Restitution.....	25
3.3.2 Determination of Vehicle Crush for Vehicle-to-Barrier Collisions.....	27
3.3.3 Determination of Barrier Force and Crush Energy in Vehicle-to-Barrier Collisions.....	30
3.3.4 Comparison of Vehicle-to-Barrier and Vehicle-to-Vehicle Cases.....	30
Chapter 4: Analytical Procedure.....	32
4.1 DESCRIPTION OF DATA.....	32
4.2 TEST SELECTION AND ORGANIZATION.....	33
4.3 DATA PROCESSING AND ANALYSIS.....	34
4.3.1 Accelerometer Data.....	34
4.3.2 Barrier Load Cell Data.....	39

Chapter 5: Frontal Collision -- Crash Test Results and Restitution.....	40
5.1 FULL-WIDTH VEHICLE-TO-BARRIER COLLISIONS	40
5.1.1 Passenger Type Vehicles.....	42
5.1.2 Non-Passenger Type Vehicles	78
5.2 PARTIAL-WIDTH VEHICLE-TO-BARRIER COLLISIONS	80
5.2.1 Impact Velocity.....	80
5.2.2 Case Study - 1987 Hyundai Excel GLS	81
5.3 POLE IMPACT COLLISIONS	84
5.3.1 Impact Velocity.....	84
5.3.2 Offset	85
5.3.3 Accelerometer Location	85
5.3.4 Case Study - 1984/1987 Honda Accord	86
5.4 FULL-WIDTH VEHICLE-TO-VEHICLE COLLISIONS	89
5.4.1 Influential Parameters.....	89
5.4.2 Comparison of Vehicle-to-Vehicle and Vehicle-to-Barrier Restitution Magnitudes.....	93
5.5 PARTIAL-WIDTH VEHICLE-TO-VEHICLE COLLISIONS	99
5.6 SUMMARY	102
5.6.1 Restitution Magnitude	102
5.6.2 Restitution Mechanisms	103
Chapter 6: Side Collision -- Crash Test Results and Restitution	104
6.1 INFLUENTIAL PARAMETERS	104
6.1.1 Impact Velocity.....	104
6.1.2 Offset	105
6.1.3 Other Parameters	106
6.2 CASE STUDY - 1982 NISSAN SENTRA.....	107
6.3 SUMMARY	110
Chapter 7: Rear Collision -- Crash Test Results and Restitution.....	111
7.1 INFLUENTIAL PARAMETERS	111
7.1.1 Impact Velocity.....	111
7.1.2 Other Parameters	112
7.2 SUMMARY	114
Chapter 8: Summary	115
8.1 ACCOMPLISHMENTS	115
8.2 OBSERVATIONS AND CONCLUSIONS.....	116
8.3 RECOMMENDATIONS	118
References.....	120
Appendix A: Crash Data Spreadsheet	122
Appendix B: Integration Program Listing	183
Appendix C: MOMEX Settings and Outputs	194
Abstract.....	196

List of Tables

<u>Table</u>		<u>Page</u>
1.1	Directional Priority (DP) as a Function of Principal Direction of Force and ΔV -- Principal Directions of Force Corresponding to Clock Positions 3, 6, 9, and 12.....	5
4.1	Number of Tests Analyzed by Crash Test Description.....	34
5.1	Coefficient of Restitution by Vehicle Type at 48 and 56 kph; Vehicle-to-Fixed Rigid Barrier Full-Frontal Collisions.....	42
5.2	Coefficient of Restitution (e), Standard Deviation (s), Number of Tests, and 80% Confidence Intervals by Engine Orientation at 48 and 56 kph; Vehicle-to-Fixed Rigid Barrier Full-Frontal Collisions; Passenger Vehicles.....	43
5.3	Average Coefficient of Restitution v. Impact Speed -- Vehicle-to-Fixed Rigid Barrier Full Frontal Collisions; Passenger Vehicles with Transverse Oriented Engines.....	45
5.4	Coefficient of Restitution by Test Lab at 48 and 56 kph; Vehicle-to-Fixed Rigid Barrier Full-Frontal Collisions; Passenger Vehicles with Transverse Oriented Engines.....	52
5.5	Test Description and Restitution Results for Five Vehicle-to-Fixed Rigid Barrier Full-Frontal Tests Involving the 1992-1996 Ford Taurus with a Transverse Oriented Engine.....	53
5.6	Test Description and Restitution Results for Three Vehicle-to-Fixed Rigid Barrier Full-Frontal Tests Involving the 1982-1984 Chevrolet Celebrity with a Transverse Oriented Engine.....	59
5.7	Coefficient of Restitution at 48 and 56 kph; Vehicle-to-Fixed Rigid Barrier Full-Frontal Collisions; Passenger Vehicles with Inline Engine Orientation.....	63
5.8	Test Description and Restitution Results for Three Vehicle-to-Fixed Rigid Barrier Full-Frontal Tests Involving the 1993 Ford Taurus with an Inline Oriented Engine.....	71
5.9	Coefficient of Restitution Magnitudes at Center Rear and Outboard Rear Locations; 1993 Ford Taurus.....	72
5.10	Derived Maximum and Residual Vehicle Crush and Corrected Maximum Crush for Transverse and Inline Engine 1993 Ford Taurus Cases.....	75
5.11	Coefficient of Restitution and Number of Tests Analyzed by Vehicle Type, Engine Orientation, and Impact Velocity; Non-Passenger Type Vehicles Only.....	78

5.12	Test Description and Restitution Results for Four Vehicle-to-Fixed Rigid Barrier Tests (Two Full-Frontal and Two 50% Overlap) Involving the 1987 Hyundai Excel GLS.....	81
5.13	Test Description and Restitution Results for a Vehicle-to-Fixed Rigid Barrier Full-Frontal Test and Centered and Offset Pole Tests Involving the 1984/1987 Honda Accord	87
5.14	Closing Velocity, Mass Ratio, Calculated Coefficient of Restitution, and Predicted Value and Percent Error for Equations 2.7 and 2.8; VTB to VTV Comparison.....	95
5.15	Comparison of the Coefficient of Restitution (ϵ) in Vehicle-to-Barrier and Vehicle-to-Vehicle Tests of Identical Vehicles at Barrier Equivalent Velocity.....	96
5.16	Coefficient of Restitution at Right and Left Rear Seats, Trace Average, and Difference, by Percent Overlap.....	101
6.1	Coefficient of Restitution at 48 and 55 kph for Comparable Collisions; Impactor-to-Vehicle Side Impact.....	105
6.2	Closing Velocity, Rebound Velocity, and Coefficient of Restitution for Upper and Lower Bound Difference Curves; NHTSA Test 820.....	110
7.1	Coefficient of Restitution at 48 and 56 kph; Rigid Impactor-to-Vehicle Rear-Impact Collisions	111

List of Figures

<u>Figure</u>		<u>Page</u>
1.1	Vehicle-to-Rigid Barrier Impact	2
1.2	Percent of Total Accidents by Principal Direction of Force -- Unweighted National Accident Sampling System (NASS) Data from Years 1988-1994	4
1.3	Average Maximum Abbreviated Injury Severity v. ΔV for Clock Directions 3, 6, 9, and 12 -- Unweighted NASS Data from Years 1988-1994	5
2.1	Coefficient of Restitution v. Closing Velocity -- Rear Impact (recreated from reference 7)	9
2.2	Coefficient of Restitution v. Closing Velocity -- Frontal Rigid Barrier Impact (recreated from reference 9)	10
2.3	Coefficient of Restitution v Impact Velocity -- 1981-1985 Ford Escort, Frontal Rigid Barrier Impact (recreated from reference 10)	11
2.4	Coefficient of Restitution in the Normal Direction v. RDS -- Vehicle- to-Vehicle Frontal and Side Impact (recreated from reference 12).....	13
2.5	Coefficient of Restitution in the Tangential Direction v. GIR -- Vehicle-to-Vehicle Side Impact (recreated from reference 12).....	14
3.1	Velocity v. Time at Various Vehicle Locations -- NHTSA Test 1890: 1993 Ford Taurus into Fixed Rigid Barrier, Full-Frontal Configuration with Applicable Nomenclature.....	18
3.2	Barrier Force v. Time -- NHTSA Test 1890: 1993 Ford Taurus into Fixed Rigid Barrier, Full-Frontal Configuration	19
3.3	Velocity v. Time at Vehicle Rear and Chest and Head of Dummies at Right and Left Front Seats -- NHTSA Test 1890: 1993 Ford Taurus, Vehicle-to-Fixed Rigid Barrier; Three-Point Belt and Airbag Restraints	20
3.4	Velocity v. Time at Vehicle Rear and Chest and Head of Dummies at Right and Left Front Seats -- NHTSA Test 1777: 1993 Ford Taurus, Vehicle-to-Fixed Rigid Barrier; Airbag Restraints Only	21
3.5	Velocity v. Time at Vehicle Rear and Chest and Head of Dummies at Right and Left Front Seats -- NHTSA Test 1103: 1988 Ford Taurus, Vehicle-to-Fixed Rigid Barrier; Three-Point Belt Restraints Only	22
3.6	Influence of Vehicle Rotation on Accelerometers Mounted Away from the Center-of-Gravity	26
3.7	Influence of Velocity of Propagation; Velocity at Vehicle Rear Seat v. Time -- NHTSA Test 1890: 1993 Ford Taurus into Fixed Rigid Barrier, Full-Frontal Configuration.....	27

3.8	Vehicle Crush Illustration and Nomenclature	29
4.1	Velocity v. Time at Various Positions on the Vehicle -- NHTSA Test 1164: 50% Overlap Frontal Vehicle-to-Barrier Collision; 1987 Hyundai Excel.....	35
5.1	Coefficient of Restitution v. Impact Velocity -- Vehicle-to-Fixed Rigid Barrier Full- Frontal Collisions; All Vehicle Types	40
5.2	Coefficient of Restitution v. Impact Velocity -- Vehicle-to-Fixed Rigid Barrier Full-Frontal Collisions; Passenger Vehicles with Both Inline and Transverse Engine Orientations	42
5.3	Rebound Velocity v. Impact Velocity -- Vehicle-to-Fixed Rigid Barrier Full-Frontal Collisions; Passenger Vehicles with Transverse Oriented Engines	46
5.4	Phase One Restitution Duration v. Impact Velocity -- Vehicle-to- Fixed Rigid Barrier Full-Frontal Collisions; Passenger Vehicles with Transverse Oriented Engines	47
5.5	Average Phase One Restitution Acceleration v. Impact Velocity -- Vehicle-to-Fixed Rigid Barrier Full-Frontal Collisions; Passenger Vehicles with Transverse Oriented Engines.....	47
5.6	(a) Coefficient of Restitution v. Vehicle Mass, (b) Coefficient of Restitution v. Engine Displacement, (c) Coefficient of Restitution v. Vehicle Length.....	49
5.6 (cont'd.)	(cont'd.) (d) Coefficient of Restitution v. Vehicle Width, (e) Coefficient of Restitution v. Wheelbase, (f) Coefficient of Restitution v. Distance Between Front Axle and Center-of-Gravity	50
5.6 (cont'd.)	(cont'd.) (g) Coefficient of Restitution v. Vehicle Model Year.....	51
5.7	Velocity v. Time -- Five Vehicle-to-Fixed Rigid Barrier Full-Frontal Crash Tests Involving the 1992-1996 Ford Taurus.....	54
5.8	Vehicle Crush, Barrier Force v. Time -- NHTSA Tests 1899, 1890: Vehicle-to-Fixed Rigid Barrier Full-Frontal Tests Involving the 1993 Ford Taurus.....	56
5.9	Velocity v. Time at Vehicle Rear and Engine -- NHTSA Test 1899: Vehicle-to-Fixed Rigid Barrier Full-Frontal Involving the 1993 Ford Taurus	58
5.10	Crush Approximations -- NHTSA Tests 1899, 1890: Vehicle-to- Fixed Rigid Barrier Full-Frontal Tests Involving the 1993 Ford Taurus...	59
5.11	Velocity v. Time -- Three Vehicle-to-Fixed Rigid Barrier Full- Frontal Crash Tests Involving the 1982-1984 Chevrolet Celebrity	60
5.12	Vehicle Crush v. Time -- NHTSA Tests 776, 688: Vehicle-to- Fixed Rigid Barrier Full-Frontal Tests Involving the 1983-1984 Chevrolet Celebrity.....	61

5.13	Crush Approximations -- NHTSA Tests 776, 688: Vehicle-to-Fixed Rigid Barrier Full-Frontal Tests Involving the 1983-1984 Chevrolet Celebrity	62
5.14	Coefficient of Restitution v. Impact Velocity -- Vehicle-to-Fixed Rigid Barrier Full-Frontal Collisions; Passenger Vehicles with Inline Engine Orientation.....	63
5.15	(a) Rebound Velocity v. Impact Velocity, (b) Restitution Time v. Impact Velocity, (c) Average Restitution Acceleration v. Impact Velocity	65
5.16	(a) Coefficient of Restitution v. Vehicle Mass, (b) Coefficient of Restitution v. Engine Displacement, (c) Coefficient of Restitution v. Vehicle Length	66
5.16 (cont'd.)	(cont'd.) (d) Coefficient of Restitution v. Vehicle Width, (e) Coefficient of Restitution v. Wheelbase, (f) Coefficient of Restitution v. Distance Between Front Axle and Center-of-Gravity	67
5.16 (cont'd.)	(cont'd) (g) Coefficient of Restitution v. Vehicle Model Year.....	68
5.17	Velocity v. Time -- NHTSA Tests 1201 - 1205; Repeated Vehicle-to-Barrier Full-Width Frontal Collisions; 1986 Ford Taurus with an Inline Engine	69
5.18	Velocity v. Time -- NHTSA Tests 1216 - 1221; Repeated Vehicle-to-Barrier Full-Width Frontal Collisions; 1985 Ford Escort with an Inline Engine.....	69
5.19	Velocity v. Time -- Three Vehicle-to-Fixed Rigid Barrier Full-Frontal Crash Tests Involving the 1993 Ford Taurus with an Inline Engine.....	71
5.20	Velocity at Various Locations v. Time -- Three Vehicle-to-Fixed Rigid Barrier Full-Frontal Crash Tests Involving the 1993 Ford Taurus with an Inline Engine.....	73
5.21	Vehicle Crush v. Time -- NHTSA Tests 1973, 1976: Vehicle-to-Fixed Rigid Barrier Full-Frontal Tests Involving the Inline 1993 Ford Taurus	74
5.22	Velocity v. Time at Vehicle Rear and Engine -- NHTSA Test 1973: Vehicle-to-Fixed Rigid Barrier Full-Frontal Involving the 1993 Ford Taurus.....	76
5.23	Crush Approximations -- NHTSA Tests 1973, 1976: Vehicle-to-Fixed Rigid Barrier Full-Frontal Tests Involving the 1993 Ford Taurus with an Inline Engine	77
5.24	Coefficient of Restitution v. Impact Velocity -- Vehicle-to-Fixed Rigid Barrier Full-Frontal Collisions; Non-Passenger Type Vehicles.....	78
5.25	Coefficient of Restitution v. Impact Velocity -- Vehicle-to-Barrier Frontal Collisions; Passenger Vehicles	80

5.26	Impact Velocity v. Time -- Vehicle-to-Fixed Rigid Barrier Full-Frontal and Fifty-Percent Overlap Collisions; 1987 Hyundai Excel GLS	81
5.27	Vehicle Crush v. Time -- Vehicle-to-Fixed Rigid Barrier Full-Frontal and Fifty-Percent Overlap Collisions; 1987 Hyundai Excel GLS	82
5.28	Coefficient of Restitution v. Impact Velocity -- Vehicle-to-Barrier Frontal Pole Impacts; Passenger Vehicles	84
5.29	Velocity v. Time Measured at Centerline and Lateral Vehicle Positions -- NHTSA Test 662: Vehicle-to-Barrier -330 mm Offset Pole Impact Involving a 1981 Volkswagen Rabbit	86
5.30	Impact Velocity v. Time -- Vehicle-to-Barrier Full-Frontal and Centered and Offset Pole Collisions; 1984/1987 Honda Accord	87
5.31	Coefficient of Restitution v. Closing Velocity -- Vehicle-to-Vehicle Full-Frontal Collisions; Passenger Type Vehicles	89
5.32	Coefficient of Restitution v. Closing Velocity by Engine Orientation -- Vehicle-to-Vehicle Full-Frontal Collisions; Passenger Type Vehicles.....	91
5.33	Coefficient of Restitution v. Difference Between Colliding Vehicles' Masses -- Full-Frontal Vehicle-to-Vehicle Collisions.....	92
5.34	Percentage Difference Between Coefficient of Restitution Values for VTV and VTB Collisions v. VTV Closing Velocity	93
5.35	Percentage Difference Between Coefficient of Restitution Values for VTV and VTB Collisions v. Mass Ratio of Colliding Vehicles.....	94
5.36	Velocity v. Time -- Vehicle-to-Barrier v. Vehicle-to-Vehicle. (a) NHTSA Tests 975, 974, 976, (b) NHTSA Tests 1054, 785, (c) NHTSA Tests 874, 796.....	97
5.37	Coefficient of Restitution v. Percent Overlap -- Vehicle-to-Vehicle Frontal Collisions.....	99
5.38	Coefficient of Restitution v. Percent Overlap -- Vehicle-to-Vehicle Frontal Collisions.....	100
6.1	Coefficient of Restitution v. Impact Velocity -- Side Collisions: NHTSA Deformable Impactor-to-Vehicle; Passenger Vehicles	104
6.2	Coefficient of Restitution v. Dimensionless Offset -- Side Collisions: NHTSA Deformable Impactor-to-Vehicle; Passenger Vehicles	106
6.3	MOMEX Results for NHTSA Test 820: Crabbed Impactor into Side of 1982 Nissan Sentra.....	107
6.4	Nissan Sentra Velocities - Derived from Right Rear Sill Accelerometer; NHTSA Test 820.....	108
6.5	Impactor Velocities - Derived from Center-of-Gravity Accelerometer; NHTSA Test 820.....	109

6.6	Derived PDOF Components of Impulse Center Velocities for the Nissan Sentra and the Impactor Using Various Accelerometers; NHTSA Test 820	109
7.1	Coefficient of Restitution v. Closing Velocity -- Rear Collisions: Rigid Impactor-to-Vehicle and Front-to-Rear Vehicle-to-Vehicle; Passenger Vehicles	111
7.2	(a) Coefficient of Restitution v. Mass Difference, (b) Coefficient of Restitution v. Vehicle Width, (c) Coefficient of Restitution v. Vehicle Model Year; Rear Impactor-to-Vehicle Collisions.....	113

Acknowledgements

As is generally the case, when one person is able to accomplish something good, it is a result of assistance and sacrifice by many others. The same is true of this thesis.

I wish to thank Dr. Geoff J. Germane for his friendship, support, and example during the course of this project. Dr. Germane has not only provided valuable insight and direction in the completion of this research, but has also provided funding for its completion.

I also want to thank Dr. Craig Smith and Dr. Ken Chase for their willingness to participate in this research as members of my advisory committee.

I am grateful to Brigham Young University and the Mechanical Engineering Department for their commitment to excellence and their unique dedication to learning by study and by faith.

I especially wish to thank my good wife, Jill, and my daughter, Lauren, for their willingness to sacrifice time spent with me and some of the luxuries of life in order to allow me to complete this research.

Nomenclature

Roman Symbols

<u>Symbol</u>	<u>Units</u>	<u>Definition</u>
a	m/s^2	Acceleration
a_{lin}	m/s^2	Linear Acceleration
a_t	m/s^2	Tangential Component of Acceleration
a_n	m/s^2	Normal Component of Acceleration
a_x	m/s^2	Component of Acceleration in X-direction
$C_{m,a}$	m	Actual Maximum Dynamic Crush
$C_{r,c}$	m	Calculated Residual Crush
c	m/s	Velocity of Propagation
E	Pa	Modulus of Elasticity
$E_{maxcrush}$	Joule	Work of Maximum Dynamic Deformation
$E_{rescrush}$	Joule	Work of Residual Deformation
F	N	Force
k	N/m	Stiffness
k_{eff}	N/m	Effective Stiffness
m	kg	Mass
r	M	Radius
t	sec	Time
t_{imp}	sec	Time of Impact
t_{cv}	sec	Time of Common Velocity
t_{mrv}	sec	Time of Maximum Rebound Velocity
t_{sep}	sec	Time of Vehicle-barrier Separation
v	m/s	Velocity
$v_{a,i}$	m/s	Initial Velocity of Body A
$v_{b,f}$	m/s	Final Velocity of Body B
x	m	Position

Greek Symbols

<u>Symbol</u>	<u>Units</u>	<u>Definition</u>
ϵ	-	Coefficient of Restitution
ϵ_A	-	Coefficient of Restitution for Barrier Impact of Body A
ϵ_{AB}	-	Coefficient of Restitution for Vehicle Impact Between Body A and Body B
ρ	kg/m ³	Density
θ	rad	Angle
ω	rad/sec	Angular Velocity

Chapter 1: Introduction

1.1 BACKGROUND

1.1.1 Problem Description

During recent years, automotive safety technology has become increasingly more advanced. Occupants are better protected by automobiles that are more effectively designed for safety. Success in advancing safety technology is a result of increased understanding of vehicle and occupant dynamics during collision. As might be expected, statistical studies demonstrate a strong correlation between collision severity and occupant injury severity. A common measure of collision severity is vehicle change in velocity during impact, or ΔV . Much of government rule-making regarding automobile safety is based upon the correlation of injury severity with vehicle ΔV . The Federal Motor Vehicle Safety Standards (FMVSS) have been implemented as standards of occupant protection in vehicles marketed in the United States. The applied standards, however, can only be as effective as the accuracy of the injury severity- ΔV correlation. Due to the complexity of vehicle behavior in accidents, it is difficult to determine the exact ΔV associated with a collision. A major contributing factor to this complexity is a lack of understanding regarding the influence of structural restoration of the vehicle following the time of maximum crush. When structural restoration occurs, forces between colliding bodies act not only to bring the bodies to a common velocity but also to accelerate them away from one another, resulting in an increased change in velocity. The coefficient of restitution defines the extent of this restoration in an indirect way by comparing the colliding bodies' velocities before and after collision. According to the classical definition attributed to Issac Newton, the coefficient is equal to the ratio of the separation and approach velocities of two colliding particles, as shown in Equation 1.1, and varies in magnitude between 0

$$\epsilon = \frac{v_{B,f} - v_{A,f}}{v_{A,i} - v_{B,i}} \quad (1.1)$$

and 1, for perfectly plastic and elastic collisions, respectively. Velocities are measured relative to the impact plane, which is generally determined by the collision geometry. Pre-impact velocities are independent of collision conditions, while post-impact velocities are determined by collision geometry as well as structural characteristics and material properties of the involved bodies. Figure 1.1 shows pre-impact and post-impact diagrams

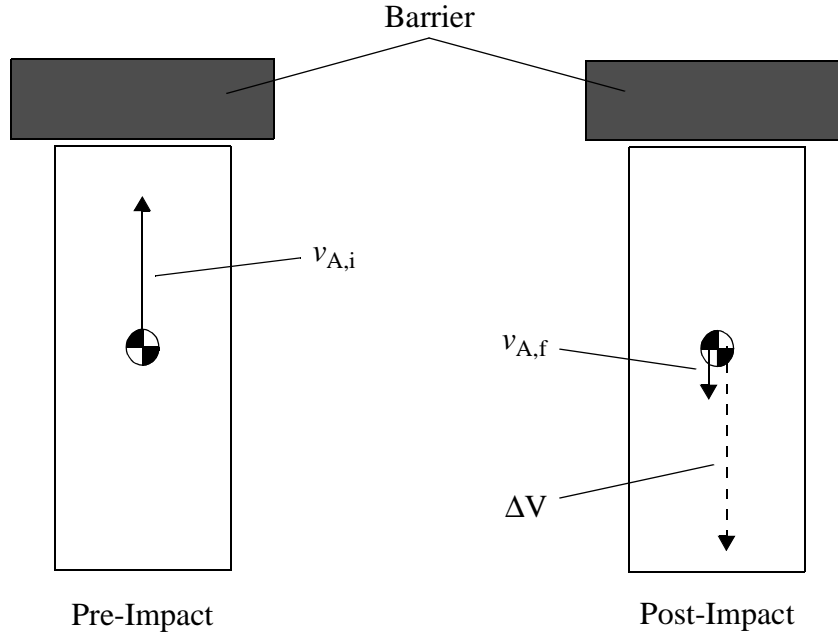


FIGURE 1.1 Vehicle-to-Rigid Barrier Impact

of a full-frontal, vehicle-to-fixed rigid barrier impact and graphically defines ΔV as the sum of the initial and final velocities. Because the barrier is immovable, velocities for vehicle B of Equation 1.1 are equal to zero. As a result, the coefficient of restitution is equal to the ratio of the final and initial velocities. With the fairly accurate assumption that the vehicle in the figure is rigid for central barrier impact, Equation 1.1 is applicable at any point on the vehicle.

In addition to promoting more effective laws that encourage safer vehicle design, correct understanding of the coefficient of restitution is critical to many other areas of automotive safety as well. Accident reconstructionists, for example, often use computer algorithms to investigate different collision scenarios. These programs implement well-known physical laws, such as conservation of energy and momentum, to determine the behavior of vehicles in a collision. In order to apply these laws, programs require a number of input values, many of which are not very well defined because of the complexity of vehicle behavior in accidents. The coefficient of restitution is one such parameter. Knowledge of the extent of restitution is necessary to determine colliding bodies' ΔV values and, thus, expected levels of occupant injury severity. Higher restitution results in more severe occupant injury. Because of the complex inhomogeneous structure of automobiles, calculating exact coefficient values for automobile collisions is impossible

in most cases, so values must be estimated. Some reconstruction programs seek to overcome the difficulty of determining a value for the coefficient by assuming perfectly plastic impact. This is a reasonably accurate assumption for some collisions, but it has been shown that in many cases restitution is significant. Other programs fully incorporate the effects of restitution by requiring the user to input some value for the coefficient. Because of uncertainty regarding the coefficient of restitution, it is difficult to choose an appropriate value.

Analysis of the literature sheds light on the level of uncertainty concerning the application of the coefficient. Marquardt reports that the coefficient will never be higher than 0.1 and that such a small value may be neglected without significant error [1]. Emori similarly states that high speed, uni-directional collisions may be considered plastic [2]. In contrast, Strother [3] and Tamny [4] both report that restitution is significant at speeds up to 48 kph, and Brach [5] reports coefficient values as high as 0.475. Some of these statements obviously conflict, but in many cases the literature is incomplete in specifying collision conditions associated with measured values for the coefficient, so it is difficult to determine how presented results compare. It is clear, though, that the complex behavior of the coefficient in automobile collisions is generally not well defined. Smith and Tsongos present the additional complication of a large spread in experimental results for the coefficient [6].

1.1.2 Impact Direction and ΔV

Unweighted data from the National Accident Sampling System (NASS) [7], years 1988-1994, reveal that frontal collisions are easily the most common type of collision, as shown in Figure 1.2. The figure illustrates the percent of the total number of accidents that occurred at each principal direction of force corresponding to the presented clock directions, where 12 and 3 represent forces contacting a vehicle directly at its front and right side, respectively. Figure 1.2 is based on a total of 42,698 accidents reported during the seven indicated years. Considering only clock directions 3, 6, 9, and 12, the sum of the percentages for directions 3 and 9, the side-impact cases, is approximately equal to nine percent, similar in magnitude to the percentage associated with rear cases, or direction 6. Both rear and side impacts, however, are less than one-fourth as common as accidents giving forces at the direct front of a vehicle. If clock directions are lumped, such that frontals include clock directions eleven through one, right side impacts include directions

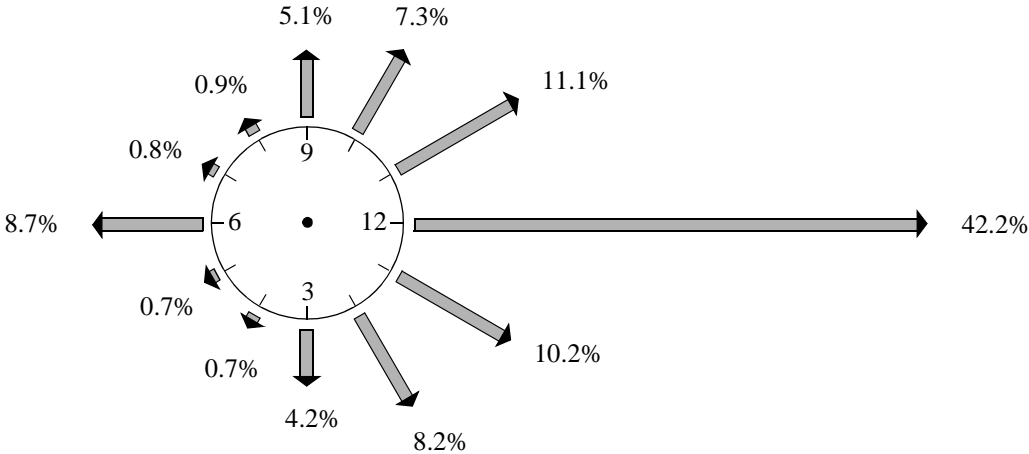


FIGURE 1.2 Percent of Total Accidents by Principal Direction of Force -- Unweighted National Accident Sampling System (NASS) Data from Years 1988-1994

two to four, and so forth, frontal impacts become even more dominant. The percentage of total accidents classified as side impacts also grows significantly, while the percentage associated with rear impacts grows only slightly.

Given the fact that the most common type of collision is front impact, it also becomes important to determine the injury scale associated with each direction of impact. Figure 1.3 plots average maximum abbreviated injury scale (AIS) as a function of velocity change, ΔV , for accidents with principal directions of force corresponding to clock directions 3, 6, 9, and 12. Abbreviated injury scale is a measure from one to six, with six being the most severe, that describes the severity of each injury sustained by a vehicle occupant in a collision [8]. The maximum AIS (MAIS) is equal to the largest AIS value reported for any one occupant, and all MAIS values for a given clock direction are averaged at each ΔV value. Averages, again determined from data reported for years 1988-1994, as well as linear regression plots for each clock direction are given in the figure. The figure is based on reports of 26,058 total occupants.

Based on the linear regression lines for each clock direction, the figure demonstrates that side impacts have the highest level of injury severity, with left-side impacts being slightly more severe than right-side collisions. Frontal collisions are next in severity, with rear impacts being the least severe of all collision directions. Slopes of the regression lines indicate that the largest increase in injury severity for a given velocity change occurs in left-side impacts, again followed by right-side, frontal, and rear cases. Consideration of the occupants' seating positions and whether or not they were belted properly, along with

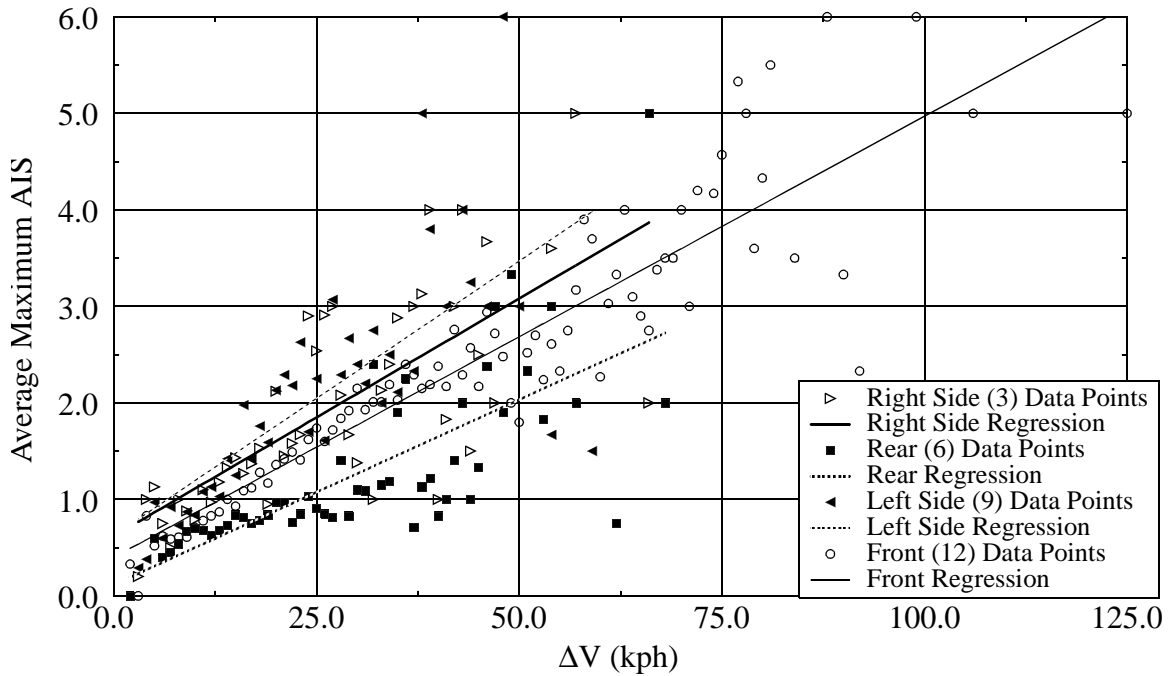


FIGURE 1.3 Average Maximum Abbreviated Injury Severity v. ΔV for Clock Directions 3, 6, 9, and 12 -- Unweighted NASS Data from Years 1988-1994

other variables, would no doubt provide valuable insight into the analysis of injury severity associated with direction of principal force. It should thus be noted that Figure 1.3 does not account for such details.

The results presented by the previous two figures can be used to estimate a priority value for impact direction in the study of collisions. Directional Priority (DP) is here defined as the product of the percentage of total accidents with a chosen principal direction of force (Pct) and the average maximum AIS for that principal direction of force (Avg. MAIS), at a chosen value of ΔV. The variable is calculated for principal directions of

TABLE 1.1 Directional Priority (DP) as a Function of Principal Direction of Force and ΔV -- Principal Directions of Force Corresponding to Clock Positions 3, 6, 9, and 12

ΔV	Clock Position Corresponding to Principal Direction of Force											
	3 - Right Side			6 - Rear			9 - Left Side			12 - Front		
	Pct (%)	Avg. MAIS	DP	Pct (%)	Avg. MAIS	DP	Pct (%)	Avg. MAIS	DP	Pct (%)	Avg. MAIS	DP
12.5	4.2	1.23	5.2	8.7	0.59	5.1	5.1	1.33	6.8	42.2	0.96	40.5
25.0	4.2	1.85	7.8	8.7	1.06	9.2	5.1	2.05	10.5	42.2	1.53	64.6
37.5	4.2	2.45	10.3	8.7	1.54	13.4	5.1	2.75	14.0	42.2	2.10	88.6
50.0	4.2	3.08	13.0	8.7	2.03	17.7	5.1	3.46	17.7	42.2	2.68	113.1

force associated with clock positions 3, 6, 9, and 12, at ΔV magnitudes of 12.5, 25, 37.5, and 50 kph. Results presented in Table 1.1 show that Directional Priority, as defined above, is around six times higher at every ΔV for frontal impacts than for left-side impacts, the direction with the next highest Directional Priority values. When left and right-side values are summed, they result in values approximately twice those calculated for rear impacts. Based on these results, it is determined that frontal collisions have the highest priority for analysis, and side impacts carry the next highest priority, followed by rear collisions. These results assume that the percentages of total accidents for the different principal directions of force, as given in Figure 1.2, remain constant through the range of reported ΔV magnitudes.

1.2 OBJECTIVES AND SCOPE

1.2.1 Objectives

- (1) Using existing automobile crash data, determine expected magnitudes of the coefficient of restitution for front, side, and rear collisions, giving frontal and then side impacts the highest priority in analysis. Focus primarily on passenger vehicles, but also briefly include results for pickup trucks, sport utility vehicles, and vans, in full-frontal barrier impact cases. Investigate the influence of impact speed, offset, and other collision/vehicle descriptors. Discuss the repeatability of the results.
- (2) For frontal collisions, additionally compare restitution magnitudes in vehicle-to-barrier tests to values in front-to-front vehicle-to-vehicle tests. Additionally study the affect of repeated impacts in frontal collisions.
- (3) Rationalize the determined magnitudes of the coefficient by investigating the physical mechanisms of restitution in representative case-studies.

1.2.2 Delimitations

- (1) The purpose of this thesis is not to develop an exact model for the coefficient of restitution for individual vehicles in specific collisions but to assemble generally applicable guidelines for accurately choosing the coefficient, based on an increased understanding of the mechanisms controlling restitution.
- (2) The developed criteria are applicable mainly to central, or near central, impacts, but principles learned may be applied to eccentric collisions, where appropriate.

- (3) Only tests with principal directions of force associated with clock positions 3, 6, 9, and 12, are considered.
- (4) The research does not include investigation of other related collision parameters, such as tangential slip or vehicle stiffness.

1.3 CONTRIBUTION OF THE THESIS

Even though some have researched the value of the coefficient of restitution for different collision conditions, the expected value of the coefficient for different collisions remains largely unclear. Further research, especially that which focuses on the mechanisms that influence restitution rather than just on the value of the coefficient itself, will more clearly define the extent of restitution and provide a rational means for properly applying the coefficient in collision analysis. Because restitution is inseparable from other issues of collision dynamics, this research will also increase general understanding of the complex behavior of motor vehicles in accidents. This increased understanding will assist safety engineers, accident reconstructionists, and government rule-makers, in better serving society. It is the intent of this thesis to develop specific criteria for selecting the coefficient based upon collision conditions and to clarify mechanisms influencing restitution.

Chapter 2: Analysis And Review Of Previous Work

The use of the coefficient of restitution in accident analysis has historically been a source of uncertainty. A comprehensive search of the literature shows that much of the work done in quantifying the coefficient has been accomplished in recent years. Some of the most rigorous research on restitution has investigated the influence of impact speed on the coefficient of restitution. The effects of a variety of other parameters have also been studied through methods of statistical correlation. Other efforts focus on developing impact models that re-define the coefficient of restitution for a variety of collision configurations, including sideswipes and corner impacts. Researchers have also presented methods for calculating the coefficient of restitution for the collision of two vehicles based on knowledge of the restitution behavior of the two vehicles in vehicle-to-barrier collisions. Because researchers define restitution differently and are often incomplete in reporting results, it is difficult to compare and combine results.

2.1 RESTITUTION AND IMPACT VELOCITY

Howard *et al*, of the Biodynamic Research Corporation, and Siegmund *et al*, of MacInnis Engineering Associates, both present research on the influence of impact speed on restitution in low-speed rear-impacts, while Prasad, at the Transportation Research Center, and a multi-company group of engineers report work on restitution and impact speed over a larger speed range.

A group at Biodynamic Research Corporation, led by Howard, reports research on restitution in a 1993 paper [9]. Their testing was limited to low velocity collisions (closing velocities ranging from 1.6 to 13.7 kph) where values of the coefficient of restitution are expected to be high. Through nine front-to-rear vehicle-to-vehicle tests, in which the rear-impacted vehicle was instrumented, and six rear-impact vehicle-to-barrier tests, results show that the coefficient of restitution tends to decrease from 1.0 as closing speed increases from zero. Most of the coefficients are in the 0.2 to 0.4 range, with the one 1.6 kph test (vehicle-to-barrier) resulting in a coefficient of 0.86. Based on the results, the authors estimate that the coefficient behaves according to the line plotted in Figure 2.1. They also report that vehicle-to-barrier coefficients tend to be slightly higher than vehicle-

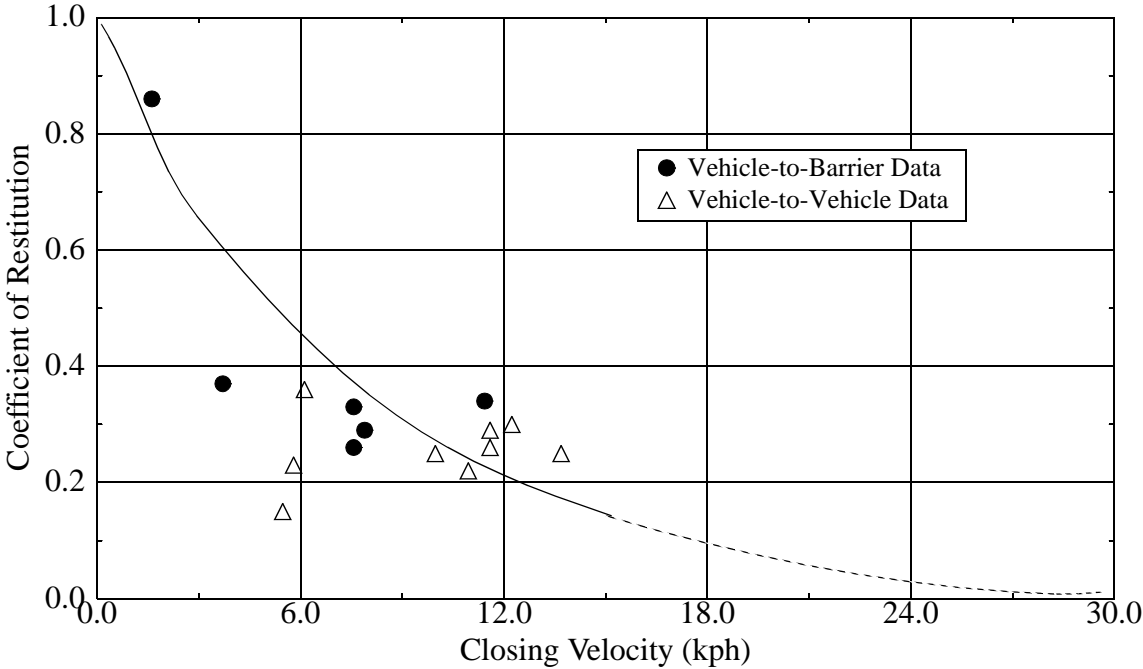


FIGURE 2.1. Coefficient of Restitution v. Closing Velocity -- Rear Impact (recreated from reference 7)

to-vehicle coefficients. Howard *et al* also note that some of the tested vehicles had energy absorbers installed in their bumpers while others did not, but the expected increase in restitution for vehicles without the energy absorbing bumpers was not seen.

Similar to the work of the Biodynamic Research group, a group at MacInnis Engineering Associates, led by Gunter P. Siegmund, reports research on restitution in low velocity collisions in a 1996 paper [10]. A total of 983 aligned, vehicle-to-vehicle and vehicle-to-barrier tests was conducted using five vehicles. Although it is not explicitly stated in the paper, discussion indicates that the tests were rear-impacts. The five tested vehicles were a 1981 Chevrolet Chevette, a 1982 Ford Granada, a 1980 Ford Mustang, a 1985 Hyundai Stellar, and a 1976 Volkswagen Rabbit. In the paper, coefficient of restitution magnitudes are plotted against speed change rather than impact speed, but impact speed is easily determined, given the coefficient of restitution and delta-V. Because the data are not detailed in the paper, plots could not be re-created, but each of the vehicles shows a general decrease in restitution with impact speed, similar to the pattern suggested by Howard *et al*. Typical coefficient values for speeds just over 0 kph are 0.8, decreasing to magnitudes between 0.2 and 0.5 at impact speeds around 8 kph. Coefficient magnitudes for vehicle-to-barrier cases are not consistently higher than values for vehicle-to-vehicle

collisions, as noted by Howard *et al.* Rather, differences between coefficient magnitudes for collisions between a subject vehicle and a rigid barrier and impacts between the same vehicle with another vehicle are similar to differences in the coefficient for collisions between the subject vehicle and two different vehicles. For a chosen vehicle, coefficient of restitution values are shown to vary by an extent of about 0.2 for collisions with different collision partners.

Another study on restitution is reported in a 1991 paper by Alope Kumar Prasad of the Transportation Research Center (TRC) in East Liberty, Ohio [11]. Prasad presents coefficients of restitution derived from data associated with 109 vehicle-to-barrier collisions stored in the National Highway Traffic Safety Administration (NHTSA) crash test database. Sixty-eight of the tests were front impacts, with closing velocities ranging from 8 to 56 kph, while seventeen were side impacts at velocities from 8 to 40 kph. The remaining twenty-four tests were rear impacts and were performed at approach speeds between 16 and 32 kph. It is assumed that all tests were performed in a normal configuration since no mention of angled impact is made. Prasad also does not specify whether or not collisions were centered or offset by some distance. Using regression analysis, Prasad tested the influence of approach velocity on the coefficient of restitution for each of the three collision configurations. Tests for front impacts were largely

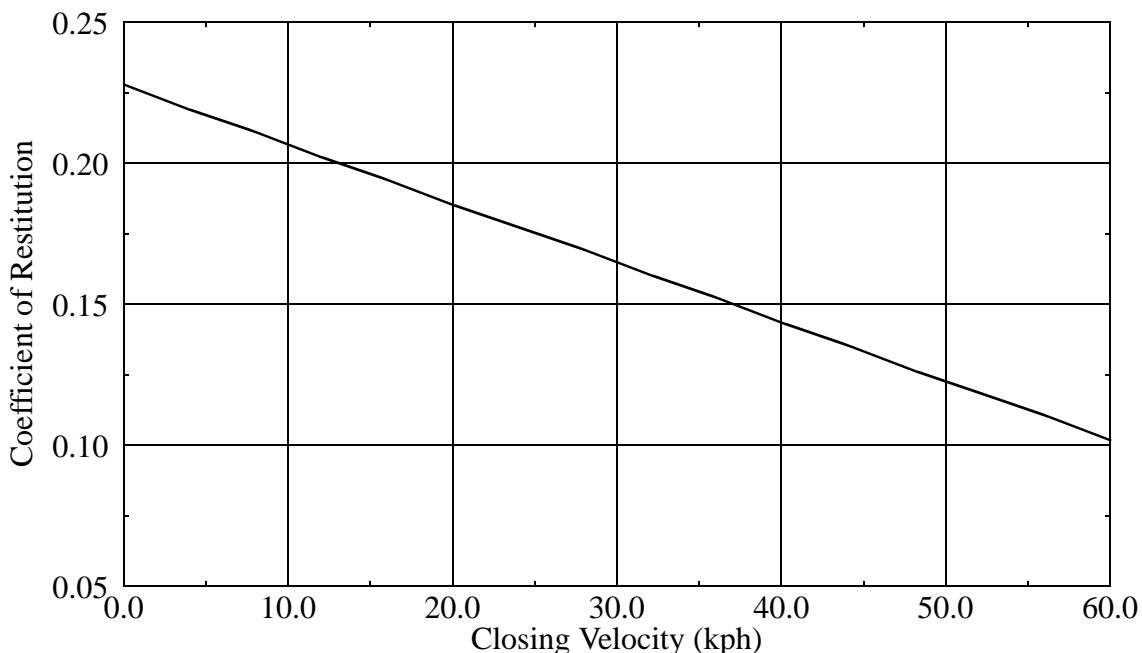


FIGURE 2.2. Coefficient of Restitution v. Closing Velocity -- Frontal Rigid Barrier Impact (recreated from reference 9)

performed at approach speeds of either 48 or 56 kph and were executed with the vehicle impacting a fixed rigid barrier. Tests at 48 and 56 kph resulted in coefficient values ranging from 0.05 to 0.18, while the few values from tests at 8 to 16 kph range between 0.10 and 0.30. Linear regression analysis predicted the best fit of the data to be the line given by Equation 2.1 and plotted in Figure 2.2. Side impact tests were conducted with either a

$$\varepsilon = 0.22771 - 0.003377 \times Velocity \quad (2.1)$$

rigid or a deformable barrier impacting the stationary vehicle at the speeds indicated above. Coefficient results vary between 0.02 and 0.27. No significant correlation was found between closing velocity and restitution for side impacts. Tests for rear impacts were also performed by moving a rigid barrier into the stationary vehicle. The coefficient of restitution for these cases ranges from 0.03 to 0.17, and as for side impacts, results indicate no correlation with closing velocity.

Coefficient of restitution values are also reported by Kerkhoff *et al* in a paper reporting the results of a series of frontal rigid barrier crash tests on the Ford Escort, model years 1981-85 [12]. Restitution results of the tests are presented in Figure 2.3. No fit of the data is attempted, but the authors note the decreasing magnitude of the coefficient with increasing impact velocity.

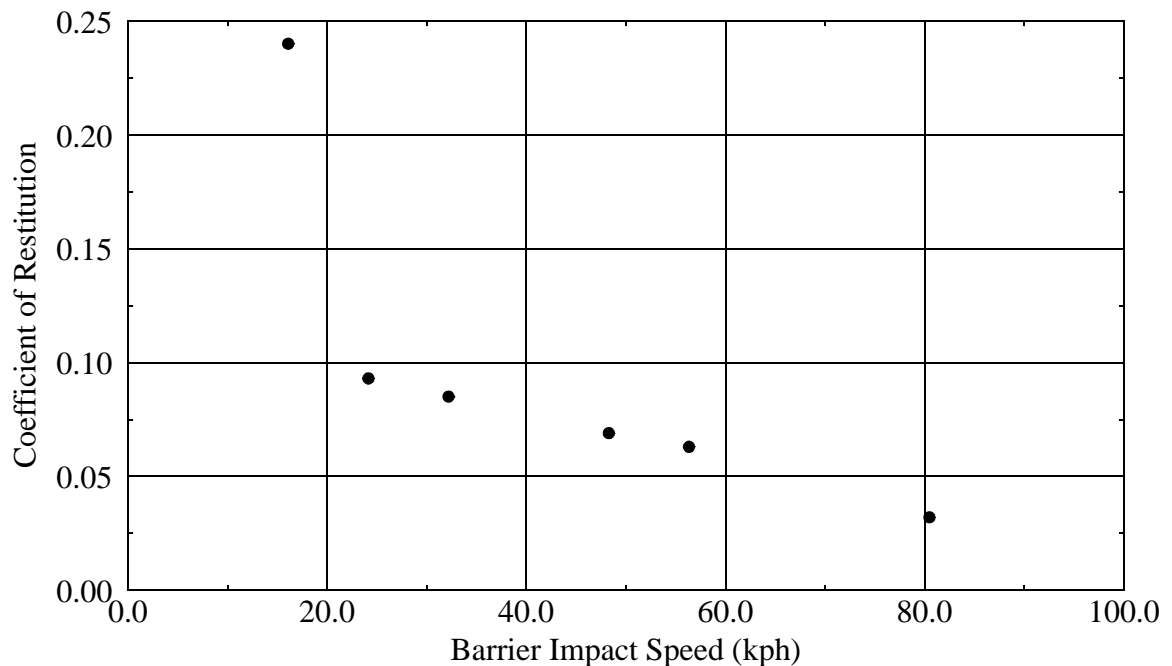


FIGURE 2.3. Coefficient of Restitution v Impact Velocity -- 1981-1985 Ford Escort, Frontal Rigid Barrier Impact (recreated from reference 10)

2.2 RESTITUTION AND OTHER INFLUENTIAL PARAMETERS

In addition to simple regression testing for correlation between restitution and closing velocity, Prasad, of the TRC, conducted multiple-variable regression analysis to test the coefficient's correlation with the following impact parameters: approach velocity, vehicle model year, body type, engine type, engine displacement, transmission type, vehicle weight, vehicle width, vehicle length, wheelbase, distance between center of gravity and front of body, and the ratios weight to width, weight to length, and weight to wheelbase [11]. Equations were generated to mathematically define the coefficient based on correlated parameters. For front impacts, the coefficient of restitution was found to correlate with approach velocity (V), vehicle model year (Y), and vehicle width (W), according to Equation 2.2.

$$\varepsilon = -0.8597 - 0.006781 \times V + 0.01128 \times Y + 0.002763 \times W \quad (2.2)$$

Surprisingly, vehicle model year is the most influential parameter. Side impact results indicate that approach velocity and the ratios weight to width (WW) and weight to length (WL) correlate with the coefficient, according to Equation 2.3.

$$\varepsilon = -0.3619 - 0.01438 \times V - 0.04177 \times WW - 0.1562 \times WL \quad (2.3)$$

As shown, the weight to length ratio is the dominant parameter in this case. Analysis of rear impacts didn't indicate significant correlation of the coefficient with any of the parameters. For this case, Prasad suggests that the average value of 0.082 be used. It should be noted, however, that the rear-impact data have a standard deviation of 0.037.

2.3 IMPACT MODEL RE-DEFINING THE COEFFICIENT OF RESTITUTION

In papers written in 1993 and 1994, Hirotoishi Ishikawa, of the Japan Automobile Research Institute, presents an impact model that re-defines the coefficient of restitution and introduces a tangential coefficient of restitution [13, 14]. As a part of the theoretical explanation of the model, Ishikawa defines GIR, RDS, and RSS. GIR, the generalized impulse ratio, is defined as the ratio of the tangential component of impulse and the normal component of impulse when the coefficient of restitution is zero. It is used as a descriptor of collision-type. RDS, relative deformation speed, and RSS, relative sliding speed, define the normal and tangential components of the colliding vehicles' relative velocity at the average location of force application during the collision, or impulse center,

respectively. The normal-tangential coordinate system is chosen based on the impact surface. The normal coefficient of restitution is defined by the ratio of the pre-impact and post-impact relative deformation speeds, as shown in Equation 2.4, while the tangential

$$\epsilon_n = \frac{-RDS}{RDS_i} \quad (2.4)$$

coefficient is defined similarly using relative sliding speed. It should be emphasized that the speeds used are measured at the impact center and not at the vehicle center-of-gravity. Ishikawa presented restitution results, based on the developed model, from sixteen vehicle-to-vehicle collisions in the 1993 paper, found that more testing was necessary in order to be conclusive, and then reported the results of forty-five vehicle-to-vehicle tests in the 1994 paper. Thirteen of the forty-five collisions were front impacts and the remaining thirty-two were side impacts. It is clear that impact angle was varied for both collision types, but the point of initial contact is not specified for all collisions. Ishikawa investigated the influence of GIR and initial RDS on the coefficient of restitution in the normal direction. The normal coefficient ranges from -0.4 to 0.5 for the side impact tests and from 0.0 to just under 0.2 for the frontal impacts, as shown in Figure 2.4. The four negative coefficient cases visible in the plot are associated with corner-to-corner impacts

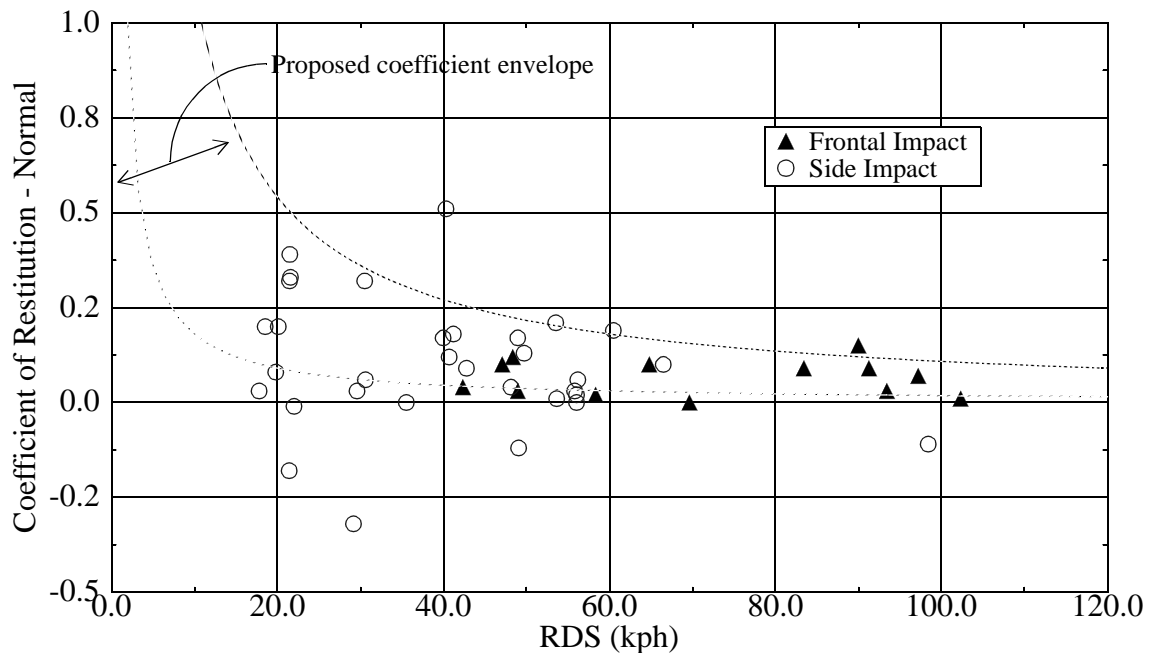


FIGURE 2.4. Coefficient of Restitution in the Normal Direction v. RDS -- Vehicle-to-Vehicle Frontal and Side Impact (recreated from reference 12)

or high speed side-swipe collisions. It should be noted that negative values result when reference points pass through or by one another. Since one mass cannot move through another, these cases occur because a coordinate frame was chosen that results in velocity components that indicate movement of the reference points past one another. Ishikawa discovered that regardless of impact geometry, the normal restitution coefficient is dependent upon the initial RDS. He proposes two lines as boundaries of an area on the plot in which most of the coefficients can be found. The lines shown in Figure 2.4 are specific cases of the family of equations given by Equation 2.5. This equation suggests

$$\epsilon_n = \frac{Const}{RDS_i} \quad (2.5)$$

that regardless of the initial relative deformation speed, the vehicle rebounds to a constant relative deformation speed. No correlation was found between the normal coefficient and GIR for either collision configuration.

As with the normal coefficient, Ishikawa investigated the influence of GIR and initial RSS on the coefficient of restitution in the tangential direction. Coefficient values for this case range from about -0.9 to just above 0.5 for side impacts and from -0.8 to 0.9 for frontal impacts. Ishikawa explains that when the coefficient is negative, the vehicles are

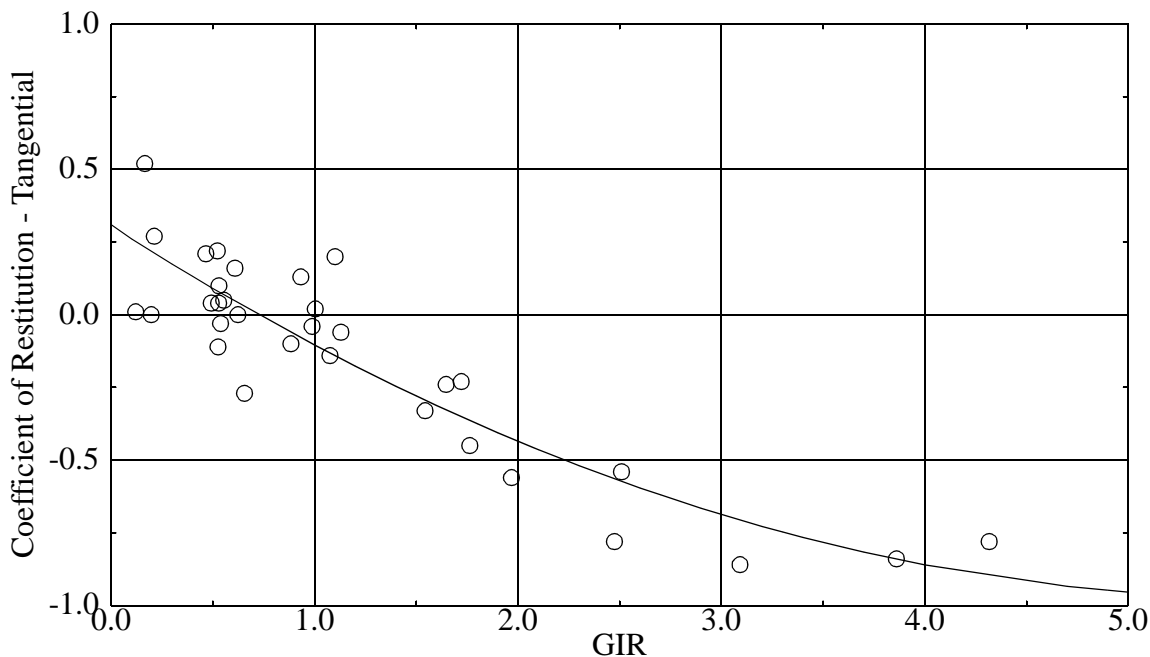


FIGURE 2.5. Coefficient of Restitution in the Tangential Direction v. GIR -- Vehicle-to-Vehicle Side Impact (recreated from reference 12)

sliding relative to one another much like a slip coefficient would indicate, while a positive value indicates restitution along the tangential axis. GIR was found to be very influential on the tangential coefficient for the side impact cases. The estimated relationship is plotted with the side impact data in Figure 2.5 and is given by Equation 2.6.

$$\varepsilon_t = 0.0396 \times GIR^2 - 0.04501 \times GIR + 0.3066 \quad (2.6)$$

Evidence of the influence of GIR on the tangential coefficient for frontal impacts and of RSS on the tangential coefficient for both impact configurations is inconclusive. Nothing is reported on the effect of impact angle or initial contact point location.

2.4 DERIVATION OF THE VEHICLE-TO-VEHICLE COEFFICIENT FROM BARRIER DATA

As a tool for determining the coefficient of restitution for a collision between two vehicles, researchers have suggested methods, generally limited to full-frontal cases, for calculating the coefficient from the vehicle-to-barrier coefficients of the involved vehicles. Howard *et al* conclude that it is impractical to quantify the coefficient for vehicle-to-vehicle collisions because each vehicle combination has a "unique restitutive response" [9]. As a result, tests would have to be performed for every possible combination. Instead, the group proposes testing to find the coefficient of restitution for a given vehicle in a vehicle-to-barrier collision and presents a method, based on the laws of conservation of momentum and energy, for combining vehicle-to-barrier coefficients for two vehicles to calculate the particular vehicle-to-vehicle coefficient, as shown in Equation 2.7. They are

$$\varepsilon_{AB} = \sqrt{1 + \frac{m_B(\varepsilon_A^2 - 1) + m_A(\varepsilon_B^2 - 1)}{m_A + m_B}} \quad (2.7)$$

careful to note that the calculation is valid only for low-velocity collisions where the collision durations and residual deformations for vehicle and barrier cases are nearly identical.

Like the group from Biodynamic Research Corporation, Prasad also derives a method for calculating a specific vehicle-to-vehicle coefficient of restitution from two vehicles' vehicle-to-barrier coefficients [11]. His final equation, however, requires knowledge of the

vehicle-to-barrier coefficients and vehicle stiffnesses, instead of vehicle masses, as given in Equation 2.8. One difficulty immediately visible in Prasad's approach is lack of

$$\epsilon_{AB} = \sqrt{\frac{\epsilon_A^2 k_B + \epsilon_B^2 k_A}{k_A + k_B}} \quad (2.8)$$

knowledge concerning vehicle stiffness characteristics.

Siegmund *et al* challenge the accuracy of such relationships [10], reporting that it is necessary to make the assumption that the durations are similar in order to derive vehicle-to-vehicle coefficients from vehicle-to-barrier coefficients as presented by Howard and Prasad. They report data showing that, at least using Howard's approach, deriving vehicle-to-vehicle coefficients from barrier coefficients generally results in an over-prediction of restitution, at least for the low velocity range in which they tested.

2.5 OTHER RESTITUTION RESEARCH

Other research gives additional information on restitution. From an analysis of eleven RICSAC (Research Input for Computer Simulation of Automobile Collisions) cases, Raymond M. Brach concludes that the coefficient of restitution is influenced by structural properties and collision geometry, as well as impact velocity [5]. Two papers written by MacInnis Engineering describe the results of extensive low-velocity collision testing, where restitution results are presented as a function of bumper isolator compression, where the isolator is a piston forced through energy-absorbing fluid. They demonstrate that the coefficient decreases with increasing isolator compression but begins to increase again when the isolator is fully compressed [10, 15].

2.6 SUMMARY

The published research on the coefficient of restitution in motor vehicle collisions indicates that restitution often reaches significant levels. It is also clear that the spread in coefficient values for similar collision conditions is high. The reported groups' studies demonstrate that restitution is influenced by certain collision properties. For example, it is apparent that approach velocity and collision geometry play important roles in the determination of the coefficient of restitution in the normal direction. Because researchers often approach the problem differently, however, it is difficult to compare and combine

results. The literature also shows a significant amount of discussion on the relation of the coefficient of restitution in vehicle-to-vehicle collisions to the individual vehicles' coefficients in barrier impacts.

Chapter 3: Theoretical Background

3.1 THE ANATOMY OF A COLLISION AND RESTITUTION

3.1.1 Vehicle Dynamics

The role of restitution in an automobile collision can best be shown by performing a "walk-through" of a specific collision. Figure 3.1 presents velocity results from a representative vehicle-to-barrier, full-frontal crash test involving a 1993 Ford Taurus (NHTSA Test 1890) [16]. In addition to showing the vehicle's velocity at its rear seat, which is assumed to accurately represent the center-of-gravity velocity, velocities are shown for the top and bottom of the engine as well as for the left and right front brake calipers. It is apparent from the figure that the rear of the vehicle begins to slow down before the engine and suspension, likely due to relatively high compliance between the components and the vehicle structure. The suspension and engine begin, however, to decelerate even more rapidly than the vehicle center-of-gravity once they are engaged by the advancing vehicle crush. The engine is the first major component of the vehicle to reach zero velocity, which occurs at under 40 ms, after which it actually restores back into the vehicle and assists in decelerating the rest of the vehicle. As is manifested by the

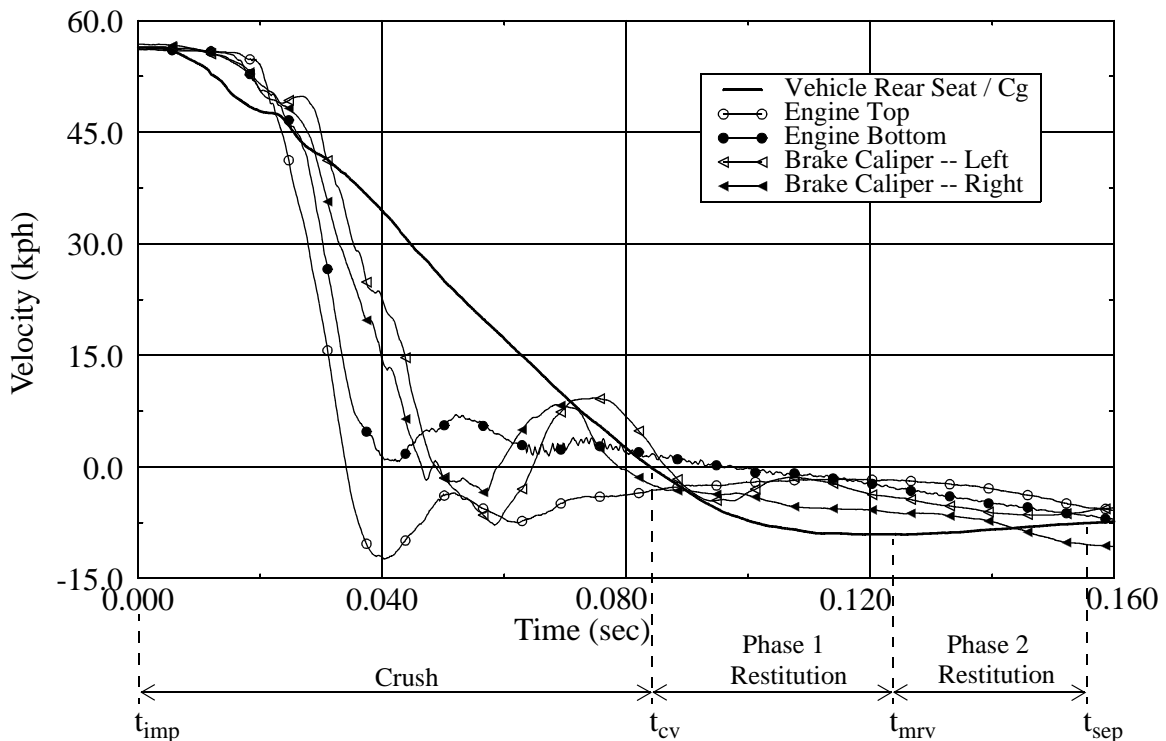


FIGURE 3.1 Velocity v. Time at Various Vehicle Locations -- NHTSA Test 1890: 1993 Ford Taurus into Fixed Rigid Barrier, Full-Frontal Configuration with Applicable Nomenclature

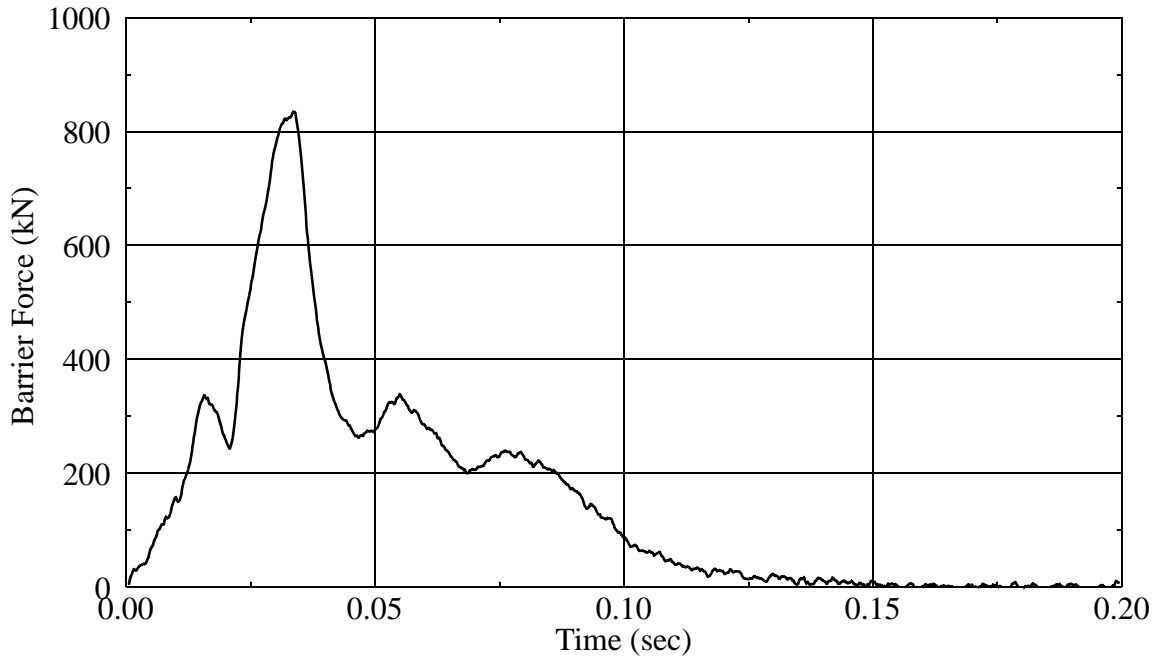


FIGURE 3.2 Barrier Force v. Time -- NHTSA Test 1890: 1993 Ford Taurus into Fixed Rigid Barrier, Full-Frontal Configuration

figure, a small amount of restitution also occurs in the suspension (brake caliper) after it reaches zero velocity about 50 ms into the collision. The velocities of both the engine and the suspension settle approximately to zero until the vehicle as a whole begins to move away from the barrier. The vehicle center-of-gravity reaches zero velocity at about 85 ms. For nomenclature purposes, the interval between the time of impact (t_{imp}) and the time of common velocity (t_{cv}), or zero velocity for this case, is designated as the crush phase of the collision. Once the vehicle center-of-gravity reaches zero velocity, restorative forces accelerate the vehicle away from the barrier. These forces continue until the time at which the vehicle and barrier separate (t_{sep}) and forces between them go to zero, which, by inspection of the force-time trace for this case shown in Figure 3.2, is about 0.155 seconds. Comparing this separation time to the time at which maximum rebound velocity (t_{mrv}) occurs, as shown in Figure 3.1, reveals that maximum rebound velocity is reached prior to vehicle-barrier separation. In other words, not all of the structural restoration that occurs contributes to a vehicle's maximum rebound velocity. The deceleration of the vehicle following acceleration to maximum rebound velocity occurs because, as restitution proceeds, barrier-vehicle forces decrease until they are lower than friction forces between the vehicle and the ground. If there were no forces due to friction, the vehicle would continue to accelerate in the direction away from the barrier until

separation. For nomenclature purposes, the period between common velocity and maximum rebound velocity is designated phase one restitution, while the period from maximum rebound velocity to vehicle-barrier separation is called phase two restitution. It should be noted that for vehicle-to-vehicle collisions, the duration of phase two restitution cannot be determined since separation time is unknown.

3.1.2 Occupant Kinematics

Restitution influences not only the dynamics of a vehicle in a collision but also occupant kinematics and injury severity. Figure 3.3 again presents the velocity trace of the vehicle in NHTSA test 1890, but this time with velocity traces associated with the longitudinal motion of the chests and heads of the crash dummies in the right and left front seats. The dummies were belted, and the air bags performed as intended at both positions. The figure shows that after an initial delay, the seat belts and air bags bring the occupants to zero velocity at about the same time the vehicle reaches zero velocity. It is clear that each of the velocity traces is in the negative region after zero velocity, with occupant velocities exceeding that of the vehicle. The erratic behavior of the dummy head traces is expected because of rotation of the heads during the course of the collision, altering the direction in which the accelerometer senses speed change. The high negative occupant

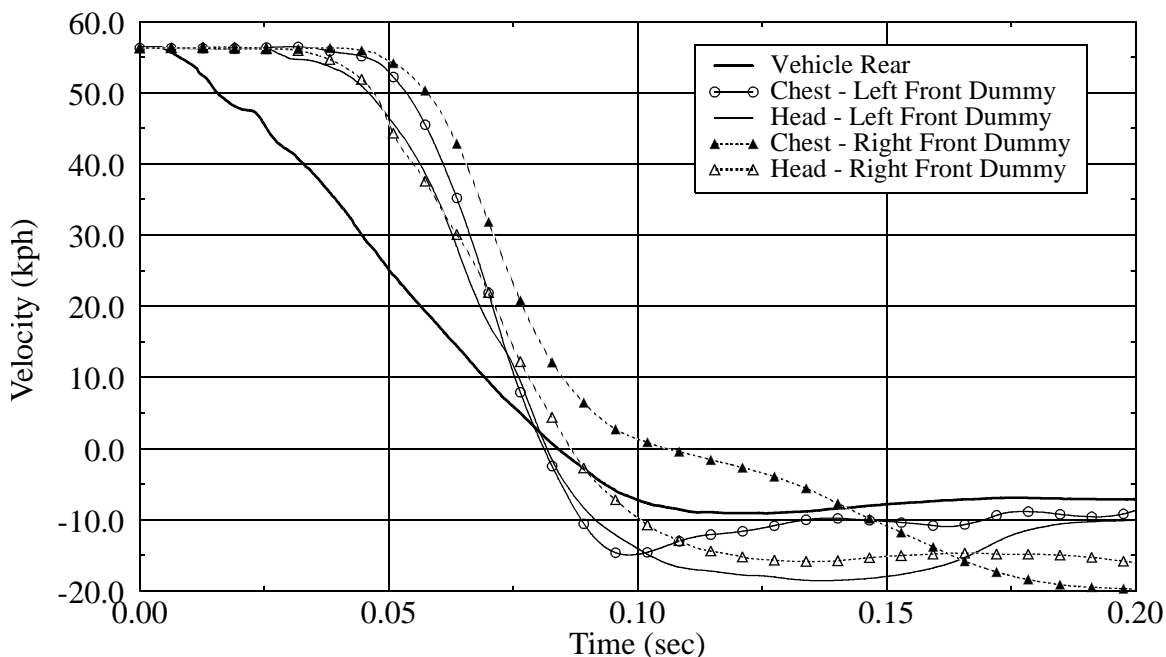


FIGURE 3.3 Velocity v. Time at Vehicle Rear and Chest and Head of Dummies at Right and Left Front Seats -- NHTSA Test 1890: 1993 Ford Taurus, Vehicle-to-Fixed Rigid Barrier; Three-Point Belt and Airbag Restraints

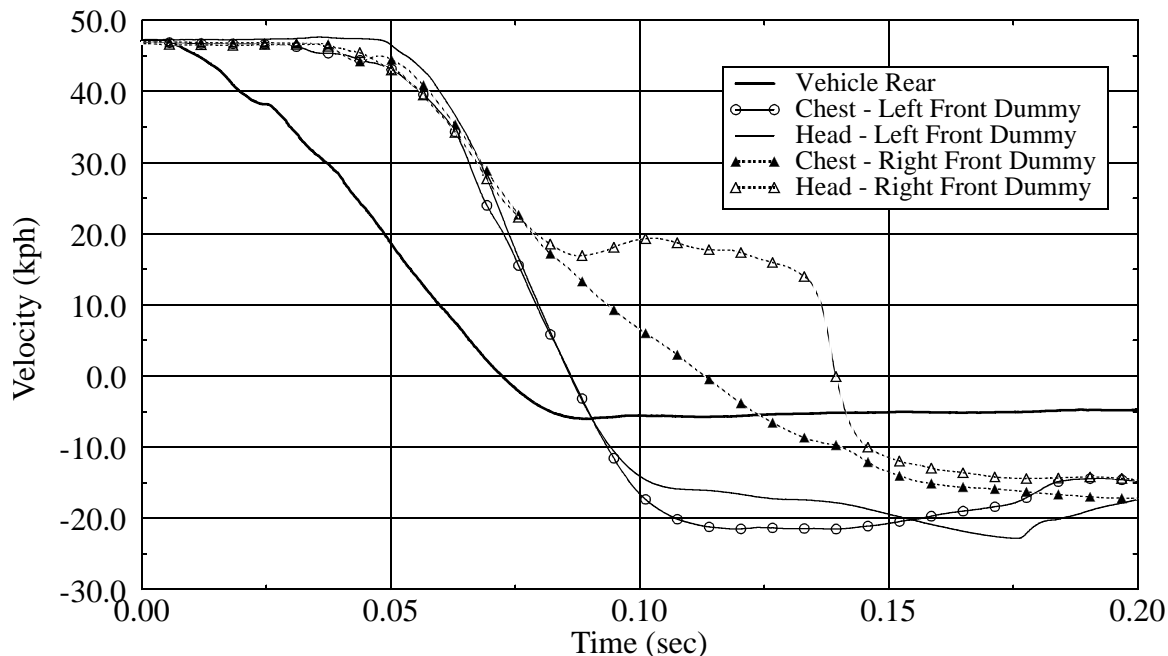


FIGURE 3.4 Velocity v. Time at Vehicle Rear and Chest and Head of Dummies at Right and Left Front Seats -- NHTSA Test 1777: 1993 Ford Taurus, Vehicle-to-Fixed Rigid Barrier; Airbag Restraints Only

velocities shown in the figure are influenced by restitution in both the impact of the vehicle with a barrier or another vehicle and the collision between the dummies and the objects they contact on the vehicle interior. It is apparent that higher vehicle restitution results in larger occupant ΔV and, therefore, greater potential injury severity.

Other cases show similar results but also demonstrate that the influence of restitution on dummy kinematics is affected by the type of restraints that are used. Two additional cases, one where airbags are the only restraint and one where only three-point belts are utilized, are presented in Figures 3.4 and 3.5 respectively. In both cases, chest and head-mounted accelerometers on two dummies in the front seat record longitudinal (relative to dummy position) velocity changes. Both tests are rigid barrier collisions involving the Ford Taurus, with impact velocities of 48 and 56 kph for Figures 3.4 and 3.5, respectively (NHTSA Tests 1777 and 1103) [16]. In the 48 kph case where only air bags are used, the dummies reach zero velocity later in the collision than when they are restrained by belts. Even though this test is conducted at a lower velocity than Test 1890, some of the occupant negative velocities are even more severe than those in the 56 kph test. The three-point belt restraint case shows similar behavior to those previously presented, except that

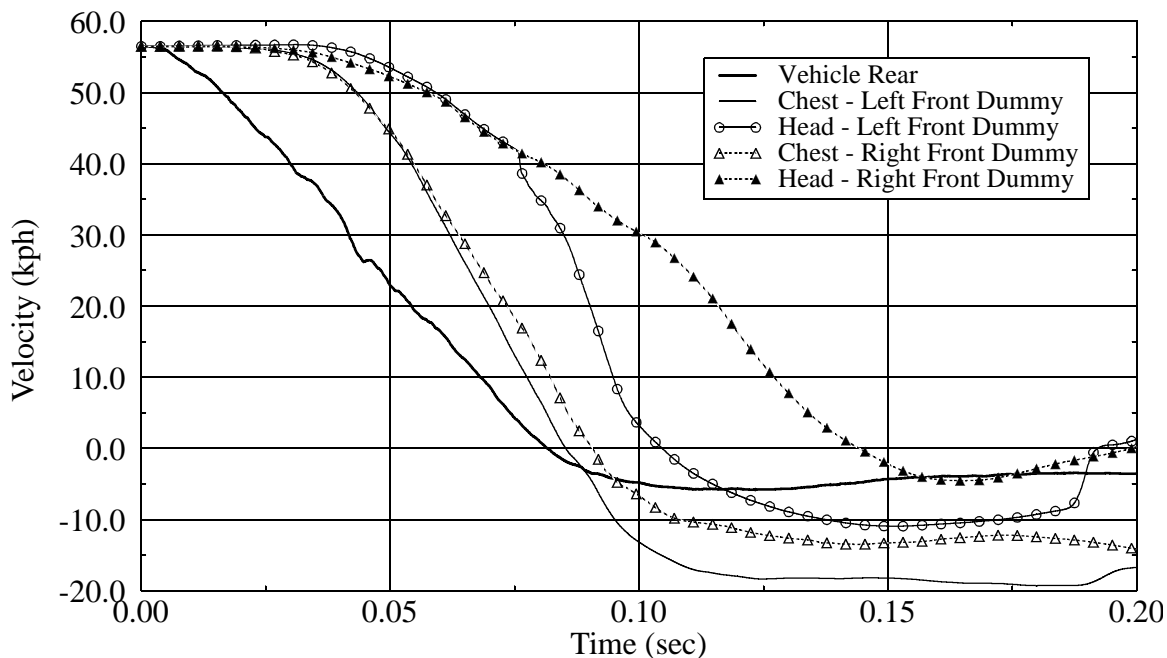


FIGURE 3.5 Velocity v. Time at Vehicle Rear and Chest and Head of Dummies at Right and Left Front Seats -- NHTSA Test 1103: 1988 Ford Taurus, Vehicle-to-Fixed Rigid Barrier; Three-Point Belt Restraints Only

head velocities do not appear to reach rebound velocities as high as the others, at least within the investigated time frame. In this case, restitution appears to be more influential in chest velocities than head velocities.

Occupant kinematics in vehicle collisions are obviously complex. Analysis is difficult because the axis along which dummy-mounted accelerometers measure acceleration is almost continuously changing due to rotation. The presented plots, however, make it clear, at least in a qualitative sense, that the extent of restitution is influential in injury severity.

3.2 AUTOMOBILE COLLISIONS AND RIGID BODY COLLISION MECHANICS

The coefficient of restitution has its foundation in the development of engineering dynamics, which defines the movement of bodies. The basic governing laws of dynamics and impact, conservation of momentum and conservation of energy, are commonly used to predict the overall behavior of automobiles in a collision. Because of the complex structures of automobiles, however, it is necessary to make certain assumptions, known as rigid body assumptions, to simplify the problem.

3.2.1 Rigid Body Assumptions

The assumptions included in assuming something to be a rigid body are accurately described by the phrase "rigid body." In other words, the body is considered to be rigid, with all points on the body maintaining their positions relative to one another. As a result, no deformation may occur. The body is also assumed to have a constant mass with a constant center-of-gravity position. There is no question that all automobile collisions, except for some very low velocity cases, violate the rigid body assumptions, but the skilled analyst can apply the governing laws in such a way that the assumptions are violated to as small degree as possible. For example, by skillfully approximating the location of the impulse center, the average point through which forces act during the collision, and the principal direction of force, an accurate exchange of momentum can be calculated, even in cases of deformation.

3.2.2 Conservation of Momentum and the Coefficient of Restitution

Conservation of momentum requires, neglecting outside forces such as tire forces in the case of automobiles, that the vector momentum be conserved during the course of a collision. For rigid bodies in central collisions (no rotation), this principle is defined by Equation 3.1 The most general expression for conservation of momentum of rigid bodies

$$\sum m\vec{v}_i = \sum m\vec{v}_f \quad (3.1)$$

includes Equation 3.1, along with a similar expression for angular momentum and equations governing restitution and slip, or relative tangential motion between colliding bodies. The equation governing the coefficient of restitution in this most general case is Equation 1.1, with velocities measured at the impulse center. For the simplified case of Equation 3.1, velocities at the center-of-gravity may be used to determine the coefficient's value, as they are equivalent to impulse center velocities. The coefficient defines the extent of elasticity of a collision such that it has a value of 1 for a perfectly elastic collision, where no permanent deformation occurs, and a value of 0 for a perfectly plastic collision, where there is residual deformation.

3.2.3 Conservation of Energy and the Coefficient of Restitution

Conservation of energy requires that energy be neither created nor destroyed. This requires that the energy of a system prior to collision must be accounted for through work or energy after the collision. The total system energy prior to a collision of two

automobiles is the sum of the kinetic energies of the vehicles, while the work and energy following the collision consists of the sum of kinetic energy and energy dissipated through structural deformation, heat, and sound. Work done through heat and sound is commonly neglected so that the sum of the post-impact kinetic energy and the work done by deformation is equal to the pre-impact kinetic energy. Using this relation and applying the definition of the coefficient of restitution described by Equation 1.1 allows an expression for total collision residual crush energy in terms of the coefficient, as given by Equation 3.2. This equation is limited to central collisions, so velocities apply to center-of-gravity

$$E_{resCrush} = \left(\frac{1 - \epsilon_{AB}^2}{2} \right) \left(\frac{m_A m_B}{m_A + m_B} \right) (v_{A,i} - v_{B,i})^2 \quad (3.2)$$

positions on the colliding bodies.

Conservation of energy may be applied at any time during the collision, such as when two vehicles in a direct, central collision or a vehicle and a barrier reach common velocity. At this time in such a collision, the decrease in kinetic energy has been transferred to crush energy, so that the work done in crush is equal to the change in kinetic energy of the system. This allows calculation of the coefficient of restitution in terms of the maximum crush energy (occurring at the time of common velocity) and the residual crush energy. Equation 3.3 shows this relationship for a vehicle impacting a rigid barrier.

$$e_A = \sqrt{\frac{E_{maxCrush} - E_{resCrush}}{E_{maxCrush}}} \quad (3.3)$$

3.3 APPLICATION OF CRASH TEST DATA

3.3.1 Derivation of the Coefficient of Restitution

Crash test data are generally available as measured by accelerometers at various locations on a vehicle. As given by Equation 3.4, velocity can be determined through

$$v(t) = \int a(t)dt \quad (3.4)$$

proper integration of a chosen acceleration trace. The coefficient of restitution is calculated using Equation 1.1, where approach velocity is simply determined as the relative velocity of two bodies' just prior to collision. Restitution velocity is determined as the maximum separation velocity of the colliding bodies occurring during the course of the collision, taken from an integrated acceleration trace. For central collisions, where no rotation occurs, data used to calculate the maximum separation velocity in a collision are obtained from accelerometers mounted at an undeformed location on the vehicle near to or along the line of action of force for the collision. Accelerometers located in this way accurately approximate the dynamics of the impulse center. In cases where data are not available at the preferred location, accelerometers in an undeformed region near that location may, with caution, be used to represent its dynamics, as long as the point is rigidly linked to the preferred location. In many cases, data from multiple accelerometers on a single vehicle may reasonably be applied to give the velocity at the desired location. All applicable traces should be averaged to minimize instrumentation error.

In cases where the estimated line of action of force does not act through the center-of-gravity of a vehicle, rotation results, and any restitution affects both linear and angular velocity changes. As a result, the rebound velocity used to determine the coefficient of restitution must be taken at the average point of force application, defined as the impulse center, and in the direction of the principal direction of force. The location of the impulse center moves deeper into a vehicle during crush and then becomes more superficial during restitution, so its average position must be estimated. Because the impulse center and principal direction of force must be approximated, determining the coefficient of restitution in this manner can only be as accurate as the approximations.

Accelerometers mounted at positions away from the center-of-gravity, in addition to measuring linear accelerations, are influenced by tangential and normal accelerations associated with vehicle rotation. Figure 3.6 illustrates this influence on two rear-mounted accelerometers in an offset frontal collision causing counter-clockwise rotation. The

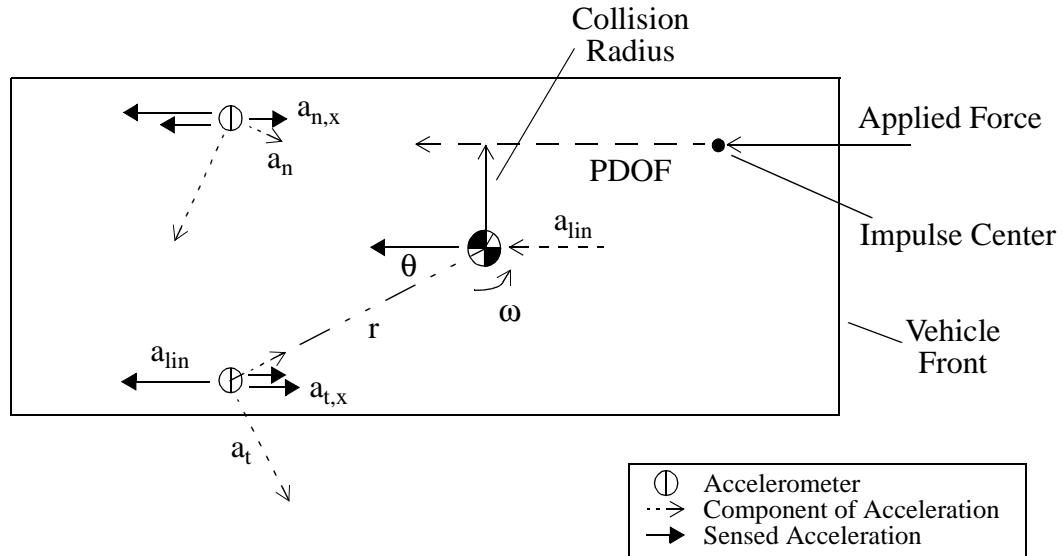


FIGURE 3.6 Influence of Vehicle Rotation on Accelerometers Mounted Away from the Center-of-Gravity

accelerometers are mounted such that they measure acceleration in the longitudinal direction. Longitudinal components of acceleration are shown as solid lines with filled arrowheads. The figure shows the same translational acceleration present at the center-of-gravity to be present at the two accelerometers, as is the case for a rigid body impact. Tangential and normal accelerations, due to rotation relative to the center-of-gravity, are shown as dashed lines. They also contribute to the sensed acceleration with components in the longitudinal direction. Because normal acceleration is due to change in velocity direction rather than change in magnitude, its influence must be subtracted from the velocity magnitude trace derived by integration. The effects of tangential and normal acceleration vary depending on the side of the vehicle on which an accelerometer is mounted. The expression given by Equation 3.5 shows the necessary steps for correcting

$$v_{cg} = v_{rr} - [\int \omega^2 r dt] \cos(\theta) - \omega r \sin \theta \quad (3.5)$$

for the influence of rotation-induced acceleration in order to determine the longitudinal component of center-of-gravity velocity from the velocity trace derived from the right rear accelerometer in Figure 3.6. It should be noted that Thomas Bundorf, in a 1996 technical paper, discusses the procedure for accounting for the influence of rotation-induced accelerations in collisions where rotation is significant [17].

3.3.2 Determination of Vehicle Crush for Vehicle-to-Barrier Collisions

Although knowledge of dynamic vehicle crush in a collision does not aid in the calculation of the magnitude of the coefficient of restitution, it is instructive in researching mechanisms that influence restitution. Knowledge of crush and vehicle structure makes it possible to determine what vehicle components and structures were contacted by the advancing crush, and therefore, were potentially influential in restitution. For vehicle-to-rigid-barrier collisions, vehicle dynamic crush is considered to be equivalent to the position change of undeformed locations on the vehicle during the time of barrier contact, and therefore, may be determined by integrating a vehicle's velocity trace, as given by Equation 3.6. Although total crush could be determined for a collision between two

$$x(t) = \int v(t) dt \quad (3.6)$$

deformable bodies in a similar way, crush for an individual body in such a collision cannot be calculated, since the velocity of the crush interface between two crushable objects is generally unknown. When a velocity trace is integrated to determine crush, however, the extent of the crush is generally overestimated, because impact waves do not travel fast enough for a rear-mounted accelerometer to sense exactly when crush begins at the front of a vehicle. Figure 3.7 shows evidence of lag in a rear-mounted accelerometer by repeating the rear seat velocity trace from Figure 3.1. Assuming that impact time was

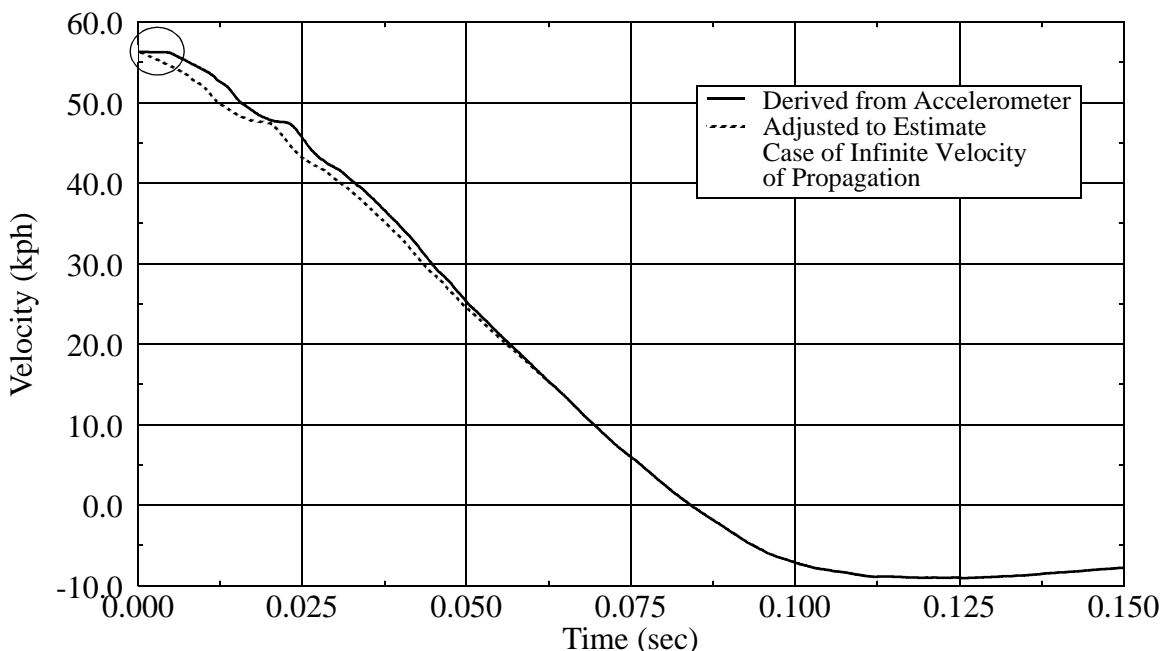


FIGURE 3.7 Influence of Velocity of Propagation; Velocity at Vehicle Rear Seat v. Time -- NHTSA Test 1890: 1993 Ford Taurus into Fixed Rigid Barrier, Full-Frontal Configuration

correctly determined, it is clear from the circled portion of the derived trace that no deceleration occurs at the point where the accelerometer is mounted until about 4 ms after impact. The speed of impact waves, known as the velocity of propagation, is defined by material properties as given in Equation 3.7. For a solid steel rod, with a modulus of

$$c = \sqrt{\frac{E}{\rho}} \quad (3.7)$$

elasticity of 207 GPa and a density of 7801 kg/m³, the velocity of propagation is calculated to be 5151 m/s. A wave at this speed would travel a distance of approximately 21 meters in 4 ms. Considering only the applicability of the concept of the velocity of propagation to a vehicle system, it is expected that wave propagation velocity in an automobile would be significantly less, due to pin and compliant connections between components that allow more than one degree of freedom and introduce a higher level of flexibility than a solid rod. Assuming that the distance through which a wave must travel to reach a rear-mounted accelerometer is 5 meters and using the time of 4 ms, a velocity of 1250 m/s is calculated. This represents a reduction to about one-fourth of the velocity for the solid case. Based on this approximation, the relationship of Equation 3.8 must also be

$$\frac{c_{ROD}}{c_{CAR}} = 4 = \frac{\sqrt{E_{ROD}/\rho_{ROD}}}{\sqrt{E_{CAR}/\rho_{CAR}}} \quad (3.8)$$

true. It is then assumed that the materials through which impact waves travel in an automobile have a slightly lower effective density than the solid rod. For the relationship to hold, the modulus of elasticity of the involved components of the vehicle must be less than one-sixteenth of the value of the modulus for the rod, which seems to be reasonable. Based on this reasoning, it is determined that lags on the order of 4 ms are explainable for tests similar to Test 1890. The adjusted trace shown in the figure is a copy of the accelerometer-derived trace that was altered in length. It qualitatively estimates the velocity that would result if the velocity of propagation were infinite, from which, if it were available, dynamic crush could be accurately calculated. It is expected that, as the vehicle crushes and velocity decreases, the difference between the derived and adjusted traces will become negligible because the speed of the crush face is decreasing. As a result, the derived velocity is considered to accurately represent the dynamics of the

vehicle during the restitution portion of the collision. The error that results from integrating the derived pulse is equal to the difference of the areas under the two traces. Because of the accuracy of the derived trace during the restitution period, error generated in determining maximum dynamic crush may be corrected by subtracting the difference of the calculated residual crush and the measured residual crush, from the calculated dynamic crush, as given by Equation 3.9.

$$C_{m,a} = C_{m,c} - (C_{r,c} - C_{r,a}) \quad (3.9)$$

Another consideration to be made in determining crush depth from velocity traces is that crushed material builds up between the vehicle-barrier interface, or crush face, and the location where crushed material is adjacent to uncrushed material, as shown in Figure 3.8. The integrated velocity trace gives the position change of the accelerometer, so only the distance moved by the crush face relative to the accelerometer is accounted for. Crush depth is defined here as being equal to the sum of the calculated position change of the vehicle center-of-gravity (Δx) and the thickness of the crushed region (Δc). Jones and Birch, in a 1990 technical paper, report that, for tubes, the distance travelled by the crush face is, at most, 75% of the original length of the material [18]. In other words, for fully-crushed tubes, the expected thickness of the crushed material would be 25% of the original

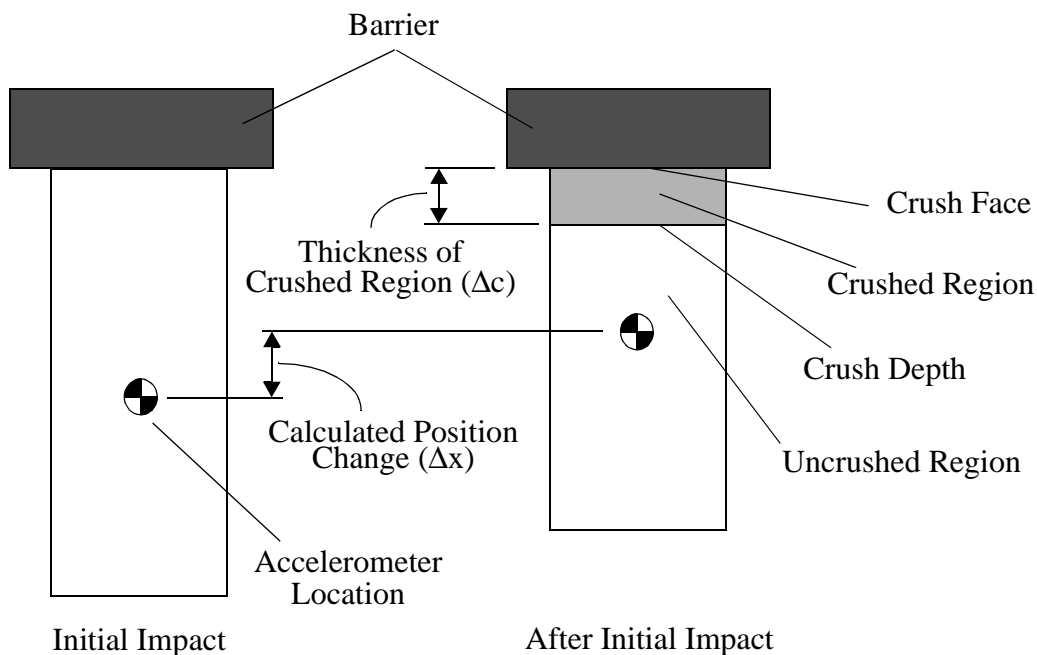


FIGURE 3.8 Vehicle Crush Illustration and Nomenclature

length of the tubes. Wood and Mooney, of Wood & Associates, report frontal crash test results that show the "75% rule" proposed by Jones *et al* to be applicable to automobiles [19]. Wood *et al*, however, do not make particular mention of how well the engine obeys the cited rule. It is likely that due to its extremely high stiffness, it probably doesn't crush nearly as much as other parts of the vehicle. As a result, crush depth is almost immediately extended into the vehicle, in the region directly behind the engine, by a distance equal to the engine's longitudinal dimension, once it is engaged by the advancing crush. Therefore, maximum crush depth can be approximated by multiplying the result of Equation 3.9 by 1.33 (inverse of 0.75). For cases where the engine is engaged by the crush in a frontal collision, the depth of crush behind the engine is found by adding the longitudinal dimension of the engine to the previous calculation.

3.3.3 Determination of Barrier Force and Crush Energy in Vehicle-to-Barrier Collisions

For many barrier collisions, barrier load cell data are also available. The load cell information may be combined to give a total barrier force. In a barrier collision, the calculated position trace represents the average crush of the vehicle. Barrier force can then be plotted against vehicle crush. Integration of the force-crush data results in an estimation of crush energy as a function of vehicle crush, according to Equation 3.10. The slope of a

$$E(x) = \int F(x)dx \quad (3.10)$$

crush energy versus vehicle crush curve is vehicle stiffness, which may be influential in the extent of restitution.

3.3.4 Comparison of Vehicle-to-Barrier and Vehicle-to-Vehicle Cases

In order to compare vehicle-to-barrier collisions to vehicle-to-vehicle impacts, it is necessary to utilize the concept of barrier equivalent velocity (BEV). BEV is defined as the impact velocity, in a vehicle-to-barrier collision, which gives the same crush energy as results in some other collision. Therefore, the BEV for a full-frontal VTV collision between identical vehicles is equal to exactly half the closing velocity between the two vehicles. In a non-identical VTV collision, BEV is likely different for each vehicle.

In order to apply the relation presented by Prasad for calculating a VTV coefficient of restitution value from VTB values, shown in Equation 2.8, stiffness values for analyzed vehicles are necessary. Using Equation 3.10 and assuming that a vehicle's structure can be

modeled as a linear spring (thus allowing the use of the fundamental expression for strain energy: $E = (1/2)kx^2$), an effective stiffness can be determined for a chosen vehicle.

Setting Equation 3.10 equal to the strain energy expression, with maximum dynamic crush implemented for displacement, and solving for k gives the definition of effective vehicle stiffness shown in Equation 3.11. Collision force in the expression is best determined

$$k_{eff} = \frac{2 \times \int F dx}{C_m^2} \quad (3.11)$$

through analysis of barrier load cell data. It may also, however, be approximated as the product of mass and acceleration. This is only an approximation because, in reality, the effective mass of a vehicle changes during the course of a collision, as some portions of the vehicle decelerate to zero velocity before others. By using the total mass of the vehicle, then, effective stiffness is overestimated. In Prasad's expression, however, proportional changes in stiffness cancel out. Therefore, it is accurate in this application to use the product of mass and acceleration to approximate collision force.

Chapter 4: Analytical Procedure

4.1 DESCRIPTION OF DATA

Crash test data are the primary source of information for vehicle collision dynamics research. Pre-impact and post-impact vehicle velocities can be easily determined from the acceleration traces available for a variety of vehicles. These velocities are used to determine the coefficient of restitution. Many of the tests include acceleration data for locations on the vehicle other than the center-of-gravity. These provide additional insight into vehicle dynamics.

This thesis assumes that the utilized crash test data are largely accurate in describing the studied collision dynamics. Film analysis, which could be used as a tool to verify the accuracy of the data and to provide additional insight, is not applied in the research. Conclusions and observations of the thesis are based upon the foundation assumption that the data are accurate.

The crash test data used in this research are available from the National Highway Traffic Safety Administration (NHTSA). Under the direction of the NHTSA, crash tests have been systematically performed on a sample of vehicles currently in use to determine the vehicles' levels of compliance with current government standards (FMVSS). For frontal collisions, FMVSS 208 requires vehicles to pass a 30 mph (48.3 kph) vehicle-to-rigid-barrier (VTB) test. Additionally, New Car Assessment Program (NCAP) tests, also under the direction of the NHTSA, are performed at 35 mph (56.3 kph) against a rigid barrier instrumented with load cells on its face. As a result, the great majority of frontal VTB tests is performed at one of these two speeds. Side and rear impactor-to-vehicle (ITV) crash tests are required by FMVSS 214 and 301, respectively. Compliance tests for side impact require a crabbed, moving deformable barrier that impacts a stationary vehicle at 33 mph (53.1 kph) resulting in a principal direction of force (PDOF) of 280 degrees. Rear compliance tests utilize a moving rigid barrier to produce an aligned collision at an impact speed of 30 mph (48.3 kph). For various purposes, other tests are also executed to study vehicle behavior under a variety of conditions, such as higher or lower speeds, varying overlap percentages, and vehicle-to-vehicle collisions.

Acceleration and force traces are available in digital X-Y format (acceleration in g's v. time in seconds; force in Newtons v. time in seconds) and were obtained through use of the NHTSA's web page on the internet [16]. Although there is some variation from test to test, data are generally available from accelerometers and load cells mounted at key locations on the vehicle, on crash test dummies, and on barriers. Barrier load cell data most commonly comprise four rows of nine cells, resulting in thirty-six individual traces. Typical time steps in the data are on the order of 0.0001 sec, with traces generally reporting data from before the time of collision to at least 0.2 sec following initial contact.

4.2 TEST SELECTION AND ORGANIZATION

Tests were selected by scanning the vehicle crash test catalog. Greater attention was given to popular, recent model year vehicles with a comparatively high number of tests, such as the Ford Taurus and the Honda Accord. To provide a general statistical basis for any conclusions, tests were also selected for many other similar vehicles, even though a large number of tests may not have been available for a particular model. Preliminary test selection was followed by analysis of test reports to verify that the tests provided necessary information, such as results from accelerometers mounted at undeformed sites like the center-of-gravity and at locations in line with the estimated principal direction of force of the collision. Vehicle-to-barrier tests where barrier load cell information is available were also noted.

Potential tests for analysis were organized into testing groups with consideration given to various parameters such as test type, overlap percentage, vehicle type, engine orientation, and impact speed. The sorting process was necessary to make it possible to study the influence of collision-defining parameters independently. Then tests that are identical (or nearly so), except in the subject parameter, could be compared to determine

the influence of the parameter. The distribution of analyzed passenger vehicle tests is outlined in Table 4.1. Five front-to-rear vehicle-to-vehicle tests were analyzed and are included in the table's totals for both front and rear VTV totals.

TABLE 4.1 Number of Tests Analyzed by Crash Test Description

Vehicle Type	Front				Side	Rear	
	Aligned		Offset/Pole		ITV	ITV	VTV
	VTB	VTV	VTB	VTV			
Passenger	142	26	22	13	33	24	5
Pickup Truck	10						
Sport Utility	14						
Van	15						
TOTAL	181	26	22	13	33	24	5

4.3 DATA PROCESSING AND ANALYSIS

Selected data, both from accelerometers and barrier load cells, were obtained from the indicated web site of the NHTSA and were analyzed to investigate restitution. A spreadsheet was utilized to list test characteristics and results and is included in Table A.1 of the Appendix.

4.3.1 Accelerometer Data

4.3.1.1 Derivation of the Coefficient of Restitution

Efforts focused on obtaining data from accelerometers mounted at the vehicle center-of-gravity and locations in line with the principal direction of force. Other traces, however, were also analyzed to study the influence of accelerometer location. Once downloaded, acceleration traces were first multiplied by the gravitational constant (9.807 m/s^2) to give acceleration in units compatible with integration over time in seconds. The data were then integrated to give velocity as a function of time. Integration was performed using the trapezoidal rule. Because the NHTSA's database reports velocities in kilometers per hour (kph), the velocity traces were converted to kph from meters per second and were then shifted so that the impact speed of the trace matched the reported impact speed. A simple program, VelCalc, was written in the ANSI C programming language to process the data to this point. The listing is included in Appendix B.

Once the velocity traces were obtained in the proper units, their validity was assessed. In the case where multiple similar traces were available, similar traces were compared. It was immediately apparent that some traces were not dependable. The following two criteria were established to sift inaccurate data:

- (1) A trace is not physically reasonable if it indicates that a vehicle regains positive velocity after restitution has reversed its incoming velocity.
- (2) A trace is not physically reasonable if it shows that a vehicle's velocity continues to increase after the restitution period of a collision has ended.

Beyond the application of these two rules, judgement was applied to determine the validity of the data. Figure 4.1 presents a sample case, NHTSA Test 1164, a 50 percent overlap vehicle-to-barrier collision involving a 1987 Hyundai Excel. The figure shows traces from accelerometers mounted at various locations on the vehicle, including primary and redundant accelerometers at the right and left rear seat positions. The center rear seat and rear axle traces were immediately eliminated from consideration since they indicate that after the vehicle decelerates to a negative velocity, it regains a positive velocity, violating the first of the above criteria. Of the remaining four traces, two are nearly a perfect match, while the others give relatively high rebound velocities. The two sets of traces both include data from the left and right rear seat locations. The question at this point was

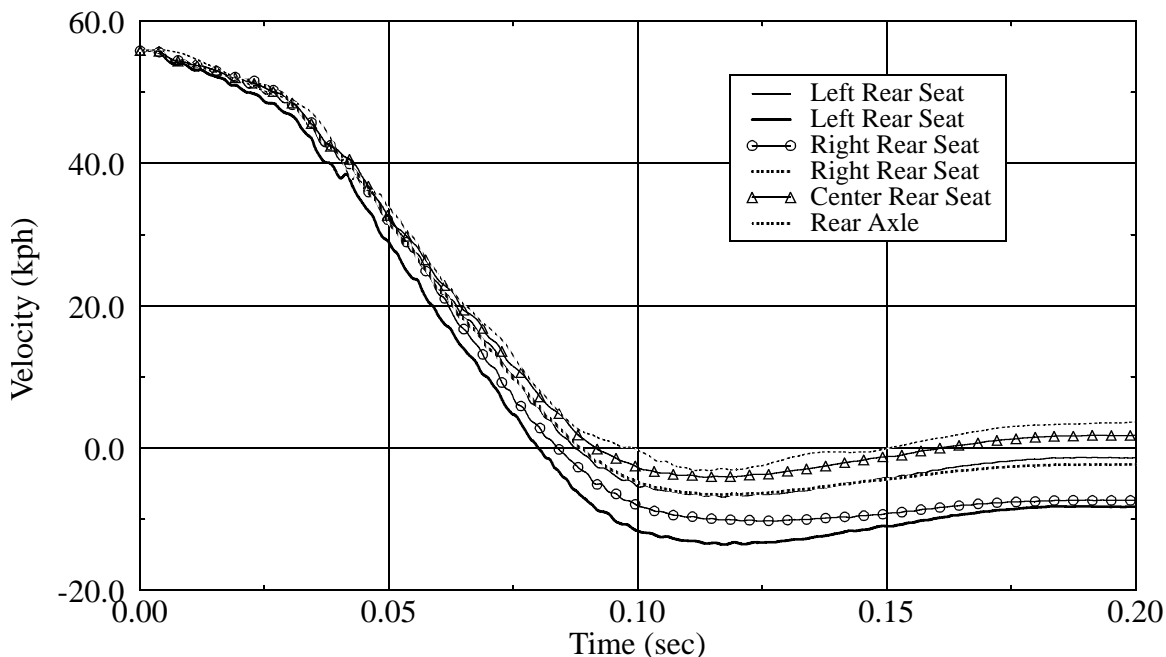


FIGURE 4.1 Velocity v. Time at Various Positions on the Vehicle -- NHTSA Test 1164: 50% Overlap Frontal Vehicle-to-Barrier Collision; 1987 Hyundai Excel

whether the remaining four traces should be averaged or if some of them should be eliminated. It was determined that the two traces giving higher rebound velocity should be eliminated, since the other two traces match so well. Also, if the high rebound velocity traces were included in an average with the other two traces, the resulting coefficient of restitution would be considerably higher than expected values based on the general passenger vehicle population. Thus, the representative trace was given by the average of the two matching traces.

After valid traces had been selected, they were averaged, and the maximum separation velocity was determined and used to calculate the coefficient of restitution for the collision. Impulse center velocities were not directly available because the impulse center represents an average position on the crush face. For central collisions, velocities at the vehicles' center-of-gravity were used to approximate the velocities at the impulse center, consistent with the discussed theory. Where information was available, the coefficient was calculated for multiple locations on the vehicle, and the difference between the coefficient at that location and the coefficient resulting from the trace with the highest maximum separation velocity was noted. Partial-contact barrier collisions and offset pole impacts are generally not central collisions, but analysis showed that rotation was insignificant for these tests. As a result, center-of-gravity velocities were also used to approximate impulse center velocities for these cases. Rotation was significant in many of the analyzed vehicle-to-vehicle, partial-width frontal and impactor-to-vehicle side collisions. For vehicle-to-vehicle, partial-contact frontal cases, data were averaged from accelerometers that were mounted symmetrically (or nearly so) to one another about the line including the vehicle center-of-gravity and parallel to the principal direction of force. Based on the discussion of vehicle rotation in Chapter Three, it is noted here that such averaging cancels the influence of the tangential acceleration due to rotation relative to the center-of-gravity but preserves normal acceleration introduced by rotation. This normal acceleration acts in such a way that, for accelerometers mounted on the side of the center-of-gravity opposite the impact, rebound velocity is reduced. Because the rebound velocity at the impulse center would be enhanced by both tangential and normal acceleration, the calculated coefficient of restitution magnitudes are lower than a more rigorous technique would produce. For side impact cases, the far side rear sill accelerometer was used to estimate the impulse center velocity of the struck vehicle, without averaging the signals of other

accelerometers. Although the right rear sill position is generally quite far from the impulse center in a left-side collision, it is almost always closer to the line of action of force than any of the other accelerometers. For cases with little rotation, this is an accurate representation of impulse center velocity. The impactor's rebound velocity was determined using an accelerometer at its center-of-gravity, which is generally also offset from the line of action of force. Unfortunately, rotation was significant in nearly all of the analyzed side impact cases. As a result, the influence of both tangential and normal acceleration due to rotation are present in the signals, making the results even more of an estimate than the results of the technique described for vehicle-to-vehicle, partial contact frontal cases. This method is also particularly subject to error because it uses only one accelerometer on each vehicle, allowing noisy, and possibly unreasonable, data to be influential. Errors are expected to be larger for cases with higher angular accelerations.

In an effort to determine the magnitude of error associated with the technique discussed for finding rebound velocity in side impact tests, one test was rigorously analyzed. By matching accelerometer data from the test, the impulse center and principal direction of force of the collision were estimated using MOMEX, a vehicle momentum exchange software package developed in conjunction with this study [20]. Using accelerometer-derived velocity traces and accelerometer position information from the test report, and applying rigid body assumptions to the tested vehicle and impactor, rebound velocities at the position of the impulse center and in the principal direction of force were determined. This value was then compared to coefficient magnitude approximated by using velocities derived with the right rear sill and center-of-gravity accelerometers.

The theoretical definition of the coefficient of restitution developed in this thesis requires impulse center velocities of the colliding bodies. The coefficient for tests of each type, except partial-width, vehicle-to-vehicle frontals and impactor-to-vehicle side impacts, was consistently calculated according to the stated definition. Because of rotation, coefficient values for the other two tests types were estimated, not meeting the requirements of the definition.

4.3.1.2 Study of Influential Parameters

In order to determine the influence of vehicle and collision parameters on the coefficient of restitution, coefficient values for different collision types were analyzed separately. In many cases, average coefficient of restitution values were calculated as a

tool in identifying trends in the data. It should be noted, however, that because each vehicle has unique structural characteristics, an average coefficient of restitution is somewhat misleading unless a comparable mix of vehicles is analyzed to determine each compared average value. Vehicle-to-barrier full-frontal impacts at 48 and 56 kph are likely the only cases treated in this thesis where comparable mixes were achieved. When an influential parameter was identified for a particular collision type, its effect was studied to determine why it is influential. The data were then further categorized based on the determined influential parameter to remove its effect from further analysis. This process continued until none of the remaining variables exhibited any visible influence on the coefficient of restitution.

Influential parameters within collision classifications were further researched through case studies. This included analysis of vehicle deformation dynamics for vehicle-to-barrier cases. Dynamic crush face position was estimated by integrating the average velocity trace for a given test, from which maximum crush face penetration was determined. The applicable force-time plot was then analyzed to find the time of vehicle-barrier separation. Using this time, residual crush face position was determined. This value was compared to the reported residual crush face position at the center of the vehicle, where crush is generally most extensive. Because errors due to the velocity of propagation, as discussed in Chapter Three, are not considered to be significant during the restitution phase of the collision, the calculated maximum dynamic crush face penetration was corrected by subtracting from it the difference of the calculated and measured residual values, defined respectively as $C_{r,c}$ and $C_{r,a}$ in Equation 3.9. The corrected dynamic value was then multiplied by 1.33 to determine maximum crush depth. In cases where the engine was engaged, the length of its longitudinal dimension was added to the previous calculation to extend the crush depth. The crush depth result was then used to determine which vehicle components were engaged.

4.3.1.3 Comparison of Vehicle-to-Vehicle Impacts to Vehicle-to-Barrier Collisions

Where vehicle-to-vehicle tests are available that involve vehicles for which barrier tests are also available at comparable velocities, resulting values of the coefficient of restitution were compared. Only full-width cases were considered. Mirror impacts, where identical vehicles collide in an aligned fashion, and collisions involving non-identical vehicles were considered. For non-identical vehicle cases, it was assumed that because

structural differences are not extreme between colliding vehicles in any of the analyzed tests, the barrier equivalent velocity (BEV) for each vehicle could be reasonably approximated by using half the closing velocity of the comparable VTV collision.

The accuracy of the relations presented by Howard and Prasad, as given in Equations 2.7 and 2.8, respectively, was also studied. Even though Howard notes that Equation 2.7 is valid only for low speed collisions, it was considered at high speeds. Effective stiffness, defined by Equation 3.11, was calculated to apply Prasad's expression, with collision force approximated as the product of mass and acceleration.

4.3.2 Barrier Load Cell Data

For selected case studies where vehicle crush was considered, barrier force magnitude traces were also analyzed. Total barrier force as a function of time was simply determined by summing the thirty-six load cell traces. After summing the traces, the result was inspected to determine if it was reasonable (e.g. to make sure the force had a magnitude of zero at the end of the collision). The total force trace was utilized to determine when barrier contact ceased, rather than estimating separation time from the velocity trace. This information was needed to determine what residual crush value was predicted by the deformation trace.

Barrier force data were examined in a variety of other ways to study the magnitude of restorative forces as a function of crush and time. Plots of force and crush energy versus vehicle crush were generated to study the influence of crush depth on barrier forces. Additionally, three-dimensional plots were created to visualize how barrier forces change across the width of the barrier. These additional barrier force studies led to interesting observations that may prove to be useful in the study of restitution. They were, however, determined to be beyond the scope of this thesis. A program was written using ANSI C code, FCFCalc, to manipulate the load cell data to give the described relationships. The code listing is included in Appendix B.

Chapter 5: Frontal Collision -- Crash Test Results and Restitution

In addition to being the most frequent collision type, frontal collisions easily have the highest Directional Priority values at a range of ΔV , as shown in Chapter One, and, as a result, generally receive the most attention in collision research. The same is true of this thesis. In order to understand the behavior of the coefficient of restitution, magnitudes of the coefficient are studied and compared for a variety of collision conditions. Vehicle-to-fixed rigid barrier collisions are first considered, with full-width cases considered first, followed by partial-width cases. Pole impacts are then studied. Following pole impacts, vehicle-to-vehicle collisions, both full-width and partial-width cases, are considered.

5.1 FULL-WIDTH VEHICLE-TO-BARRIER COLLISIONS

The coefficient of restitution for a total of 181 full-width vehicle-to-barrier collisions are presented in Figure 5.1 as a function of impact velocity. Bin averages are also shown for velocity bins where more than one test was analyzed. It should be noted that the lines connecting the bin averages are meaningless, except to locate the averages within the data. The figure combines results from tests on 142 passenger vehicles, 10 pickup trucks, 14 sport utility vehicles, and 15 vans, so averages are largely dominated by passenger vehicle

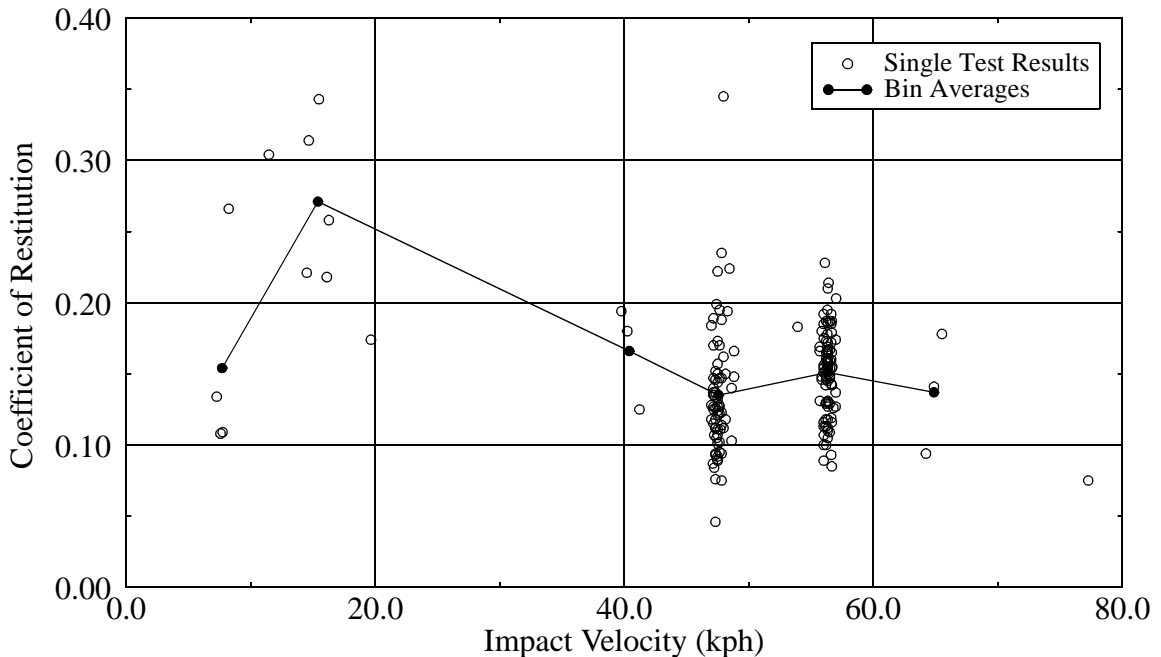


FIGURE 5.1 Coefficient of Restitution v. Impact Velocity -- Vehicle-to-Fixed Rigid Barrier Full- Frontal Collisions; All Vehicle Types

results. It is obvious from the plot that tests at speeds of about 48 and 56 kph (corresponding to 30 and 35 mph), the compliance (FMVSS 208) and New Car Assessment Program (NCAP) velocities, are much more frequent than those at other speeds. Results from tests at speeds other than 48 and 56 kph all involved passenger vehicles.

The results of the figure are generally not surprising as they largely agree with the generally-accepted idea that the coefficient of restitution decreases with increasing impact velocity. The fact, though, that the magnitude of the coefficient of restitution is greater at 56 kph than at 48 kph clearly contradicts the anticipated pattern. Based on the literature, it is clear that the opposite relationship is expected. The data look quite similar to that presented by Prasad, which is no surprise, since he also utilized the NHTSA's crash test database, but he does not note the high coefficient value at 56 kph [11]. The low value of the first bin average is also unexpected. Each of the tests used to obtain the average for the low-velocity bin involved a 1979 Ford LTD, so the average is likely not representative of the general vehicle population. It is anticipated that if more data were available, the average coefficient at such low speeds would be significantly higher, as has been reported in the literature. The results at all velocities, except for 48 and 56 kph, are similarly questionable because of the small amount of data available. With the exception, however, of the lowest velocity bin, the results appear to be reasonable, at least in their expected relationship with the more reliable averages at 48 and 56 kph. Figure 5.1 suggests that the coefficient of restitution, at least on average, is not expected to drop below 0.1 until impact velocities exceed 70 kph. Even though averages are calculated, it is important to realize that different vehicles are expected to have different restitution characteristics. The averages are most useful when averages with similar vehicle mixes are compared, as is the case for the 48 and 56 kph collisions.

To further investigate the behavior of the coefficient, it is necessary to study results associated with individual vehicle types. Bin averages for each vehicle type, as well as the standard deviation associated with each average and the number of tests analyzed for each case, are shown in Table 5.1 at compliance and NCAP impact velocities (48 and 56 kph). The table shows that the average coefficient of restitution at 56 kph is greater, to varying degrees, than that at 48 kph, regardless of vehicle type. The difference is most dramatic for pickup trucks. Coefficient magnitudes are similar throughout vehicle types, excepting a

value of 0.105 for pickup trucks at 48 kph, while the expected coefficient for all other vehicle types at that speed is around 0.135. Standard deviations are on the same order for each case. Influential parameters are investigated by further studying the behavior of the coefficient of restitution within each vehicle type.

TABLE 5.1 Coefficient of Restitution by Vehicle Type at 48 and 56 kph; Vehicle-to-Fixed Rigid Barrier Full-Frontal Collisions

Vehicle Type	FMVSS 208 Compliance Tests (48 kph)			NCAP Tests (56 kph)		
	Avg. ϵ	Standard Deviation	Number of Tests	Avg. ϵ	Standard Deviation	Number of Tests
Passenger	0.139	0.045	53	0.152	0.028	70
Pickup Truck	0.105	0.023	5	0.160	0.036	5
Sport Utility	0.135	0.058	6	0.146	0.026	8
Van	0.131	0.044	7	0.143	0.041	8

5.1.1 Passenger Type Vehicles

To further investigate the behavior of the coefficient, it is necessary to study results associated with individual vehicle types. Figure 5.2 repeats the data from Figure 5.1 that were obtained from tests involving passenger vehicles. In this case, however, the data are further categorized by indicating the engine orientation of the vehicle in each test. The average coefficient of restitution for inline and transverse orientations at compliance and

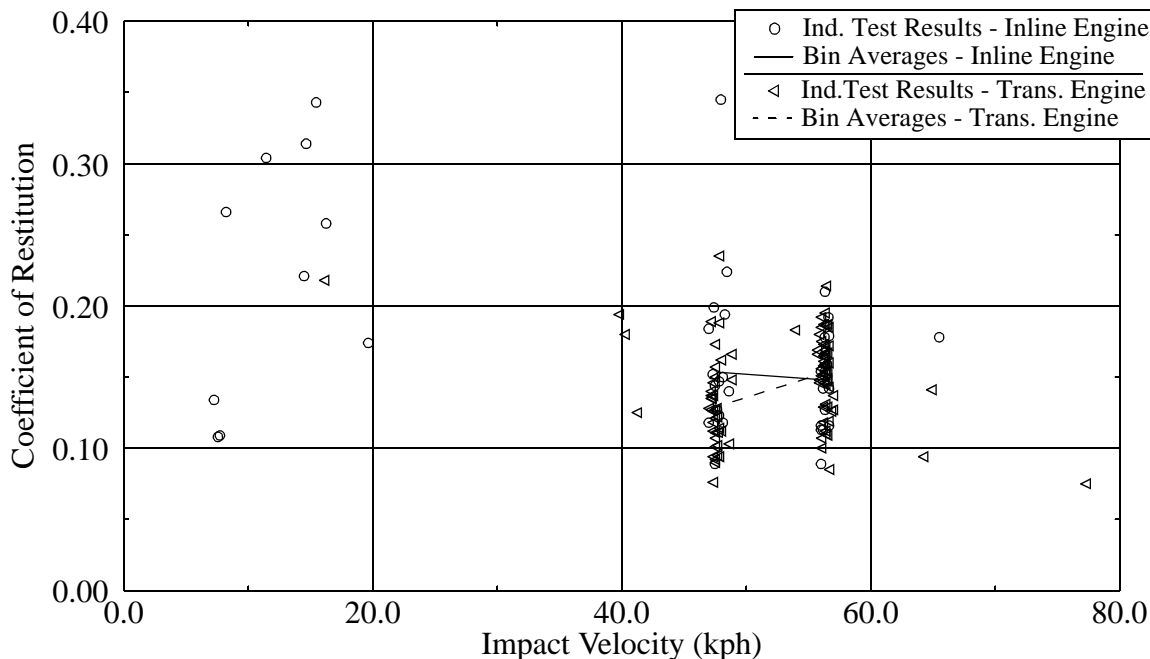


FIGURE 5.2 Coefficient of Restitution v. Impact Velocity -- Vehicle-to-Fixed Rigid Barrier Full-Frontal Collisions; Passenger Vehicles with Both Inline and Transverse Engine Orientations

NCAP impact velocities, where inline means that the engine crankshaft is parallel to the roll axis of the vehicle, are also given in the figure. Of 142 total tests shown in Figure 5.2, 42 involve vehicles with inline engines, with the remaining 100 points representing tests on vehicles with transverse-mounted engines. As in the previous figure, the two averages for each engine orientation are connected with lines to locate the average within the locus of points. The lines themselves are meaningless except at their endpoints.

The figure demonstrates that the effect of engine orientation is significant, at least at the two averaged velocities. This is no surprise since the engine represents a relatively large part of the vehicle mass and is a factor in any collision with enough crush to engage the engine. For transverse-mounted engines, the pattern previously demonstrated, where the coefficient of restitution is higher at 56 kph than at 48 kph, is clearly present. Inline engines, on the other hand, contradict the pattern, appearing to behave according to the theory that the coefficient of restitution decreases as impact velocity increases. The average coefficient of restitution values, again presented with standard deviation and number of points contributing to the average, are given in Table 5.2. Eighty-percent confidence intervals are also shown. Figure 5.2 shows that one reported coefficient value for inline engine 48 kph collisions is exceptionally high relative to other results. It was

TABLE 5.2 Coefficient of Restitution (ϵ), Standard Deviation (σ), Number of Tests, and 80% Confidence Intervals by Engine Orientation at 48 and 56 kph; Vehicle-to-Fixed Rigid Barrier Full-Frontal Collisions; Passenger Vehicles

Engine Orientation	FMVSS 208 Compliance Tests (48 kph)					NCAP Tests (56 kph)				
	Avg. ϵ	σ	No. of Tests	80% Conf. Interval		Avg. ϵ	σ	No. of Tests	80% Conf. Interval	
				Low	High				Low	High
Inline	0.151 (0.164)	0.037 (0.062)	14 (15)	0.138	0.164	0.148	0.035	16	0.136	0.160
Transverse	0.129	0.032	38	0.122	0.136	0.153	0.027	54	0.148	0.158

neglected in primary calculations, but its effect is shown by the results in the table in parentheses. The table shows that both engine orientations result in similar averages for NCAP test velocities. For inline engines, the difference between the average coefficients at the two speeds is 0.003, while the same difference for transverse engines is -0.024. For both engine types, standard deviation values are slightly lower in the 56 kph collisions than in the 48 kph tests. It also true that variance is lower for transverse engine vehicles

than for tests with inline engines at each impact velocity. Confidence interval calculations were included to determine statistical significance in differences between averages. Because so few tests were analyzed involving vehicles with inline engines, a student-t distribution was used to calculate confidence intervals, resulting in large intervals. The average coefficient values at 48 and 56 kph for the inline tests are nearly equal, so it may be impossible, with additional data, to show significant difference between those values, especially with differing vehicle properties. The transverse engine cases, on the other hand, could be approximated with a normal distribution. The eighty-percent confidence intervals in the table show that the average coefficients at the two speeds are significantly different. As a matter of fact, these values can be shown to be significantly different with 99% confidence. The eighty percent intervals in the table demonstrate that the average coefficient values for the two engine types at 48 kph are significantly different. The same cannot be said of the values at 56 kph. It should be noted that because these data were used to create Figure 5.1, the figure is dominated by the influence of transverse-mounted engines.

Considering the dramatic effect of engine orientation on the magnitude of the coefficient of restitution, it is necessary to consider collisions involving vehicles with transverse and inline engines separately.

5.1.1.1 Transverse Oriented Engines

Data taken from full-frontal vehicle-to-barrier collision tests involving passenger vehicles with transverse-mounted engines were further exercised to determine the influence of other collision conditions upon the coefficient of restitution. Among the parameters studied are impact velocity, as previously mentioned, and various vehicle parameters including vehicle mass, engine displacement, vehicle length, vehicle width, wheelbase, distance between the front axle of the vehicle and its center-of-gravity, and vehicle model year. Prasad also performed research on the influence of these parameters on the coefficient of restitution [11]. Variability in coefficient results among contracted test labs and repeatability of the coefficient of restitution for similar collisions are also discussed.

Specific test cases are also analyzed to further investigate broad observations of parameters influencing the coefficient and to allow discussion of specific restitution behavior. Insights gained are useful in understanding general characteristics of restitution.

5.1.1.1.1 Impact Velocity

Figure 5.2 and Table 5.2 clearly establish expected values for the coefficient of restitution at velocities of 48 and 56 kph for passenger vehicles with transverse-mounted engines. Only eight tests outside of the two main impact speeds were available for analysis - one at about 16 kph, three at about 40 kph, one at about 54 kph, two at about 65 kph, and one at approximately 77 kph. They are also plotted in Figure 5.2. Even though there are so few tests that an expected value for the coefficient really cannot be established, it is beneficial to investigate the behavior of the available points. The vehicles tested at these velocities include a 1985 Pontiac Grand Am, a 1984 Chevrolet Cavalier, a 1989 Hyundai Excel GLS, a 1989 Toyota Celica, a 1993 Chevrolet Corsica, two 1980 Chevrolet Citations, and one 1982 Citation, so together they represent a wide variety in the passenger vehicle population. From Figure 5.2, it is apparent that the average coefficients of restitution at these points follow the general rule of decreasing magnitude with increasing impact velocity. Their decrease appears to be approximately linear, with the second half of the points being shifted upward beginning at about 54 kph. Average values for all points, including those at 48 and 56 kph are presented in Table 5.3.

TABLE 5.3 Average Coefficient of Restitution v. Impact Speed -- Vehicle-to-Fixed Rigid Barrier Full Frontal Collisions; Passenger Vehicles with Transverse Oriented Engines

	16 kph	40 kph	48 kph	54 kph	56 kph	65 kph	77 kph
Average Coefficient of Restitution	0.218	0.166	0.129	0.183	0.153	0.117	0.075
Number of Points	1	3	38	1	54	2	1

Another interesting way to view the influence of impact velocity on the coefficient of restitution is by plotting rebound velocity as a function of impact velocity. The coefficient of restitution is the ratio of these two velocities, whose relationship for passenger vehicles with transverse engines is shown in Figure 5.3. Individual test results and bin averages are again presented for the same tests shown in Figure 5.2. It appears that rebound velocity generally increases with impact velocity until it reaches a maximum near 9 kph at an impact velocity of 56 kph. It then decreases with higher impact velocities. The low average coefficient of restitution at 48 kph is due to the low rebound velocity shown in the figure at that speed. The coefficient of restitution boundary lines proposed by Ishikawa, defined in Equation 2.5 and plotted in Figure 2.4, are based upon the premise that rebound velocity is constant no matter what the impact speed [13, 14]. Figure 5.3 challenges the

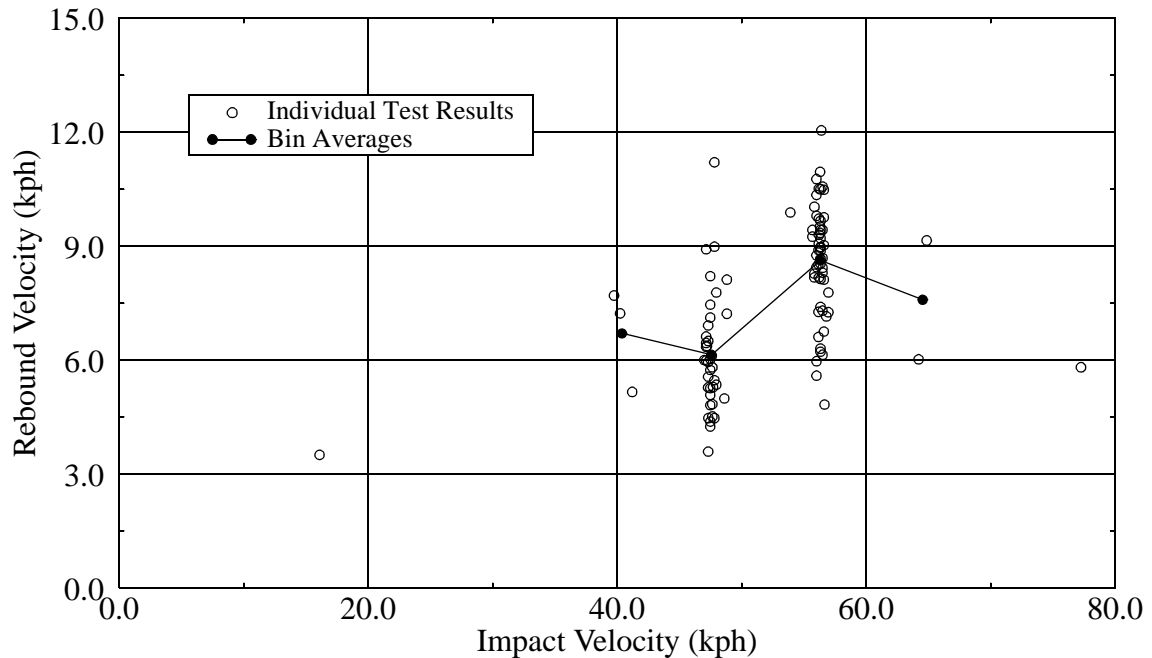


FIGURE 5.3 Rebound Velocity v. Impact Velocity -- Vehicle-to-Fixed Rigid Barrier Full-Frontal Collisions; Passenger Vehicles with Transverse Oriented Engines

validity of that premise. For the data shown, such an approach could only coarsely approximate the value of the coefficient of restitution at the four velocities where averages are presented. Approximations at speeds above and below the averaged values would be even less accurate, especially at the lower velocities, where a small change in rebound velocity causes a large deviation in the coefficient's value.

For a given closing velocity, the change in velocity of a collision, ΔV , increases as rebound velocity increases, so by this measure of collision severity, as the coefficient of restitution increases, the severity of the collision increases also. The influence of restitution on collision severity, however, may more accurately be characterized by considering acceleration during the restitution phase of the collision. The time between zero velocity and maximum rebound velocity, or the duration of phase one restitution as defined in Chapter Three, is shown as a function of impact velocity in Figure 5.4. The duration of the phase one restitution period at an impact speed of 40 kph is significantly less than its duration at the other speeds. Averages are plotted only for the cases where

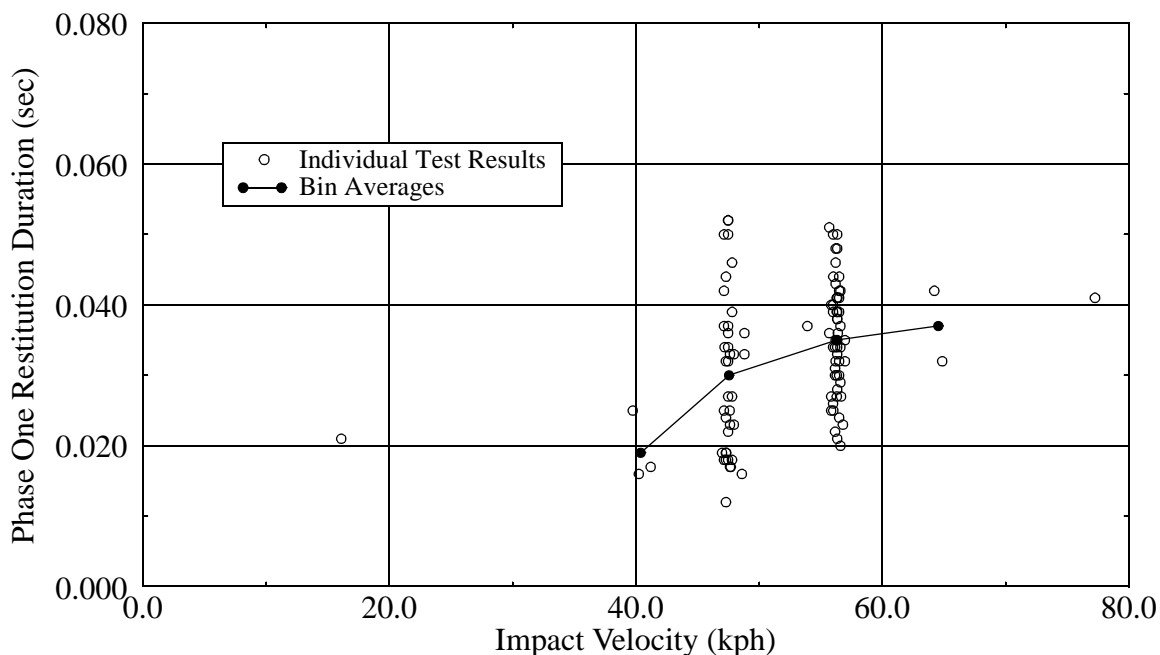


FIGURE 5.4 Phase One Restitution Duration v. Impact Velocity -- Vehicle-to-Fixed Rigid Barrier Full-Frontal Collisions; Passenger Vehicles with Transverse Oriented Engines

more than one test was available. Using these durations and the rebound velocities plotted in Figure 5.3, average accelerations during the first phase of restitution are calculated and plotted as a function of impact velocity in Figure 5.5. Surprisingly, the most severe

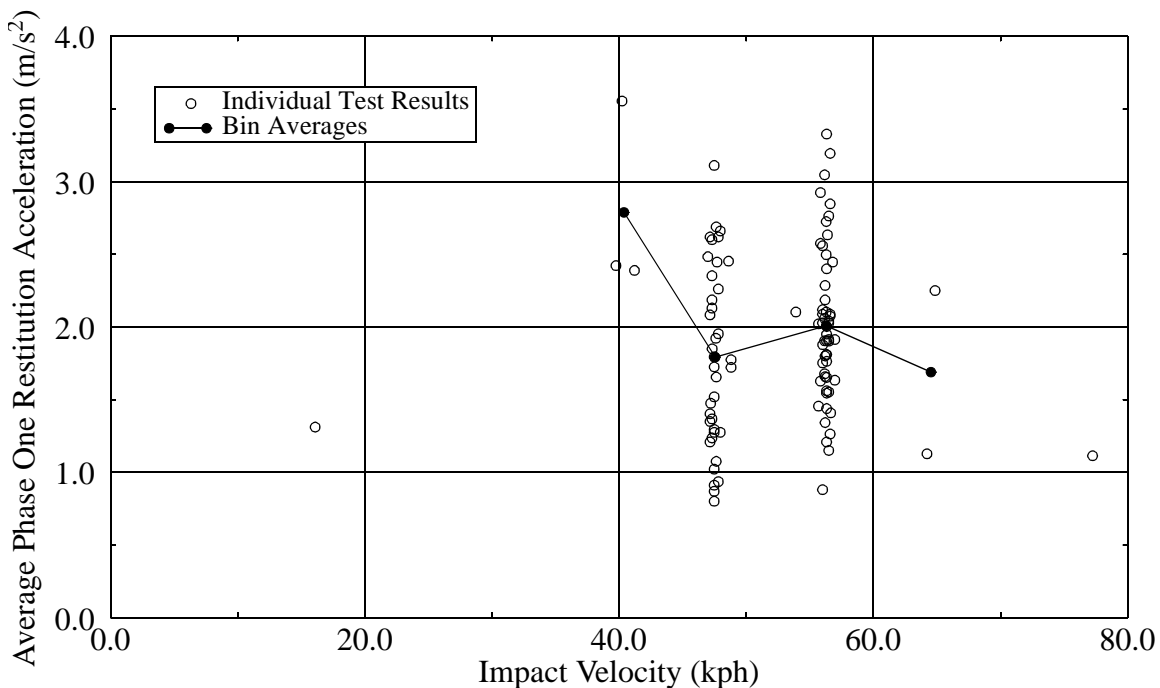


FIGURE 5.5 Average Phase One Restitution Acceleration v. Impact Velocity -- Vehicle-to-Fixed Rigid Barrier Full-Frontal Collisions; Passenger Vehicles with Transverse Oriented Engines

restitution phase acceleration, on average, occurs at 40 kph, and the accelerations at 48, 56, and 65 kph are closely similar in magnitude. Again, though, it is important to note that the results at 40 and 65 kph are based upon only three and two tests, respectively. If the other points on the plot are considered, at 16 and 77 kph, where only one test each was available, it appears that increased acceleration due to restitution is low for low velocities, it increases to a maximum around 40 kph, and then decreases with increasing velocity. It begins again to decrease at higher velocities because restitution time increases while rebound velocity decreases.

5.1.1.1.2 Vehicle Parameters

To satisfactorily determine the influence of the selected vehicle parameters on the coefficient of restitution, it is helpful to eliminate the influence of impact velocity by studying the coefficient magnitudes within the two main velocity bins separately. Figure 5.6(a) shows the coefficient of restitution and calculated averages as a function of vehicle mass within the 48 and 56 kph impact velocity bins. As before, average values are connected by line segments to make it easier to view the averages; the lines themselves are meaningless. As well, averages are calculated only for cases where more than one point resides within a bin. Bin averages are not considered to be statistically sound, since some involve only two or three tests. They are only included to help clarify trends in the data. Based on the figure, there is no visible influence of vehicle mass on the coefficient of restitution for the chosen test cases. Similarly, results are presented in Figures 5.6(b-g) showing the coefficient of restitution as a function of engine displacement, vehicle length, vehicle width, wheelbase, distance between the front axle and the center-of-gravity, and vehicle model year. Bins are 100 kg wide for vehicle mass, 0.5 L wide for engine displacement, 250 mm wide for length, 50 mm wide for width, 100 mm wide for wheelbase, 50 mm wide for distance between front axle and center-of-gravity, and 5 years wide for model year. In each case, except that of vehicle year, the parameters have no visible influence on restitution. In Figure 5.6(b), it appears that engine displacement may be influential in the range of 1.5 to 2.5 L, with the coefficient of restitution increasing with displacement, but the trend does not continue with larger displacements. The influence of vehicle model year is shown in Figure 5.6(g). Based on the population tested, later model vehicles tend to have a slightly higher coefficient of restitution. It appears that vehicle model years from 1985 to 1990 have the lowest average coefficients, with a steady

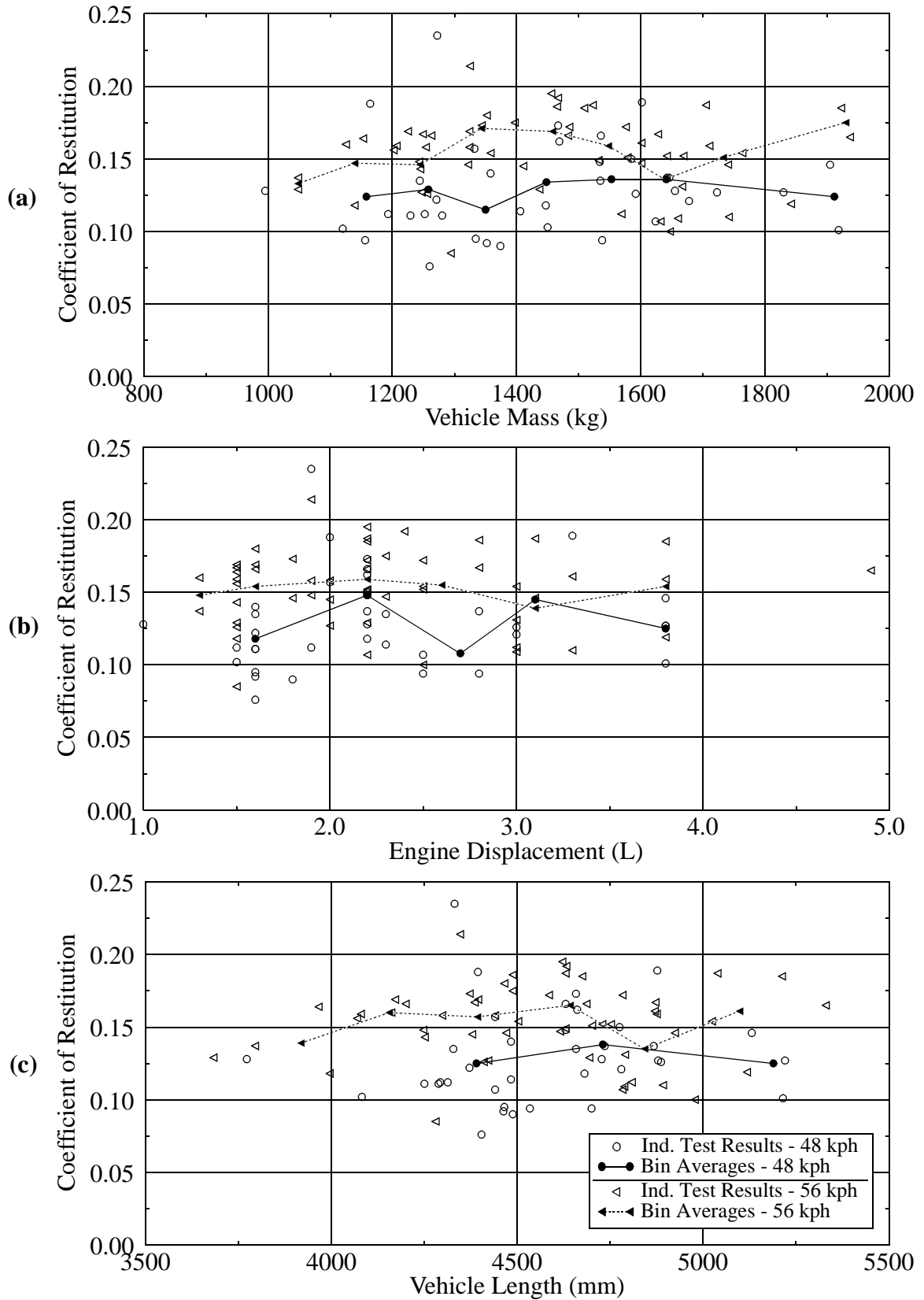


FIGURE 5.6 (a) Coefficient of Restitution v. Vehicle Mass, (b) Coefficient of Restitution v. Engine Displacement, (c) Coefficient of Restitution v. Vehicle Length

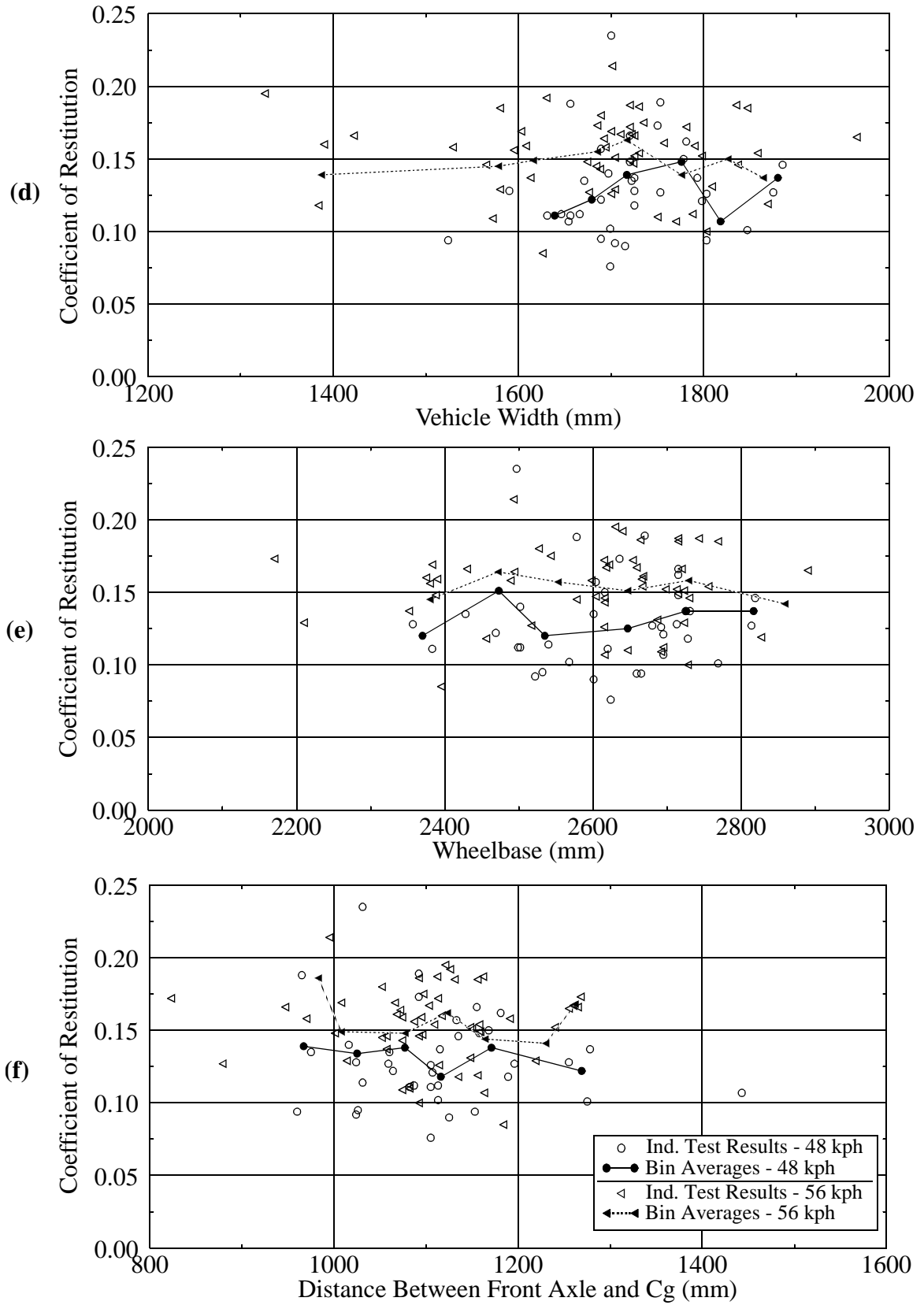


FIGURE 5.6 (cont'd.) (d) Coefficient of Restitution v. Vehicle Width, (e) Coefficient of Restitution v. Wheelbase, (f) Coefficient of Restitution v. Distance Between Front Axle and Center-of-Gravity

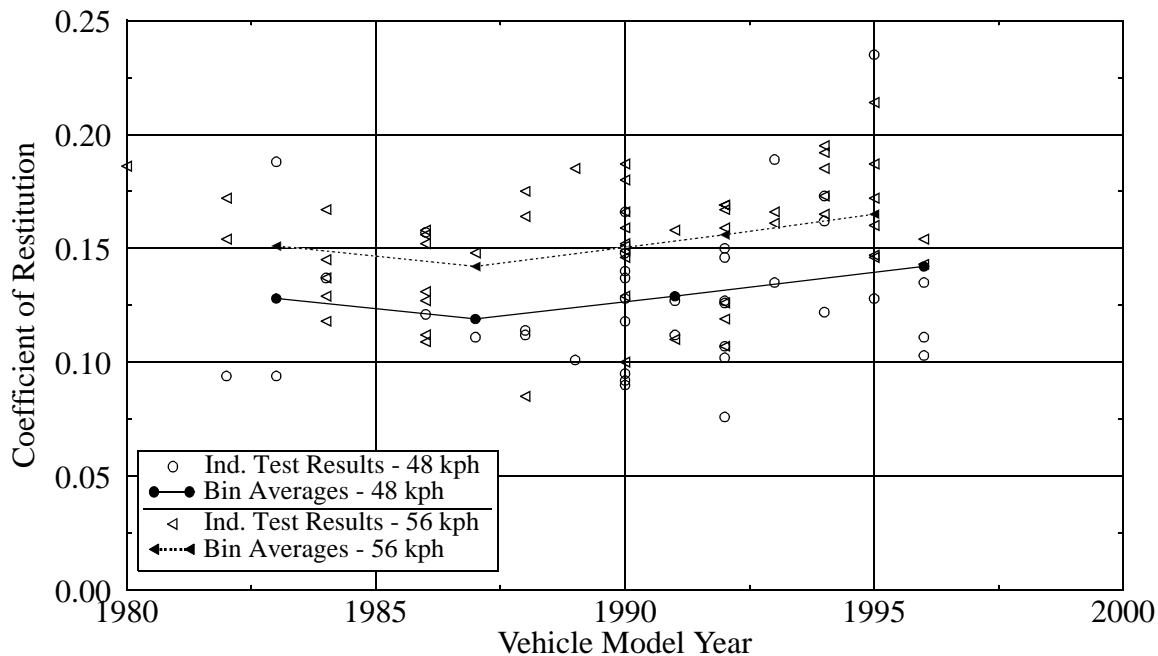


FIGURE 5.6 (cont'd.) (g) Coefficient of Restitution v. Vehicle Model Year

increase of about 0.03 to cars in the latest years. In his study of vehicle parameters on restitution, Prasad agrees that vehicle model year is influential but also reports vehicle width as influential in frontal collisions, as given by Equation 2.2 [11]. Chapter Two states that Prasad performed a multiple-variable regression analysis to reach his conclusions on influential vehicle parameters. Because such analyses were not conducted as part of this study, it is possible that the influence of vehicle width, or one of the other parameters, remains hidden in the data. Following the chosen method of analysis, however, there is no basis for further categorization of the data.

5.1.1.1.3 Test Labs

The crash tests analyzed in this thesis are found in the NHTSA's crash test database, but they are not performed by the government agency. Test labs around the United States receive contracts to perform the tests in behalf of the government. Close analysis of the data reveals that, in some cases, coefficient of restitution results vary significantly between the test labs. Table 5.4 presents the average coefficients, along with applicable standard deviations and the number of tests used to arrive at each average, resulting from tests with impact velocities of 48 and 56 kph. Four of the main test contractors are included: Calspan Corporation, MGA Research Corporation, Mobility Systems, and Transportation

Research Center of Ohio. Averages are not reported for MGA Research and Mobility

TABLE 5.4 Coefficient of Restitution by Test Lab at 48 and 56 kph; Vehicle-to-Fixed Rigid Barrier Full-Frontal Collisions; Passenger Vehicles with Transverse Oriented Engines

Test Lab	Compliance Tests (48 kph)			NCAP Tests (56 kph)		
	Coefficient Average	Standard Deviation	Number of Tests	Coefficient Average	Standard Deviation	Number of Tests
Calspan	0.112	0.021	16	0.145	0.025	25
MGA Research	-	-	3	0.184	0.022	7
Mobility Systems	-	-	2	0.145	0.032	9
TRC of Ohio	0.136	0.023	17	0.157	0.014	11

Systems at 48 kph because so few tests were run. Both Calspan and TRC of Ohio ran a significant number of tests at both speeds. They both report lower average coefficients at 48 kph than at 56 kph, as expected, yet the magnitudes of the coefficients are significantly different. TRC's results are higher than Calspan's for both cases. For 56 kph tests, MGA Research's average is exceptionally high, while Mobility Systems reports results very similar to those of Calspan. It is interesting to note that the standard deviations associated with each contractor are generally lower than 0.032 and 0.027, the values reported for 48 and 56 kph impacts, respectively, in Table 5.2 that are independent of test lab. This result seems to indicate a real difference in results between test labs. Testing procedures for contracted tests are rigorously defined by the NHTSA, so if differences between test labs are as repeatable as they appear to be, they must be a result of some part of the test that is not clearly defined. Through personal communication with both TRC and MGA, it was learned that accelerometer mounting procedures are not specified by NHTSA [21, 22]. The two companies' techniques seem to be quite similar, but perhaps this is one of the sources of the difference manifest in the data.

5.1.1.1.4 Repeatability

Variability in coefficient of restitution data is expected due to the complex nature of automobile impact and varying automobile properties. Coefficient values have been shown to vary because of differences in collision and vehicle parameters. Expected variability is difficult to quantify because variability in crash test instrumentation is generally inseparable from any variability in the actual behavior of the coefficient. Table 5.2 reports average coefficient of restitution values of 0.129 and 0.153 for passenger vehicles with transverse-mounted engines at the two main impact speeds. Their respective standard

deviations, from sets of 38 and 54 tests, are 0.032 and 0.027, respectively. The previous section, discussing discrepancies between test labs, demonstrates that the variance in the data is significantly reduced when data from one lab is considered. Table 5.4 gives standard deviations of 0.021 and 0.023 for Calspan tests and TRC tests, respectively, at 48 kph. Standard deviations for the various test labs for crashes at 56 kph range from 0.014 to 0.032, with an average deviation similar to those reported for the 48 kph tests. From these results, it appears that, for passenger vehicles with transverse-mounted engines in full frontal barrier collisions, a standard deviation of about 0.025 is expected in the magnitude of the coefficient of restitution, regardless of vehicle model.

5.1.1.1.5 Case Studies

To further investigate the characteristics of restitution, crash tests involving two specific vehicles are analyzed, the Ford Taurus, model years 1992 and 1996, and the 1982-1984 Chevrolet Celebrity. Two vehicles are studied because barrier data from tests at both 48 and 56 kph are necessary to study some aspects of restitution. This information is available for the Celebrity. The Taurus does not satisfy this requirement because of some barrier load cell errors in one of its tests, but it is still studied to a limited extent as representative of late model vehicles.

1992-1996 Transverse Engine Ford Taurus

Crash test information and results for five full-frontal fixed rigid barrier crash tests involving the 1992 and 1996 Ford Taurus are outlined in Table 5.5. The table includes test number, structure model year, contracted test lab, and number of accelerometers averaged to obtain the representative trace and their locations. Test velocities and the calculated coefficient of restitution are also included. Each vehicle has a transverse oriented engine.

TABLE 5.5 Test Description and Restitution Results for Five Vehicle-to-Fixed Rigid Barrier Full-Frontal Tests Involving the 1992-1996 Ford Taurus with a Transverse Oriented Engine

NHTSA Crash Test No.	Model Year	Test Lab	Accelerometers		Impact Velocity (kph)	Maximum Rebound Velocity (kph)	ϵ
			No. Avg'd.	Location			
1777	1993	TRC	2	right, left rear seat	47.15	5.99	0.127
1899	1993	Calspan	3	right, center, left rear seat	47.31	5.95	0.126
2450	1996	Calspan	2	right, left rear seat	48.60	4.99	0.103
1890	1993	TRC	4	right(2), left(2) rear seat	56.30	8.96	0.159
2312	1996	TRC	4	right(2), left(2) rear seat	56.50	8.69	0.154

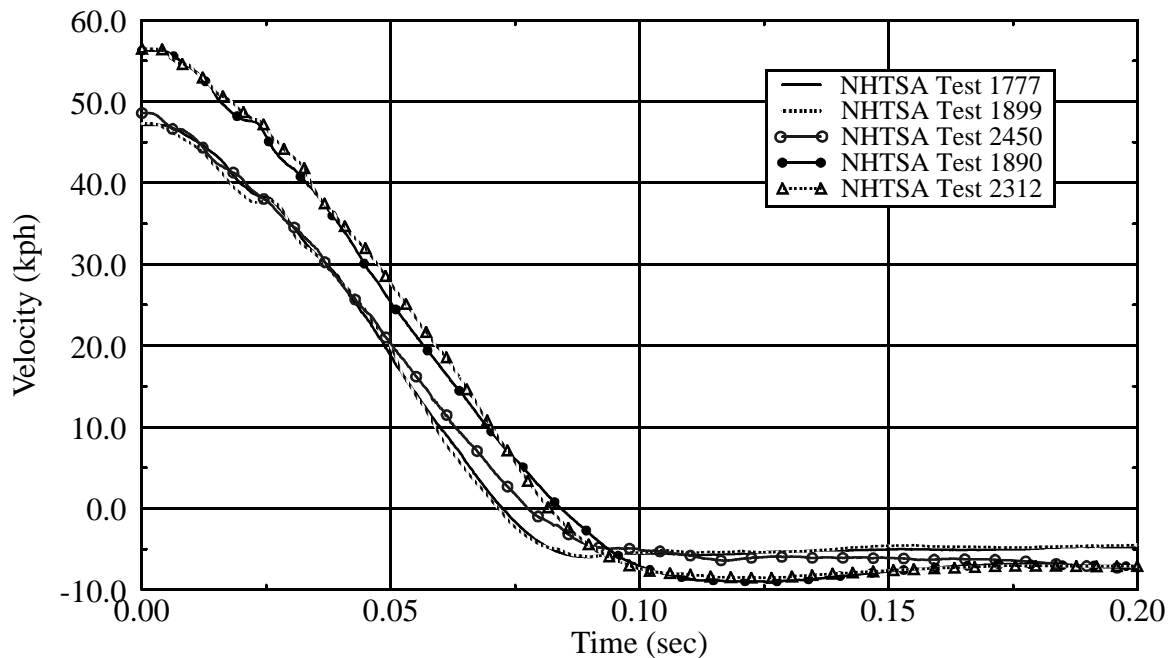


FIGURE 5.7 Velocity v. Time -- Five Vehicle-to-Fixed Rigid Barrier Full-Frontal Crash Tests Involving the 1992-1996 Ford Taurus

Velocity traces for the tests are shown in Figure 5.7. According to the Hollanders Interchange Manual [23], the Ford Taurus structure remained unchanged for model years 1992-1995 and for 1996 to present. Three tests, two of which involve the 1992 structure, were performed at impact velocities of approximately 48 kph, while two tests, one from each structure group, were completed at 56 kph. Both structure groups were analyzed together because of the similarity of the 56 kph traces. The figure shows that the traces for two tests at each speed are virtually identical, but test 2450 does not match the other two traces at 48 kph very well. It is a difficult trace to analyze in terms of restitution, because, according to the data, rebound velocity continues to increase even after the impulse has ended. In order to calculate the coefficient of restitution for this trace, rebound velocity was taken at about 90 ms into the collision. The fact that rebound velocity continues to increase is an indicator that something went wrong with the instrumentation during the test, but it is difficult to know to what extent differences from the other tests are due to instrument error and how much they are due to actual vehicle behavior. Even though test 2450 exhibits notable differences in comparison to the other tests, the differences are not extreme enough to warrant its elimination from analysis.

As is the case for the overall analysis of passenger vehicles with transverse engines, the coefficient of restitution for the Taurus is higher at 56 kph than at 48 kph. In this case, the difference between the coefficient magnitudes at the two speeds is around 0.030. For the overall case, the difference between the values reported in Table 5.2 is 0.024, so the difference between the coefficients for the Taurus is similar to that in the overall study. When test 2450 is not considered, the remaining two tests at each speed indicate a very high repeatability, if repeatability can really be measured for just two tests. Differences between coefficients at 48 and 56 kph are 0.001 and 0.005, respectively. For this case study, there is no noticeable variation in results for tests performed by Calspan in comparison to those conducted by TRC.

It should be noted here that, for the presented tests, traces from individual accelerometers used in the same test differ from one another by small amounts, giving coefficients of restitution magnitudes that differ by as much as 0.037 in the case of test 1890. Differences, however, between right, center, and left-mounted accelerometer traces are not consistent from test to test, so variation between them is attributed to instrumentation error rather than location-related vehicle dynamics. The fact that repeatability of the average of the traces for each test is high when there is still significant variation in individual accelerometers within the same test is an indication that the coefficient of restitution is the same for identical vehicles and test conditions. It illustrates the importance of averaging results from multiple accelerometers to minimize instrumentation error.

In order to investigate the pattern of a higher coefficient of restitution at 56 kph than at 48 kph, it is useful to integrate the velocity traces to determine the magnitude of dynamic crush. Two representative tests were chosen for analysis, since, excepting test 2450, tests at the same velocities are nearly identical. Tests 1899 and 1890, with impact velocities of

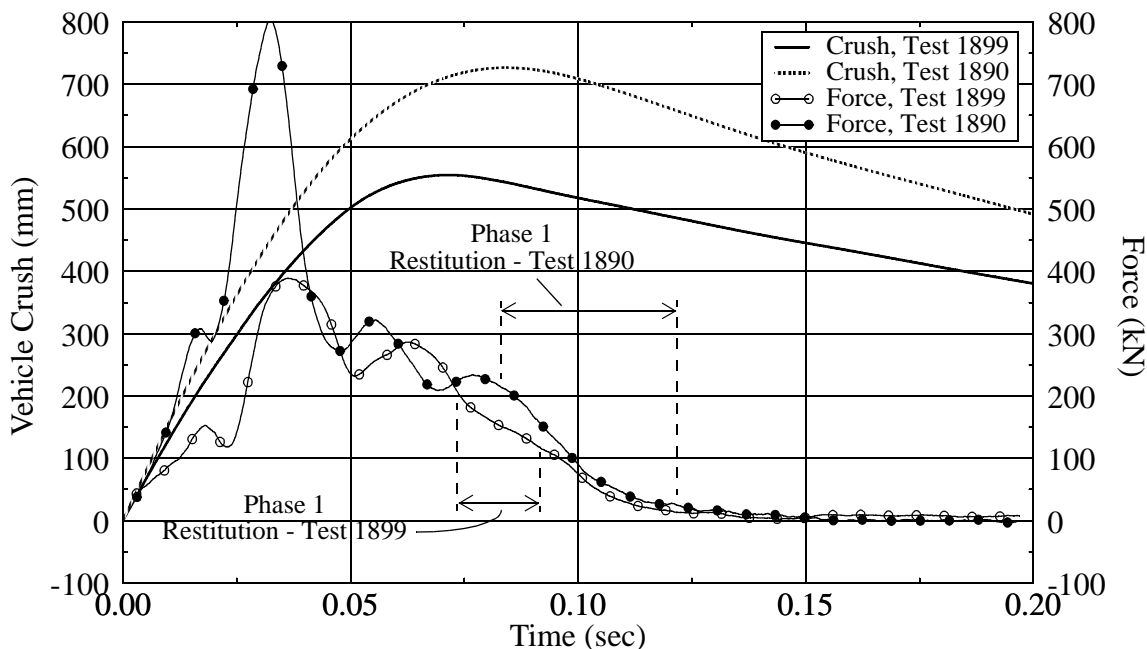


FIGURE 5.8 Vehicle Crush, Barrier Force v. Time -- NHTSA Tests 1899, 1890: Vehicle-to-Fixed Rigid Barrier Full-Frontal Tests Involving the 1993 Ford Taurus

47.15 and 56.50 kph, respectively, are integrated and shown in Figure 5.8. The plot is only representative of crush until the vehicle separates from the barrier. As expected, higher impact velocities result in more extensive crush. Maximum dynamic crush face depths for the two tests, measured at the end of the crash phase and prior to the restitution phase of the collision, are 554 and 727 mm. In order to determine residual crush values for each case, it is necessary to know the time when the vehicle separates from the barrier. The figure also shows barrier force as a function of time for the two tests. Each force trace has been smoothed by calculating running averages at every 50 data points. Separation from the barrier occurs when all barrier forces cease, which for test 1890 occurs around 0.155 seconds. For test 1899, the trace reaches zero and then becomes positive again. This is a result of bad data in some of the load cells, but the zero-force time can be estimated as 0.14 seconds. Analysis of the velocity traces presented in Figure 5.7 shows that phase one restitution extends from 72 to 90 ms for Test 1899 and from 84 to 123 ms for Test 1890, meaning that the duration of the period is twice as long in the 56 kph collision than in the 48 kph test. These intervals are included in Figure 5.8 to allow easy identification of the forces present during the periods. It is apparent that the barrier forces at the end of phase one restitution are significantly higher for the 48 kph test than for the 56 kph collision. The two periods are expected to end with approximately the same force, since phase one

restitution ends when friction forces exceed barrier forces. The figure suggests that there are dramatically different friction forces between the tests, but that cannot be the case. The Taurus has a mass of about 1700 kg, so even for an approximation of the coefficient of friction of 1.0, the friction force will not exceed 17 kN. It is, therefore, concluded that the magnitudes of the load cell traces, especially in Test 1899, are in error, although their timing seems accurate based on comparison to similar tests. It is, however, clear from Figure 5.9 that restitution forces are sustained longer in the 56 kph collision than in a 48 kph crash.

Using the times determined for vehicle-barrier separation and the crush data of Figure 5.8, residual crush face depth is found to be 459 and 580 mm for tests 1899 and 1890, respectively. Measured residual crush values found in the test reports at the lateral centers of the vehicles are 318 and 482. Based on the conclusion of the influence of the velocity of propagation in Chapter Four, derived maximum dynamic crush face depth is reduced by the magnitude of the difference between the calculated and measured residual crush values, giving corrected maximum dynamic crush values of 413 and 627 mm for the two tests.

Knowledge of vehicle maximum dynamic crush and vehicle dimensions reveals what vehicle components were engaged during a collision and sheds light on why restitution forces are generally more significant in collisions at 56 kph than at 48 kph. In a technical paper written in 1997, Denis P. Wood and Stephen Mooney discuss the influence of dynamic crush depth on vehicle stiffness [19]. They report that, for full-frontal barrier collisions, among other collision types, force transitions (from one approximately constant force to another) occur at crush depths 75% of the distance to the front of the engine and to the front of the occupant compartment, or cowl panel, from the front of tested vehicles. The accuracy of the observation of Jones *et al* discussed in Chapter Three for automobiles is not established beyond the work of Wood *et al*, but using the observation, they determine that the front portion of a vehicle may be characterized by three constant stiffness crush zones, made up of the portion of the vehicle in front of the engine, the engine and rear front structure, and the occupant compartment. They find stiffness to be highest in the engine and rear front structure zone.

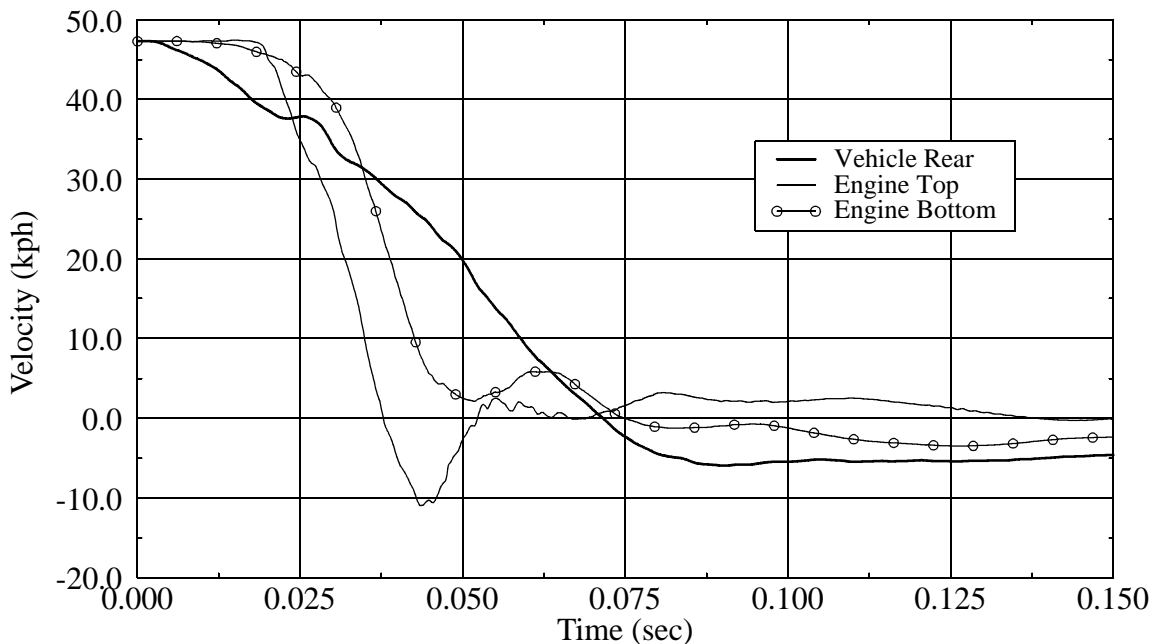


FIGURE 5.9 Velocity v. Time at Vehicle Rear and Engine -- NHTSA Test 1899: Vehicle-to-Fixed Rigid Barrier Full-Frontal Involving the 1993 Ford Taurus

Measurement of a transverse engine Ford Taurus from the years 1992-1995 gives about 570 mm to the front of the engine from the front of the bumper and about 1215 mm to the cowl panel from the front of the bumper, two depths of force transition identified by Wood *et al.* The longitudinal dimension of the engine is approximately 381 mm. Applying the "75% rule" to the calculated corrected maximum crush face penetrations of 413 and 627 mm gives crush depth values of 551 and 836 mm for the 48 and 56 kph collisions, respectively. This indicates that the depth of crush for the 48 kph case approximately reached the region of the front of the engine. A close look at the dynamics of the engine, however, illustrated in Figure 5.9, indicates that the engine was engaged fairly early in the collision. The error in the penetration estimate is potentially a result of inaccurate residual measurement values, but it is more likely that the validity of the "75% Rule" is questionable. Therefore, it is concluded that crush in the 48 kph collision engaged the engine, extending the crush depth by the longitudinal dimension of the engine, and pushed the engine back a small distance before restitution occurred, as shown by the diagram of Figure 5.10. It is unlikely, however, that any contact with the cowl panel region occurred. Because the crush in the 56 kph collision obviously engaged the engine, the longitudinal dimension of the engine is added to 836 mm to give a total penetration of 1217 mm, a depth nearly equal to the distance to the cowl panel. These calculations, along with the

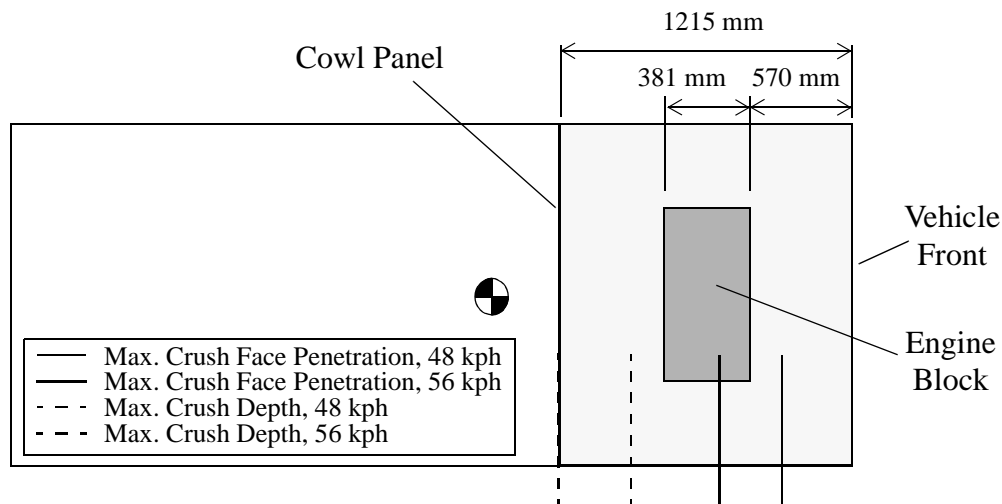


FIGURE 5.10 Crush Approximations -- NHTSA Tests 1899, 1890: Vehicle-to-Fixed Rigid Barrier Full-Frontal Tests Involving the 1993 Ford Taurus

presented fact that the coefficient of restitution is repeatably higher at 56 kph than at 48 kph, suggest that the relatively high restitution at 56 kph is due to higher restorative forces in the cowl panel region than at the depth where crush engaged the engine but was not deep enough to push the engine into the cowl panel.

1982-1984 Transverse Engine Chevrolet Celebrity

In a study related to that presented for the Ford Taurus, the 1982-1984 Chevrolet Celebrity with a transverse oriented engine was also analyzed. Crash test information, including contracted test lab and number of averaged accelerometers and their locations, is outlined in Table 5.6 for three vehicle-to-fixed rigid barrier full-frontal collisions involving the Celebrity. Calculated coefficient of restitution values for the tests are also included. Velocity traces corresponding to the tests are included in Figure 5.11. The Hollander's Interchange Manual reports that the Celebrity structure remained the same through the

TABLE 5.6 Test Description and Restitution Results for Three Vehicle-to-Fixed Rigid Barrier Full-Frontal Tests Involving the 1982-1984 Chevrolet Celebrity with a Transverse Oriented Engine

NHTSA Crash Test No.	Model Year	Test Lab	Accelerometers		Impact Velocity (kph)	Maximum Rebound Velocity (kph)	ϵ
			No. Avg'd.	Location			
776	1983	TRC	4	right (2), left (2) rear seat	47.80	4.47	0.094
451	1982	Dynamic Science	2	left rear floor; cg	56.33	9.67	0.172
688	1984	Calspan	2	left rear seat; cg	56.33	9.43	0.167

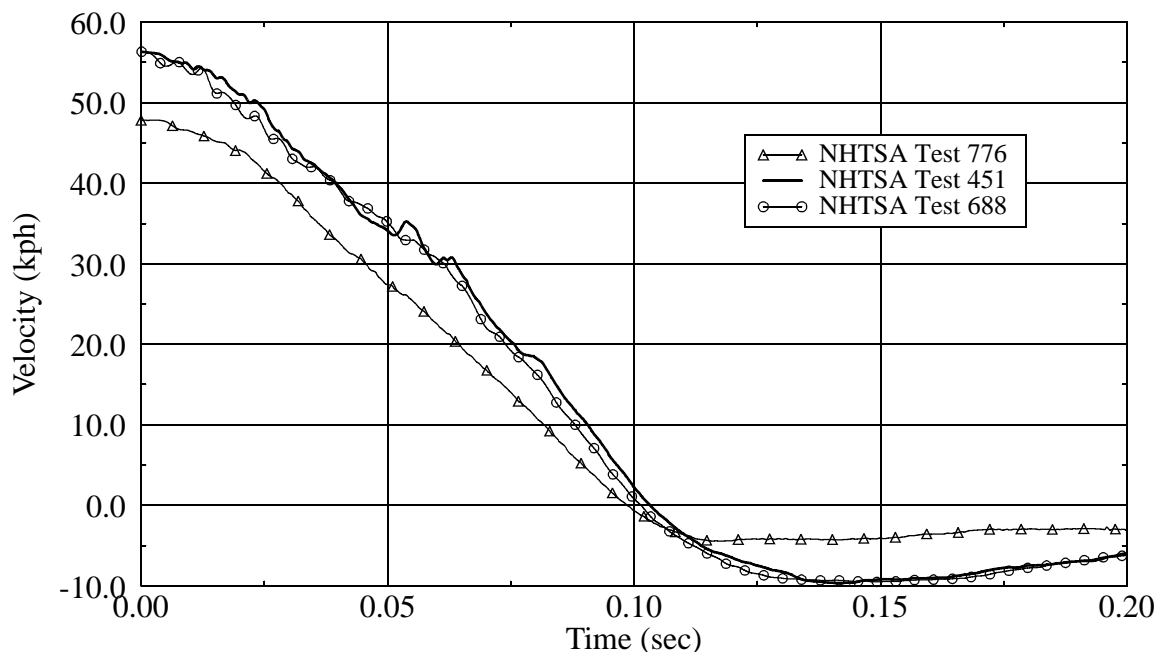


FIGURE 5.11 Velocity v. Time -- Three Vehicle-to-Fixed Rigid Barrier Full-Frontal Crash Tests Involving the 1982-1984 Chevrolet Celebrity

years 1982-1985 [23]. Two tests are presented at 56 kph, while only one test was available at 48 kph. Figure 5.11 shows that, except for some noise, the two traces at 56 kph are very similar, as their coefficient of restitution magnitudes reported in Table 5.6 attest. As is the case with Taurus, it is again apparent that there is a significant difference between the magnitudes of the average coefficient of restitution at 48 and 56 kph. For these Celebrity cases, however, the difference is much higher than the overall case, 0.076 compared to 0.024. Repeatability, at least at 56 kph, is again quite good, as coefficient values vary only by 0.005. It should be noted that each test was performed by a different contractor, but it is impossible to tell if the test lab variable contributes to variation in these tests.

Coefficients of restitution calculated from individual traces within the same test vary by as much 0.067 in the case of test 451, but errors in accelerometers located at the vehicle rear average out such that results from the two 56 kph tests are quite similar.

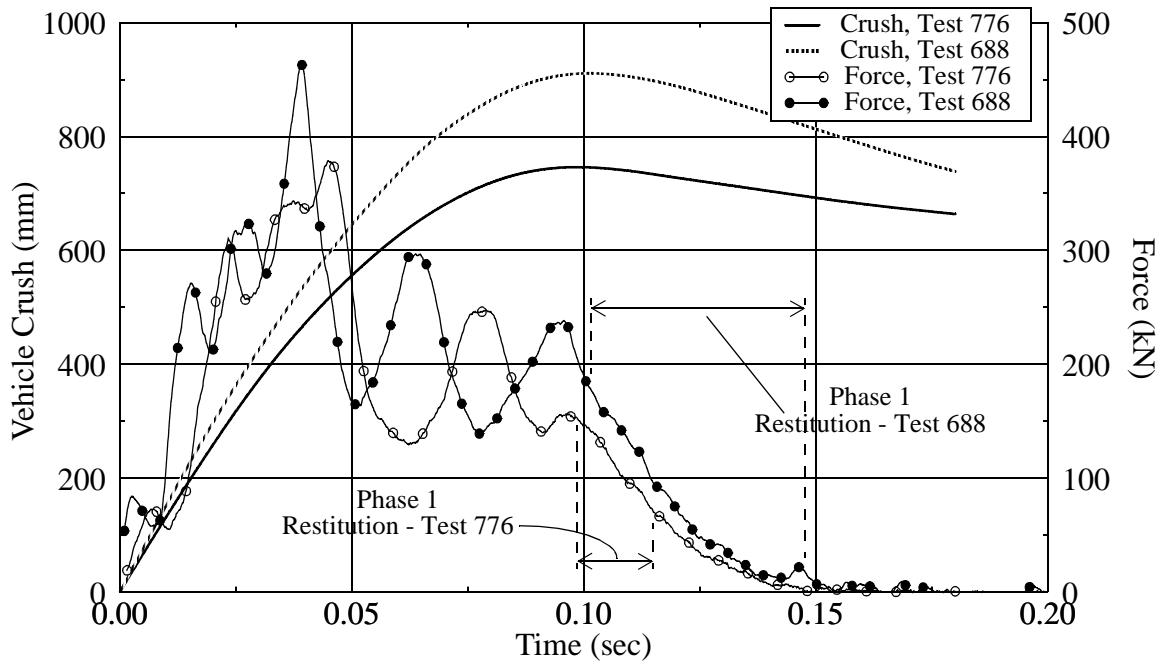


FIGURE 5.12 Vehicle Crush v. Time -- NHTSA Tests 776, 688: Vehicle-to-Fixed Rigid Barrier Full-Frontal Tests Involving the 1983-1984 Chevrolet Celebrity

As a part of the process of determining the maximum dynamic crush for the tests, integrated velocity traces, or vehicle dynamic crush, are plotted in Figure 5.12 for tests 776 and 688. Maximum dynamic crush face depths from the plotted data are 746 and 911 mm. Smoothed barrier load cell data for each of the tests are also included in the figure. It is estimated that the vehicle in test 776 separates from the barrier at about 0.150 seconds, while separation time in test 688 is at about 0.155 seconds. Analysis of the velocity traces for these tests reveals that phase one restitution for Test 776 begins at 99 ms and ends at 117 ms, while it extends from 101 to 149 ms in Test 688, as indicated in Figure 5.12. Again, the period in the 56 kph test is well over twice its length in the 48 kph test. Although not to the extent of the Taurus case, these force traces also give different values of force at the end of the phase one restitution period. The differences are again largely attributed to error in the barrier load cell signals.

Using the vehicle-barrier separation times and crush data given in Figure 5.12 leads to derived residual crush face values of 692 and 800 mm. Measured residual crush values for the lateral center of the vehicle are reported to be 566 and 736 mm, resulting in corrected maximum dynamic crush face depths of 620 and 847 mm for tests 776 and 688, respectively.

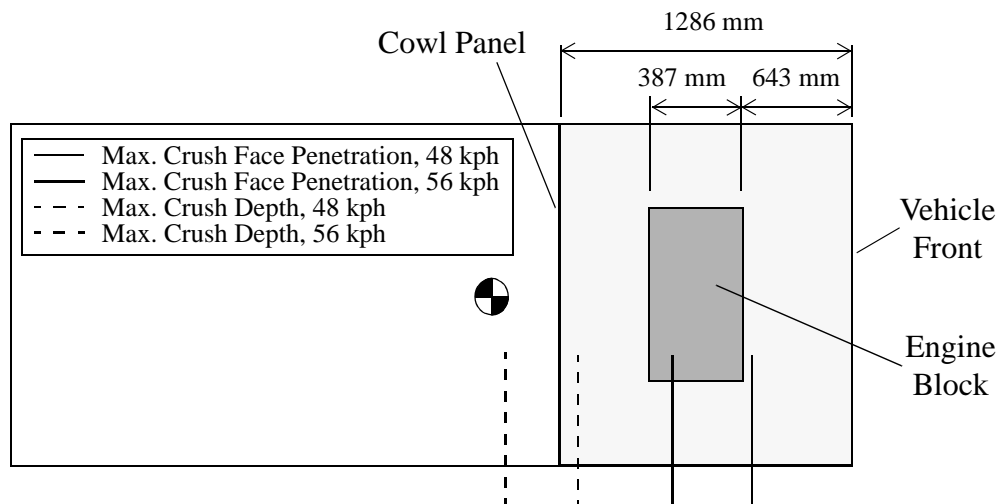


FIGURE 5.13 Crush Approximations -- NHTSA Tests 776, 688: Vehicle-to-Fixed Rigid Barrier Full-Frontal Tests Involving the 1983-1984 Chevrolet Celebrity

For the Celebrity, the distances from the front of the car to the front of the engine and to the cowl panel region are 643 and 1286 mm, respectively, as shown in Figure 5.13. The longitudinal dimension of the engine is 387 mm. Applying the "75% rule" approximates that the 48 kph test results in a penetration of 827 mm, a distance between the front of the engine and the cowl panel. Because crush was determined to be deeper than the front of the engine, it was engaged by crush, extending the crush depth to about 1214, just short of the distance measured to the cowl panel region. The 56 kph test is calculated to have penetrated a distance of 1129 mm, placing it just short of penetrating the occupant compartment. When the engine dimension is added, however, the penetration distance grows to 1516 mm, such that crush penetrated the cowl panel.

5.1.1.2 Inline Oriented Engines

Similar to the analysis performed in studying restitution in passenger vehicles with transverse-mounted engines, restitution in vehicles with inline engines is considered. The influence of impact velocity, vehicle parameters, and repeated impacts, along with variability in test lab results and repeatability are investigated. A case study of tests involving a 1993 Ford Taurus with an inline engine is also presented.

5.1.1.2.1 Impact Velocity

Data from Figure 5.2 that pertain to vehicles with inline-oriented engines are repeated in Figure 5.14. The applicable portion of Table 5.2 is also repeated in Table 5.7, summarizing the results of the figure. Individual tests, as well as bin averages at the compliance (FMVSS 208) and NCAP impact velocities are reported. As is noted previously for vehicles with inline engines, the pattern of higher restitution at impact velocities of 56 kph than at 48 kph is not seen. Rather, the coefficient of restitution

TABLE 5.7 Coefficient of Restitution at 48 and 56 kph; Vehicle-to-Fixed Rigid Barrier Full-Frontal Collisions; Passenger Vehicles with Inline Engine Orientation

FMVSS 208 Compliance Tests (48 kph)			NCAP Tests (56 kph)		
Coefficient Average	Standard Deviation	Number of Tests	Coefficient Average	Standard Deviation	Number of Tests
0.151	0.037	14	0.148	0.035	16

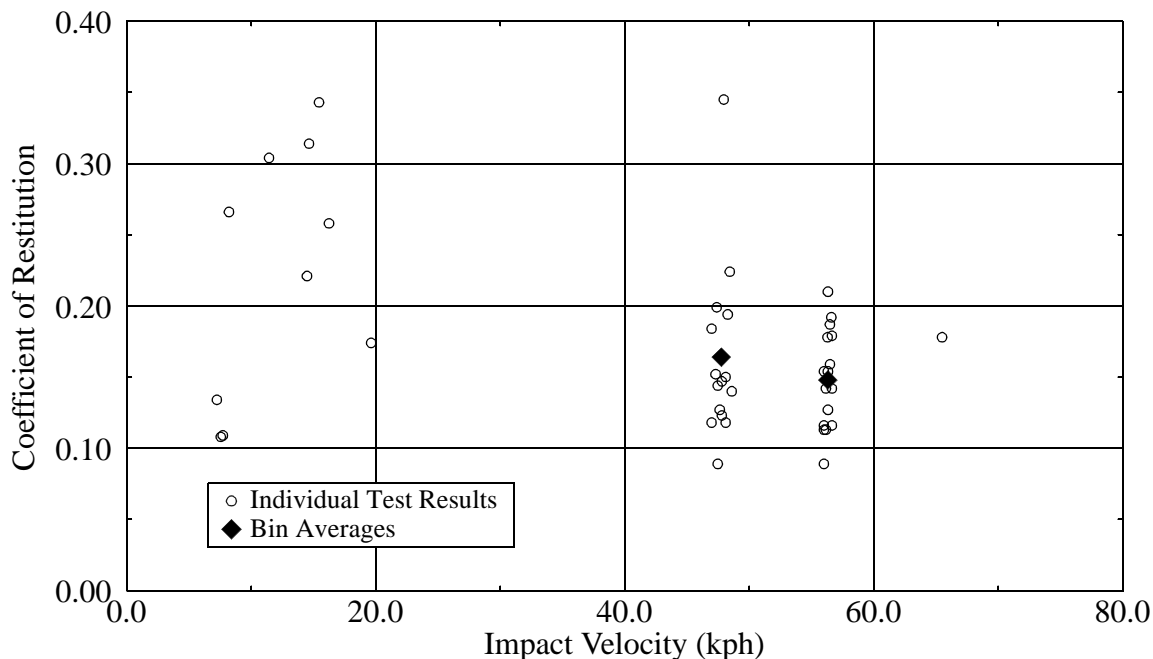


FIGURE 5.14 Coefficient of Restitution v. Impact Velocity -- Vehicle-to-Fixed Rigid Barrier Full-Frontal Collisions; Passenger Vehicles with Inline Engine Orientation

generally decreases with increasing impact velocity. Coefficient values reported at lower speeds in the figure, except for the unexpectedly low LTD values, also generally decrease with increasing impact velocity.

Plots of rebound velocity, restitution time, and average restitution acceleration, all as a function of impact velocity, are presented in Figure 5.15. Figure 5.15(a) indicates that rebound velocity increases with impact velocity, contrary to the same plot, Figure 5.3, for vehicles with transverse oriented engines, which shows that rebound velocity reaches a maximum and then begins to decrease. It is expected that if more data were available at higher speeds for the inline case, it would give similar results, but no data are available to support such a conclusion. Comparing Figure 5.15(b) to Figure 5.4, it is evident that average restitution times for both engine orientations are similar at 56 kph but significantly different at 48 kph. For transverse engines, the average restitution time at 48 kph is 0.040 seconds versus 0.030 seconds shown in Figure 5.15(b). According to Figures 5.15(c) and 5.5, average acceleration during the restitution period is similar for inline and transverse engines at the well documented impact velocities. Accelerations at other speeds really can't be compared because of lack of data.

5.1.1.2.2 Vehicle Parameters

As is shown for vehicles with transverse engines, a variety of vehicle parameters were also tested for their influence on the coefficient of restitution for vehicles with inline engines. The parameters' affects on the coefficient for inline engines are established in Figure 5.16. Similar bin sizes are utilized for averaging as for the transverse cases. Plots of the coefficient of restitution as a function of vehicle mass, engine displacement, vehicle length, vehicle width, wheelbase, distance between the front axle and center-of-gravity, and vehicle model year are shown in Figure 5.16(a-g). As was the case for transverse oriented engines, the coefficient of restitution for the inline engine cases shows no visible reliance upon any of the vehicle parameters, except for vehicle model year. The influence

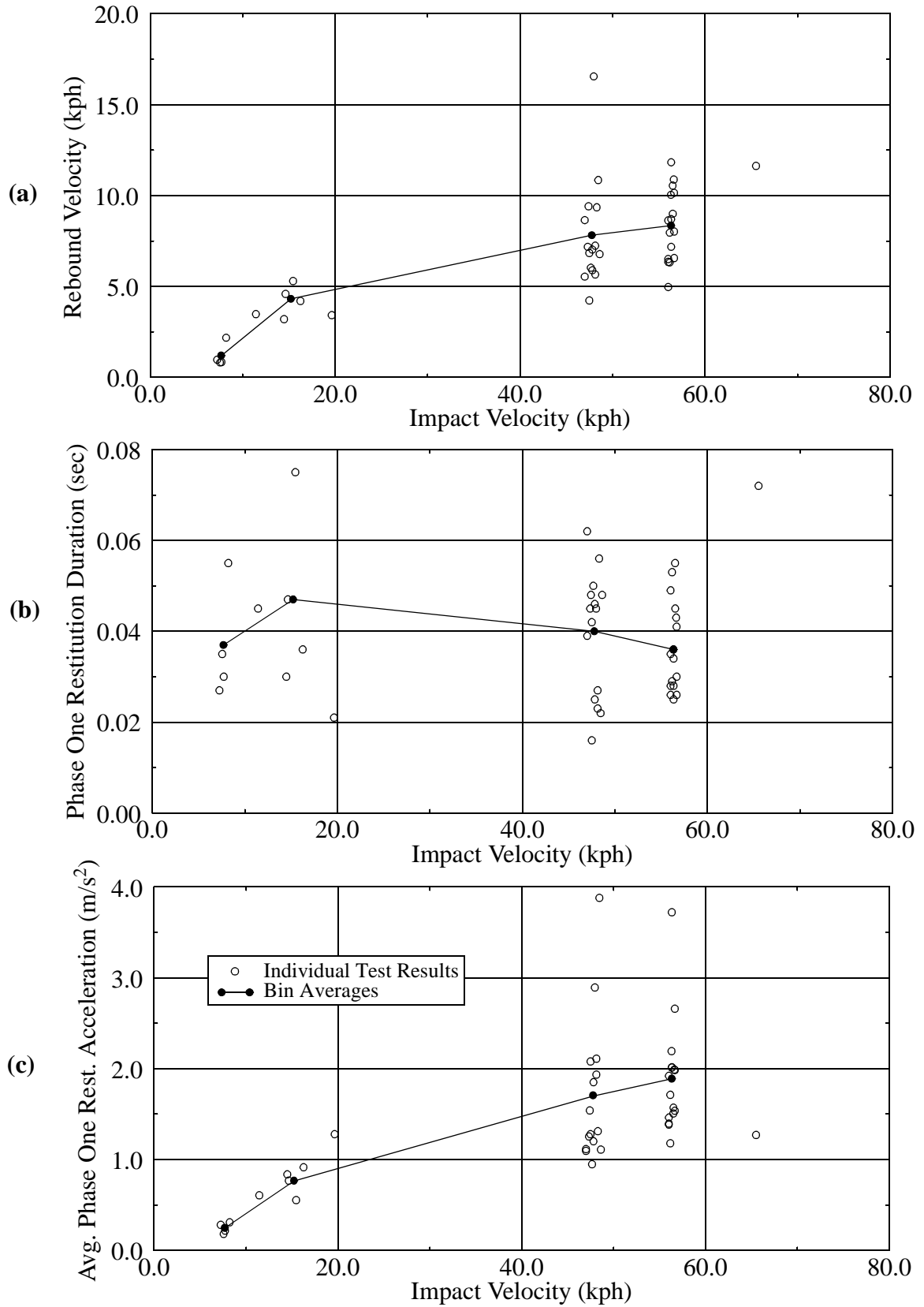


FIGURE 5.15 (a) Rebound Velocity v. Impact Velocity, (b) Restitution Time v. Impact Velocity, (c) Average Restitution Acceleration v. Impact Velocity

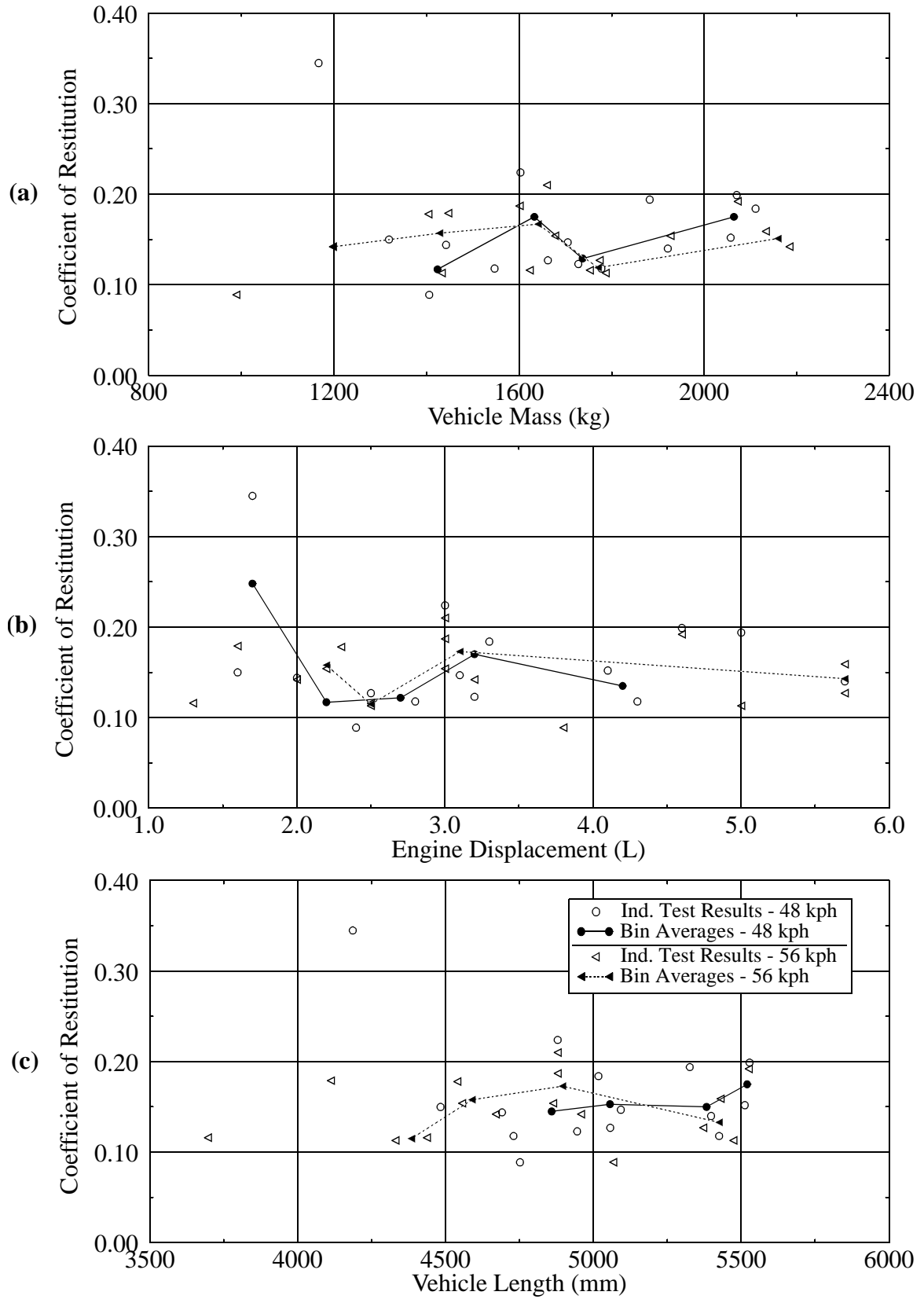


FIGURE 5.16 (a) Coefficient of Restitution v. Vehicle Mass, (b) Coefficient of Restitution v. Engine Displacement, (c) Coefficient of Restitution v. Vehicle Length

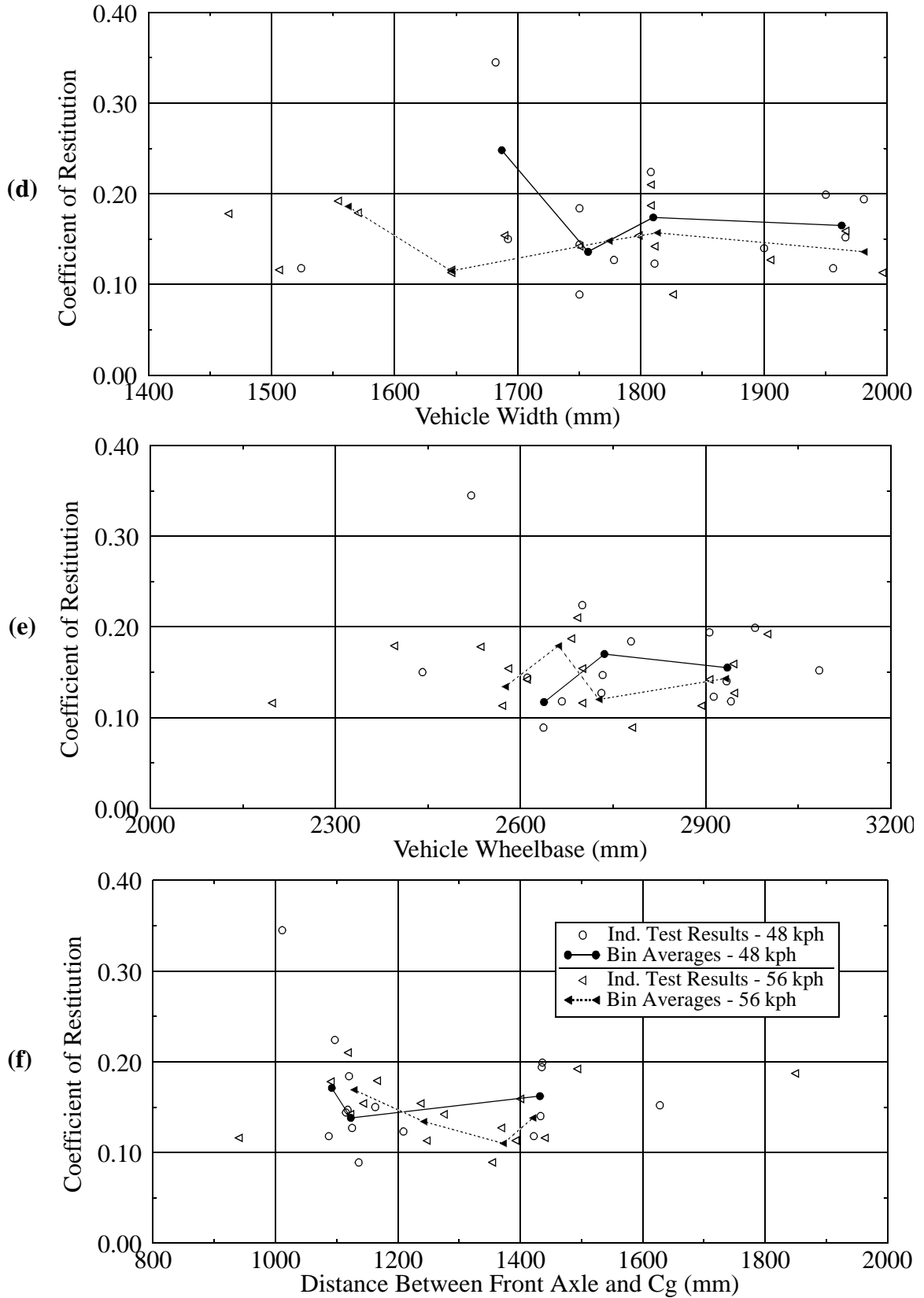


FIGURE 5.16 (cont'd.) (d) Coefficient of Restitution v. Vehicle Width, (e) Coefficient of Restitution v. Wheelbase, (f) Coefficient of Restitution v. Distance Between Front Axle and Center-of-Gravity

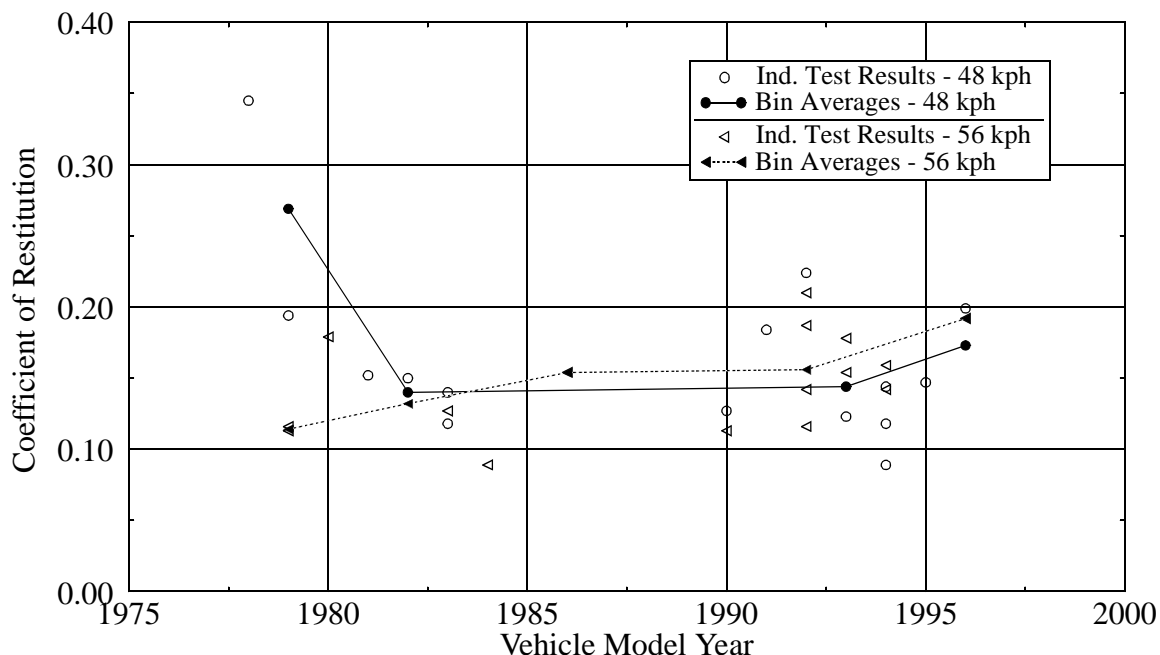


FIGURE 5.16 (cont'd) (g) Coefficient of Restitution v. Vehicle Model Year

of vehicle model year for the inline cases, shown in Figure 5.16(g), is similar to its effect in the transverse case. The average coefficient generally increases by a magnitude of about 0.03 between model years from 1985-1990 and model years from 1995-2000.

5.1.1.2.3 Repeated Impacts

The repeated test technique has been applied as a tool to investigate vehicle stiffness, but it is also useful in revealing some characteristics of restitution. Velocity traces from a series of frontal barrier impacts involving the same 1986 Ford Taurus (inline engine) are presented in Figure 5.17. Each of the traces was derived from an accelerometer mounted at the vehicle center-of-gravity. The calculated coefficient of restitution for each test is included in the figure. The second, third, and fourth tests were all performed at speeds near 30 kph, so they are particularly useful to compare. The second of the three traces is noisy, so its value is approximated. It is interesting to note that the third of the three similar traces displays the most restitution. It is also true that the coefficient of restitution in the final test is significantly higher than single impact tests at the same speed. It appears, therefore, that repeated impacts act to increase the elastic properties of a vehicle.

Another similar series of tests, shown in Figure 5.18, involves a 1985 Ford Escort. In this case, there are six total tests, with four of them at the comparable intermediate impact velocity. Velocity traces for the Escort cases were derived from an accelerometer mounted

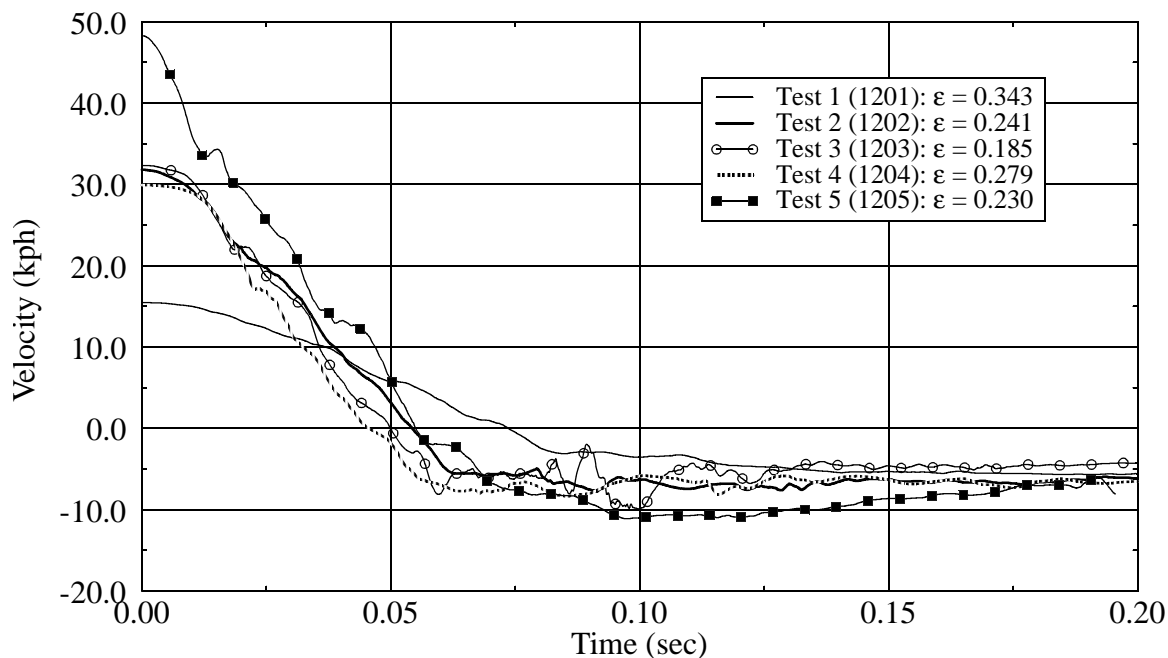


FIGURE 5.17 Velocity v. Time -- NHTSA Tests 1201 - 1205; Repeated Vehicle-to-Barrier Full-Width Frontal Collisions; 1986 Ford Taurus with an Inline Engine

at the vehicle's rear deck. As in Figure 5.17, the coefficient of restitution for each test is given in the figure. For the intermediate tests, there is a notable increase in the coefficient of restitution from the first test to the third, followed by a decrease in its value in the fourth test. Perhaps this is due to penetration through a relatively elastic part of the vehicle

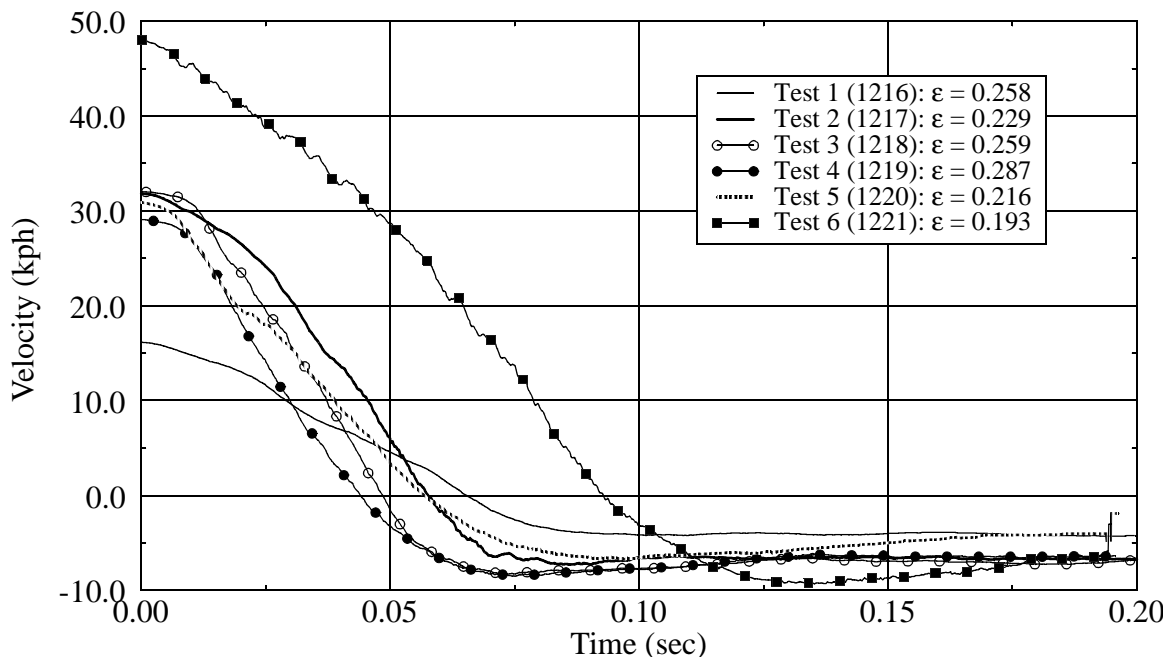


FIGURE 5.18 Velocity v. Time -- NHTSA Tests 1216 - 1221; Repeated Vehicle-to-Barrier Full-Width Frontal Collisions; 1985 Ford Escort with an Inline Engine

structure, reducing its ability to return energy. Again, the value of the coefficient of restitution in the 48 kph test is relatively high compared to values for single impacts at comparable speeds.

It is likely that the relatively high restitution displayed by repeated impact cases is due to an increase in the energy stored by more elastic vehicle components as less plastic portions of the structure lose their ability to store, or dissipate, energy.

5.1.1.2.4 Test Labs

For vehicles with inline engine orientations, the limited amount of data allows, at best, a questionable comparison between test labs. Calspan performed five tests at 48 kph and nine at 56 kph, while TRC performed six and two tests at the same impact velocities. Other contractors performed even fewer tests. A possible comparison may be made between Calspan and TRC for 48 kph tests. Reported average coefficients for the two companies at 48 kph are 0.159 and 0.145, respectively. Even though five and six tests don't provide a strong statistical basis, it is interesting to note that the test lab with lower coefficient results is TRC in this case, a reversal from what was found in the more complete analysis on transverse engines. Neglecting one test that gives an uncharacteristically high coefficient of 0.345, the overall standard deviation for inline engine tests at this speed is 0.037, while the standard deviations resulting from the two companies' tests are 0.045 and 0.027. The fact that the data from one of companies has a higher standard deviation magnitude than the overall value indicates that there is no visible difference in the results reported by the two test labs.

5.1.1.2.5 Repeatability

The standard deviation value reported in Table 5.2 for vehicles with inline engines at 48 kph is very high because of a coefficient of restitution value of 0.345 determined for one test. If that value is dropped from the analysis, the standard deviation falls to 0.037. The standard deviation presented in the same table for tests at 56 kph is 0.035. These values are about 0.01 greater than the expected value for vehicles with transverse engines. Because the amount of data analyzed for vehicles with inline engines is small, it is impossible to determine whether or not differences among test labs contribute to this standard deviation, as was the case for transverse engine vehicles, or if vehicles with inline engines, for some reason, demonstrate less repeatability in the coefficient of restitution.

5.1.1.2.6 Case Study - 1993 Inline Engine Ford Taurus

Further analysis of the coefficient of restitution in vehicle-to-barrier collisions involving passenger vehicles with inline oriented engines is accomplished by studying some individual cases. Test information and restitution results for three crash tests involving the 1993 Ford Taurus with an inline oriented engine are outlined in Table 5.8. Velocity traces corresponding to the tests are presented in Figure 5.19. Two tests are analyzed at 56 kph, while only one at 48 kph is available for study. As is the case for the overall analysis of vehicles with inline engines, the coefficient of restitution for this case is higher at 48 kph than the average value at 56 kph. Rebound velocities for the two speeds are quite similar. It is immediately apparent from the figure that each of the traces is

TABLE 5.8 Test Description and Restitution Results for Three Vehicle-to-Fixed Rigid Barrier Full-Frontal Tests Involving the 1993 Ford Taurus with an Inline Oriented Engine

NHTSA Crash Test No.	Model Year	Test Lab	Accelerometers		Impact Velocity (kph)	Maximum Rebound Velocity (kph)	ϵ
			No. Avg'd.	Location			
1973	1993	Calspan	1	center rear cross-member	48.44	10.85	0.224
1974	1993	Calspan	1	center rear cross-member	56.49	10.55	0.187
1976	1993	Calspan	1	center rear cross-member	56.33	11.83	0.210

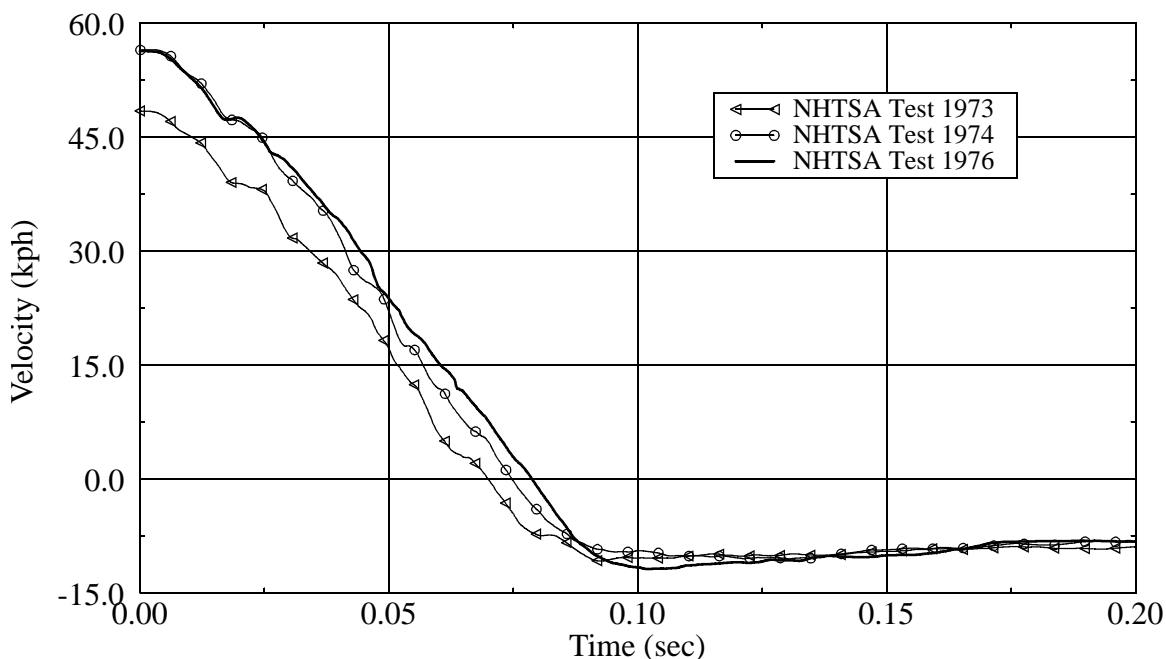


FIGURE 5.19 Velocity v. Time -- Three Vehicle-to-Fixed Rigid Barrier Full-Frontal Crash Tests Involving the 1993 Ford Taurus with an Inline Engine

somewhat noisy. The observed noise is likely the reason why the two coefficient values at 56 kph are so different; a difference of 0.023 for tests at the same impact velocity is more than a factor of four higher than the largest of the differences reported in case studies for transverse engine vehicles. Each of the tests was performed by the same test lab, so differences in contractor results cannot contribute to the variation.

Each of the traces shown in Figure 5.19 was determined through the use of just one accelerometer, which is likely the factor causing relatively noisy traces and wide variation in the coefficient of restitution. The accelerometer utilized in each test was mounted at the center rear cross-member of the vehicle, so the tests are consistent with one another, but without the use of additional accelerometers to be used in averaging, instrumentation noise can have a large influence. For Tests 1973 and 1976, additional data from accelerometers mounted in outboard rear positions are also available, but they were not used to generate the traces because they give consistently lower accelerations than accelerometers at the longitudinal centerline of the vehicle. Velocity traces derived from rear-mounted accelerometers located at the vehicle centerline and lateral positions are compared in Figure 5.20. Table 5.9 summarizes coefficient of restitution magnitudes and differences for the two mounting positions. The figure shows velocities from accelerometers at both mounting locations for Tests 1973 and 1976. An outboard accelerometer is not available for Test 1974, but its centerline trace is included to validate the centerline trace of Test 1976. Even though only one test is available at each impact velocity that reports both lateral and centerline velocities, it is clear that there is a definite, repeatable difference in the velocities at compared locations. Table 5.9 shows that the coefficient of restitution at lateral positions is nearly the same for both impact speeds. The largest difference between coefficient magnitudes at center and outboard positions is 0.145 at 48 kph. It is unclear, though, why the coefficients at the lateral positions for these cases

TABLE 5.9 Coefficient of Restitution Magnitudes at Center Rear and Outboard Rear Locations; 1993 Ford Taurus

NHTSA Crash Test No.	Calculated Coefficient of Restitution		Difference
	Center Rear	Outboard Rear	
1973	0.224	0.079	0.145
1974	0.187	-	-
1976	0.210	0.076	0.134

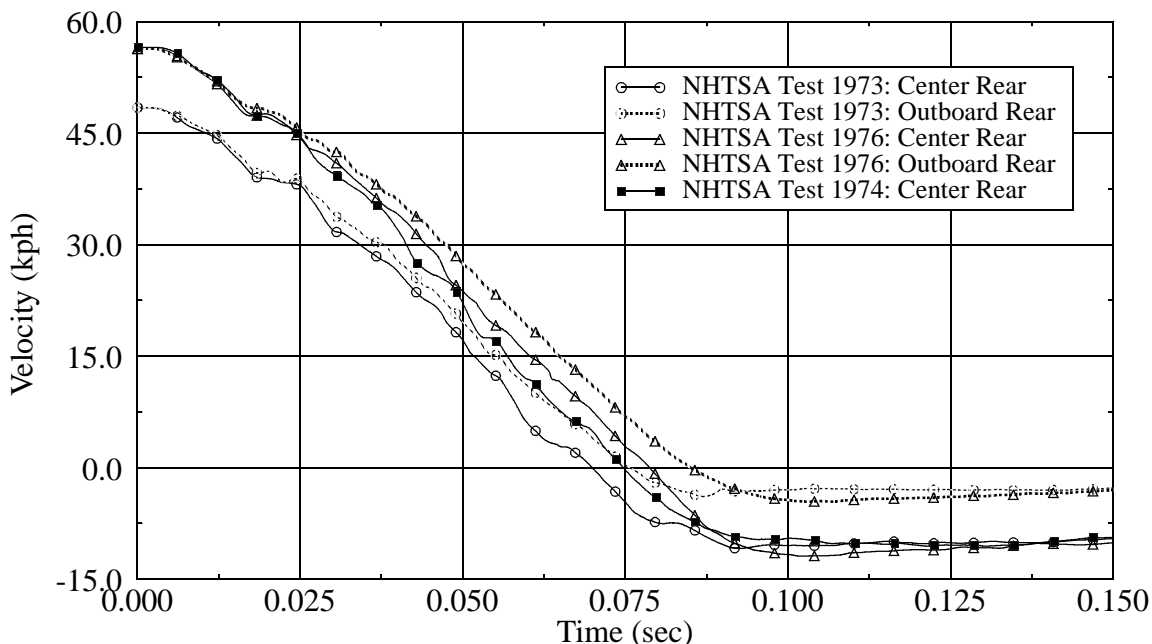


FIGURE 5.20 Velocity at Various Locations v. Time -- Three Vehicle-to-Fixed Rigid Barrier Full-Frontal Crash Tests Involving the 1993 Ford Taurus with an Inline Engine

are so low, both below 0.08, compared to the averages of 0.151 and 0.148 reported in Table 5.7 for impacts at 48 and 56 kph, respectively. The coefficients of restitution associated with nearly all of the other inline cases were calculated using accelerometers in outboard rear positions and, therefore, are expected to produce results similar to those reported at lateral rear locations for the 1993 Taurus. Because of this inconsistency, it is difficult to know if velocity differences between center and lateral locations are a consistent property of vehicles with inline engines or if the effect is limited to the case presented. Additional research of tests involving vehicles with accelerometers located in both positions is necessary. Based on the study, it appears that, at least for the 1993 Taurus, an inline engine orientation results in higher accelerations for central seating locations than for lateral positions.

To further compare results between tests at 48 and 56 kph for the inline 1993 Taurus, the centerline velocity traces for Tests 1973 and 1976 are integrated, as shown in Figure 5.21, to determine vehicle dynamic crush. Test 1976 is used to represent the 56 kph case because there appears to be less noise in its velocity trace than in the trace from Test 1974. From the figure, maximum dynamic crush values are determined to be 534 and 695 mm for Tests 1973 and 1976, respectively. Smoothed force-time traces, also given in the figure, show that vehicle-barrier separation times can be approximated to be 0.113 and 0.138

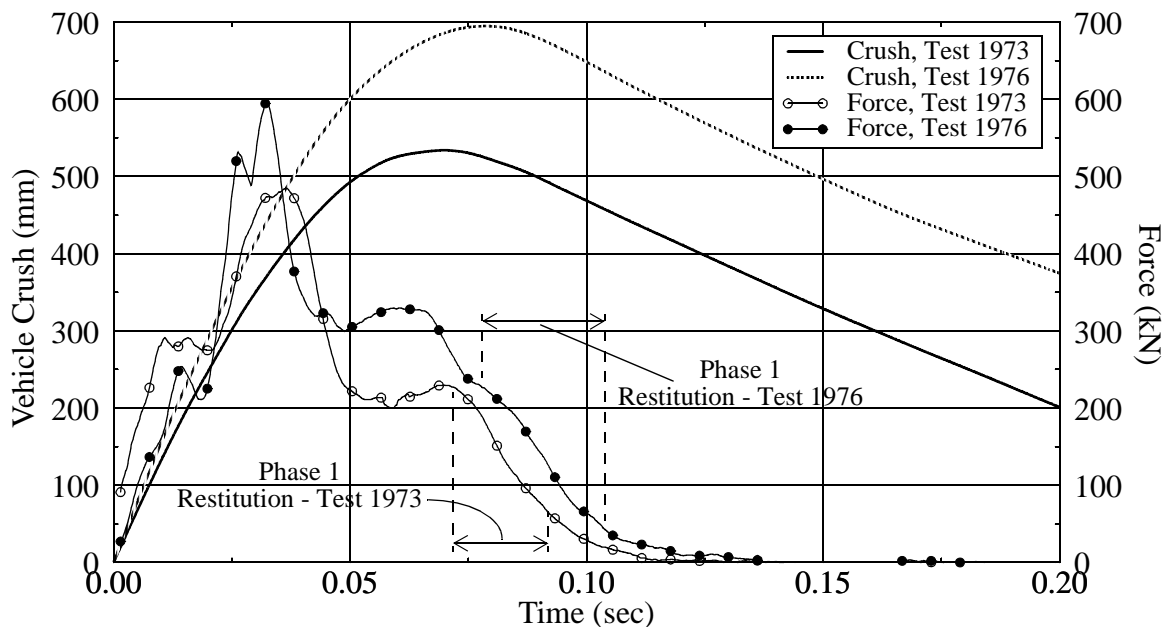


FIGURE 5.21 Vehicle Crush v. Time -- NHTSA Tests 1973, 1976: Vehicle-to-Fixed Rigid Barrier Full-Frontal Tests Involving the Inline 1993 Ford Taurus

seconds for Tests 1973 and 1976, respectively. The velocity traces associated with these tests show that the duration of phase one restitution extends from 70 to 92 ms for Test 1973, while for Test 1976 it lasts from 79 to 104 ms. The intervals are indicated in Figure 5.21. In contrast to the investigated transverse engine cases, these intervals differ by only 3 seconds. The force magnitudes reported during the period for each test are comparable, thus resulting in comparable magnitudes of rebound velocity, as shown in Figure 5.19. The fact that the barrier forces acting at the end of phase one restitution for this inline study are basically equivalent at both speeds while there is a difference in forces manifest in the two case studies for transverse engines suggests that the force difference is related to engine orientation. As stated previously, however, there is no physical basis for believing that post-phase one restitution forces vary for different impact velocities, so the inconsistency is attributed to error in the load cell signals.

The vehicle-barrier separation times drawn from Figure 5.21 can be applied to determine derived residual crush values, which are 431 and 531 mm for Tests 1973 and 1976, respectively. Reported residual crush values are not available, however, so the same method used to determine corrected maximum dynamic crush values for the transverse engine studies cannot be applied to these cases. Rather, because of the similarity between the derived vehicle dynamic crush results shown in Figures 5.8 and 5.21, the corrected

maximum dynamic crush values for the inline Taurus cases are approximated using the transverse Taurus results. Comparison of the two figures shows that derived crush for the transverse cases ranges between 20 and 49 mm greater than that for the inline cases, as shown in Table 5.10. Derived maximum dynamic crush values for the transverse cases are

TABLE 5.10 Derived Maximum and Residual Vehicle Crush and Corrected Maximum Crush for Transverse and Inline Engine 1993 Ford Taurus Cases

Engine Orientation	Derived Maximum Dynamic Crush (mm)		Derived Residual Crush (mm)		Corrected Maximum Dynamic Crush (mm)	
	48 kph	56 kph	48 kph	56 kph	48 kph	56 kph
Transverse	554	727	459	580	413	627
Inline	534	695	431	531	383	595
Difference	20	32	28	49	20	32

20 and 32 mm higher than values for the inline cases at 48 and 56 kph, respectively. Corrected maximum dynamic crush values for the inline cases are approximated by subtracting 20 and 32 mm from the corrected maximum dynamic crush values determined for the transverse cases. This results in corrected dynamic crush magnitudes of 383 and 595 mm for the inline cases at 48 and 56 kph, respectively. It is expected that crush depth would be slightly less for inline engine cases than for transverse vehicles, because the longitudinal dimension of the engine is longer, allowing less "empty space" between the rear of the engine and the cowl panel region.

Measurements from the test reports for NHTSA Tests 1973 and 1976 indicate that the distances from the front of the vehicle to the front of the engine and to the firewall are about 582 and 1218 mm, respectively. As expected, these distances are approximately the same as those reported for the transverse engine Taurus. The longitudinal dimension of the engine is reported to be 406 mm, about 25 mm longer than the transverse engine. Applying the "75% Rule" to the corrected dynamic crush values of 383 and 595 mm gives penetration depths of 511 and 793 mm, respectively. Based on the previously discussed transverse engine case studies and the high value of the coefficient of restitution at 48 kph for inline engines, it is hypothesized that penetration in the 48 kph collision reached the cowl panel. The estimate of crush depth, though, places maximum penetration short of the

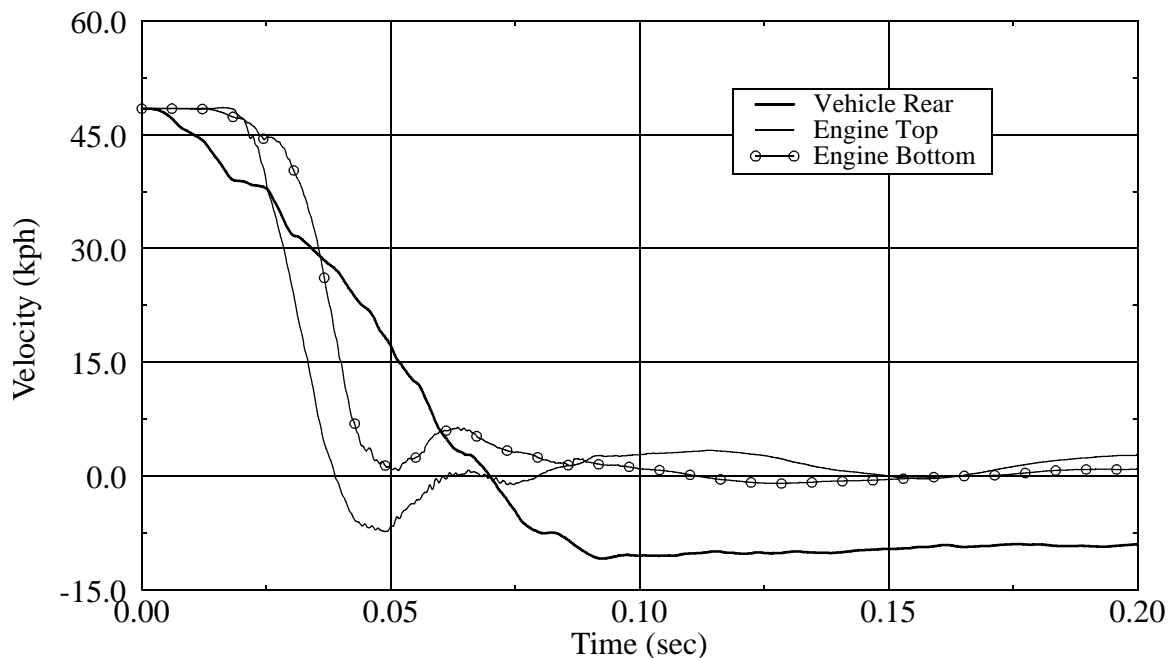


FIGURE 5.22 Velocity v. Time at Vehicle Rear and Engine -- NHTSA Test 1973: Vehicle-to-Fixed Rigid Barrier Full-Frontal Involving the 1993 Ford Taurus

front of the engine. Velocity traces in Figure 5.22 show that the engine reached zero velocity before the rear end of the vehicle, so, like the transverse case, the engine must have been engaged by crush. The estimated penetration depth, therefore, is an underestimate of the actual depth, the extent of which is unknown. After having determined that the engine was engaged, crush depth is extended by the longitudinal dimension of the engine. Even with this addition, penetration is still short of the cowl panel, but because the engine is inline, there would be an assortment of pulleys and shafts on the end of the engine that could potentially extend the dimension of the stiff region enough to initiate contact and generate increased restorative forces. Depth estimates are shown in Figure 5.23. Because inline engines are generally associated with rear-wheel drive vehicles, it is also possible that the relatively high coefficient of restitution in 48 kph collisions is influenced by restitution properties of the driveshaft and connected

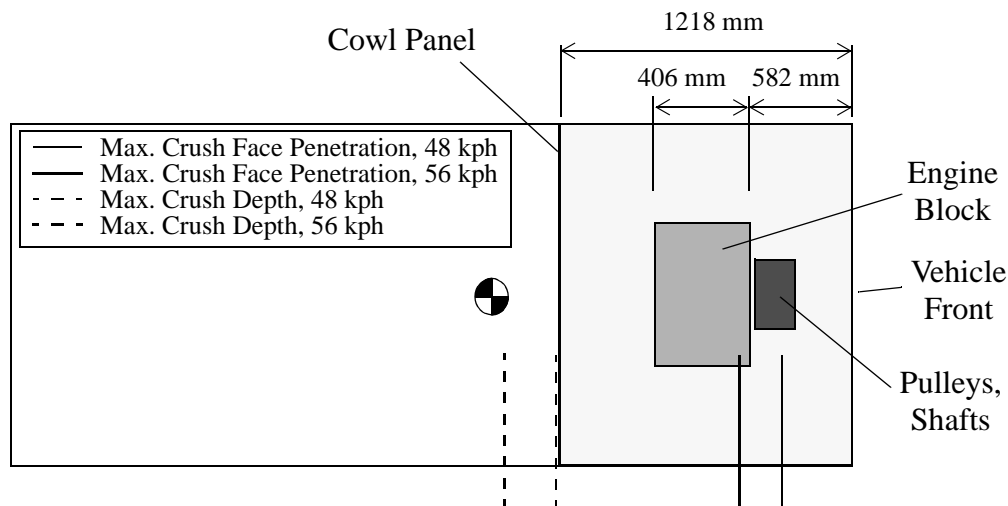


FIGURE 5.23 Crush Approximations -- NHTSA Tests 1973, 1976: Vehicle-to-Fixed Rigid Barrier Full-Frontal Tests Involving the 1993 Ford Taurus with an Inline Engine

components. In the 56 kph collision, it is evident from the measurements that crush extends at least to the front of the cowl panel. If the dimension of the engine is extended to account for pulley and shafts, the crush would be deeper than in the 56 kph transverse Taurus collision. This reasoning could explain why the expected coefficient of restitution at 56 kph is slightly less for inline engine cases than for transverse engine vehicles. Based on the speculation that the 48 kph inline engine penetration depth is similar in magnitude to the 56 kph transverse engine crush depth, restorative forces, and rebound velocities, are expected to be similar. The difference between the coefficient of restitution for these two cases could reasonably be due to the difference in impact velocity. Information is not available to show whether or not the series of adjustments and rationale required to show that crush in the 48 kph impact penetrated to the cowl panel are reasonable, so it is impossible to draw any certain conclusions with regard to the relative influence of vehicle components and structure. The evidence, however, shows that the preceding rationale may be reasonable and should be further investigated.

5.1.2 Non-Passenger Type Vehicles

Figure 5.24 repeats Figure 5.1, plotting the coefficient of restitution as a function of impact velocity for non-passenger type vehicles only, while Table 5.11 summarizes the coefficient of restitution data for pickup trucks, sport utility vehicles, and vans, by engine orientation. As the figure shows, only tests at 48 and 56 kph are presented. Totals of 18 and 21 tests at 48 and 56 kph, respectively, are shown. The tests are fairly evenly distributed among the three vehicle types. The overall distribution of the coefficient, as seen in the figure, and the overall average values given in the table reveal that the coefficient of restitution is, on average, higher at 56 kph than at 48 kph, as is the case with passenger vehicles. Individual vehicle type data outlined in Table 5.11, however, shows

TABLE 5.11 Coefficient of Restitution and Number of Tests Analyzed by Vehicle Type, Engine Orientation, and Impact Velocity; Non-Passenger Type Vehicles Only

Impact Velocity (kph)	Pickup		Sport Utility		Van				OVERALL	
	Inline		Inline		Inline		Transverse			
	Avg. ϵ	No. Tests	Avg. ϵ	No. Tests	Avg. ϵ	No. Tests	Avg. ϵ	No. Tests	Avg. ϵ	No. Tests
48	0.105	5	0.135	6	0.107	4	0.162	3	0.125	18
56	0.160	5	0.146	8	0.130	5	0.164	3	0.148	21

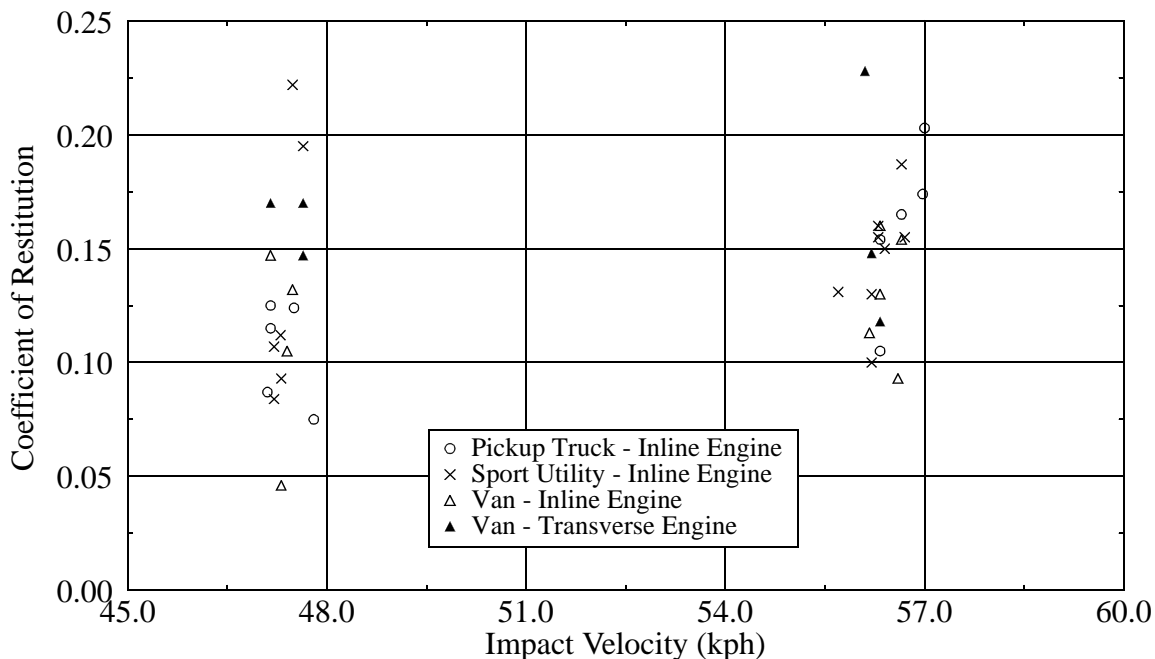


FIGURE 5.24 Coefficient of Restitution v. Impact Velocity -- Vehicle-to-Fixed Rigid Barrier Full-Frontal Collisions; Non-Passenger Type Vehicles

that behavior varies among vehicle types, assuming that the small amount of tests collected for each type are representative. Each vehicle type has a higher coefficient at 56 kph than at 48 kph, but the extent of difference varies. As Table 5.11 illustrates, the difference between coefficient magnitudes at the two speeds is most dramatic for pickup trucks with inline engines, while it is least dramatic for vans with transverse oriented engines. Inline-engined sport utility vehicle coefficient values are most similar to the reported passenger type vehicle magnitudes of 0.139 and 0.152 at 48 and 56 kph, respectively.

5.2 PARTIAL-WIDTH VEHICLE-TO-BARRIER COLLISIONS

Very few partial-contact vehicle-to-barrier collisions are available in the NHTSA crash test database. Six tests, all fifty percent overlap case, were downloaded and analyzed.

5.2.1 Impact Velocity

Coefficient of restitution results from the six available 50 percent overlap rigid barrier tests are shown in Figure 5.25. Of the six vehicle-to-barrier fifty-percent overlap tests shown in the figure, two are at an impact velocity of 16 kph, involving the 1988 Ford Taurus and the 1987 Ford Escort. The four remaining tests involve the 1987 Toyota Celica and the 1987 Hyundai Excel GLS, with tests conducted at 40 and 56 kph for each vehicle. In each case, the vehicle has a transverse engine. For comparison purposes, averages from the analyses on full-frontal vehicle-to-barrier collisions performed in section 5.1 are also included. The line segments connecting the averages are meaningless except to differentiate the averages they connect from other points in the figure. The plot demonstrates that partial-width impacts generally result in lower coefficient of restitution values than full-width impacts, and that the value of the coefficient tends to decrease with increasing impact velocity. There appears, however, to be an increase in the average value

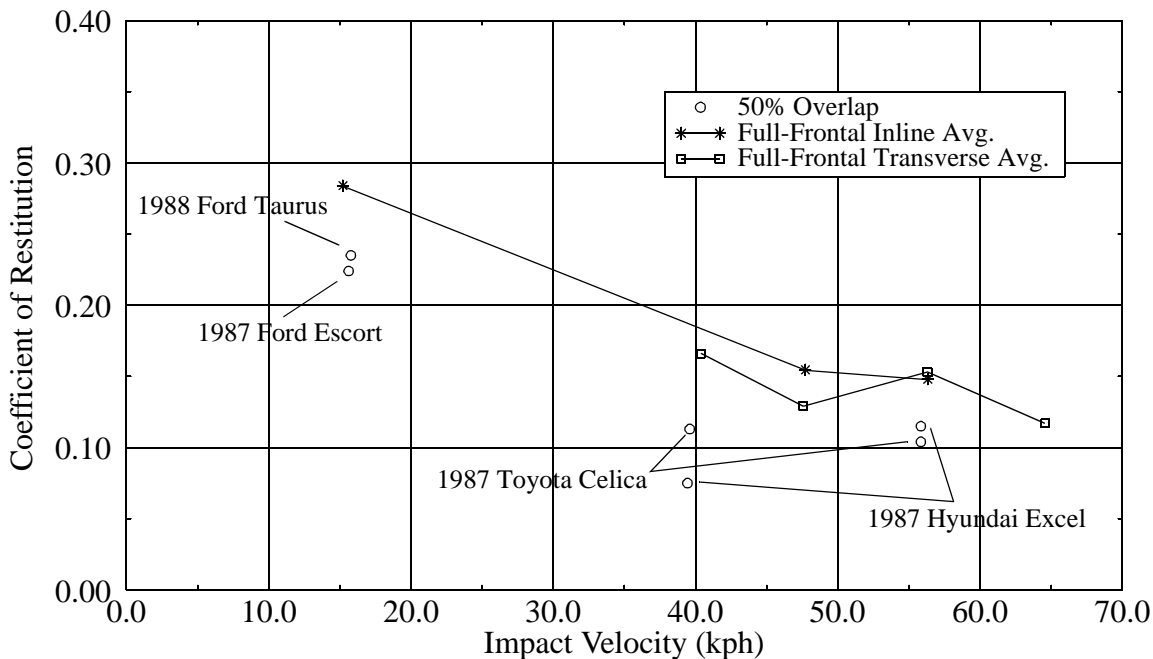


FIGURE 5.25 Coefficient of Restitution v. Impact Velocity -- Vehicle-to-Barrier Frontal Collisions; Passenger Vehicles

for the coefficient between 40 and 56 kph, much like the contradiction of the decreasing coefficient trend sited for full-width vehicle-to-barrier collisions. The figure shows that the coefficient increases from 40 to 56 kph for the Excel but not for the Celica.

5.2.2 Case Study - 1987 Hyundai Excel GLS

In order to illustrate why partial-contact cases generally result in lower coefficient of restitution values than do full-contact tests, two of the fifty-percent overlap cases, the 40 and 56 kph Hyundai Excel tests, are studied and compared to full-frontal tests at the same speeds. Information and results for the four tests are outlined in Table 5.12. The table includes NHTSA crash test number, percent overlap, contracted test lab, and number of accelerometers averaged and their locations. Velocity traces for the tests are included in Figure 5.26. The figure and table show that at both impact velocities, the coefficient of

TABLE 5.12 Test Description and Restitution Results for Four Vehicle-to-Fixed Rigid Barrier Tests (Two Full-Frontal and Two 50% Overlap) Involving the 1987 Hyundai Excel GLS

NHTSA Crash Test No.	Percent Overlap	Test Lab	Accelerometers		Impact Velocity (kph)	Maximum Rebound Velocity (kph)	ϵ
			No. Avg'd.	Location			
1156	50	Calspan	4	left rear seat (2)	39.43	2.97	0.075
1092	100	Calspan	2	right, left rear cross-member	39.75	7.70	0.194
1164	50	Calspan	2	right, left rear seat	55.84	6.40	0.115
1101	100	Calspan	4	right (2), center, left rear seat	56.00	8.76	0.156

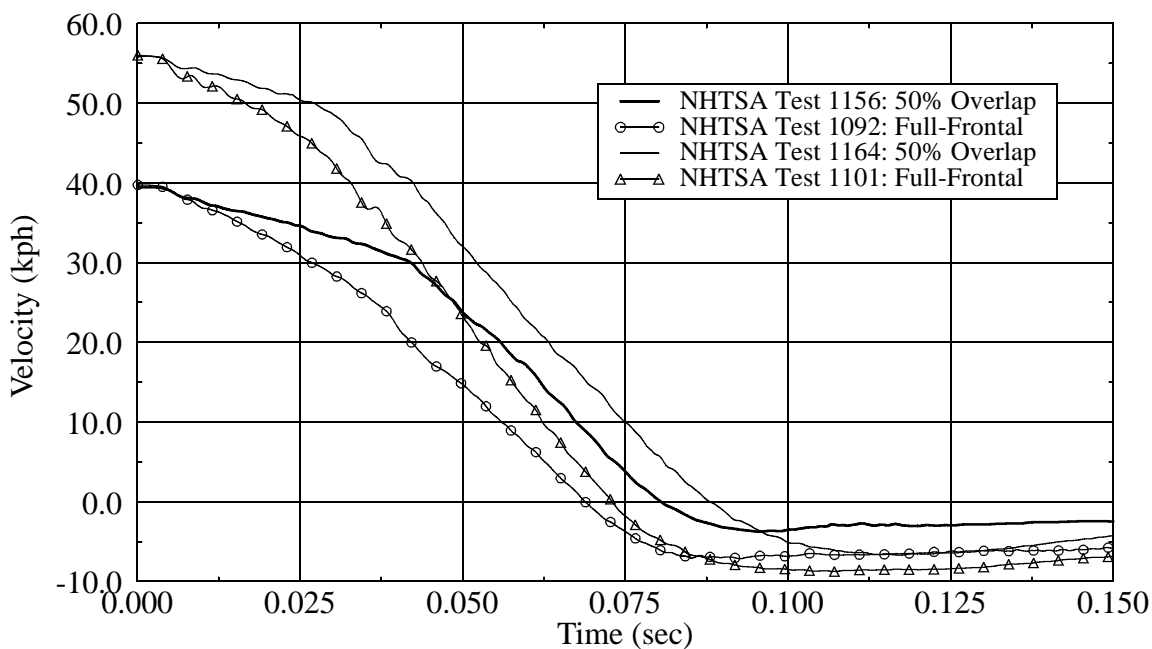


FIGURE 5.26 Impact Velocity v. Time -- Vehicle-to-Fixed Rigid Barrier Full-Frontal and Fifty-Percent Overlap Collisions; 1987 Hyundai Excel GLS

restitution is higher for the full-frontal cases than the fifty-percent overlap tests, just as Figure 5.25 suggests. Coefficient values differ by 0.119 at 40 kph and by 0.041 at 56 kph. The coefficient of restitution results at 40 kph are unexpectedly high and low for the full-frontal and fifty-percent overlap tests, respectively, but multiple accelerometers for both tests were used to determine their traces. In both cases, additional data that were consistent with the averaged data were discarded because of noise, so the presented traces are believed to be accurate. Table 5.12 also shows that while the coefficient of restitution for the full-frontal tests is higher at 40 kph than at 56 kph, the opposite is true for the fifty-percent overlap cases. Figure 5.26 additionally illustrates that the transition in deceleration during the crush phase is more pronounced in partial-contact collisions than in full-width tests.

Because the coefficient of restitution was earlier shown to be a function of crush depth, the presented Hyundai Excel tests are integrated and shown in Figure 5.27. The figure shows derived maximum penetration depths to be 572, 451, 828, and 674 mm, for Tests 1156, 1092, 1164, and 1101, respectively. It is apparent that a collision with only partial barrier contact results in deeper penetration than a full-contact case at the same speed. Residual crush measurements are not reported for any of these tests, so corrected maximum dynamic crush values cannot be determined. Based on the previous analyses on

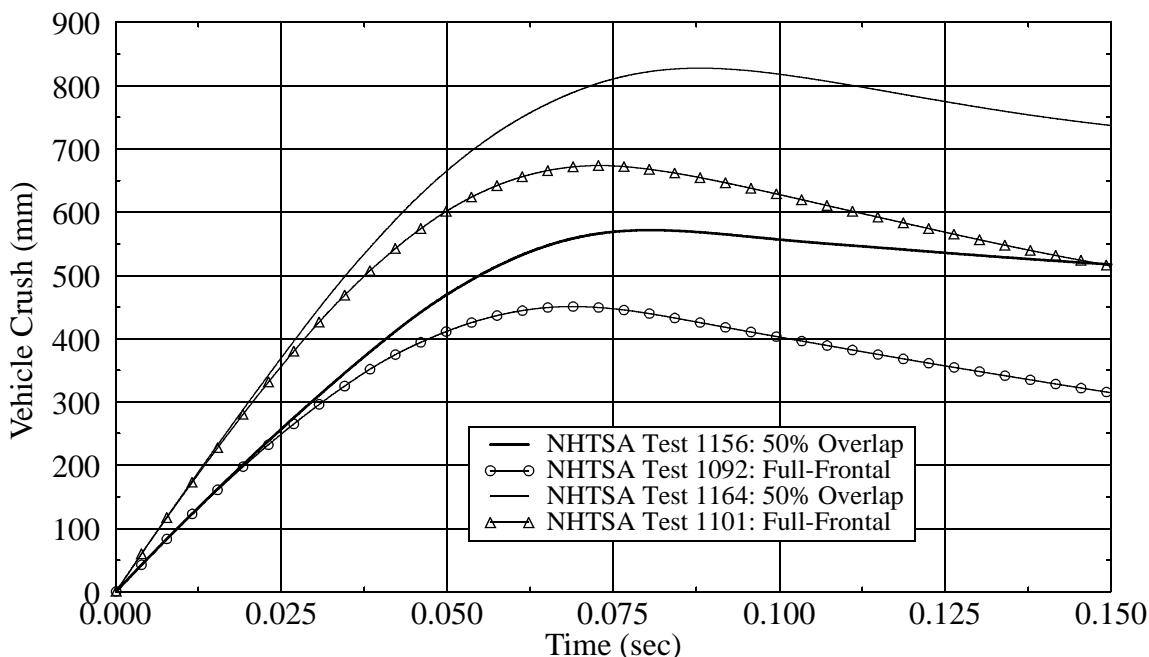


FIGURE 5.27 Vehicle Crush v. Time -- Vehicle-to-Fixed Rigid Barrier Full-Frontal and Fifty-Percent Overlap Collisions; 1987 Hyundai Excel GLS

the influence of crush depth in full-frontal collisions, however, it appears, for Test 1092, that crush penetrated to a depth near the front of the engine, giving a fairly high coefficient of restitution. Crush in Test 1156 likely penetrated to a point short of the cowl panel / toe pan area, giving a very low coefficient. Calculated coefficient of restitution values and penetration depth estimations suggest that the crush in Test 1101 penetrated to the depth of the cowl panel region, resulting in a high coefficient, while penetration in Test 1164 reached into the occupant compartment, causing less restitution than that seen in Test 1101.

5.3 POLE IMPACT COLLISIONS

Tests involving the collision of vehicles into poles, both centered and offset cases, are included in the NHTSA crash test database. The influence of restitution for pole impact cases is here studied.

5.3.1 Impact Velocity

Figure 5.28 presents calculated coefficient of restitution values for pole impact tests as a function of impact velocity. For comparison purposes, average coefficient values for full-frontal barrier collisions are also included. The pole impact results include both inline and transverse oriented engine vehicles, as well as centered and offset impacts. Four velocity bins at 8, 16, 32, and 48 kph are visible. As the figure shows, pole impact restitution coefficients vary widely in magnitude, but, as a whole, their averages tend to decrease with increasing impact velocity. A slight increase in the average magnitude of the coefficient, however, appears to occur between 32 and 48 kph, much like the demonstrated increase between 48 and 56 kph for full-frontal tests on transverse engine vehicles. The centered impact data considered alone, however, for both engine orientations, offer no basis for believing that the trend of decreasing coefficient of restitution with increasing impact velocity is violated at any speed. Rather, the presented data largely behave according to the stated trend. Based on the evidence presented in the analysis of vehicle-to-barrier, full-

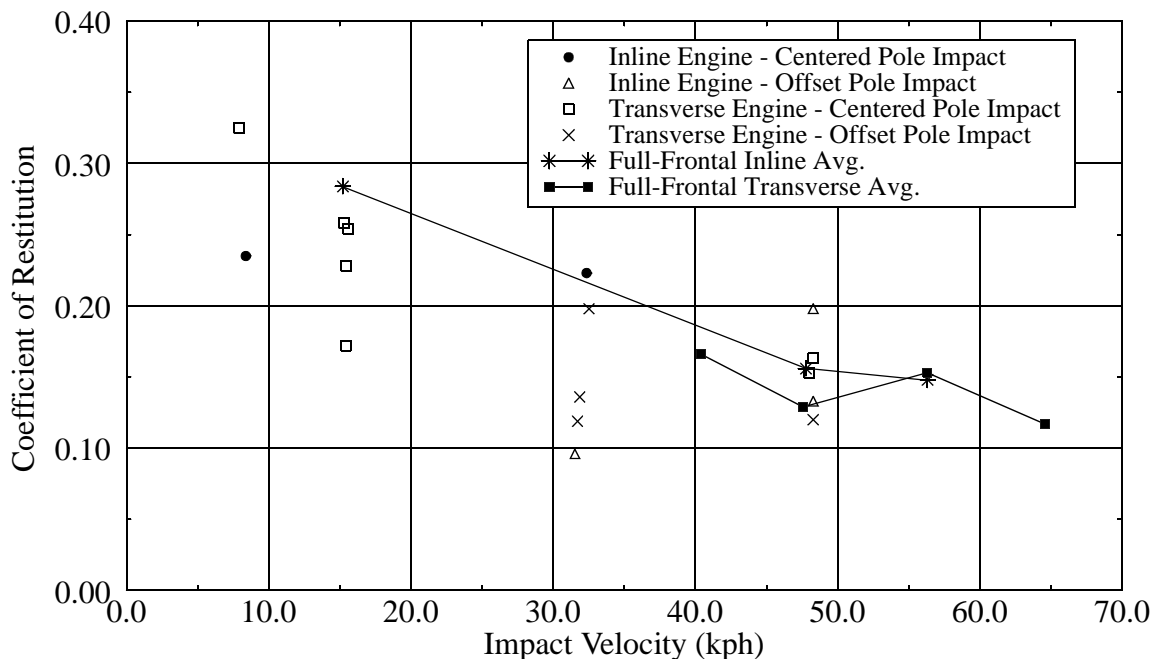


FIGURE 5.28 Coefficient of Restitution v. Impact Velocity -- Vehicle-to-Barrier Frontal Pole Impacts; Passenger Vehicles

frontal collisions, though, it is expected that if more data were available, contradictions of the trend would become visible. Sharp changes in the value of the coefficient would likely appear at lower speeds than for full-frontal collisions, however, since more penetration generally occurs in pole impacts than in full-frontal collisions at the same speed. Without information on increases in the coefficient's behavior with increasing velocity for centered pole impacts, expected values of the coefficient appear to be similar in magnitude to those expected for vehicle-to-barrier, full-frontal collisions. In some pole impact cases, however, the deformed vehicle structure "captures" the pole, causing forces that act opposite to restorative forces, resulting in a lower coefficient of restitution. Because it is difficult from the data to see when this may occur, pole impacts would be more effectively studied using film analysis, coupled with the study of accelerometer data.

5.3.2 Offset

A small amount of information can also be drawn from Figure 5.28 regarding the influence of offset in pole impacts. It appears from the tests around 32 kph that offset may result in lower magnitudes of restitution. The only centered impact value that can be used to contrast the offset cases, however, is an inline engine case that seems to be higher than what might be expected. The lack of available data makes it difficult to make a confident observation on the matter. It is interesting to note that the three transverse engine, offset impact cases at 32 kph have offset distances of 140, 229, and 330 mm, and give restitution coefficients of 0.136, 0.119, and 0.198, respectively. Based on these values, if offset distance in pole impact has a significant influence on restitution, which it likely does, the relationship is not linear.

5.3.3 Accelerometer Location

Velocity traces from NHTSA Test 662, a 330 mm left-side offset pole impact involving a 1981 Volkswagen Rabbit, are presented in Figure 5.29. Traces measured at the center-of-gravity and at left and right rear floor locations are compared. Interestingly, the traces from the laterally-mounted accelerometers are quite similar, indicating that even though the impact was offset, very little rotation occurred. The illustrated case has the largest offset distance of all of the pole impacts analyzed. Most of the other offset cases show similar results while some indicate that rotation was significant. This effect is a good example of the complex nature of automobile collisions and would not occur if vehicles were rigid bodies. The unexpected behavior is likely due to the generation of a load path,

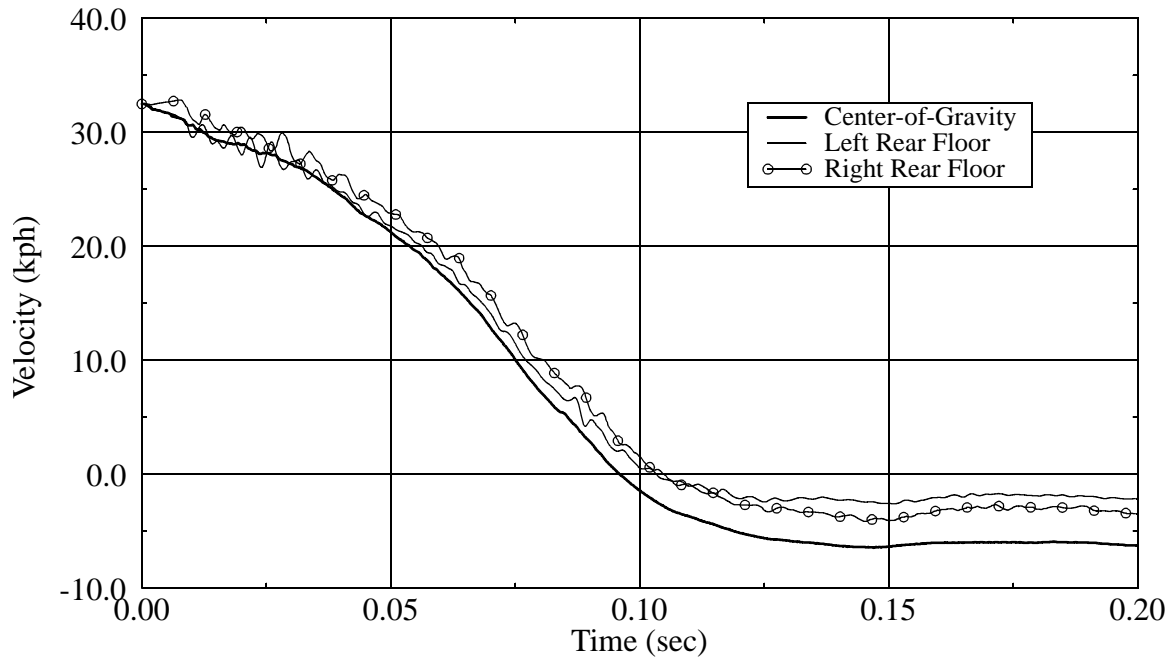


FIGURE 5.29 Velocity v. Time Measured at Centerline and Lateral Vehicle Positions -- NHTSA Test 662: Vehicle-to-Barrier -330 mm Offset Pole Impact Involving a 1981 Volkswagen Rabbit

by virtue of oblique contact with the engine, that acts to the side of the center-of-gravity opposite that of the principal direction of force estimated for a rigid body collision. Perhaps this is the reason why the relationship between offset distance and the coefficient of restitution doesn't seem to be linear.

Figure 5.29 also indicates that the center-of-gravity trace has the highest rebound velocity of the presented traces. This difference is common to nearly all of the analyzed pole impact cases where an accelerometer was mounted at the center-of-gravity. In addition, the analyzed tests seem to show that the difference increases with impact velocity. The fact that the difference in rebound velocity is present for both offset and centered cases and when rotation is significant in the collision, and when it is not, is puzzling. More research on additional tests is necessary to clarify the nature of the discrepancy with rebound velocity.

5.3.4 Case Study - 1984/1987 Honda Accord

In order to further illustrate the behavior of the coefficient of restitution in pole impact cases, centered and offset pole impact cases involving the Honda Accord were compared to a vehicle-to-barrier full frontal case. Table 5.13 outlines information, including test number, vehicle model year, contracted test lab, and number of accelerometers averaged and their locations, for NHTSA Tests 1054, 819, and 873, which are vehicle-to-barrier

full-frontal and centered and offset pole collisions, respectively. Restitution results are also included in the table. As before, the 1984 and 1987 Honda Accord are compared. Even though a structure change occurred in the Accord between these years, the change does not seem to be significant in terms of restitution. Velocity traces associated with each of the tests are presented in Figure 5.30. For test 1054, the portion of the trace after about 110 ms is ignored. It is immediately apparent from the figure that the crush duration is significantly longer for the pole impact cases than for the barrier test. The wide contact of the barrier impact initially provides much higher resistance to crush than does the narrow pole impact, and as a result, generates higher forces that decelerate the vehicle earlier. In the case of pole impact, shortly after the engine is engaged by crush, a sharp transition

TABLE 5.13 Test Description and Restitution Results for a Vehicle-to-Fixed Rigid Barrier Full-Frontal Test and Centered and Offset Pole Tests Involving the 1984/1987 Honda Accord

NHTSA Crash Test No.	Model Year	Test Lab	Accelerometers		Impact Velocity (kph)	Maximum Rebound Velocity (kph)	ϵ
			No. Averaged	Location			
1054	1987	TRC	2	right, left rear seat	47.48	7.46	0.157
819	1984	TRC	6	right (2), left(2) rear seat; right, left b-pillar	48.28	7.87	0.163
873	1984	TRC	2	left rear seat; left b-pillar	48.28	5.80	0.120

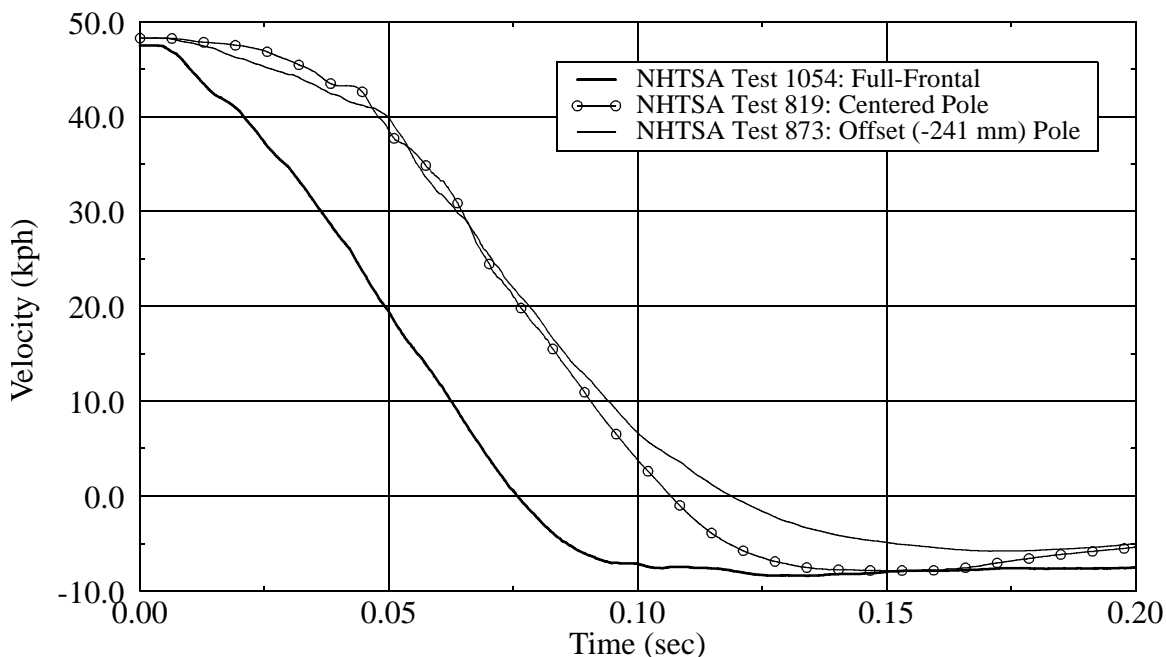


FIGURE 5.30 Impact Velocity v. Time -- Vehicle-to-Barrier Full-Frontal and Centered and Offset Pole Collisions; 1984/1987 Honda Accord

occurs in the vehicle's acceleration such that it decelerates at a rate nearly identical to that of the full-frontal case. The transition in deceleration is less visible for the full-width case, because the full-contact resists crush with a stiffness similar in magnitude to that of the engine. Besides this difference in the crush behavior, the traces for the barrier and centered pole impacts are nearly identical and result in very similar coefficient of restitution values, as shown in Table 5.13. It is unknown why the coefficient of restitution for the offset case is lower than the other two. The table shows that the two pole impact test traces result from data taken from laterally-mounted accelerometers. Based on the discussion associated with Figure 5.29, it is likely that values for the coefficient would be higher than shown at the vehicle centerline for these tests.

5.4 FULL-WIDTH VEHICLE-TO-VEHICLE COLLISIONS

Even though significantly fewer tests are reported for vehicle-to-vehicle collisions than for vehicle-to-barrier tests, the coefficient of restitution for full-frontal VTV cases was investigated. Its behavior is studied as a function of closing velocity and engine orientation, along with a brief discussion on the influence of difference in mass between colliding vehicles. Comparisons are made between coefficient magnitudes obtained in VTB and VTV tests for identical vehicles.

5.4.1 Influential Parameters

5.4.1.1 Closing Velocity

The coefficient of restitution from twenty-six vehicle-to-vehicle full-frontal collisions is presented as a function of closing velocity in Figure 5.31. Each of the collisions involves passenger vehicles only. Twenty-one of the collisions are front-to-front collisions, while the remaining five are front-to-rear type collisions. It should be noted that full-frontal vehicle-to-vehicle tests are generally not available in the NHTSA database for late model vehicles. Model years of vehicles involved in the presented front-to-front tests range from 1980-1984, while the front-to-rear tests all involve 1971 vehicles. As a result, it is unknown how closely the presented results apply to late model vehicles. It is

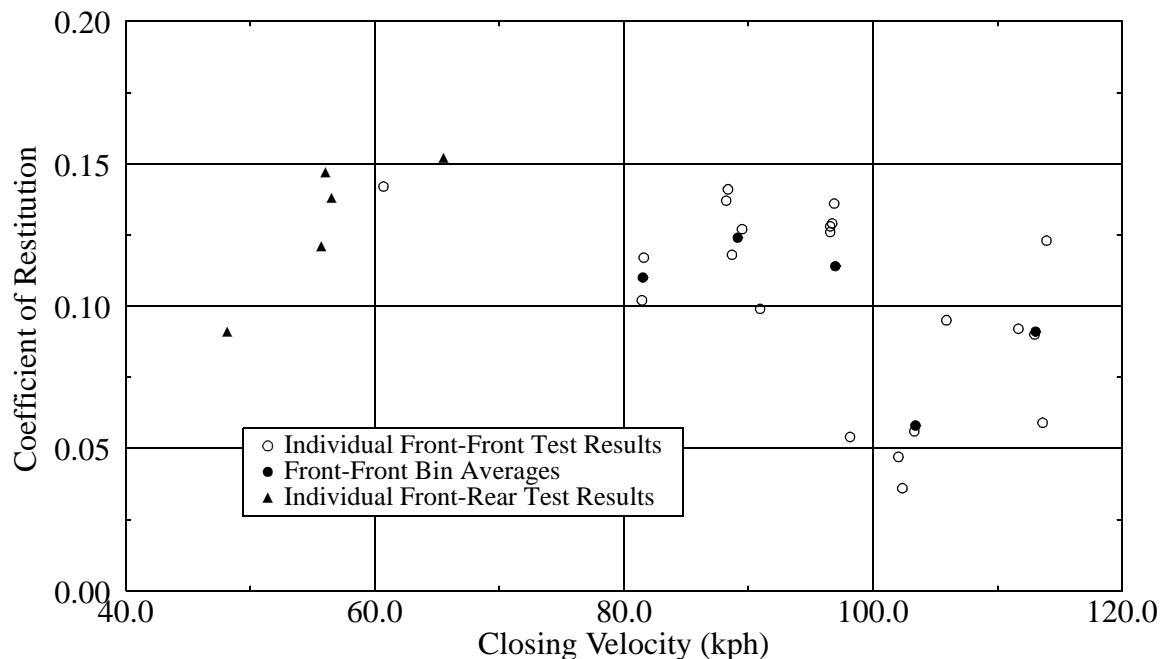


FIGURE 5.31 Coefficient of Restitution v. Closing Velocity -- Vehicle-to-Vehicle Full-Frontal Collisions; Passenger Type Vehicles

anticipated, however, that since the coefficient of restitution has been shown to be higher in later model vehicles in frontal barrier collisions, the same behavior would apply to vehicle-to-vehicle cases.

The figure generally demonstrates the trend of decreasing magnitude in the coefficient of restitution with increasing closing velocity. The majority of tests available at the lower velocities are front-to-rear type collisions, as shown, and except for one test indicating relatively low restitution, the front-to-rear collisions appear to demonstrate similar coefficient of restitution magnitudes in comparison to front-to-front cases. Data are not available to substantiate this observation at higher velocities, but further analysis does not differentiate between the two types of vehicle-to-vehicle collisions.

Apparent contradictions to the trend of decreasing coefficient with increasing velocity are visible in Figure 5.31 at about 82 and 103 kph. The discrepancy at 82 kph is small and may not represent a true average, as only two tests are reported at that closing speed. The large difference at 103 kph, however, is the average of five tests and so is expected to be more reliable. Based on the research presented for vehicle-to-barrier collisions, contradictions of the decreasing-coefficient-with-increasing-velocity trend are expected, but because of relative differences between colliding vehicles' stiffnesses and variation in engine orientation, it is difficult to determine where the contradictions might occur for vehicle-to-vehicle collisions.

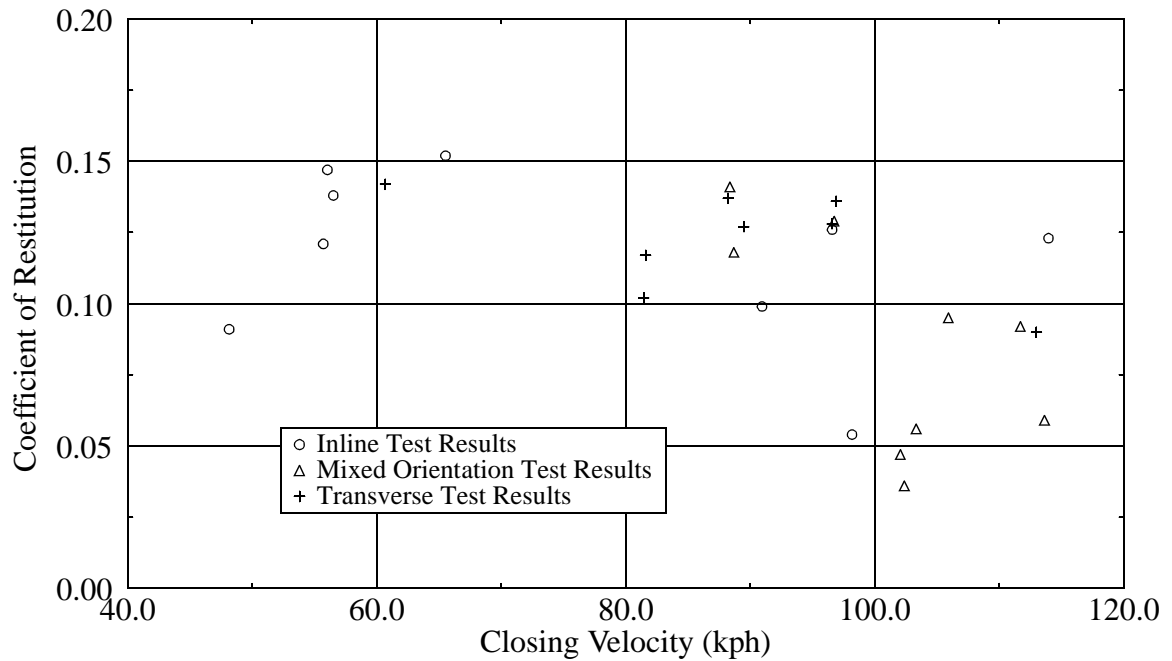


FIGURE 5.32 Coefficient of Restitution v. Closing Velocity by Engine Orientation -- Vehicle-to-Vehicle Full-Frontal Collisions; Passenger Type Vehicles

5.4.1.2 Engine Orientation

Because research into vehicle-to-barrier collisions shows engine orientation to be influential on the coefficient of restitution, the data of Figure 5.31 are further studied by separating them according to the involved vehicles' engine orientations. Figure 5.32 presents the coefficient of restitution, again as a function of closing velocity, for tests where the two colliding vehicles both have inline engines and both have transverse engines and where both orientations are represented in one collision. Front-to-rear cases are categorized according to the engine orientation of the striking vehicle. Nine, nine, and eight of the tests apply to inline, mixed, and transverse categories, respectively. The figure doesn't show any particular trends associated with engine orientation for the presented vehicle-to-vehicle cases. It is apparent, though, that the decrease in coefficient of restitution magnitude at 82 kph is represented only by transverse engine tests, so it is unknown whether the decrease applies to other orientations. The low coefficient values around 100 kph result mostly from tests with mixed orientations. One inline engine test, however, also gives a low coefficient at that speed.

5.4.2 Comparison of Vehicle-to-Vehicle and Vehicle-to-Barrier Restitution Magnitudes

The nature of restitution in vehicle-to-vehicle collisions is further investigated by comparing coefficient of restitution magnitudes obtained in vehicle-to-vehicle and vehicle-to-fixed rigid barrier tests. All applicable tests are studied first from a general perspective, after which only collisions of identical vehicles are considered. In addition to discussing the relative magnitudes of VTV and VTB coefficient values, the first section studies the accuracy of the relations developed by Howard and Prasad, as given in Equations 2.7 and 2.8, respectively, for predicting VTV coefficient values from VTB test results.

5.4.2.1 General

5.4.2.1.1 VTV and VTB Coefficient Magnitude Comparisons

Nine total full-width, vehicle-to-vehicle tests where comparable barrier impacts had been performed were found in the NHTSA's database. In every case, the coefficient of restitution for the vehicle-to-vehicle case was smaller than both coefficients associated with comparable barrier impacts of the colliding vehicles. Figure 5.34 shows the percentage difference between VTV coefficients and VTB coefficients for comparable tests as a function of the closing velocity associated with the VTV collisions. The

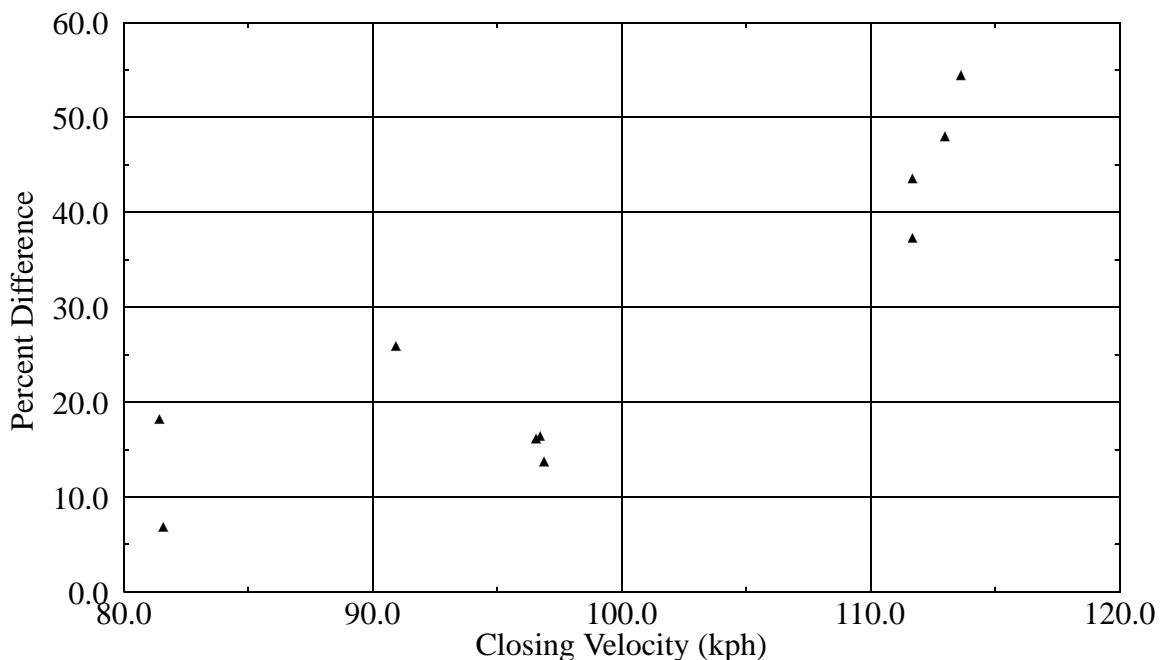


FIGURE 5.34 Percentage Difference Between Coefficient of Restitution Values for VTV and VTB Collisions v. VTV Closing Velocity

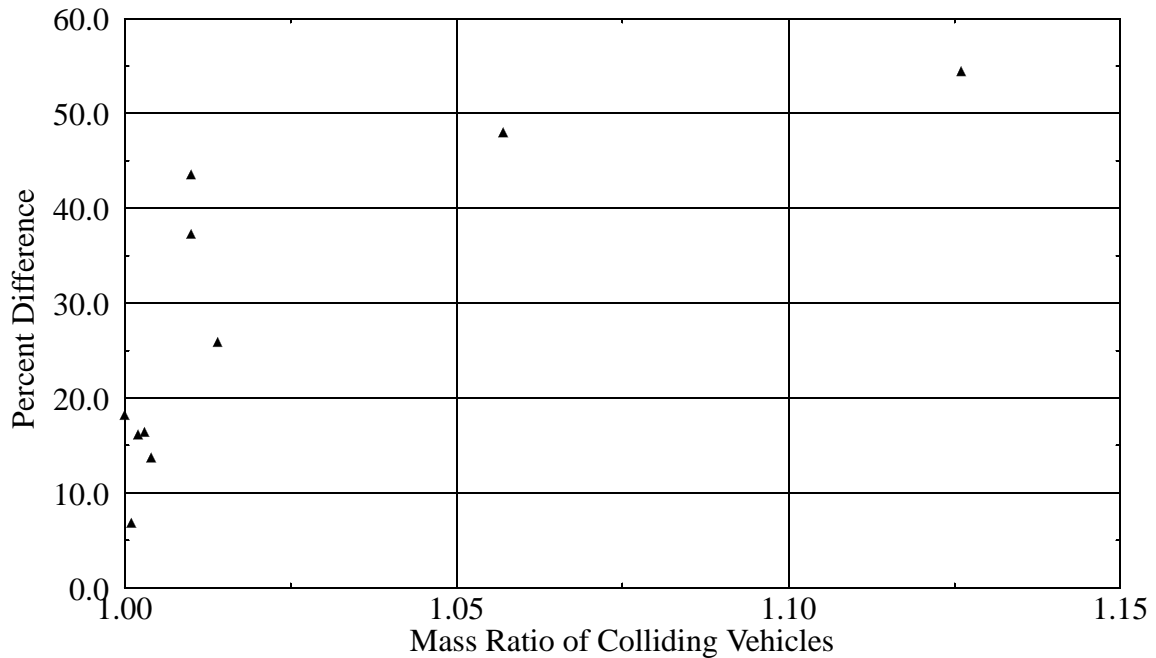


FIGURE 5.35 Percentage Difference Between Coefficient of Restitution Values for VTV and VTB Collisions v. Mass Ratio of Colliding Vehicles

percentage is calculated as the ratio of the VTV coefficient and the average of the comparable VTB coefficients subtracted from one, as given by Equation 5.1. Ten points are shown in the figure because for one of the VTV tests, there were two sets of comparable barrier impact tests available. The data show that the difference between

$$Percent = 1 - \frac{2 \times \epsilon_{AB}}{\epsilon_A + \epsilon_B} \quad (5.1)$$

coefficient values for the two tests increases with increasing closing velocity. Figure 5.35 seems to indicate that the percent difference in the coefficients is also a function of the mass ratio of the colliding vehicles. The mass ratio was calculated so that it is always greater than one. According to the figure, increase in percent difference is dramatic with a slight increase in mass difference, while, as mass difference becomes larger, the increase in percent difference is considerably less dramatic. The percent difference between the coefficients for cases with mass ratios near 1.0 is around 15%, while it increases to 55% for the case with a mass ratio of 1.126. The four points with the highest percent difference value in both figures are cases with relatively high mass ratios and are from tests performed at relatively high velocities. In Figure 5.34, these four coefficients are shown just above 110 kph. The point with the highest percent difference is also the point with the

highest mass ratio. Even though the other three points are from tests performed at approximately the same impact velocity, their percent difference values decrease with their mass ratios. From the data presented in the figures, it is apparent that both closing velocity and mass difference are influential in the magnitude of the difference between vehicle-to-vehicle coefficients and comparable vehicle-to-barrier coefficient values.

5.4.2.1.2 Accuracy of Published Equations for VTV and VTB Coefficient Relation

The same ten tests presented in Figures 5.34 and 5.35 were applied to Equations 2.7 and 2.8 developed by Howard and Prasad, respectively, for deriving a full-width, vehicle-to-vehicle coefficient of restitution from barrier test coefficients for the colliding vehicles. Table 5.14 shows the calculated value of the coefficient of restitution for each test and the

TABLE 5.14 Closing Velocity, Mass Ratio, Calculated Coefficient of Restitution, and Predicted Value and Percent Error for Equations 2.7 and 2.8; VTB to VTV Comparison

NHTSA Crash Test No.	Closing Velocity (kph)	Mass Ratio	ϵ Calculated	Equation 2.7		Equation 2.8	
				ϵ	Percent Error	ϵ	Percent Error
456	113.62	1.126	0.059	0.136	56.98	0.136	56.82
132	112.98	1.057	0.090	0.172	47.79	0.171	47.51
447	111.68	1.010	0.092	0.165	44.42	0.164	44.35
447	111.68	1.010	0.092	0.147	37.61	0.147	37.68
824	90.93	1.014	0.099	0.136	27.16	0.134	26.11
974	81.43	1.000	0.102	0.125	18.22	0.125	18.22
976	81.59	1.001	0.117	0.125	6.84	0.125	6.84
796	96.56	1.002	0.126	0.150	16.16	0.150	16.16
804	96.72	1.003	0.129	0.154	16.44	0.153	16.23
785	96.88	1.004	0.136	0.157	13.74	0.157	13.74

predicted values of the two equations, along with the percent error associated with each prediction. Test 447 is included twice because two sets of comparable vehicle-to-barrier tests were utilized. The table demonstrates that errors are significant, although the errors associated with the two approaches are remarkably similar. Cases where the exact same errors are reported are generally associated with mirror impacts, so mass ratios are basically equal to 1.0. The two approaches reach the same conclusion in these cases because they are mass-weighted and stiffness-weighted averages, respectively. Thus, for two equal barrier coefficients, both equations predict the same value for the VTV collision. Percent error appears to increase with closing velocity and mass ratio.

5.4.2.2 Identical Vehicle Cases

Table 5.15 outlines the three cases where identical-vehicle tests were available. Two VTV tests are compared to one VTB test in the case of the Chevrolet Cavalier. Otherwise,

TABLE 5.15 Comparison of the Coefficient of Restitution (ϵ) in Vehicle-to-Barrier and Vehicle-to-Vehicle Tests of Identical Vehicles at Barrier Equivalent Velocity

Test Vehicle (Engine Orientation)	Vehicle-to-Barrier				Vehicle-to-Vehicle			
	Model Year	Test No.	Impact Velocity (kph)	ϵ	Model Year	Test No.	Closing Velocity (kph)	ϵ
Chevrolet Cavalier (T)	1984	975	41.20	0.125	1984	974	81.43	0.102
					1984	976	81.59	0.117
Honda Accord (T)	1987	1054	47.48	0.157	1984	785	96.88	0.136
Renault Fuego (I)	1982	872	48.12	0.150	1983	796	96.56	0.126

one test of each type is presented for each vehicle. A structure change was made in the Accord between the compared model years, but its test results seem consistent enough with those of the other presented tests to indicate that the change in structure did not affect the coefficient of restitution and to warrant inclusion of the Accord case in this study.

The Cavalier barrier test was conducted at 41.20 kph, just greater than half the speed of the two reported VTV tests. The barrier test, in this case, results in a coefficient of restitution that is greater by about 0.015 than the average of the two VTV tests. Barrier tests for the Honda Accord and the Renault Fuego similarly show the coefficient of restitution for the barrier tests at 48 kph to be around 0.02 higher than the coefficient for the VTV tests at 96 kph. As reported in the previous section for collisions with mass ratios near 1.0, vehicle-to-vehicle values, on average, are about 15% lower than vehicle-to-barrier values. From the reported 48 kph collisions, engine orientation apparently has no influence on the magnitude of the difference. The Fuego results, are, however, based upon accelerometers mounted at positions lateral to the vehicle centerline.

In order to more deeply examine the relationship between vehicle-to-barrier and vehicle-to-vehicle tests of identical vehicles at barrier equivalent velocities, velocity traces for the tests outlined in Table 5.15 are presented in Figure 5.36. Parts (a-c) of the figure show results for the Cavalier, the Accord, and the Fuego, respectively. Traces are plotted such that individual vehicles in the vehicle-to-vehicle collisions are compared to the vehicles in the barrier collisions. Parts (a-b) of the figure, both involving vehicles with transverse oriented engines, show similar relationships between the vehicle-to-barrier

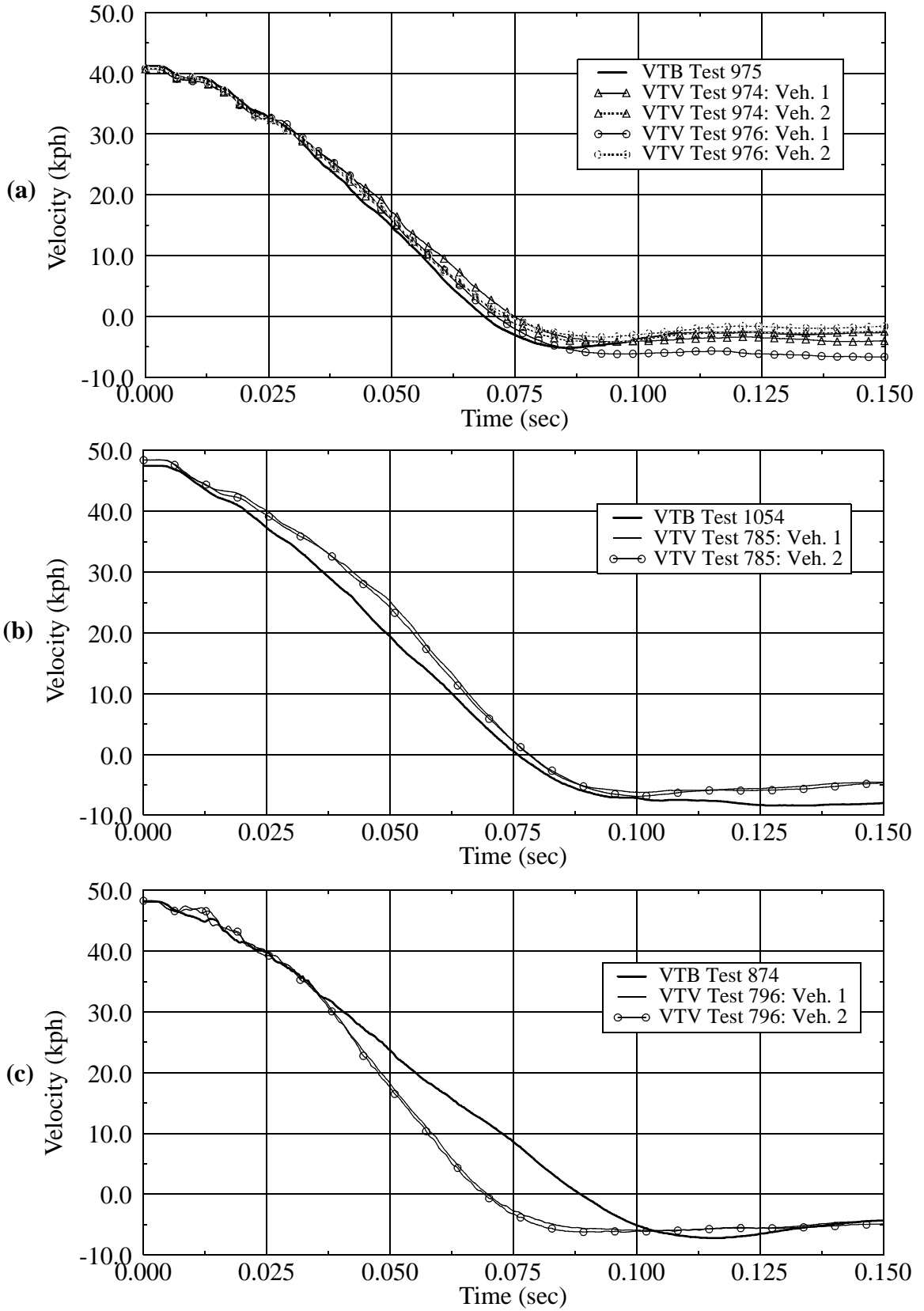


FIGURE 5.36 Velocity v. Time -- Vehicle-to-Barrier v. Vehicle-to-Vehicle. (a) NHTSA Tests 975, 974, 976, (b) NHTSA Tests 1054, 785, (c) NHTSA Tests 874, 796

traces and the individual vehicle velocities from the VTV collisions. In all three plots, the barrier traces reach a slightly higher rebound velocity in comparison to the VTV traces. In Figure 5.36(a), the trace representing vehicle one of Test 976 reaches a higher maximum rebound velocity than does the Cavalier VTB trace, but its partner vehicle has a significantly lower rebound velocity. As a result, the average between the two vehicles of Test 976 results in a lower rebound velocity than the VTB trace shows. In part (b) of the figure, maximum rebound velocity for the vehicle-to-barrier trace was taken at about 110 ms such that the physically unreasonable post-separation increase in rebound velocity was ignored. Parts (a) and (b) of Figure 5.36 also demonstrate that the vehicle-to-vehicle traces slightly lag the barrier traces. In part (c) of the figure, however, the vehicle-to-vehicle traces reach zero velocity about 20 ms before the vehicle-to-barrier trace. It is unknown if this is common to all vehicles with inline oriented engines.

5.4.2.3 Summary of VTV and VTB Restitution Comparison

The concept of obtaining a coefficient of restitution value for a vehicle-to-vehicle collision from the vehicle-to-barrier coefficients of the colliding vehicles is a very useful one, if it can be properly modeled. Closing velocity and mass difference are shown to be influential in differences between the test types' results. In the case of identical vehicles colliding, Equations 2.7 and 2.8 both predict a VTV coefficient equal in magnitude to the VTB coefficient of the vehicle. In this section, that has been shown to be inaccurate by about 15% for identical vehicle collisions, and by greater percentages for non-identical vehicle cases. Potential reasons for the slight drop in the magnitude of the coefficient of restitution in vehicle-to-vehicle collisions include that flat barrier collisions involve the entire front end of a colliding vehicle, without under-ride or over-ride. In addition, vehicle crush is more uniform in barrier collisions, involving hard as well as soft spots, so vehicle components are more evenly involved in energy restoration. Because the load distribution in a barrier collision is generally more uniform than for vehicle-to-vehicle cases, it is also likely that the ΔV is more nearly parallel with the ground.

5.5 PARTIAL-WIDTH VEHICLE-TO-VEHICLE COLLISIONS

Figure 5.37 shows coefficient of restitution results for 34 frontal vehicle-to-vehicle collisions as a function of percent overlap. Twenty-one of the tests are full-contact cases, which show a large degree of variation. The linear regression line for the individual data is also included, illustrating the tendency for the coefficient of restitution to decrease with percent overlap. Averages are also shown for 60 and 100 percent overlap cases. These results are similar to those shown for vehicle-to-barrier cases, where the coefficient tends to be higher for full-frontal tests than for partial-contact cases. The data in Figure 5.37 account for tests with closing velocities ranging from 61 to 118 kph, while Figure 5.38 shows results for two velocity bins centered about 96 and 114 kph. The 96 kph bin includes seven tests with closing velocities ranging from 94 to 97 kph, while the 114 kph bin shows the results of thirteen cases with velocities between 110 and 118 kph. Overlap bin averages are also shown where more than one test in the same velocity bin is reported. These cases validate the results of Figure 5.37 that the magnitude of the coefficient of restitution decreases with percent overlap.

Because the coefficient for each of the presented tests was derived using the average of the data from laterally symmetric, rear-mounted accelerometers, the influence of the normal component of any angular acceleration that may have occurred in the tests was not

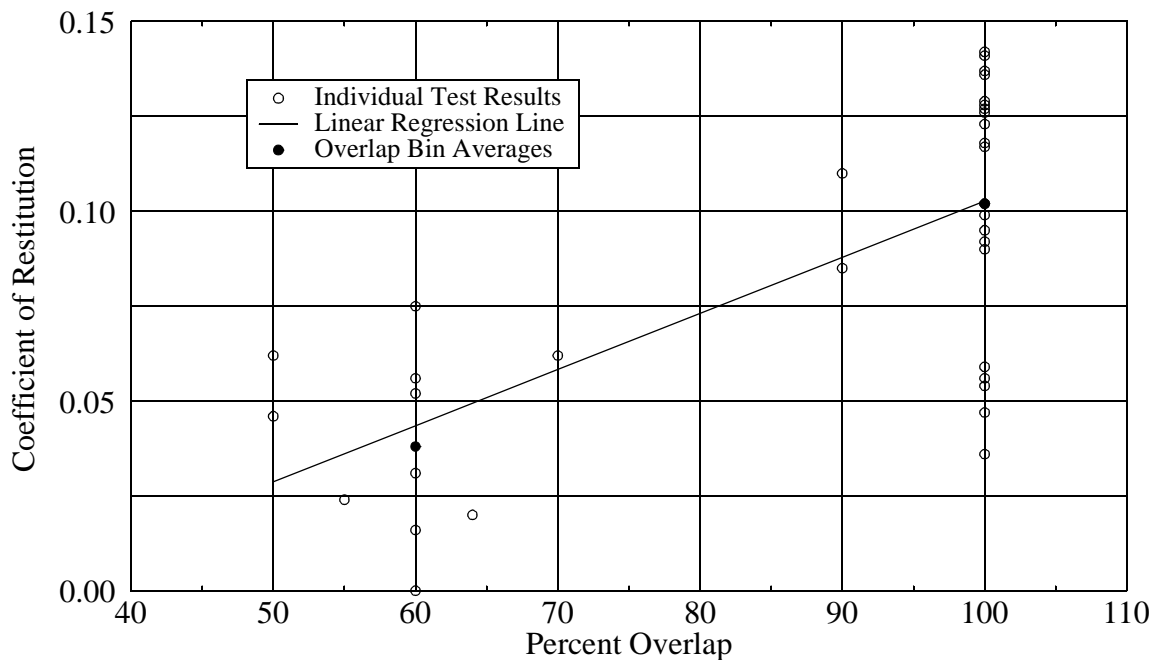


FIGURE 5.37 Coefficient of Restitution v. Percent Overlap -- Vehicle-to-Vehicle Frontal Collisions

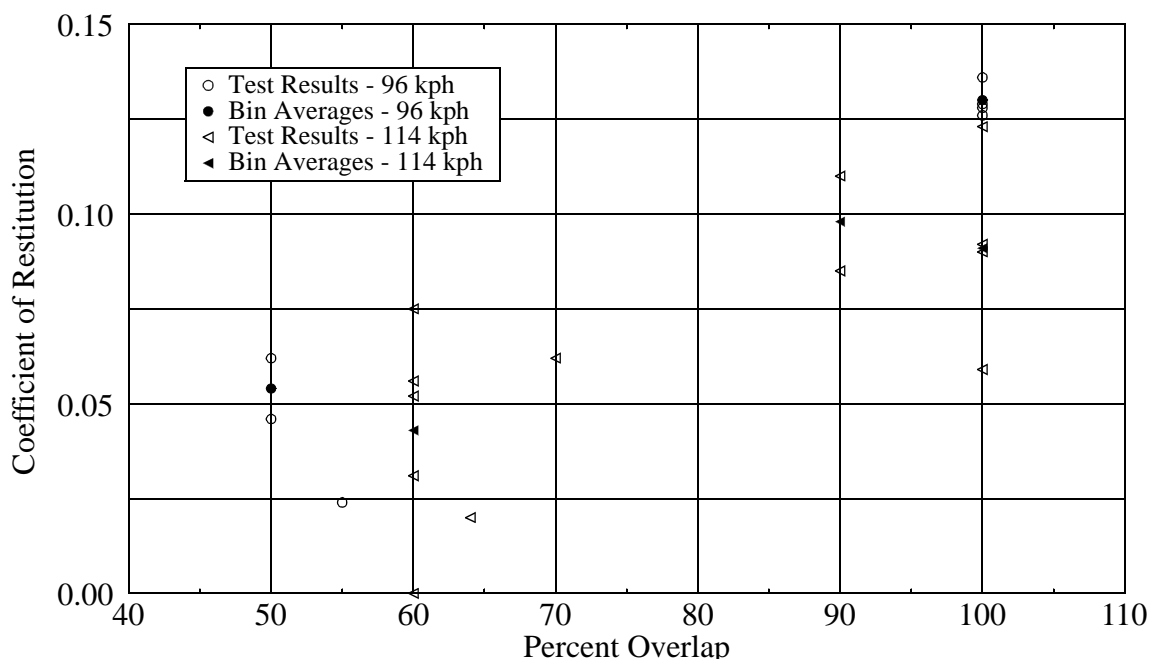


FIGURE 5.38 Coefficient of Restitution v. Percent Overlap -- Vehicle-to-Vehicle Frontal Collisions

eliminated as the influence of the tangential component was, resulting in lower calculated rebound velocities than actual. Based on rigid body assumptions, less overlap leads to more rotation and, therefore, greater reduction of the measured rebound velocity. As a result, it is suspected that the coefficient of restitution magnitudes for partial-contact cases reported in Figures 5.37 and 5.38 are slightly in error, giving lower values than actual, with the greatest error occurring in the cases with the least amount of overlap. Corrections in the data, however, are not expected to change the basic observation that the coefficient of restitution decreases with percent overlap, but the slope of a linear regression of the data would likely decrease in magnitude.

Although averaging the data from two symmetric, rear-mounted accelerometers provides a way to estimate the value of the coefficient of restitution in frontal, offset, vehicle-to-vehicle collisions, it doesn't fully express the nature of the velocity change at the positions of the accelerometers, as it cancels out velocity due to tangential acceleration. The most common accelerometer mounting positions for these tests are at the right and left rear seats, locations of particular interest since the rear seats may be occupied by passengers during actual collisions. The coefficient of restitution was calculated at these two positions prior to averaging by comparing the velocity at the left seat of one vehicle to the velocity at the left seat of the other. The same was done for the

right seat locations. Results are shown in Table 5.16. Offset in the presented collisions was always to the left, so, when rotation occurs, the magnitude of the coefficient of restitution is larger on the left than the right. Because of rotation, a passenger seated in the left rear seat would, therefore, experience a larger ΔV than one in the right rear seat in such a collision. It should be noted that the individual traces include the influence of both components of angular velocity. It is expected that if more data were available, the difference between the coefficients measured at the two locations would decrease as percent overlap increases. Negative values reported in most of the cases for the right rear seat indicate that the velocities never became negative due to rotation. The average of the two data signals is not always equal to the average of the reported coefficients for the two seats shown in the table because maximum negative velocities, or minimum velocities, didn't always occur at the same time in the individual traces.

TABLE 5.16 Coefficient of Restitution at Right and Left Rear Seats, Trace Average, and Difference, by Percent Overlap

Percent Overlap	Right Rear Seat	Left Rear Seat	Trace Average	Difference	NHTSA Crash Test No.
50	-0.002	0.094	0.046	0.096	864
50	0.062	0.066	0.062	0.004	845
55	-0.039	0.085	0.024	0.124	865
60	-0.024	0.017	0.000	0.041	1618
60	0.006	0.108	0.056	0.102	1665
60	-0.043	0.106	0.031	0.149	1666
60	-0.026	0.136	0.052	0.162	1544
60	-0.044	0.076	0.016	0.120	1551
60	0.033	0.118	0.075	0.151	1676
64	-0.072	0.118	0.020	0.190	1374
70	0.003	0.121	0.062	0.118	1770
90	0.085	0.085	0.085	0	1373
90	0.110	0.110	0.110	0	1372

5.6 SUMMARY

5.6.1 Restitution Magnitude

5.6.1.1 Impact Velocity

Coefficient of restitution results for frontal collisions of all studied collision and vehicle types demonstrate that restitution is a function of impact velocity. As impact velocity increases, the coefficient of restitution generally decreases. A contradiction of the decreasing coefficient trend is, however, shown to exist. In full-width vehicle-to-barrier collisions involving passenger vehicles, the coefficient of restitution is shown to decrease from about 0.27 at 8 kph (consistent with values reported by others for low-speed collisions) to values near 0.1 at around 70 kph. The increase in the coefficient's value generally appears between 48 and 56 kph. Tests on pickup trucks, sport utility vehicles, and vans also result in an increase of the coefficient in a similar impact velocity range. Coefficient values for other test types involving passenger vehicles, including partial-width barrier impacts, pole impacts, and full and partial-width vehicle-to-vehicle collisions, are generally lower than those determined for full-width vehicle-to-barrier tests at comparable velocities. Of these other test types, only partial-width barrier cases suggest a contradiction of the decreasing coefficient trend.

5.6.1.2 Engine Orientation

Engine orientation does not appear to be significant in the magnitude of restitution, except where the mentioned contradiction of the decreasing coefficient trend occurs. For all studied vehicle types in full-width vehicle-to-barrier collisions, the magnitude of the increase in the coefficient of restitution associated with the contradiction, and possibly the impact velocity at which it occurs, are shown to be dependent upon engine orientation. In passenger vehicles with transverse engines, the trend reversal occurs between 48 and 56 kph, with respective average coefficient values of 0.129 and 0.153. Tests involving inline engine passenger vehicles, on the other hand, show no trend contradiction, resulting in average coefficient of restitution values of 0.151 and 0.148 for impact velocities of 48 and 56 kph, respectively. Engine orientation is not, however, found to be influential in other types of tests involving passenger vehicles.

5.6.1.3 Repeated Impact

Study of repeated impact tests shows that multiple impacts involving the same vehicle generally tend to increase restitution. In repeated impacts, it is likely that the increased restitution is due to an increase in the percent of crush energy stored by relatively elastic components of the vehicle as less plastic portions of the structure lose their ability to store, or dissipate, energy.

5.6.1.4 Overlap

A comparison of partial-width tests and related full-width tests indicates that as percent of overlap decreases, the magnitude of restitution decreases. Pole impact tests, on average, similarly result in lower average coefficient of restitution values than full-width tests at the same impact velocity.

5.6.1.5 Barrier Impacts Compared to Vehicle-to-Vehicle Collisions

A small set of vehicle-to-vehicle collisions with comparable barrier impacts demonstrate that differences between the test types' coefficient values are influenced by closing velocity and the mass ratio of colliding vehicles. Based on the analyzed data, VTV coefficients are always smaller than barrier impact values at comparable speeds. Mirror impact vehicle-to-vehicle coefficient of restitution values are, on average, about 15% smaller than comparable vehicle-to-barrier coefficients. Tests involving non-identical vehicles result in even greater differences. Equations developed to predict the VTV coefficient from barrier values are shown to be subject to a similar magnitude of error.

5.6.1.6 Differences in Colliding Vehicles' Masses

Linear regression the coefficient of restitution determined from full-width vehicle-to-vehicle tests indicates a tendency for the coefficient's value to decrease as the difference between the colliding vehicles' masses increases.

5.6.2 Restitution Mechanisms

Restitution is shown to be related to depth of vehicle crush and what vehicle components are engaged by the crush. The unexpected increase in transverse engine vehicles is speculated to be a result of engine contact with the cowl panel region occurring at velocities higher than 48 kph. Restitution behavior in inline engines is considered to be due to the engine (and satellite components) contacting the cowl panel at 48 kph and/or the restitution properties of the drive shaft and connected rear-end components.

Chapter 6: Side Collision -- Crash Test Results and Restitution

As shown in Chapter One, side collisions occur about one-fourth as often as frontal collisions. When they do occur, however, occupant injuries are generally slightly more severe than they are for frontals, according to Figure 1.3. The influence of restitution in side impact collisions is investigated by studying impactor-to-vehicle crash tests performed under the direction of the NHTSA.

6.1 INFLUENTIAL PARAMETERS

6.1.1 Impact Velocity

Figure 6.1 presents estimated coefficient of restitution magnitudes for 33 impactor-to-vehicle, side impact crash tests as a function of impact speed. As the figure shows, most of the available tests for side impact cases were executed at impact velocities around 48 kph. The results include all analyzed side collision cases, regardless of offset and principal direction of force. Seven of the tests were conducted with a principal direction of force of 270 degrees, while the remaining 26 tests were executed to give a PDOF of 280 degrees. No difference associated with the small difference in angle was apparent in test results, so they are included together in the analysis. The plot shows individual test results as well as

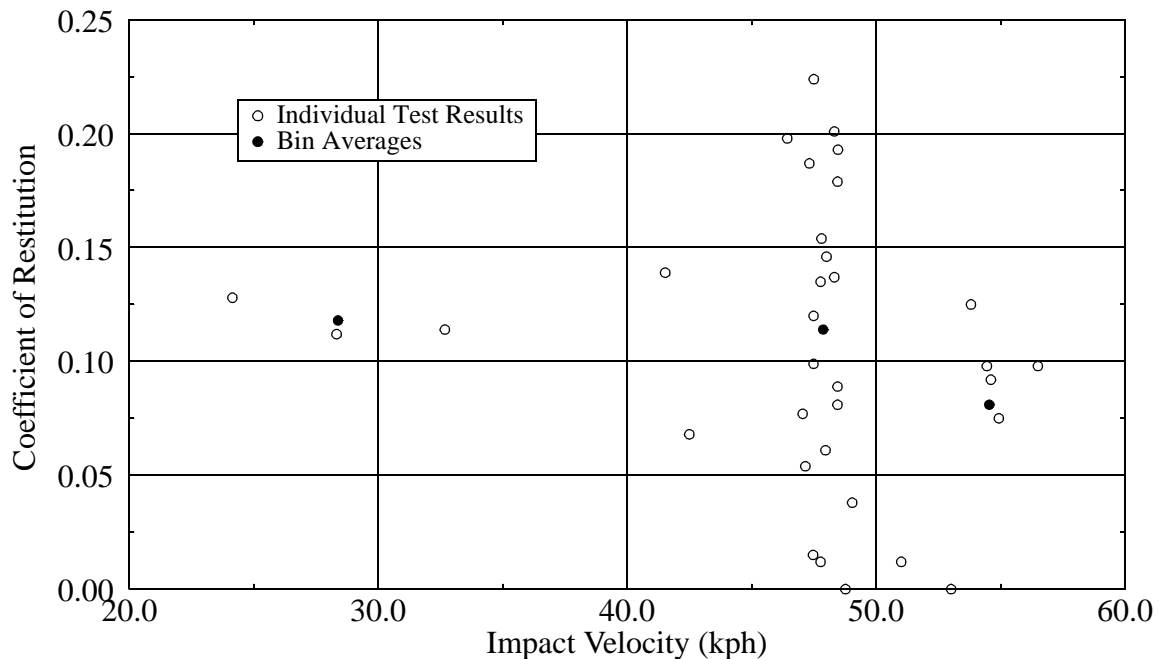


FIGURE 6.1 Coefficient of Restitution v. Impact Velocity -- Side Collisions: NHTSA Deformable Impactor-to-Vehicle; Passenger Vehicles

bin averages. It is apparent from the figure that there is a large amount of variation in the magnitude of the coefficient of restitution for side impacts, especially at impact velocities around 48 kph. Because it does not remove the influence of angular acceleration from the analyzed traces and relies upon only one accelerometer for each vehicle, the technique used to approximate rebound velocities for side impacts is expected to introduce a degree of error in the calculated coefficient of restitution, but it is not anticipated that it would introduce enough error to mask the effect of influential parameters. Even with the large variation in coefficient values, the figure vaguely suggests that the magnitude of the coefficient of restitution decreases slightly as impact velocity increases. The relative magnitudes of the coefficient at 48 and 55 kph is further investigated in Table 6.1 by

TABLE 6.1 Coefficient of Restitution at 48 and 55 kph for Comparable Collisions; Impactor-to-Vehicle Side Impact

Impact Velocities Around 48 kph				Impact Velocities Around 55 kph			
NHTSA Test No.	Vehicle Description	Offset (mm)	ϵ	NHTSA Test No.	Vehicle Description	Offset (mm)	ϵ
1921	93 Acura Legend	nr	0.146	1960	93 Acura Legend	nr	0.125
1961	93 Honda Civic	nr	0.154	1962	93 Honda Civic	nr	0.092
2087	94 Honda Accord	102	0.120	1867	92 Honda Accord	135	0.075

comparing tests that involve related vehicles at the two speeds. Of the three cases shown, offset is not reported for two of them, so it is difficult to know how closely they can be compared. If offset is not considered, the table verifies that, within the narrow velocity window shown, the coefficient of restitution has a tendency to decrease with increasing impact velocity. If the bin averages in Figure 6.1 are utilized, it appears that expected magnitudes for the coefficient at 48 and 55 kph are around 0.12 and 0.08, respectively. It is interesting to note that the expected value for side collisions at 48 kph is approximately equal to that expected for frontal collisions involving transverse engine vehicles at the same speed, while the expected magnitude at 55-56 kph for frontal collisions are significantly higher than for side impacts.

6.1.2 Offset

Offset distance (the longitudinal distance between the impact point and the center-of-gravity of the struck vehicle) is anticipated to be influential in side collisions. The impact point is defined to be the center of initial barrier contact on the struck vehicle. Offset

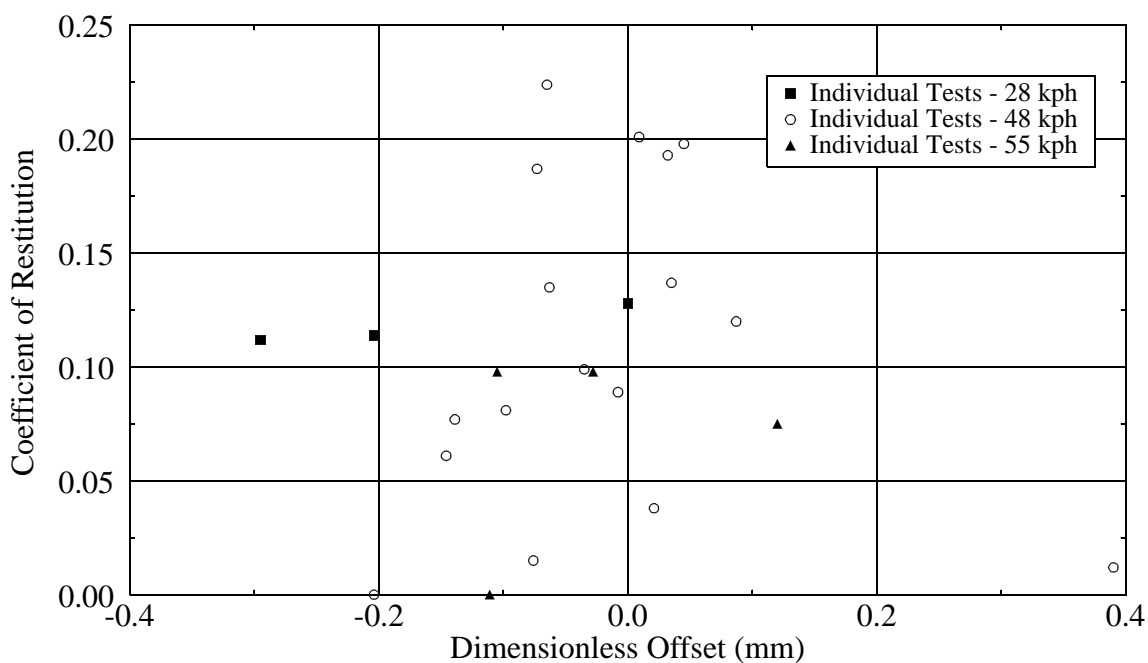


FIGURE 6.2 Coefficient of Restitution v. Dimensionless Offset -- Side Collisions: NHTSA Deformable Impactor-to-Vehicle; Passenger Vehicles

distance for most of the 48 kph tests varies by about 770 mm, while offset distance variation in tests at speeds around 28 and 55 kph is less than half that, so it is likely that the large spread in coefficient results is partially due to offset variation. Figure 6.2 shows the coefficient of restitution as a function of dimensionless offset, calculated as the percent of the distance from the vehicle center-of-gravity to the front and rear axle for offsets forward and rearward of the center-of-gravity, respectively. Results are shown for tests with impact velocities around 28, 48, and 55 kph. The figure, however, suggests that the coefficient of restitution does not appear to be a function of dimensionless offset, at least in the range of offset the analyzed tests give. Although it is not visible in the analyzed side impact data, it is expected that the magnitude of the coefficient of restitution would be influenced by larger dimensionless offset magnitudes that involve the stiff region of the axles.

6.1.3 Other Parameters

The influence of the difference between vehicle and impactor masses on the coefficient of restitution for side impact cases was also investigated but no indications of any influence were detected.

6.2 CASE STUDY - 1982 NISSAN SENTRA

In an effort to determine the error introduced into the coefficient of restitution results by estimating its magnitude without accounting for the influence of rotation, the coefficient's value is rigorously determined for one case and compared to the estimated value. The chosen test, NHTSA Test 820, involves a 1982 Nissan Sentra, with an impact point located 41 mm forward of the vehicle center-of-gravity. The crash test was performed to test compliance according to FMVSS 214, so the impactor was crabbed at 27 degrees, resulting in a principal direction of force of 280 degrees. Using accelerometers mounted at the impactor's center-of-gravity and the Sentra's right rear sill, the estimated value of the coefficient of restitution is 0.137. Accelerometers located at the right front and rear sills and rear deck of the vehicle, along with accelerometers at the impactor center-of-gravity and left rear, were utilized in the rigorous analysis.

Using MOMEX, a momentum exchange software package, to match the test's accelerometer data, the position of the impulse center, denoted by an X on a small circle in Figure 6.3, was estimated to be 64 mm rearward and 635 mm to the left of the Sentra center-of-gravity. Its location with respect to the impactor center-of-gravity is 1969 mm forward and 356 mm to the right. With the impulse center located as shown, the principal direction of force, as determined by the software, is 285 degrees with reference to the Sentra, while the test report gives a PDOF of 280 degrees. A coefficient of restitution of

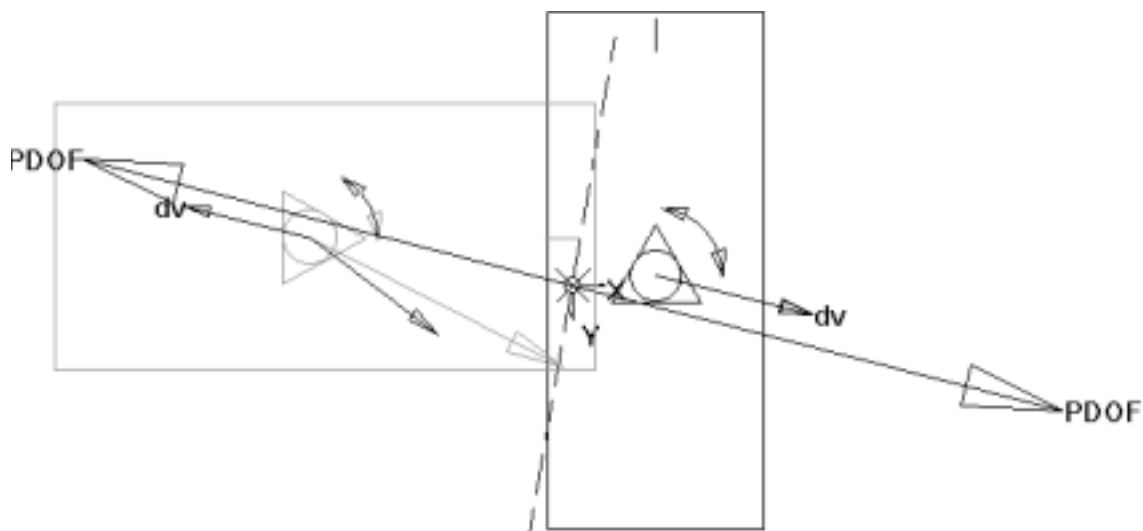


FIGURE 6.3 MOMEX Results for NHTSA Test 820: Crabbed Impactor into Side of 1982 Nissan Sentra

0.1, with the impact plane set at 80 degrees as shown by the dashed line in Figure 6.3, was used to approximate the impulse center location. It is interesting to note that in a run where the coefficient was set to 0.0, the resulting angular velocities changed by less than 0.1 radians/second when compared to the case with restitution. It is apparent, therefore, that restitution has very little influence on rotation in this case. Complete MOMEX settings and results for this analysis are included in Appendix C. Once the location of the impulse center was accurately estimated, velocities at the locations on the two vehicles corresponding to the impulse center were calculated. Figures 6.4 and 6.5 show the results for the Sentra and impactor, respectively. In these figures, the X direction is relative to the vehicle coordinate system, referring to the forward direction of the vehicle. Sentra velocities in the figure were derived from the right rear sill accelerometer, while center-of-gravity accelerometer data were applied for the impactor. As a point of interest, Figure 6.4 also displays the magnitude of the velocity due to normal acceleration, affecting the right rear accelerometer. It never reaches a velocity greater than about 1 kph and, therefore, is not very influential in this case. Velocity differences at different points on the vehicles are due to the influence of angular velocity, with the extent of each component's influence varying depending on the relative positions of points of interest. Using the derived impulse center velocities, x and y-direction components of velocity were combined and the components of the two vehicles' velocities in the direction of the PDOF were applied to

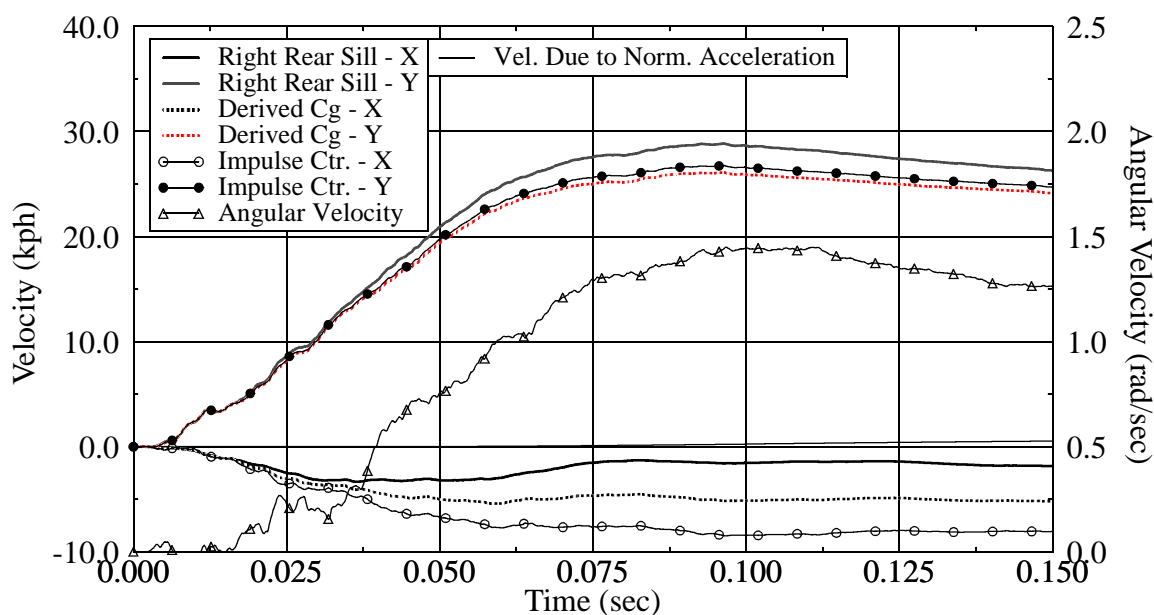


FIGURE 6.4 Nissan Sentra Velocities - Derived from Right Rear Sill Accelerometer; NHTSA Test 820

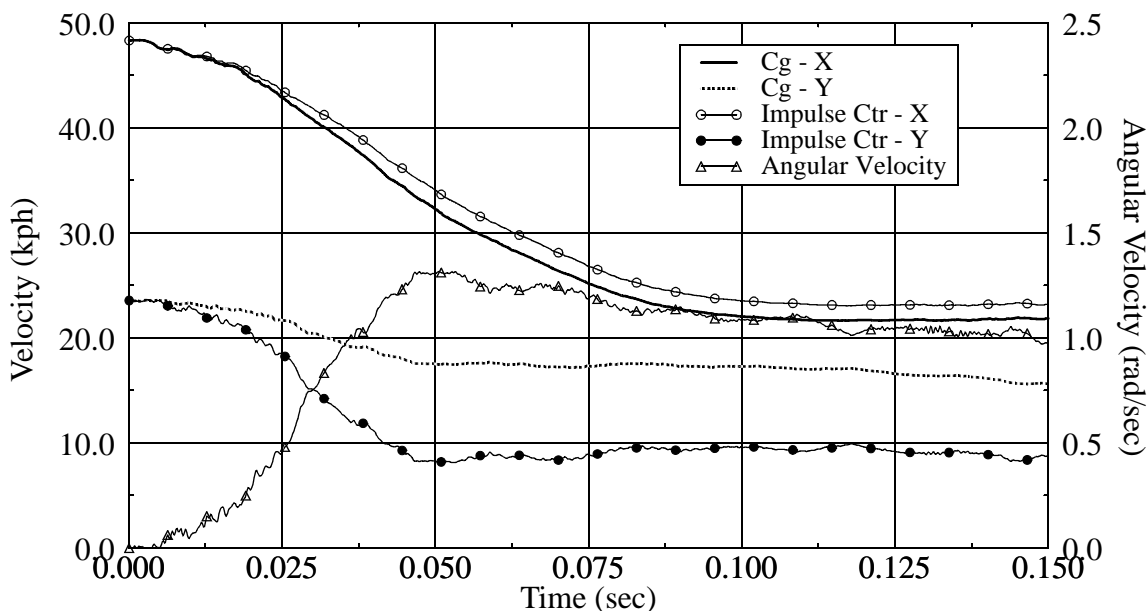


FIGURE 6.5 Impactor Velocities - Derived from Center-of-Gravity Accelerometer; NHTSA Test 820

determine the coefficient of restitution. Figure 6.6 presents velocities at the impulse center of both vehicles, as determined by two impactor accelerometers and three Sentra accelerometers. The difference between impactor and Sentra velocities determine the closing and rebound velocities needed to calculate the coefficient of restitution. Because of variability in the signals, two difference curves are presented in the figure that give the

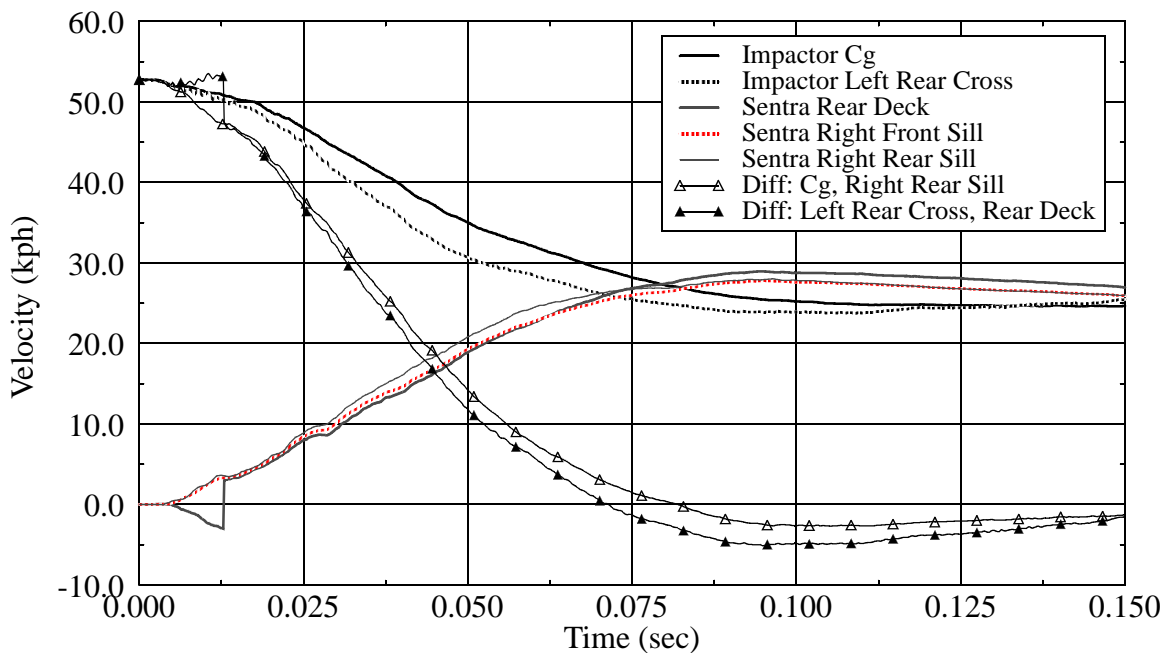


FIGURE 6.6 Derived PDOF Components of Impulse Center Velocities for the Nissan Sentra and the Impactor Using Various Accelerometers; NHTSA Test 820

largest and smallest differences available with the applied accelerometers. Table 6.2 shows closing and rebound velocities, along with calculated coefficient of restitution values, associated with the two difference traces. The calculated magnitudes of the coefficient of

TABLE 6.2 Closing Velocity, Rebound Velocity, and Coefficient of Restitution for Upper and Lower Bound Difference Curves; NHTSA Test 820

	Closing Velocity (kph)	Rebound Velocity (kph)	ϵ
Upper Bound	52.76	5.13	0.097
Lower Bound	52.76	2.65	0.050

restitution are low compared to the estimated value of 0.137. The estimated value resulted from using the forward velocity of the impactor at its center-of-gravity and the lateral velocity of the Sentra at its right rear sill. These velocities, however, have a larger difference than do the components of the two vehicles' impulse center velocities in the direction of the PDOF. As a result, the coefficient of restitution is overestimated.

6.3 SUMMARY

Based on estimates made of the coefficient of restitution, general analysis of the data does not appear to demonstrate that impact velocity has any influence on the magnitude of restitution in side impact cases. Individual comparisons, however, of same vehicle models in collisions with similar offsets show that restitution does decrease with increasing impact velocity. These individual cases give coefficient values of around 0.13 and 0.10 at impact velocities of 48 and 56 kph, although there is significant variation between the cases. Dimensionless offset was also studied as a possible influential parameter, but no relationship is visible. It is likely that it is influential, but its effect is not apparent because of scatter in the estimated data. It is also possible that the coefficient of restitution in side impacts does not change significantly in the small range of offset tested.

A case study of a test involving a 1982 Nissan Sentra shows that the error introduced into the coefficient of restitution's value by the applied estimation technique is significant; the estimated value is 0.137, while rigorous analysis envelopes the value between 0.097 and 0.050. Magnitudes of error likely vary from test to test based on the extent of offset. If information is available, it is preferable to perform a rigorous analysis in cases where rotation is influential.

Chapter 7: Rear Collision -- Crash Test Results and Restitution

Rear collisions occur at a frequency similar to that of side collisions but result in average MAIS values of about half the magnitude of those experienced in side collisions. Restitution in rear impact cases is determined and the influence of various parameters is investigated.

7.1 INFLUENTIAL PARAMETERS

7.1.1 Impact Velocity

Coefficient of restitution results for 24 rigid impactor-to-vehicle tests and five front-to-rear vehicle-to-vehicle tests are presented in Figure 7.1. The impactor-to-vehicle tests were only available at closing velocities of 48 and 56 kph, as is evident from the figure. Bin averages for the test type at the two speeds, along with standard deviations and

TABLE 7.1 Coefficient of Restitution at 48 and 56 kph; Rigid Impactor-to-Vehicle Rear-Impact Collisions

48 kph			56 kph		
Coefficient Average	Standard Deviation	Number of Tests	Coefficient Average	Standard Deviation	Number of Tests
0.113	0.067	13	0.115	0.033	11

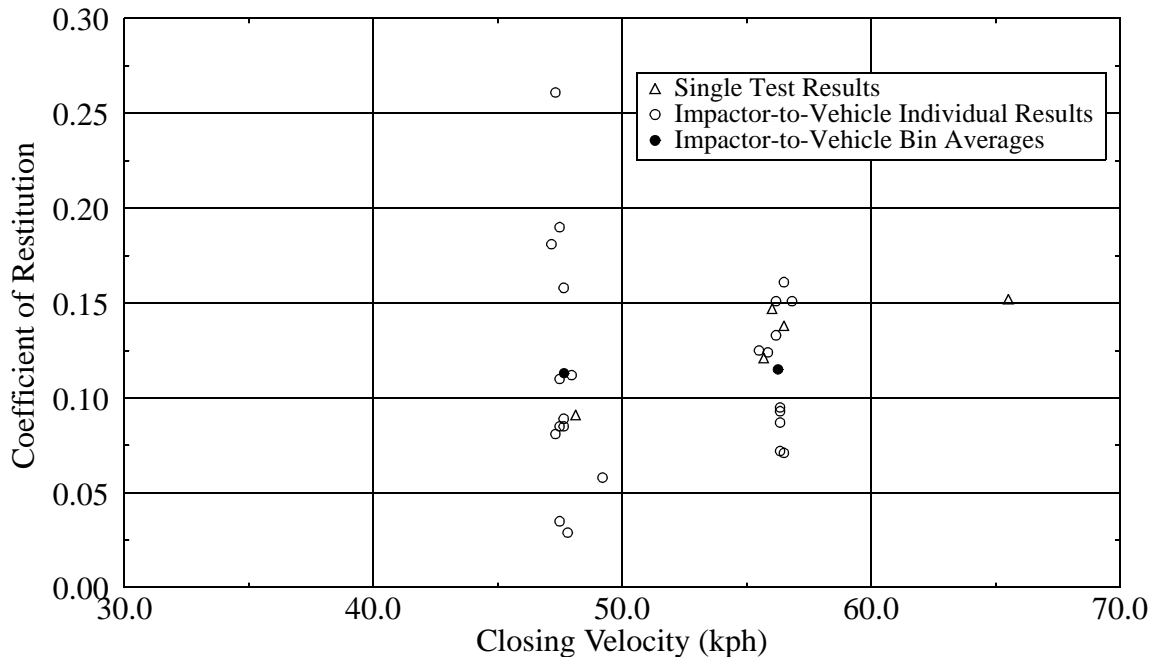


FIGURE 7.1 Coefficient of Restitution v. Closing Velocity -- Rear Collisions: Rigid Impactor-to-Vehicle and Front-to-Rear Vehicle-to-Vehicle; Passenger Vehicles

number of tests analyzed, are outlined in Table 7.1. The table shows that the averages are nearly equal to one another, but the standard deviation for the tests at 48 kph is more than twice as large as that given at 56 kph. Because no abrupt changes in stiffness are expected as the rear structure crushes (in contrast to the front and the engine), it is anticipated that rear impacts would produce restitution coefficients that decrease in magnitude with increasing impact velocity. Data at just 48 and 56 kph are, of course, not sufficient to determine behavior at other speeds, but it appears that the curve representing the functional relationship of the coefficient of restitution and impact velocity is quite flat in the region of the tested velocities.

The front-to-rear impact cases give coefficient magnitudes that lie close to the reported average values for impactor-to-vehicle tests, but the number of tests available make it difficult to conclude how the two test types compare. One front-to-rear test is also reported at about 65 kph. Front-to-rear collisions are more complex than barrier impacts, since they involve the complicated front structural characteristics of the striking vehicle as well as the struck vehicle's rear characteristics. In order to determine behavior, it is necessary to combine knowledge from study of barrier impacts for both front and rear collisions. The limited number and scope of tests of this type in the NHTSA database do not provide enough information for sufficient study, but barrier impact research provides foundational principles for rigorous study of more complex cases like front-to-rear impacts.

7.1.2 Other Parameters

The impactor-to-vehicle collision tests are further investigated by studying the magnitude of the coefficient of restitution as a function of the difference in mass between impactor and vehicle, vehicle width, and vehicle model year. Figure 7.2 shows these relationships in parts (a-c), respectively. Linear regression lines are included in the plots for mass difference and vehicle width. Part (a) of the figure shows that as the difference between the masses of the impactor and the struck vehicle increases, the coefficient of restitution decreases. In every case, vehicle mass was less than, or equal to, impactor mass. Conversely, part (b) of the figure demonstrates that as vehicle width increases, the coefficient of restitution also increases. In both plots, the slope of the regression line is steeper for tests at 48 kph than at 56 kph, although the behavior is manifest at both speeds. If cases at 48 kph are truly more easily influenced by these parameters, it would explain why the standard deviation of the data presented in Table 7.1 at that speed is so much

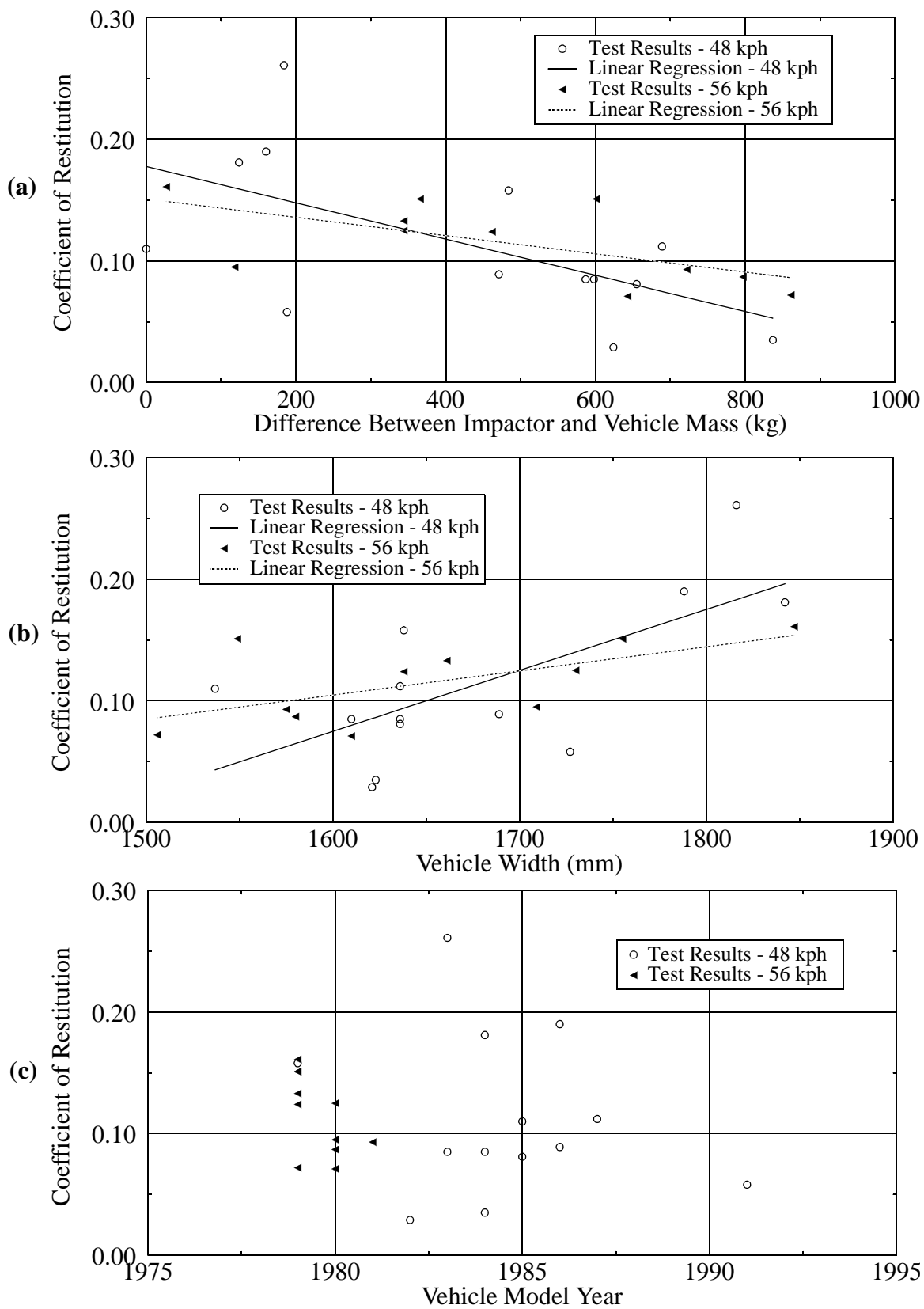


FIGURE 7.2 (a) Coefficient of Restitution v. Mass Difference, (b) Coefficient of Restitution v. Vehicle Width, (c) Coefficient of Restitution v. Vehicle Model Year; Rear Impactor-to-Vehicle

higher than that at 56 kph. It is interesting to note that vehicle mass and vehicle width are studied for their influence on the coefficient of restitution in full-frontal barrier collisions in Chapter Five but were found to not be influential. As has been mentioned, Prasad reports vehicle width to be influential for the full-frontal case. Perhaps the dominant influence of engine mass in the frontal cases masks the effect of vehicle width and possibly vehicle mass. Figure 7.2(c) is included to show the difference in the vehicle model years analyzed at 48 and 56 kph. 48 kph test model years centered around 1985, while 56 kph model years were mostly around 1980. The data are not sufficiently broad to draw conclusions on the influence of vehicle model year. As is the case for some other test types, the impactor-to-vehicle tests available for analysis generally involve early model vehicles. Tests have been and are performed on more recent vehicle models, but recent tests generally do not report data for the barrier, which is requisite for determining the coefficient of restitution.

7.2 SUMMARY

Because of scatter in coefficient of restitution data from rear impacts, no relationship with impact velocity is apparent. Average values demonstrate coefficient values around 0.12 at speeds of 48 and 56 kph. It is possible that the change in the coefficient's value in this small region of velocity is insignificant, but data are not available to determine whether or not this is true. Linear regression indicates that the coefficient of restitution is influenced by the magnitude of the difference of the colliding vehicles' masses, as was manifest by study of full-width vehicle-to-vehicle impacts in Chapter Five. As is the case for the vehicle-to-vehicle collisions, the coefficient in rear impacts decreases as difference in mass increases. Through linear regression, it is also apparent that vehicle width is influential in restitution in rear impacts. As vehicle width increases, the coefficient of restitution increases.

Chapter 8: Summary

8.1 ACCOMPLISHMENTS

The research objectives outlined in Chapter One of this thesis have been completed. A number of different types of collisions were investigated, including front, side, and rear directions of impact. In each case, expected values of the coefficient of restitution were determined, and collision/vehicle descriptors were investigated to determine their influence on the magnitude of the coefficient. Accomplishments of the research can be summarized as follows:

- (1) A total of 181 vehicle-to-barrier full-frontal collisions was analyzed, and magnitudes of the coefficient of restitution were determined for each case. One hundred and forty-two of the total number involved passenger vehicles, while ten, fourteen, and fifteen tests were analyzed for pickup trucks, sport utility vehicle, and vans, respectively.
- (2) Passenger vehicles in full-frontal, vehicle-to-barrier collision tests, 100 with transverse engines and 42 with inline engines, were further analyzed to determine the influence of various collision/vehicle parameters on the coefficient of restitution, including impact velocity and depth of crush, engine orientation, vehicle mass, engine displacement, vehicle length, vehicle width, wheelbase, distance from center-of-gravity to front axle, and vehicle model year. Data from contracted test labs were also compared, and repeatability of the coefficient of restitution in full-contact barrier collisions was outlined. The influence of repeated impacts was also investigated for inline engine cases. Expected magnitudes of the coefficient of restitution for given conditions were outlined. Three specific cases were studied to investigate the mechanisms influencing the coefficient of restitution in such collisions.
- (3) Coefficient of restitution values for full-frontal, vehicle-to-barrier tests involving non-passenger type vehicles were analyzed to determine influential parameters. Results were compared to those obtained for passenger vehicles in similar collisions.

- (4) The coefficient of restitution in frontal, partial-contact, vehicle-to-barrier collisions and pole impacts was investigated. Sixty-five percent overlap, vehicle-to-barrier tests and sixteen pole impact cases, centered as well as offset, were considered. Case studies, both for barrier and pole impact cases, were completed to investigate the mechanisms of restitution. Results were compared to full-frontal, vehicle-to-barrier results.
- (5) Full-frontal, vehicle-to-vehicle collisions involving passenger type vehicles were researched. Five of the tests analyzed were front-to-rear cases, and 21 were front-to-front tests. Coefficient of restitution magnitudes were compared to results from vehicle-to-barrier tests involving the same vehicles at barrier equivalent velocity. The accuracy of relations developed to predict the VTV coefficient value based on VTB coefficients was studied.
- (6) The coefficient of restitution for thirteen vehicle-to-vehicle, partial-contact, frontal collisions was determined and compared to full-frontal, vehicle-to-vehicle cases. The influence of restitution on rear-seated occupants in cases of restitution was also discussed.
- (7) The extent of restitution in 33 impactor-to-vehicle, side impact collisions, ranging in magnitude of offset, was estimated. One test was rigorously analyzed to determine the error introduced in the value of the coefficient through estimation techniques.
- (8) A total of 24 impactor-to-vehicle, full-contact, rear collisions was studied to investigate restitution in rear impact cases. The five front-to-rear impacts researched with the vehicle-to-vehicle full-frontal cases were also examined with the rear impact cases.

8.2 OBSERVATIONS AND CONCLUSIONS

Conclusions and observations associated with the research presented in this thesis may be stated as follows:

- (1) Regardless of impact direction, the coefficient of restitution is a function of impact velocity, which is directly related to extent of vehicle crush. As a general rule, the magnitude of the coefficient of restitution decreases as impact velocity, and crush depth, increase. For frontal barrier collisions, this trend is applicable

until a velocity where an upward offset in the value of the coefficient occurs. After the offset, however, the trend continues. The contradiction of the trend seems to occur as crush penetrates deep enough to engage the cowl panel region, which exhibits relatively elastic properties, resulting in relatively high restorative forces. With increasing velocity and further penetration, the coefficient of restitution again decreases. Engine orientation is a significant parameter in determining the depth of crush penetration. The velocity at which the trend contradiction occurs is generally between 48 and 56 kph for passenger vehicles with transverse engines, while it appears to occur earlier for cars with inline engines. The exact velocity at which crush penetrates deep enough to result in the increase in restitution is expected to vary for different vehicles. Non-passenger vehicles show similar behavior, although the magnitude of the increase in the coefficient varies with vehicle type. The influence of impact velocity on the coefficient of restitution in vehicle-to-vehicle collisions is not so defined because crush occurs at soft points in the vehicle rather than forcing crush into stiffer components. This generally results in lower coefficient values.

- (2) Overlap percent and vehicle width are influential in determining the extent of restitution, with overlap percent demonstrating greater influence than width. The coefficient of restitution increases as overlap increases and also increases slightly in full-contact collisions as vehicle width increases. Like impact velocity, these parameters are related to crush depth, which determines what components are engaged and the magnitude of the restorative forces. Fractional overlap collisions generally result in deeper crush, so transitions in the coefficient occur earlier than in full-contact cases.
- (3) In front and rear full-width, vehicle-to-vehicle collisions the magnitude of the coefficient of restitution decreases as differences between the masses of colliding bodies increase.
- (4) Coefficient of restitution values for vehicle-to-vehicle collisions are smaller than coefficients of comparable barrier impacts. For mirror impacts around 40 to 48 kph, the VTB coefficient is higher than the VTV case by about 15%. Differences for non-identical vehicles are higher.

- (5) In collisions that result in rotation, such as vehicle-to-vehicle, partial-overlap frontals, an occupant seated on the side of the vehicle center-of-gravity through which the line of action of force acts is subject to restitution-enhanced linear and angular accelerations, while accelerations due to restitution on the opposite side of the vehicle partially neutralize one another.
- (6) Repeated impacts generally result in coefficient of restitution values that are greater than coefficient values in comparable single impact tests.
- (7) For full-frontal collisions, the magnitude of the coefficient is higher in late model vehicles than in earlier models.
- (8) Results from different test labs sometimes show repeatable differences for identical tests.
- (9) The repeatability of test results increases significantly when multiple accelerometers, instead of one, are used to characterize vehicle dynamics.

8.3 RECOMMENDATIONS

- (1) The significance of restitution in occupant injury severity should be further characterized to provide greater motivation for its study. Perhaps it would be possible to design a sled test with no restitution that is identical to a barrier impact excepting the lack of restitution. Dummy kinematics could then be compared to clearly characterize the influence of vehicle restitution in terms of injury severity.
- (2) More data are needed for analysis of the coefficient of restitution in all collision geometries. The only case where enough data are available to firmly establish the behavior of the coefficient is full-frontal, vehicle-to-barrier collisions at 48 and 56 kph. It seems to have become common practice to not instrument the impactor in some impactor-to-vehicle collisions, probably because compliance with safety standards can be determined without it. Adding an accelerometer to the impactor center-of-gravity, however, would allow the tests to be analyzed for restitution, among other things.
- (3) Contradictions of the tendency for the coefficient of restitution to decrease with increasing impact velocity in frontal collisions need to be investigated. The influence of the cowl panel on the coefficient of restitution should be clarified through analysis of more tests. In order to investigate other points, further analysis needs

to be made at speeds between 15 and 48 kph and above 56 kph. Because engaging the front of the engine represents a significant change in stiffness, it represents another possible crush depth where a restitution increase may occur and should be further studied.

- (4) Vehicle crush stack-up needs to be studied more rigorously to determine how closely it follows patterns such as the one applied in this thesis, herein referred to as the "75% Rule."
- (5) More research should be conducted to determine the repeatability of differences in results between test labs.

References

1. Marquardt, James F., "Vehicle and Occupant Factors that Determine Occupant Injury," SAE 740303, 1974.
2. Emori, Richard I., "Vehicle Mechanics of Intersection Collision Impact," SAE 700177, 1970.
3. Strother, Charles E., "Velocity Histories as an Accident Reconstruction Tool," SAE 850249, 1985.
4. Tamny, Simon, "The Linear Elastic-Plastic Vehicle Collision," SAE 921073, 1992.
5. Brach, Raymond M., "Analysis of Planar Vehicle Collisions Using Equations of Impulse and Momentum," *Accident Analysis and Prevention*, Vol. 15, No. 2, pp. 105-120, 1983.
6. Smith, Russell A. and Tsongos, Nicholas G., "Crash Phase Accident Reconstruction," SAE 860209, 1986.
7. National Accident Sampling System, General Estimates System, 1988-1994; United States Department of Transportation, National Highway Traffic Safety Administration, National Center for Statistics and Analysis.
8. National Accident Sampling System, 1994 Crashworthiness Data System, Data Collection, Coding, and Editing Manual, United States Department of Transportation, National Highway Traffic Safety Administration, National Center for Statistics and Analysis, Washington, D.C., January 1994.
9. Howard, Richard P.; Bomar, John and Bare, Cleve, "Vehicle Restitution Response in Low Velocity Collisions," SAE 931842, 1993.
10. Siegmund, Gunter P.; King, David J., and Montgomery, Darcy T., "Using Barrier Impact Data to Determine Speed Change in Aligned, Low-Speed, Vehicle-to-Vehicle Collisions," SAE 960887, 1996.
11. Prasad, Alope Kumar, "Coefficient of Restitution of Vehicle Structures and its Use in Estimating the Total ΔV in Automobile Collisions," *Crashworthiness and Occupant Protection in Transportation Systems-1991 ASME*, Applied Mechanics Division, pp. 217-246.
12. Kerkhoff, John F.; Husher, Stein E.; Varat, Michael S.; Busenga, Alison M., and Hamilton, Kevin, "An Investigation into Vehicle Frontal Impact Stiffness, BEV and Repeated Testing for Reconstruction," SAE 930899, 1993.
13. Ishikawa, Hirotooshi, "Impact Model for Accident Reconstruction-Normal and Tangential Restitution Coefficients," SAE 930654, 1993.
14. Ishikawa, Hirotooshi, "Impact Center and Restitution Coefficients for Accident Reconstruction," SAE 940564, 1994.
15. Bailey, Mark N.; Wong, Bing C. and Lawrence, Jonathan M., "Data and Methods for Estimating Severity of Minor Impacts," SAE 950352, 1995.

16. Vehicle Crash Test Database (Internet Site: <http://www.nhtsa.dot.gov/nrd10/nrd11/databases.html>), United States Department of Transportation, National Highway Traffic Safety Administration.
17. Bundorf, R. Thomas, "Analysis and Calculation of Delta-V from Crash Test Data," SAE 960899, 1996.
18. Jones, N. and Birch, R.S., "Dynamic and Static Axial Crushing of Axially Stiffened Tubes," Journal of Mechanical Engineering Science, Vol. 204, No. C5, pp. 204-210, 1990.
19. Wood, Denis P. and Mooney, Stephen, "Modelling of Car Dynamic Frontal Crush," SAE 970943, 1997.
20. Germane, Geoff, MOMEX, 1997.
21. Personal communication with Jeff Sankey, Manager of Project Operations, TRC; July 1997.
22. Personal communication with John Fluck, Facility Director, MGA Research; July 1997.
23. The Hollander, 61st Edition, Auto-Truck Interchange, ADP Hollander Inc., 1995.

Appendix A

TABLE A.1 Crash Test Data Spreadsheet

The data in the Table A-1 are organized such that each set of three pages fully describes a set of crash tests. The first of each set of three pages includes general information that characterizes the test, such as force direction and impact velocity, along with descriptive information on the involved vehicle(s). The calculated coefficient of restitution is included on this page. The second page characterizes the crush profile, where given, of the tested vehicle and presents specific vehicle information related to this research. The third page in each set of three gives information on averaged accelerometers, shows comments, and presents information on differences in the coefficient of restitution at various locations on the vehicle. Tests that were not suitable for analysis are italicized. Units used in the chart are kph for velocity, mm for length, kg for mass, L for volume, seconds for time, and kph/sec for acceleration.

<u>Dir</u>	<u>Test Type</u>	<u>Ovrlp %</u>	<u>Veh Type</u>	<u>Eng Or</u>	<u>Off</u>	<u>Make</u>	<u>Model</u>	<u>Yr</u>	<u>Tst No.</u>	<u>Rep No</u>	<u>Imp Vel</u>	<u>Crsh</u>	<u>Imp Time</u>	<u>Zero Time</u>	<u>Reb Time</u>	<u>Reb Vel</u>	ϵ	<u>Crsh Δt</u>	<u>Rest Δt</u>	<u>Crsh Acc</u>	<u>Rest Acc</u>
F	VTDB	Pole	PAS	I		Renault	Fuego	83	847		48.12	352	0.000	0.088	0.117	-6.50	0.135	0.088	0.029	15.49	6.35
F	VTDB	40	PAS	I		Ford	Taurus	92	2290		64.40	nr	0.000	0.125	0.172	-7.15	0.111	0.125	0.047	14.59	4.31
F	VTDB	40	PAS	T		Honda	Accord	94	2286		63.90	nr	0.000	0.121	0.152	-5.64	0.088	0.121	0.031	14.96	5.15
F	VTDB	50	PAS	T		Ford	Taurus	92	2143		64.70	735	0.000	0.000	0.000	0.00	0.000	0.000	0.000		
F	VTDB	100	PAS	I		Volvo	244	75	13		72.58	847	0.000	0.102	0.149	-9.89	0.136	0.102	0.047	20.15	5.96
F	VTDB	100	PAS	T		Honda	Civic	75	18		65.66	545	0.000	0.091	0.139	-8.22	0.125	0.091	0.048	20.44	4.85
F	VTRB	Pole	PAS	I		Chevrolet	Caprice	92	2185		8.40	6	0.000	0.120	0.201	-1.97	0.235	0.120	0.081	1.98	0.69
F	VTRB	Pole	PAS	I		Chevrolet	Vega	73	709		32.35	200	0.000	0.095	0.126	-7.23	0.223	0.095	0.031	9.65	6.61
F	VTRB	Pole	PAS	I		Ford	LTD	82	666		48.44	nr	0.000	0.000	0.000	0.00	0.000	0.000	0.000		
F	VTRB	Pole	PAS	I	-241	Dodge	Omni	83	876		48.28	462	0.000	0.102	0.143	-9.54	0.198	0.102	0.041	13.41	6.59
F	VTRB	Pole	PAS	I	-241	Renault	Fuego	83	872		48.28	363	0.000	0.105	0.147	-6.42	0.133	0.105	0.042	13.02	4.33
F	VTRB	Pole	PAS	I	246	Dodge	Colt	81	473		0.00	202	0.000	0.000	0.000	0.00		0.000	0.000		
F	VTRB	Pole	PAS	I	292	Chevrolet	Vega	73	698		31.54	235	0.000	0.142	0.168	-3.03	0.096	0.142	0.026	6.29	3.30
F	VTRB	Pole	PAS	T		Dodge	Omni	83	846		47.96	525	0.000	0.106	0.135	-7.35	0.153	0.106	0.029	12.82	7.18
F	VTRB	Pole	PAS	T		Ford	Escort	87	1836	1	15.45	93	0.000	0.123	0.160	-2.66	0.172	0.123	0.037	3.56	2.04
F	VTRB	Pole	PAS	T		Ford	Escort	87	1837	2	15.77	142	0.000	0.074	0.114	-4.40	0.279	0.074	0.040	6.04	3.12
F	VTRB	Pole	PAS	T		Ford	Escort	87	1838	3	23.98	204	0.000	0.054	0.091	-7.31	0.305	0.054	0.037	12.58	5.60
F	VTRB	Pole	PAS	T		Ford	Escort	87	1839	4	32.19	340	0.000	0.046	0.071	-8.61	0.267	0.046	0.025	19.82	9.75
F	VTRB	Pole	PAS	T		Ford	Escort	87	1840	5	53.91	603	0.000	0.062	0.110	-12.42	0.230	0.062	0.048	24.63	7.33
F	VTRB	Pole	PAS	T		Ford	Taurus	86	2170	1	7.90	26	0.000	0.165	0.275	-2.57	0.325	0.165	0.110	1.36	0.66
F	VTRB	Pole	PAS	T		Ford	Taurus	86	2171	2	15.90	136	0.000	0.133	0.183	-4.76	0.299	0.133	0.050	3.39	2.70
F	VTRB	Pole	PAS	T		Ford	Taurus	86	2172	3	15.90	148	0.000	0.089	0.136	-5.75	0.362	0.089	0.047	5.06	3.47
F	VTRB	Pole	PAS	T		Ford	Taurus	86	2173	4	32.00	179	0.000	0.065	0.099	-8.30	0.259	0.065	0.034	13.94	6.91
F	VTRB	Pole	PAS	T		Ford	Taurus	86	2174	5	56.20	381	0.000	0.079	0.128	-9.86	0.175	0.079	0.049	20.15	5.70
F	VTRB	Pole	PAS	T		Ford	Tempo	85	1846		15.45	nr	0.000	0.127	0.172	-3.53	0.228	0.127	0.045	3.45	2.22
F	VTRB	Pole	PAS	T		Honda	Accord	84	819		48.28	478	0.000	0.107	0.154	-7.87	0.163	0.107	0.047	12.78	4.74
F	VTRB	Pole	PAS	T		Honda	Civic	81	449		32.19	190	0.000	0.000	0.000	0.00	0.000	0.000	0.000		
F	VTRB	Pole	PAS	T		Hyundai	Excel GLS	86	1648		15.29	105	0.000	0.104	0.141	-3.95	0.258	0.104	0.037	4.16	3.02
F	VTRB	Pole	PAS	T		Nissan	Sentra	85	1841		15.61	143	0.000	0.115	0.156	-3.96	0.254	0.115	0.041	3.84	2.74
F	VTRB	Pole	PAS	T	-330	Volkswagen	Rabbit	81	662		32.51	210	0.000	0.096	0.147	-6.45	0.198	0.096	0.051	9.59	3.58
F	VTRB	Pole	PAS	T	-241	Honda	Accord	84	873		48.28	480	0.000	0.119	0.171	-5.80	0.120	0.119	0.052	11.49	3.16
F	VTRB	Pole	PAS	T	-229	Volkswagen	Rabbit	81	614		31.70	206	0.000	0.102	0.124	-3.76	0.119	0.102	0.022	8.80	4.84
F	VTRB	Pole	PAS	T	-140	Dodge	Colt	81	663		31.86	168	0.000	0.089	0.105	-4.32	0.136	0.089	0.016	10.14	7.65
F	VTRB	Pole	PAS	T	-114	Honda	Civic	81	700		32.03	96	0.000	0.000	0.000	0.00	0.000	0.000	0.000		

Test No.	Vehicle Crush Information						Test Lab	Eng Mass	Eng Desc	Eng Disp	Trans	Drive	Door	Length	Width	Whl-base	FAxle to		Barr Data
	C1	C2	C3	C4	C5	C6											Cg	DL'd	
847	41	305	597	577	246	25	TRC	1372	4IF	1.6	M	F	3	4476	1430	2438	1120	X	A
2290							IIHS	1433	S6IF				4	4877	1803	2692		X	
2286							IIHS	1314						4674	1778	2718		X	
2143	1465	1460	1480					1560						1800					
13	851	848	869	861	823	820	DS	1520	4IF	2.0	A	R	4	4892	1707	2642	1257	X	
18	569	610	640	617	572	0	DS	1000	4TF	1.5	M	F	2	3808	1506	2197	945	X	A
2185	2	8	1	11	5	6	TRC	1906	V8IF	5.7	A	R	4	5450	1956	2944	1444	X	
709	-5	127	386	376	122	-20	MS	1206	4IF	2.3	M	R	3	4369	1676	2477	1077	X	
666								1976						1857					
876	445	696	691	455	241	10	TRC	1265	4IF	2.2	M	F	5	4161	1689	2515	1085	X	
872	460	464	612	340	53	226	TRC	1335	4IF	1.6	M	F	3	4473	1689	2438	1168	X	
473	0	127	338	445	102	0		1027						1585					
698	-41	-28	191	536	445	102	MS		4IF	2.3	A	R	3	4349	1687	2564	1057	X	
846	229	508	732	716	455	203	TRC	1310	4TF	2.2	M	F	5	4158	1689	2520	1120	X	A
1836	0	64	152	173	76	0	TRC	1101	4TF	1.9	A	F	3	4237	1636	2383	1473	X	
1837	0	119	180	279	130	0	TRC	1101	4TF	1.9	A	F	3	4237	1636	2383	1473	X	
1838	0	130	218	450	208	30	TRC	1101	4TF	1.9	A	F	3	4237	1636	2383	1473	X	
1839	43	218	539	627	259	71	TRC	1101	4TF	1.9	A	F	3	4237	1636	2383	1473	X	
1840	300	330	920	998	419	399	TRC	1101	4TF	1.9	A	F	3	4237	1636	2383	1473	X	
2170	12	22	23	52	23	8	TRC	1619	S6TF	3.0	A	F	4	4790	1813	2690	1056	X	
2171	171	35	269	91	124	148	TRC	1619	S6TF	3.0	A	F	4	4790	1813	2690	1056	X	
2172	199	8	231	280	37	173	TRC	1619	S6TF	3.0	A	F	4	4790	1813	2690	1056	X	
2173	18	162	309	350	52	24	TRC	1619	S6TF	3.0	A	F	4	4790	1813	2690	1056	X	
2174	92	162	1023	410	201	127	TRC	1619	S6TF	3.0	A	F	4	4790	1813	2690	1056	X	
1846							TRC	1280	4TF	2.3	A	F	4	4468	1737	2535	920	X	
819	48	452	719	732	445	38	TRC	1333	4TF	1.8	M	F	4	4468	1656	2459	1201	X	
449	0	152	254	368	178	0		950						1580					
1648	79	41	165	224	23	64	TRC	985	4TF	1.5	M	F	4	4150	1610	2388	1024	X	
1841	61	66	201	290	99	56	TRC	1042	4TF	1.6	M	F	4	4171	1626	2393	884	X	
662	127	379	330	218	97	-71	MS	988	4TF	1.7	A	F	5	3927	1565	2410	775	X	
873	244	564	795	605	295	36	TRC	1281	4TF	1.8	M	F	4	4455	1651	2451	1092	X	A
614	79	302	384	249	89	-69	MS	982	4TF	1.7	M	F	5	3927	1577	2413	800	X	
663	-64	31	315	412	173	-114	MS	981	4TF	1.5	M	F	3	3800	1595	2306	810	X	
700	-157	91	155	345	36	-142		948						1610					

<u>Test No.</u>	<u>No. Acc</u>	<u>Trace No.</u>	<u>Location</u>	<u>Notes</u>	ϵ <u>Low</u>	ϵ <u>Loc</u>	ϵ <u>High</u>	ϵ <u>Loc</u>	ϵ <u>Diff</u>
847	6	49,51,52,64,68,69	right-2, left-2 rear seat; right, left b-pillar	good crush transition point and second phase restitution					
2290	1	29	cg	crush transition, second phase restitution visible;					
2286	1	29	cg	similar to 40% Taurus case; earlier crush transition;					
2143				BAD DATA					
13	3	49,61,67	rear deck; left b-pillar-2	58 consistent but noisy; crush transition not as pronounced					
18	2	47,60	rear deck; left b-pillar	56, 74 bad or not consistent; crush transition not as pronounced					
2185	3	1,4,6,8,10	right, left rear seat; right, left front sill; cg						
709	1	23	cg	compared to offset Vega (698), higher restitution					
666				<i>bad data</i>					
876	2	37,40	left rear seat-2	43 inconsistent; restitution may be artificially high					
872	2	37,40	right, left rear seat	43 inconsistent					
473									
698	1	11	cg	14, 15 located at outboard rear - similar decel. as cg but no rest					
846	5	49,51,52,64,69	right, left-2 rear seat; right, left b-pillar	68 bad data					
1836	3	1,2,3	right rear sill; left rear door; cg						
1837	3	1,2,3	right rear sill; left rear door; cg						
1838	3	1,2,3	right rear sill; left rear door; cg						
1839	2	1,2	right rear sill; left rear door	3 (cg) noisy and inconsistent					
1840	2	1,2	right rear sill; left rear door	3 (cg) noisy and inconsistent;					
2170	2	1,5	left rear sill; cg	3 inconsistent					
2171	3	1,3,5	right, left rear sill; cg	spread of .275 to .33 among averaged accelerometers					
2172	2	1,3	right, left rear sill	5 (cg) curve smooth but significantly smaller restitution					
2173	1	1	left rear sill	3 inconsistent; 5 (cg) same phenomena as previous case					
2174	1	3	right rear sill	1 noisy; 5 (cg) same phenomena as above					
1846	3	1,2,3	right rear sill; left rear door; cg						
819	6	49,51,52,64,68,69	right-2, left-2 rear seat; right, left b-pillar						
449				<i>bad data at cg</i>					
1648	2	1,3	right, left rear seat						
1841	3	1,2,3	right rear sill; left rear door; cg						
662	1	23	cg	26, 27 typical outboard response					
873	2	40,44	left rear seat; left b-pillar	43, 48 response typical for non-impacted side in pole impact					
614	1	23	cg	26 typical outboard response; 27 inconsistent					
663	1	23	cg	26 bad; 27 typical outboard response to pole impact					
700				<i>bad data at cg</i>					

<u>Dir</u>	<u>Test Type</u>	<u>Ovrlp %</u>	<u>Veh Type</u>	<u>Eng Or Off</u>	<u>Make</u>	<u>Model</u>	<u>Yr</u>	<u>Tst No.</u>	<u>Rep No</u>	<u>Imp Vel</u>	<u>Crsh</u>	<u>Imp Time</u>	<u>Zero Time</u>	<u>Reb Time</u>	<u>Reb Vel</u>	<u>ε</u>	<u>Crsh Δt</u>	<u>Rest Δt</u>	<u>Crsh Acc</u>	<u>Rest Acc</u>	
F	VTRB	?	PAS	T		Volkswagen	Rabbit	76	432	0.00	0	0.000	0.000	0.000	0.00		0.000	0.000			
F	VTRB	?	PAS	T		Volkswagen	Rabbit	76	441	30.60	0	0.000	0.000	0.000	0.00	0.000	0.000	0.000			
F	VTRB	?	PAS	T		Volkswagen	Rabbit	81	741	0.00	0	0.000	0.000	0.000	0.00		0.000	0.000			
F	VTRB	?	PAS	T	-361	Volkswagen	Rabbit	81	476	32.19	163	0.000	0.000	0.000	0.00	0.000	0.000	0.000			
F	VTRB	50	PAS	T		Ford	Escort	87	1948	1	15.61	78	0.000	0.086	0.142	-3.50	0.224	0.086	0.056	5.14	1.77
F	VTRB	50	PAS	T		Ford	Escort	87	1949	2	32.03	237	0.000	0.079	0.114	-6.09	0.190	0.079	0.035	11.48	4.93
F	VTRB	50	PAS	T		Ford	Escort	87	1950	3	32.19	396	0.000	0.054	0.098	-8.53	0.265	0.054	0.044	16.88	5.49
F	VTRB	50	PAS	T		Ford	Escort	87	1951	4	56.49	751	0.000	0.111	0.167	-2.00	0.035	0.111	0.056	14.41	1.01
F	VTRB	50	PAS	T		Ford	Taurus	86	1935	1	15.77	54	0.000	0.097	0.144	-3.70	0.235	0.097	0.047	4.60	2.23
F	VTRB	50	PAS	T		Ford	Taurus	86	1936	2	31.87	235	0.000	0.076	0.117	-6.03	0.189	0.076	0.041	11.88	4.17
F	VTRB	50	PAS	T		Ford	Taurus	86	1937	3	32.19	352	0.000	0.049	0.083	-9.21	0.286	0.049	0.034	18.61	7.67
F	VTRB	50	PAS	T		Ford	Taurus	86	1938	4	56.33	481	0.000	0.000	0.000	0.00	0.000	0.000	0.000		
F	VTRB	50	PAS	T		Hyundai	Excel GLS	86	1156		39.43	nr	0.000	0.082	0.096	-2.97	0.075	0.082	0.014	13.62	6.01
F	VTRB	50	PAS	T		Hyundai	Excel GLS	86	1164		55.84	nr	0.000	0.089	0.117	-6.40	0.115	0.089	0.028	17.77	6.47
F	VTRB	50	PAS	T		Toyota	Celica	86	1155		39.59	nr	0.000	0.077	0.087	-4.47	0.113	0.077	0.010	14.56	12.66
F	VTRB	50	PAS	T		Toyota	Celica	86	1158		55.84	nr	0.000	0.077	0.094	-5.81	0.104	0.077	0.017	20.54	9.68
F	VTRB	100	PAS	I		Acura	Legend	92	1733		56.17	nr	0.000	0.079	0.108	-6.32	0.113	0.079	0.029	20.14	6.17
F	VTRB	100	PAS	I		Acura	Legend	93	1880		47.80	nr	0.000	0.068	0.093	-5.89	0.123	0.068	0.025	19.91	6.67
F	VTRB	100	PAS	I		BMW	325I	90	1453		56.00	515	0.000	0.072	0.107	-6.51	0.116	0.072	0.035	22.03	5.27
F	VTRB	100	PAS	I		BMW	325I	92	1659		56.65	nr	0.000	0.081	0.107	-6.56	0.116	0.081	0.026	19.81	7.15
F	VTRB	100	PAS	I		Cadillac	De Ville	81	355		47.31	622	0.000	0.106	0.151	-7.18	0.152	0.106	0.045	12.64	4.52
F	VTRB	100	PAS	I		Chevrolet	Caprice	94	2007		46.99	nr	0.000	0.095	0.157	-8.65	0.184	0.095	0.062	14.01	3.95
F	VTRB	100	PAS	I		Chevrolet	Caprice	94	2072		56.50	652	0.000	0.091	0.136	-9.00	0.159	0.091	0.045	17.59	5.66
F	VTRB	100	PAS	I		Chevrolet	Celebrity	83	773		48.12	577	0.000	0.095	0.118	-5.66	0.118	0.095	0.023	14.35	6.97
F	VTRB	100	PAS	I		Chevrolet	Chevette	80	270		47.32	460	0.000	0.000	0.000	0.00	0.000	0.000	0.000		
F	VTRB	100	PAS	I		Chevrolet	Chevette	80	284		44.26	nr	0.000	0.000	0.000	0.00	0.000	0.000	0.000		
F	VTRB	100	PAS	I		Chevrolet	Chevette	80	426		56.65	535	0.000	0.089	0.130	-8.02	0.142	0.089	0.041	18.03	5.54
F	VTRB	100	PAS	I		Chevrolet	Impala	83	861		48.60	573	0.000	0.093	0.141	-6.78	0.140	0.093	0.048	14.80	4.00
F	VTRB	100	PAS	I		Chevrolet	Impala	83	891		56.33	676	0.000	0.087	0.121	-8.70	0.154	0.087	0.034	18.34	7.25
F	VTRB	100	PAS	I		Chevrolet	Lumina	90	1378		47.64	462	0.000	0.093	0.143	-6.03	0.127	0.093	0.050	14.51	3.42
F	VTRB	100	PAS	I		Chevrolet	MonteCarlo	95	2234		47.80	481	0.000	0.092	0.138	-7.03	0.147	0.092	0.046	14.72	4.33
F	VTRB	100	PAS	I		Chrysler	New Yorker	91	1599		46.99	nr	0.000	0.093	0.132	-5.54	0.118	0.093	0.039	14.31	4.02
F	VTRB	100	PAS	I		Dodge	Diplomat	78	774		14.48	nr	0.000	0.064	0.094	-3.20	0.221	0.064	0.030	6.41	3.02
F	VTRB	100	PAS	I		Dodge	Omni	78	299		47.96	127	0.000	0.067	0.112	-16.56	0.345	0.067	0.045	20.28	10.42

Test No.	Vehicle Crush Information						Test Lab	Eng Mass	Eng Desc	Eng Disp	Trans	Drive	Door	Length	Width	Whl-base	FAxle to		Barr Data
	C1	C2	C3	C4	C5	C6											Cg	DL'd	
432	0	0	0	0	0	0													
441	0	0	0	0	0	0													
741	0	0	0	0	0	0													
476	0	76	114	191	432	0		1138						1610					
1948	64	99	135	74	48	8	TRC	1135	4TF	1.9	M	F	3	4216	1676	2388	912	X	
1949	66	406	467	257	13	15	TRC	1135	4TF	1.9	M	F	3	4216	1676	2388	912	X	
1950	122	371	635	638	244	69	TRC	1135	4TF	1.9	M	F	3	4216	1676	2388	912	X	
1951	566	907	1168	1179	175	84	TRC	1135	4TF	1.9	M	F	3	4216	1676	2388	912	X	
1935	51	56	79	71	36	8	TRC	1495	S6TF	3.0	A	F	4	4724	1803	2692	927	X	
1936	165	356	348	239	132	33	TRC	1495	S6TF	3.0	A	F	4	4724	1803	2692	927	X	
1937	343	523	516	373	158	41	TRC	1495	S6TF	3.0	A	F	4	4724	1803	2692	927	X	
1938	229	940	950	229	173	3	TRC	1495	S6TF	3.0	A	F	4	4724	1803	2692	927		
1156							CAL	1202	4TF	1.5	M	F	5	4069	1435	2380	1069	X	A
1164							CAL	1188	4TF	1.5	M	F	4	4265	1435	2380	1135	X	A
1155							CAL	1261	4TF	2.0	M	F	2	4422	1397	2517	1014	X	A
1158							CAL	1252	4TF	2.0	M	F	2	4422	1397	2517	993	X	A
1733							CAL	1787	V6IF	3.2	A	F	4	4958	1811	2906	1275	X	
1880							CAL	1728	V6IF	3.2	M	F	4	4945	1811	2913	1209	X	
1453	485	508	541	531	513	478	MS	1753	V6IF	2.5	M	R	2	4331	1646	2570	1247	X	A
1659							CAL	1623	S6IF	2.5	A	R	4	4437	1646	2700	1440	X	A
355	607	610	686	681	569	518	DS	2057	V6IF	4.1	A	R	4	5512	1966	3084	1628	X	
2007							CAL	2111	V8IF	4.3	A	R	4	5425	1956	2941	1422	X	
2072	589	632	651	678	690	628	TRC	2133	V8IF	5.7	A	R	4	5430	1966	2945	1400	X	A
773	561	584	605	587	554	546	TRC	1547	V6IF	2.8	A	F	4	4730	1524	2667	1087	X	
270	465	447	485	483	442	424		1173						1570					
284								1220						1570					
426	577	597	617	597	574		DS	1198	4IF	1.6	A	R	3	4112	1570	2395	1166	X	A
861	523	569	605	597	572	523	TRC	1921	V8IF	5.7	A	R	4	5398	1900	2934	1433	X	
891	638	668	732	719	643	594	TRC	1927	V8IF	5.7	A	R	4	5372	1905	2946	1369	X	
1378	411	437	490	544	434	396	TRC	1662	4IF	2.5	A	R	4	5057	1778	2731	1125	X	
2234	389	457	490	511	531	442	CAL	1705	V6IF	3.1	A	F	2	5093		2733	1118	X	
1599							CAL	1778	V6IF	3.3	A	F	4	5017	1750	2779	1120	X	
774							TRC	1647	V8IF	5.2	A	R	2	5146	1842			X	
299	432	419					NTS	1167	4IF	1.7	M	F	5	4186	1682	2520	1011	X	

<u>Test No.</u>	<u>No. Acc</u>	<u>Trace No.</u>	<u>Location</u>	<u>Notes</u>	ϵ <u>Low</u>	<u>Loc</u>	ϵ <u>High</u>	<u>Loc</u>	ϵ <u>Diff</u>
432				<i>luminare</i>					
441				<i>luminare</i>					
741				<i>luminare</i>					
476				<i>luminare</i>					
1948	2	1,5	left rear sill; cg	3 not consistent					
1949	2	1,5	left rear sill; cg	3 (rr) lower, as expected	0.117	rr	0.203	lr	0.086
1950	1	5	cg	1,3 (lr,rr) lower than cg??????	0.190	rear	0.265	cg	0.075
1951	1	5	cg	all traces suspect	0.000	rear	0.035	cg	0.035
1935	3	1,3,5	left, right rear sill; cg		0.219	rr	0.247	lr	0.028
1936	3	1,3,5	left, right rear sill; cg		0.166	rr	0.220	lr	0.054
1937	1	5	cg	1,3 (lr,rr) give lower restitution, as in Escort case	0.218	rear	0.286	cg	0.068
1938				<i>accurate restitution value cannot be determined</i>					
1156	4	45,46	left-2 rear seat						
1164	2	47,50	right, left rear seat	48,49 unreasonable; 51, 54 not consistent; 60 bad data					
1155	4	46,47,48,50	left-2, center, right rear seat	49,53,59 unreasonable/bad data					
1158	5	44,45,46,47,48	left-2, center, right-2 rear seat	51 consistent but noisy; 57 bad data					
1733	3	23,24,30	right-2, left rear sill	29 noisy; no center traces					
1880	2	17,18	right, left rear sill	no center traces					
1453	2	30,31	right, left rear floor						
1659	2	23,24	right, left rear sill						
355	2	6,15	left rear, right front floor		0.140	lr	0.165	rf	0.025
2007	2	31,32	right, center rear seat						
2072	1	40	right rear seat	46, 47 bad data					
773	4	25,27,28,29	right-2, left-2 rear seat	no center traces; b-pillar traces not consistent					
270									
284				<i>bad data</i>					
426	4	9,10,20,25	left rear-2, right front-2 seat						
861	2	8,21	right, left b-pillar		0.128	lb-p	0.151	rb-p	0.023
891	1	12	left b-pillar						
1378	1	19	left rear seat						
2234	2	17,18	left, right rear seat		0.149	lr	0.149	rr	0.000
1599	2	17,18	left, right rear sill		0.132	lr	0.135	rr	0.003
774	2	1,2	front x-member	3 not consistent with others; rest taken @ .094 s					
299	1	23	left rear floor	questionable					

<u>Dir</u>	<u>Test Type</u>	<u>Ovrlp %</u>	<u>Veh Type</u>	<u>Eng Or Off</u>	<u>Make</u>	<u>Model</u>	<u>Yr</u>	<u>Tst No.</u>	<u>Rep No.</u>	<u>Imp Vel</u>	<u>Crsh</u>	<u>Imp Time</u>	<u>Zero Time</u>	<u>Reb Time</u>	<u>Reb Vel</u>	<u>ε</u>	<u>Crsh Δt</u>	<u>Rest Δt</u>	<u>Crsh Acc</u>	<u>Rest Acc</u>
F	VTRB	100	PAS	I	Ford	Escort	85	1216	1	16.25	62	0.000	0.065	0.101	-4.20	0.258	0.065	0.036	7.08	3.30
F	VTRB	100	PAS	I	Ford	Escort	85	1217	2	31.86	290	0.005	0.058	0.086	-7.30	0.229	0.053	0.028	16.89	7.38
F	VTRB	100	PAS	I	Ford	Escort	85	1218	3	32.03	432	0.005	0.049	0.074	-8.28	0.259	0.044	0.025	20.42	9.38
F	VTRB	100	PAS	I	Ford	Escort	85	1219	4	29.29	536	0.009	0.044	0.080	-8.42	0.287	0.035	0.036	24.00	6.62
F	VTRB	100	PAS	I	Ford	Escort	85	1220	5	31.06	715	0.011	0.057	0.097	-6.71	0.216	0.046	0.040	19.26	4.75
F	VTRB	100	PAS	I	Ford	Escort	85	1221	6	48.28	1328	0.012	0.093	0.135	-9.31	0.193	0.081	0.042	16.84	6.28
F	VTRB	100	PAS	I	Ford	LTD	79	203		56.17	857	0.000	0.107	0.160	-7.96	0.142	0.107	0.053	14.87	4.25
F	VTRB	100	PAS	I	Ford	LTD	79	750		8.21	nr	0.000	0.059	0.114	-2.18	0.266	0.059	0.055	3.94	1.12
F	VTRB	100	PAS	I	Ford	LTD	79	751		14.64	nr	0.000	0.060	0.107	-4.59	0.314	0.060	0.047	6.91	2.77
F	VTRB	100	PAS	I	Ford	LTD	79	752		11.43	nr	0.000	0.068	0.113	-3.48	0.304	0.068	0.045	4.76	2.19
F	VTRB	100	PAS	I	Ford	LTD	79	753		7.24	nr	0.000	0.076	0.103	-0.97	0.134	0.076	0.027	2.70	1.02
F	VTRB	100	PAS	I	Ford	LTD	79	754		48.28	562	0.000	0.103	0.159	-9.35	0.194	0.103	0.056	13.28	4.73
F	VTRB	100	PAS	I	Ford	LTD	79	758		7.72	nr	0.000	0.085	0.115	-0.84	0.109	0.085	0.030	2.57	0.79
F	VTRB	100	PAS	I	Ford	LTD	79	759		19.63	101	0.000	0.066	0.087	-3.42	0.174	0.066	0.021	8.42	4.61
F	VTRB	100	PAS	I	Ford	LTD	79	760		7.56	nr	0.000	0.075	0.110	-0.82	0.108	0.075	0.035	2.86	0.66
F	VTRB	100	PAS	I	Ford	Taurus	86	1201	1	15.45	63	0.003	0.077	0.152	-5.30	0.343	0.074	0.075	5.92	2.00
F	VTRB	100	PAS	I	Ford	Taurus	86	1202	2	31.86	206	0.005	0.054	0.091	-7.67	0.241	0.049	0.037	18.53	5.87
F	VTRB	100	PAS	I	Ford	Taurus	86	1203	3	32.35	359	0.006	0.050	0.000	0.00	0.000	0.044	-0.050	20.85	0.00
F	VTRB	100	PAS	I	Ford	Taurus	86	1204	4	29.93	465	0.007	0.046	0.085	-8.35	0.279	0.039	0.039	21.84	6.06
F	VTRB	100	PAS	I	Ford	Taurus	86	1205	5	48.28	753	0.013	0.055	0.098	-11.11	0.230	0.042	0.043	32.32	7.32
F	VTRB	100	PAS	I	Ford	Taurus	86	1600		56.33	nr	0.000	0.087	0.115	-7.18	0.127	0.087	0.028	18.34	7.26
F	VTRB	100	PAS	I	Ford	Taurus	92	1973		48.44	nr	0.000	0.070	0.092	-10.85	0.224	0.070	0.022	19.60	13.97
F	VTRB	100	PAS	I	Ford	Taurus	92	1974		56.49	nr	0.000	0.075	0.130	-10.55	0.187	0.075	0.055	21.33	5.43
F	VTRB	100	PAS	I	Ford	Taurus	92	1976		56.33	nr	0.000	0.079	0.104	-11.83	0.210	0.079	0.025	20.20	13.40
F	VTRB	100	PAS	I	Ford	Tempo	93	1858		56.30	471	0.000	0.079	0.115	-10.04	0.178	0.079	0.036	20.19	7.90
F	VTRB	100	PAS	I	Honda	Civic	79	94		56.00	53	0.000	0.074	0.102	-4.97	0.089	0.074	0.028	21.43	5.03
F	VTRB	100	PAS	I	Lincoln	Town Car	96	2334		47.40	439	0.000	0.109	0.157	-9.41	0.199	0.109	0.048	12.32	5.55
F	VTRB	100	PAS	I	Lincoln	Town Car	96	2429		56.60	662	0.000	0.104	0.147	-10.88	0.192	0.104	0.043	15.42	7.17
F	VTRB	100	PAS	I	Mazda	626	94	1981		47.48	nr	0.000	0.071	0.087	-4.23	0.089	0.071	0.016	18.94	7.49
F	VTRB	100	PAS	I	Mazda	626	94	1998		56.65	548	0.000	0.073	0.103	-10.15	0.179	0.073	0.030	21.98	9.58
F	VTRB	100	PAS	I	Mitsubishi	Galant	94	1985		47.48	nr	0.000	0.073	0.115	-6.84	0.144	0.073	0.042	18.42	4.61
F	VTRB	100	PAS	I	Oldsmobile	Cutlass	84	624		56.00	686	0.000	0.096	0.145	-8.63	0.154	0.096	0.049	16.52	4.99
F	VTRB	100	PAS	I	Plymouth	Fury	75	10		65.50	618	0.000	0.110	0.182	-11.63	0.178	0.110	0.072	16.87	4.58
F	VTRB	100	PAS	I	Renault	Fuego	82	874		48.12	441	0.000	0.089	0.116	-7.24	0.150	0.089	0.027	15.31	7.60

Test No.	Vehicle Crush Information						Test Lab	Eng Mass	Eng Desc	Eng Disp	Trans	Drive	Door	Length	Width	Whl-base	FAxle to		Barr Data
	C1	C2	C3	C4	C5	C6											Cg	DL'd	
1216	66	64	74	66	56	41	TRC	1254	4IF	1.6	A	F	3	4082	1692	2388	686	X	
1217	305	307	307	292	269	244	TRC	1254	4IF	1.6	A	F	3	4082	1692	2388	686	X	
1218	434	437	447	437	424	399	TRC	1254	4IF	1.6	A	F	3	4082	1692	2388	686	X	
1219	538	549	554	546	523	480	TRC	1254	4IF	1.6	A	F	3	4082	1692	2388	686	X	
1220	729	726	734	724	701	653	TRC	1254	4IF	1.6	A	F	3	4082	1692	2388	686	X	
1221	1273	1290	1336	1349	1356	1344	TRC	1254	4IF	1.6	A	F	3	4082	1692	2388	686	X	
203	866	869	866	861	841	831	DS	2184	V8IF	5.0	A	R	2	5474	1996	2893	1392	X	
750							TRC	1719	V8IF	5.0	A	R	4	5309	1981			X	
751							TRC	1719	V8IF	5.0	A	R	4	5309	1981			X	
752							TRC	1719	V8IF	5.0	A	R	4	5309	1981			X	
753							TRC	1799	V8IF	5.0	A	R	4	5326	1981	2906	1311	X	
754	409	536	582	615	589	564	TRC	1882	V8IF	5.0	A	R	4	5326	1981	2906	1435	X	
758							TRC	1950	V8IF	5.0	A	R	4	5227	1885	2898	1367	X	
759							TRC	1937	V8IF	5.0	A	R	4	5227	1882	2898	1402	X	
760							TRC	1932	V8IF	5.0	A	R	4	5215	1936	2898	1402	X	
1201	25	51	76	79	71	48	TRC	1591	4IF	3.0	A	F	4	4468	1768	2662	945	X	
1202	170	201	221	224	213	173	TRC	1591	4IF	3.0	A	F	4	4468	1768	2662	945	X	
1203	320	353	373	376	366	333	TRC	1591	4IF	3.0	A	F	4	4468	1768	2662	945	X	
1204	429	460	483	480	472	432	TRC	1591	4IF	3.0	A	F	4	4468	1768	2662	945	X	
1205	737	759	787	772	739	676	TRC	1591	4IF	3.0	A	F	4	4468	1768	2662	945	X	
1600							CAL	1774	V6IF	3.0	A	F	WAG	4864	1798	2700	1237	X	A
1973							CAL	1603	V6IF	3.0	A	F	4	4879	1808	2700	1097	X	X
1974							CAL	1601	V6IF	3.0	A	F	4	4879	1808	2682	1849	X	A
1976							CAL	1660	V6IF	3.0	A	F	4	4879	1808	2692	1118	X	X
1858	465	487	452	462	485	475	MGA	1404	4IF	2.3	A	F	4	4540	1465	2535	1090	X	
94	531						CAL	989	4IF	1.3	M	F	2	3696	1506	2197	940	X	A
2334	484	485	496	418	378	352	MGA	2070	V8IF	4.6	A	R	4	5528	1950	2980	1436	X	
2429	620	537	724	752	678	615	MGA	2072	V8IF	4.6	A	R	4	5525	1554	3000	1493	X	A
1981							DS	1406	4IF	2.0	M	F	4	4691	1750	2611	1115	X	
1998	445	575	570	575	570	450	CAL	1447	4IF	2.0	A	F	4	4670	1750	2610	1122	X	A
1985							TRC	1442	4IF	2.4	A	F	4	4752	1750	2637	1136	X	
624	673	676	714	711	666	648	CAL	1678	V6IF	3.8	A	R	2	5067	1826	2781	1354	X	A
10	612	622	640	635	602	574	DS	2014	V8IF	5.0	A	R	4	5535	1974	2985	1334	X	A
874	?	513	506	503	478	412	TRC	1319	4IF	1.6	M	F	3	4483	1692	2441	1163	X	A

<u>Test No.</u>	<u>No. Acc</u>	<u>Trace No.</u>	<u>Location</u>	<u>Notes</u>	ϵ <u>Low</u>	<u>Loc</u>	ϵ <u>High</u>	<u>Loc</u>	ϵ <u>Diff</u>
1216	2	5,6	rear deck						
1217	2	5,6	rear deck						
1218	2	1,2	rear deck						
1219	2	1,2	rear deck						
1220	2	1,2	rear deck						
1221	2	1,2	rear deck						
203	1	33	left rear floor	2d; no center trace					
750	1	3	left b-pillar	1,2 bad data					
751	1	3	left b-pillar	1,2 unreasonable					
752	1	3	left b-pillar	1,2 noisy					
753	2	2,9	left b-pillar; steering column						
754	1	11	left b-pillar	4d; no center trace					
758	1	1	b-pillar						
759	2	10,13	right, left b-pillar	20 consistent but noisy					
760	2	1,4	left, right b-pillar	11 not reasonable					
1201	1	1	cg	event time indicator; ugly curve-should probably be thrown out					
1202	1	1	cg						
1203	1	1	cg						
1204	1	1	cg						
1205	1	1	cg						
1600	2	23,24	right, left rear sill	no center-mounted accelerometer available--smaller e?					
1973	1	37	center rear cross-member	38, 81 bad data; 43 consistent but noisy; all traces noisy	0.079	lr	0.224	cr	0.145
1974	1	41	center rear cross-member	48 noisy, inconsistent					
1976	1	41	center rear cross member	48 noisy; 80 mult by -1; 80,81 outboard location	0.076	l,rr	0.210	cr	0.134
1858	4	36,37,38,39	right-2, left-2 b-pillar	no center trace					
94	1	25	left rail	28 inconsistent					
2334	2	25,26	left, right rear x-member		0.200	lr	0.200	rr	0.000
2429	4	12,30,66,90	left-2, right-2 rear floor						
1981	2	17,18	right, left rear sill						
1998	4	37,38,44,45	right-2, left-2 rear seat						
1985	2	17,18	right, left rear sill						
624	1	27	right front seat	28 bad data; 29 consistent but too noisy					
10	3	49,62,70	rear deck; left b-pillar-2						
874	3	30,33,36	right, left-2 rear seat	5 bad data; 37,41 (b-pillars) are consistent; no ctr trace	0.112	b-pill	0.150	rear	0.038

<u>Dir</u>	<u>Test Type</u>	<u>Ovrlp %</u>	<u>Veh Type</u>	<u>Eng Or Off</u>	<u>Make</u>	<u>Model</u>	<u>Yr</u>	<u>Tst No.</u>	<u>Rep No</u>	<u>Imp Vel</u>	<u>Crsh</u>	<u>Imp Time</u>	<u>Zero Time</u>	<u>Reb Time</u>	<u>Reb Vel</u>	<u>ε</u>	<u>Crsh Δt</u>	<u>Rest Δt</u>	<u>Crsh Acc</u>	<u>Rest Acc</u>
F	VTRB	100	PAS	I	Subaru	Legacy	93	1885		56.00	504	0.000	0.086	0.112	-6.35	0.113	0.086	0.026	18.44	6.92
F	VTRB	100	PAS	I	Volvo	244	75	30		56.33	nr	0.000	0.000	0.000	0.00	0.000	0.000	0.000		
F	VTRB	100	PAS	T	Acura	Integra	90	1365		55.84	492	0.000	0.075	0.100	-8.18	0.146	0.075	0.025	21.09	9.27
F	VTRB	100	PAS	T	Acura	Integra	90	1445		47.48	nr	0.000	0.074	0.096	-4.25	0.090	0.074	0.022	18.17	5.47
F	VTRB	100	PAS	T	BMW	325I	92	1657		47.48	354	0.000	0.075	0.125	-5.08	0.107	0.075	0.050	17.93	2.88
F	VTRB	100	PAS	T	Buick	Century	93	1773		47.15	506	0.000	0.090	0.140	-8.92	0.189	0.090	0.050	14.84	5.05
F	VTRB	100	PAS	T	Buick	Century	93	1776		56.20	629	0.000	0.098	0.141	-9.07	0.161	0.098	0.043	16.24	5.97
F	VTRB	100	PAS	T	Buick	Park Ave	91	1603		47.48	580	0.000	0.099	0.151	-6.03	0.127	0.099	0.052	13.58	3.28
F	VTRB	100	PAS	T	Cadillac	De Ville	94	2024		56.20	614	0.000	0.096	0.128	-9.30	0.165	0.096	0.032	16.58	8.23
F	VTRB	100	PAS	T	Chevrolet	Cavalier	83	672		47.80	150	0.000	0.075	0.102	-8.99	0.188	0.075	0.027	18.05	9.43
F	VTRB	100	PAS	T	Chevrolet	Cavalier	84	661		56.33	571	0.000	0.083	0.124	-8.14	0.145	0.083	0.041	19.22	5.62
F	VTRB	100	PAS	T	Chevrolet	Cavalier	84	975		41.20	nr	0.000	0.069	0.086	-5.16	0.125	0.069	0.017	16.91	8.60
F	VTRB	100	PAS	T	Chevrolet	Celebrity	82	451		56.33	639	0.000	0.103	0.141	-9.67	0.172	0.103	0.038	15.49	7.21
F	VTRB	100	PAS	T	Chevrolet	Celebrity	83	776		47.80	547	0.000	0.099	0.117	-4.47	0.094	0.099	0.018	13.68	7.03
F	VTRB	100	PAS	T	Chevrolet	Celebrity	84	688		56.33	714	0.000	0.101	0.149	-9.43	0.167	0.101	0.048	15.80	5.56
F	VTRB	100	PAS	T	Chevrolet	Citation	80	1		64.21	215	0.000	0.096	0.138	-6.02	0.094	0.096	0.042	18.94	4.06
F	VTRB	100	PAS	T	Chevrolet	Citation	80	4		77.25	308	0.000	0.115	0.156	-5.81	0.075	0.115	0.041	19.03	4.01
F	VTRB	100	PAS	T	Chevrolet	Citation	80	5		56.33	163	0.000	0.090	0.140	-10.50	0.186	0.090	0.050	17.73	5.95
F	VTRB	100	PAS	T	Chevrolet	Citation	82	483		56.33	604	0.000	0.095	0.130	-8.67	0.154	0.095	0.035	16.79	7.02
F	VTRB	100	PAS	T	Chevrolet	Citation	82	498		47.32	515	0.000	0.085	0.104	-4.47	0.094	0.085	0.019	15.77	6.66
F	VTRB	100	PAS	T	Chevrolet	Citation	82	545		53.91	528	0.000	0.093	0.130	-9.89	0.183	0.093	0.037	16.42	7.57
F	VTRB	100	PAS	T	Chevrolet	Corsica	93	1883		64.86	705	0.000	0.090	0.122	-9.15	0.141	0.090	0.032	20.41	8.10
F	VTRB	100	PAS	T	Chevrolet	Corsica	94	2030		56.30	617	0.000	0.090	0.131	-10.96	0.195	0.090	0.041	17.72	7.57
F	VTRB	100	PAS	T	Chevrolet	Corsica	94	2124		47.48	473	0.000	0.083	0.119	-8.21	0.173	0.083	0.036	16.20	6.46
F	VTRB	100	PAS	T	Chevrolet	Lumina	90	1368		56.00	426	0.000	0.092	0.142	-5.59	0.100	0.092	0.050	17.24	3.17
F	VTRB	100	PAS	T	Chevrolet	Lumina	94	2120		47.48	460	0.000	0.093	0.125	-2.83	0.060	0.093	0.032	14.46	2.50
F	VTRB	100	PAS	T	Chevrolet	Lumina	95	2222		56.20	470	0.000	0.093	0.141	-8.18	0.146	0.093	0.048	17.12	4.83
F	VTRB	100	PAS	T	Chevrolet	MonteCarlo	95	2159		56.20	597	0.000	0.091	0.137	-10.52	0.187	0.091	0.046	17.49	6.48
F	VTRB	100	PAS	T	Chrysler	New Yorker	91	1590		56.33	nr	0.000	0.096	0.130	-6.22	0.110	0.096	0.034	16.62	5.18
F	VTRB	100	PAS	T	Dodge	Colt	88	1151		56.65	nr	0.000	0.091	0.118	-4.83	0.085	0.091	0.027	17.63	5.07
F	VTRB	100	PAS	T	Ford	Escort	87	997		55.84	533	0.000	0.077	0.117	-8.28	0.148	0.077	0.040	20.54	5.86
F	VTRB	100	PAS	T	Ford	Escort	87	1118		47.48	456	0.000	0.078	0.110	-5.26	0.111	0.078	0.032	17.24	4.66
F	VTRB	100	PAS	T	Ford	Escort	91	1517		47.96	nr	0.000	0.077	0.110	-5.35	0.112	0.077	0.033	17.64	4.59
F	VTRB	100	PAS	T	Ford	Escort	91	1523		56.17	463	0.000	0.078	0.112	-8.90	0.158	0.078	0.034	20.40	7.41

Test No.	Vehicle Crush Information						Test Lab	Eng Mass	Eng Desc	Eng Disp	Trans	Drive	Door	Length	Width	Whl-base	FAxle to		Barr Data	
	C1	C2	C3	C4	C5	C6											Cg	DL'd		
1885	424	492	530	536	516	464	CAL	1433	4IF	2.2	A	F	4	4556	1689	2580	1143	X	A	
30								1530						1702						
1365	457	495	506	503	498	457	MS	1322	4TF	1.8	M	F	4	4470	1565	2616	1057	X	A	
1445							CAL	1374	4TF	1.8	M	F	4	4488	1715	2601	1125	X		
1657	244	320	389	409	376	305	TRC	1624	S6TF	2.5	M	F	4	4440	1654	2695	1443	X		
1773	406	516	536	549	511	432	TRC	1602	S6TF	3.3	A	F	4	4877	1753	2670	1092	X		
1776	547	635	655	655	645	559	TRC	1601	S6TF	3.3	A	F	4	4870	1757	2668	1068	X	A	
1603	483	579	615	635	574	508	TRC	1830	S6TF	3.8	A	F	4	5220	1875	2814	1196	X		
2024	499	594	692	698	570	528	TRC	1937	8TF	4.9	A	F	4	5330	1965	2890	1255	X	A	
672	483	508					MS	1164	4TF	2.0	A	F	WAG	4394	1656	2578	965	X		
661	513	551	574	597	592	569	CAL	1411	4TF	2.0	A	F	-	4379	1684	2578	1052	X	A	
975							GM	1389	4TF	2.0	A	F	4	4369	1684	2571	978	X		
451	597	615	643	663	666	620	DS	1485	4TF	2.5	A	F	4	4783	1720	2654	823	X	X	
776	526	518	566	566	554	533	TRC	1538	-	2.8	A	F	4	4700	1524	2659	1153	X	X	
688	704	704	737	734	696	696	CAL	1628	S6TF	2.8	A	F	WAG	4872	1722	2659	1260	X	X	
1	716	716					CAL	1415		2.8	A	F	5	4488	1730	2665	1069	X		
4	1016	1031					CAL	1420		2.8	A	F	5	4488	1730	2660	1052	X		
5	541	544					CAL	1465	S6TF	2.8	A	F	5	4488	1730	2664	1092	X		
483	572	602	622	620	602	579	DS	1358	4TF	2.5	M	F	5	4503	1730	2667	1158	X		
498	521	518	516	513	511	508	MS	1156	4TF	2.5	A	R	3	4534	1803	2665	960	X		
545	531	533	528	544	523	490	TRC	1361	4TF	2.5	M	F	5	4488	1740	2665	1146	X		
1883	602	702	743	732	724	651	CAL	1297	4TF	2.2	A	F	4	4653	1727	2639	1163	X	X	
2030	584	589	620	649	634	604	MGA	1456	4TF	2.2	A	F	4	4621	1326	2630	1121	X		
2124	427	457	554	513	432	389	MGA	1467	4TF	2.2	A	F	4	4658	1750	2636	1092	X		
1368	363	422	447	437	442	399	MS	1647	4TF	2.5	A	F	4	4978	1803	2728	1092	X	A	
2120	437	462	485	478	452	404		1741						1781						
2222	300	473	552	505	465	414	TRC	1741	V6TF	3.1	A	F	4	4924	1837	2730	1092	X	A	
2159	527	587	622	625	613	552	MGA	1705	V6TF	3.1	A	F	2	5039	1835	2743	1112	X	A	
1590							CAL	1742	S6TF	3.3	A	F	4	4892	1750	2647	1082	X	A	
1151							MS	1294	4TF	1.5	M	F	WAG	4280	1626	2395	1184	X	A	
997	498	528	549	551	526	521	CAL	1243	4TF	1.9	M	F	3	4247	1674	2388	1001	X	A	
1118	450	455	465	470	455	417	TRC	1280	4TF	1.6	M	F	5	4288	1631	2383	1082	X		
1517							CAL	1252	4TF	1.9	M	F	3	4313	1646	2499	1087	X		
1523	478	483	460	460	457	437	MS	1254	4TF	1.9	M	F	2	4298	1694	2489	970	X	A	

<u>Test No.</u>	<u>No. Acc</u>	<u>Trace No.</u>	<u>Location</u>	<u>Notes</u>	ϵ <u>Low</u>	<u>Loc</u>	ϵ <u>High</u>	<u>Loc</u>	ϵ <u>Diff</u>
1885	3	24,30,31	right, left-2 rear sill	23 bad data; no center trace					
30									
1365	2	30,31	right, left rear floor						
1445	1	18	right rear sill						
1657	2	17,18	right, left rear seat						
1773	2	19,20	left, right rear seat						
1776	3	19,26,27	left-2, right rear seat						
1603	1	19	left rear seat	report notes both traces questionable; 20 bad data					
2024	3	40,46,47	left, right-2 rear seat		0.151	lr	0.180	rr	0.029
672	1	2	left rear floor	station wagon body; 1(right front) a little low					
661	2	28,29	cg; left rear seat	29 noisy but consistent					
975	3	4,5,6	right rear sill; right. left rear floor	3 inconsistent; higher value of restitution anticipated					
451	2	7,9	left rear floor; cg		0.137	cg	0.204	lr	0.067
776	4	39,41,42,43	right-2, left-2 rear seat						
688	2	28,29	left rear seat; cg		0.162	cg	0.177	lr	0.015
1	1	26	rear X-member	25 consistent but noisy					
4	1	26	rear X-member	25 bad data					
5	1	27	rear x-member	25 (front cross) under predicts restitution @ cg					
483	1	21	rear cross	15 bad data					
498	2	1,2	right front, left rear floor	front and rear very similar in this case					
545	4	23,24,25,27	right, left rear floor; right, left front floor						
1883	2	51,52	right, left rear seat	53 not consistent					
2030	3	12,51,52	right, left-2 rear seat	11 bad data					
2124	2	5,6	right, left rear seat						
1368	1	30	left rear floor	31 noisy, unreasonable; 30 also unreasonable					
2120	2	35,39	right, left rear seat	traces are consistent but cross again from neg. to pos. velocity					
2222	4	45,46,52,53	right-2, left-2 rear seat						
2159	4	11,12,62,63	right-2, left-2 rear floor	difference between primaries and redundants					
1590	2	25,26	left, right rear sill	big discrepancy between traces but average seems reasonable	0.072	lr	0.151	rr	0.079
1151	2	30,31	right, left rear floor						
997	1	22	left rear sill	23 inconsistent					
1118	1	25	left rear seat	26 inconsistent					
1517	2	17,18	right, left rear sill						
1523	2	30,31	right, left rear floor						

<u>Dir</u>	<u>Test Type</u>	<u>Ovrlp %</u>	<u>Veh Type</u>	<u>Eng Or Off</u>	<u>Make</u>	<u>Model</u>	<u>Yr</u>	<u>Tst No.</u>	<u>Rep No</u>	<u>Imp Vel</u>	<u>Crsh</u>	<u>Imp Time</u>	<u>Zero Time</u>	<u>Reb Time</u>	<u>Reb Vel</u>	<u>ε</u>	<u>Crsh Δt</u>	<u>Rest Δt</u>	<u>Crsh Acc</u>	<u>Rest Acc</u>
F	VTRB	100	PAS	T	Ford	Escort	94	2062		56.30	418	0.000	0.000	0.000	0.00	0.000	0.000	0.000		
F	VTRB	100	PAS	T	Ford	Escort	95	2241		47.80	333	0.000	0.073	0.112	-11.21	0.235	0.073	0.039	18.55	8.14
F	VTRB	100	PAS	T	Ford	Escort	95	2264		56.40	512	0.000	0.074	0.110	-12.05	0.214	0.074	0.036	21.59	9.48
F	VTRB	100	PAS	T	Ford	LTD	79	832		93.66	0	0.000	0.000	0.000	0.00	0.000	0.000	0.000		
F	VTRB	100	PAS	T	Ford	LTD	79	919		93.99	0	0.000	0.000	0.000	0.00	0.000	0.000	0.000		
F	VTRB	100	PAS	T	Ford	Taurus	86	944		56.33	530	0.000	0.083	0.124	-6.30	0.112	0.083	0.041	19.22	4.35
F	VTRB	100	PAS	T	Ford	Taurus	86	1103		56.49	494	0.000	0.081	0.123	-6.14	0.109	0.081	0.042	19.75	4.14
F	VTRB	100	PAS	T	Ford	Taurus	86	1177		56.33	520	0.000	0.084	0.117	-7.40	0.131	0.084	0.033	18.99	6.35
F	VTRB	100	PAS	T	Ford	Taurus	86	1385		56.17	nr	0.000	0.080	0.102	-8.52	0.152	0.080	0.022	19.89	10.97
F	VTRB	100	PAS	T	Ford	Taurus	86	1403		47.48	nr	0.000	0.074	0.126	-5.74	0.121	0.074	0.052	18.17	3.13
F	VTRB	100	PAS	T	Ford	Taurus	92	1777		47.15	305	0.000	0.072	0.090	-5.99	0.127	0.072	0.018	18.55	9.43
F	VTRB	100	PAS	T	Ford	Taurus	92	1890		56.30	464	0.000	0.084	0.123	-8.96	0.159	0.084	0.039	18.98	6.51
F	VTRB	100	PAS	T	Ford	Taurus	92	1899		47.31	304	0.000	0.072	0.090	-5.95	0.126	0.072	0.018	18.61	9.36
F	VTRB	100	PAS	T	Ford	Taurus	96	2312		56.50	403	0.000	0.082	0.126	-8.69	0.154	0.082	0.044	19.52	5.59
F	VTRB	100	PAS	T	Ford	Taurus	96	2450		48.60	nr	0.000	0.078	0.094	-4.99	0.103	0.078	0.016	17.65	8.83
F	VTRB	100	PAS	T	Ford	Tempo	88	1186		56.01	517	0.000	0.075	0.119	-9.80	0.175	0.075	0.044	21.15	6.31
F	VTRB	100	PAS	T	Ford	Tempo	88	1213		47.80	nr	0.000	0.075	0.121	-5.47	0.114	0.075	0.046	18.05	3.37
F	VTRB	100	PAS	T	Geo	Metro	95	2201		47.60	408	0.000	0.073	0.098	-6.11	0.128	0.073	0.025	18.47	6.92
F	VTRB	100	PAS	T	Geo	Metro	95	2239		56.60	603	0.000	0.081	0.115	-9.03	0.160	0.081	0.034	19.79	7.52
F	VTRB	100	PAS	T	Honda	Accord	86	1045		56.33	535	0.000	0.084	0.105	-8.88	0.158	0.084	0.021	18.99	11.98
F	VTRB	100	PAS	T	Honda	Accord	86	1054		47.48	415	0.000	0.076	0.110	-7.46	0.157	0.076	0.034	17.70	6.21
F	VTRB	100	PAS	T	Honda	Accord	90	1541		55.68	nr	0.000	0.073	0.109	-9.25	0.166	0.073	0.036	21.60	7.28
F	VTRB	100	PAS	T	Honda	Accord	90	1552		47.31	nr	0.000	0.068	0.100	-5.56	0.118	0.068	0.032	19.71	4.92
F	VTRB	100	PAS	T	Honda	Accord	90	1597		56.33	nr	0.000	0.077	0.105	-8.54	0.152	0.077	0.028	20.72	8.64
F	VTRB	100	PAS	T	Honda	Accord	90	1610		46.99	nr	0.000	0.069	0.088	-6.00	0.128	0.069	0.019	19.29	8.94
F	VTRB	100	PAS	T	Honda	Accord	90	1637		47.31	nr	0.000	0.070	0.094	-6.50	0.137	0.070	0.024	19.14	7.67
F	VTRB	100	PAS	T	Honda	Accord	90	1691		56.17	nr	0.000	0.080	0.110	-7.27	0.129	0.080	0.030	19.89	6.86
F	VTRB	100	PAS	T	Honda	Accord	90	1875		56.00	482	0.000	0.076	0.102	-8.45	0.151	0.076	0.026	20.87	9.21
F	VTRB	100	PAS	T	Honda	Accord	90	2039		48.80	401	0.000	0.072	0.105	-7.22	0.148	0.072	0.033	19.20	6.20
F	VTRB	100	PAS	T	Honda	Accord	90	2040		48.80	371	0.000	0.074	0.110	-8.12	0.166	0.074	0.036	18.68	6.39
F	VTRB	100	PAS	T	Honda	Accord	90	2041		56.50	459	0.000	0.078	0.102	-8.43	0.149	0.078	0.024	20.52	9.95
F	VTRB	100	PAS	T	Honda	Accord	90	2042		56.50	463	0.000	0.074	0.115	-10.57	0.187	0.074	0.041	21.63	7.30
F	VTRB	100	PAS	T	Honda	Accord	94	2032		47.96	nr	0.000	0.068	0.091	-7.78	0.162	0.068	0.023	19.98	9.58
F	VTRB	100	PAS	T	Honda	Accord	94	2048		56.60	523	0.000	0.077	0.106	-10.49	0.185	0.077	0.029	20.82	10.25

Test No.	Vehicle Crush Information						Test Lab	Eng Mass	Eng Desc	Eng Disp	Trans	Drive	Door	Length	Width	Whl-base	FAxle to		Barr Data
	C1	C2	C3	C4	C5	C6											Cg	DL'd	
2062	327	390	416	441	460	441		1369						1630					
2241	270	348	347	347	350	272	MGA	1272	4TF	1.9	M	F	3	4331	1700	2497	1031	X	
2264	496	513	513	520	514	500	MGA	1325	4TF	1.9	A	F	4	4346	1701	2493	995	X	
832																			
919																			
944							CAL	1569	S6TF	3.0	A	F	4	4808	1788	2695	1082	X	A
1103							CAL	1660	S6TF	3.0	A	F	4	4788	1572	2692	1074	X	A
1177	475	523	539	536	521	483	TRC	1667	S6TF	3.0	A	F	4	4790	1809	2687	1148	X	A
1385							CAL	1642	4TF	2.5	A	F	4	4752	1798	2698	1148	X	A
1403							CAL	1678	S6TF	3.0	A	F	4	4780	1798	2695	1107	X	
1777	274	320	312	305	310	279	TRC	1723	S6TF	3.8	A	F	4	4879	1753	2680	1059	X	
1890	410	460	474	490	468	443	TRC	1711	S6TF	3.8	A	F	4	4875	1790	2666	1095	X	X
1899	254	292	312	323	318	292	CAL	1592	S6TF	3.0	A	F	4	4887	1803	2692	1105	X	X
2312	351	405	410	428	410	374	TRC	1764	V6TF	3.0	A	F	4	5024	1858	2756	1109	X	A
2450							CAL	1450										X	
1186	500	533	511	516	516	516	CAL	1397	4TF	2.3	M	F	4	4488	1735	2543	1097	X	A
1213							CAL	1406	4TF	2.3	A	F	4	4483	nr	2540	1031	X	
2201	168	394	455	462	447	394	TRC	995	3TF	1.0	M	F	3	3772	1590	2357	1024	X	
2239	506	600	635	609	653	525	CAL	1125	4TF	1.3	A	F	4	4161	1390	2375	1117	X	A
1045							CAL	1324	4TF	2.0	M	F	3	4440	1529	2598	1191	X	A
1054							TRC	1332	4TF	2.0	M	F	3	4440	1689	2604	1133	X	
1541							CAL	1483	4TF	2.2	M	F	4	4686	1725	2720	1265	X	A
1552							CAL	1447	4TF	2.2	M	F	4	4681	1725	2728	1189	X	
1597							CAL	1669	4TF	2.2	A	F	WAG	4729	1725	2713	1240	X	A
1610							CAL	1655	4TF	2.2	A	F	WAG	4727	1725	2713	1255	X	
1637							CAL	1646	4TF	2.2	M	F	WAG	4735	1725	2725	1278	X	
1691							CAL	1437	4TF	2.2	M	F	4	4694	1704	2723	1219	X	A
1875							CAL	1579	4TF	2.2	A	F	4	4701	1704	2723	1150	X	A
2039	338	408	426	432	405	327	TRC	1534	4TF	2.2	A	F	4	4630	1720	2715	1158	X	A
2040	309	382	407	400	368	289	TRC	1536	4TF	2.2	A	F	4	4630	1720	2715	1155	X	A
2041	425	472	489	499	441	364	TRC	1532	4TF	2.2	A	F	4	4630	1720	2715	1159	X	A
2042	385	491	482	491	470	378	TRC	1523	4TF	2.2	A	F	4	4630	1720	2715	1162	X	A
2032							CAL	1469	4TF	2.2	M	F	4	4661	1781	2715	1181	X	
2048	470	648	525	509	465	468	MGA	1509	4TF	2.2	A	F	4	4675	1580	2715	1131	X	

<u>Test No.</u>	<u>No. Acc</u>	<u>Trace No.</u>	<u>Location</u>	<u>Notes</u>	ϵ <u>Low</u>	<u>Loc</u>	ϵ <u>High</u>	<u>Loc</u>	ϵ <u>Diff</u>
2062				<i>bad data</i>					
2241	2	5,6	right, left b-pillar	very high restitution					
2264	4	11,12,62,63	right-2, left-2 rear floor	very high restitution					
832				<i>impact attenuator</i>					
919				<i>impact attenuator</i>					
944	2	27,28	rear cross-member - 2	33 (cg) discarded -- vel never reaches 0;					
1103	1	25	left, rear sill	26 (rr) discarded -- post-impact vel too low					
1177	2	40,41	right, left rear sill		0.130	rr	0.133	lr	0.003
1385	1	25	left, rear sill	26 (rr) discarded -- post-impact vel. too high					
1403	2	17,18	right, left rear sill		0.114	lr	0.125	rr	0.011
1777	2	17,18	right, left rear seat		0.121	lr	0.134	rr	0.013
1890	4	17,18,24,25	right-2, left-2 rear seat	difference in left, right corroborated by redundant accelerometers	0.142	lr	0.179	rr	0.037
1899	3	50,51,52	right, center, left rear seat		0.120	cr	0.133	lr	0.013
2312	4	57,58,64,65	right-2, left-2 rear seat	As for 1890, difference in right, left confirmed by redundants	0.138	lr	0.166	rr	0.028
2450	2	27,28	right, left rear seat	35 bad data; all data is pretty ugly					
1186	2	23,24	right, left rear sill						
1213	2	17,18	right, left rear sill						
2201	1	20	right rear seat	19 (left rear seat) inconsistently low restitution of .064					
2239	4	37,38,44,45	right-2, left-2 rear seat						
1045	1	23	left rear sill	high frequency noise on 24 (rr) giving higher restitution					
1054	2	17,18	right, left rear seat	rest vel taken @ .11					
1541	2	23,24	right, left rear sill	left rear sill noisy but used					
1552	2	17,18	right, left rear sill	both traces noisy					
1597	2	23,24	right, left rear sill	good data	0.140	rr	0.164	lr	0.024
1610	2	17,18	right, left rear sill	dash consistent but noisy; good data	0.126	lr	0.132	rr	0.006
1637	2	17,18	right, left rear sill	dash consistent but noisy	0.116	rr	0.161	lr	0.045
1691	2	23,24	right, left rear sill		0.116	rr	0.143	lr	0.027
1875	3	23,24,31	right-2, left-1 rear sill	30 (lr) discarded -- not similar to others; good data	0.145	lr	0.156	rr	0.011
2039	2	76,77	floorpan tunnel	floorpan not compare well to sill data--diff behavior					
2040	2	72,73	floorpan tunnel	floorpan not compare well to sill data--diff behavior					
2041	2	70,71	floorpan tunnel	floorpan data not comparable to sill dynamically					
2042	2	73,74	floorpan tunnel	floorpan data not comparable to sill dynamically					
2032	2	17,18	right, left rear cross-member		0.150	lr	0.174	rr	0.024
2048	2	12,52	right rear cross-member	51 not consistent with majority	0.181	rr	0.184	rr	0.003

<u>Dir</u>	<u>Test Type</u>	<u>Ovrlp %</u>	<u>Veh Type</u>	<u>Eng Or Off</u>	<u>Make</u>	<u>Model</u>	<u>Yr</u>	<u>Tst No.</u>	<u>Rep No</u>	<u>Imp Vel</u>	<u>Crsh</u>	<u>Imp Time</u>	<u>Zero Time</u>	<u>Reb Time</u>	<u>Reb Vel</u>	<u>ε</u>	<u>Crsh Δt</u>	<u>Rest Δt</u>	<u>Crsh Acc</u>	<u>Rest Acc</u>
F	VTRB	100	PAS	T	Honda	Civic	79	833		93.34	0	0.000	0.000	0.000	0.00	0.000	0.000	0.000		
F	VTRB	100	PAS	T	Honda	Civic	79	838		96.56	0	0.000	0.000	0.000	0.00	0.000	0.000	0.000		
F	VTRB	100	PAS	T	Honda	Civic	79	916		96.88	0	0.000	0.000	0.000	0.00	0.000	0.000	0.000		
F	VTRB	100	PAS	T	Honda	Civic	79	917		83.69	0	0.000	0.000	0.000	0.00	0.000	0.000	0.000		
F	VTRB	100	PAS	T	Honda	Civic	79	918		96.88	0	0.000	0.000	0.000	0.00	0.000	0.000	0.000		
F	VTRB	100	PAS	T	Honda	Civic	84	669		56.49	563	0.000	0.084	0.114	-7.30	0.129	0.084	0.030	19.05	6.89
F	VTRB	100	PAS	T	Honda	Civic	84	694		56.17	578	0.000	0.081	0.112	-6.61	0.118	0.081	0.031	19.64	6.04
F	VTRB	100	PAS	T	Honda	Civic	84	705		56.97	536	0.000	0.072	0.104	-7.78	0.137	0.072	0.032	22.41	6.89
F	VTRB	100	PAS	T	Honda	Civic	88	1152		56.33	479	0.000	0.079	0.117	-9.21	0.164	0.079	0.038	20.20	6.86
F	VTRB	100	PAS	T	Honda	Civic	88	1288		55.68	nr	0.000	0.087	0.099	-4.88	0.088	0.087	0.012	18.13	11.52
F	VTRB	100	PAS	T	Honda	Civic	88	1447		47.31	nr	0.000	0.069	0.088	-5.28	0.112	0.069	0.019	19.42	7.87
F	VTRB	100	PAS	T	Honda	Civic	88	1561		56.33	405	0.000	0.078	0.118	-10.42	0.185	0.078	0.040	20.46	7.38
F	VTRB	100	PAS	T	Honda	Civic	92	1725		47.64	nr	0.000	0.072	0.095	-4.84	0.102	0.072	0.023	18.74	5.96
F	VTRB	100	PAS	T	Honda	Civic	92	1801		56.80	524	0.000	0.075	0.098	-7.15	0.126	0.075	0.023	21.45	8.81
F	VTRB	100	PAS	T	Honda	Civic	92	1822		47.31	nr	0.000	0.074	0.086	-3.59	0.076	0.074	0.012	18.11	8.47
F	VTRB	100	PAS	T	Honda	Civic	92	1892		56.30	490	0.000	0.072	0.102	-9.52	0.169	0.072	0.030	22.15	8.99
F	VTRB	100	PAS	T	Honda	Civic	92	2066		56.50	597	0.000	0.071	0.110	-9.43	0.167	0.071	0.039	22.54	6.85
F	VTRB	100	PAS	T	Honda	Civic	96	2362		47.70	337	0.000	0.074	0.091	-5.29	0.111	0.074	0.017	18.26	8.81
F	VTRB	100	PAS	T	Honda	Civic	96	2428		56.60	486	0.000	0.076	0.096	-8.12	0.143	0.076	0.020	21.09	11.50
F	VTRB	100	PAS	T	Hyundai	Excel GLS	86	1092		39.75	nr	0.000	0.068	0.093	-7.70	0.194	0.068	0.025	16.56	8.72
F	VTRB	100	PAS	T	Hyundai	Excel GLS	86	1101		56.00	nr	0.000	0.073	0.107	-8.76	0.156	0.073	0.034	21.73	7.30
F	VTRB	100	PAS	T	Hyundai	Excel GLS	90	1383		56.33	nr	0.000	0.076	0.115	-8.98	0.159	0.076	0.039	20.99	6.52
F	VTRB	100	PAS	T	Hyundai	Excel GLS	92	1722		55.68	571	0.000	0.081	0.132	-9.43	0.169	0.081	0.051	19.47	5.24
F	VTRB	100	PAS	T	Lincoln	Continental	89	1309		56.00	nr	0.000	0.089	0.128	-10.35	0.185	0.089	0.039	17.82	7.52
F	VTRB	100	PAS	T	Lincoln	Continental	89	1331		47.48	nr	0.000	0.091	0.128	-4.81	0.101	0.091	0.037	14.78	3.68
F	VTRB	100	PAS	T	Mercury	Cougar	79	834		96.56	0	0.000	0.000	0.000	0.00	0.000	0.000	0.000		
F	VTRB	100	PAS	T	Mercury	Cougar	79	837		96.56	0	0.000	0.000	0.000	0.00	0.000	0.000	0.000		
F	VTRB	100	PAS	T	Mercury	Cougar	79	913		96.56	0	0.000	0.000	0.000	0.00	0.000	0.000	0.000		
F	VTRB	100	PAS	T	Mercury	Cougar	79	915		96.56	0	0.000	0.000	0.000	0.00	0.000	0.000	0.000		
F	VTRB	100	PAS	T	Mitsubishi	Galant	94	1975		56.00	493	0.000	0.077	0.117	-10.77	0.192	0.077	0.040	20.60	7.63
F	VTRB	100	PAS	T	Nissan	Sentra	93	1768		47.15	392	0.000	0.064	0.101	-6.35	0.135	0.064	0.037	20.87	4.86
F	VTRB	100	PAS	T	Nissan	Sentra	93	1888		56.30	535	0.000	0.087	0.114	-9.35	0.166	0.087	0.027	18.33	9.81
F	VTRB	100	PAS	T	Oldsmobile	Cutlass	84	1215		47.15	334	0.000	0.083	0.125	-6.45	0.137	0.083	0.042	16.09	4.35
F	VTRB	100	PAS	T	Pontiac	Bonneville	92	1702		47.31	467	0.000	0.097	0.141	-6.91	0.146	0.097	0.044	13.81	4.45

Test No.	Vehicle Crush Information						Test Lab	Mass	Eng Desc	Eng Disp	Trans	Drive	Door	Length	Width	Whl-base	FAxle to		Barr Data
	C1	C2	C3	C4	C5	C6											Cg	DL'd	
833																			
838																			
916																			
917																			
918																			
669	546	582	572	566	556	528	CAL	1048	4TF	1.5	A	F	2	3683	1580	2210	1014	X	A
694	549	574	594	594	587	528	CAL	1139	4TF	1.5	M	F	WAG	3995	1384	2456	1135	X	A
705	483	546	556	546	546	485	MS	1048	4TF	1.3	M	F	3	3795	1613	2352	1057	X	A
1152							TRC	1153	4TF	1.5	A	F	3	3965	1692	2494	1072	X	A
1288								1045											A
1447							CAL	1193	4TF	1.5	M	F	4	4293	1666	2502	1113	X	
1561								1244											
1725							CAL	1120	4TF	1.5	M	F	3	4082	1699	2568	1113	X	
1801							CAL	1256	4TF	1.5	A	F	4	4410	1700	2615	1114	X	A
1822							CAL	1260	4TF	1.6	M	F	2	4404	1699	2624	1105	X	
1892							MS	1324	4TF	1.6	A	F	2	4395	1700	2622	1066	X	A
2066	465	628	637	631	607	495	TRC	1249	4TF	1.5	A	F	4	4385	1710	2618	1103	X	A
2362	209	353	369	371	358	254	MGA	1229	4TF	1.6	M	F	4	4250	1656	2620	1105	X	
2428							MGA	1245	4TF	1.5	A	F	2	4251	1688	2616	1074	X	
1092							CAL	1207	4TF	1.5	M	F	5	4069	1595	2380	1092	X	A
1101							CAL	1202	4TF	1.5	M	F	5	4069	1595	2380	1087	X	A
1383							CAL	1207	4TF	1.5	M	F	3	4079	1608	2390	1074	X	A
1722	521	554	589	602	579	544	MS	1225	4TF	1.5	A	F	4	4171	1603	2383	1008	X	
1309							CAL	1923	S6TF	3.8	A	F	4	5212	1847	2769	1156	X	A
1331							CAL	1919	S6TF	3.8	A	F	4	5215	1847	2769	1275	X	
834																			
837																			
913																			
915																			
1975	492	493	551	486	469	436	MGA	1467	4TF	2.4	A	F	4	4632	1630	2640	1126	X	
1768	351	373	399	399	419	384	TRC	1244	4TF	1.6	M	F	2	4328	1671	2428	975	X	
1888	473	524	542	551	549	544	MS	1263	4TF	1.6	A	F	4	4200	1422	2430	947	X	A
1215	274	323	335	348	358	333	TRC	1642	S6TF	2.8	A	F	2	4867	1793	2731	1115	X	
1702	414	462	526	508	442	384	TRC	1905	S6TF	3.8	A	F	4	5131	1885	2819	1135	X	

<u>Test No.</u>	<u>No. Acc</u>	<u>Trace No.</u>	<u>Location</u>	<u>Notes</u>	ϵ <u>Low</u>	<u>Loc</u>	ϵ <u>High</u>	<u>Loc</u>	ϵ <u>Diff</u>
833				<i>impact attenuator</i>					
838				<i>impact attenuator</i>					
916				<i>impact attenuator</i>					
917				<i>impact attenuator</i>					
918				<i>impact attenuator</i>					
669	1	29	left rear seat	27,28 consistent but noisy					
694	1	29	left rear seat	27,28 consistent but noisy					
705	2	25,26	right front, left rear floor		0.126	lr	0.147	rf	0.021
1152	2	25,26	right, left rear seat						
1288	1	31	right rear floorpan	<i>30 vel never reached zero; 31 is suspect but used anyway</i>					
1447	2	17,18	right, left rear sill	restitution time may be too late -- taken at first flat spot					
1561	1	26	left rear seat	<i>25 completely unreasonable--huge restitution</i>					
1725	1	?	left rear sill	right rear sill bad data					
1801	3	?	right-2, left rear sill						
1822	1	17	left rear sill	18 (rr) discarded -- not reasonable; graph is questionable					
1892	3	30,31,33	right. left rear floorpan; center trunk						
2066	1	40	right rear seat	40 noisy but consistent with expected pattern; other traces bad					
2362	2	25,26	right, left rear cross						
2428	4	12,30,66,92	right-2, left-2 rear seat						
1092	2	49,50	left, right rear cross member	47,48,54,60 discarded; 54 too noisy, inconsistent					
1101	4	47,48,49,50	right-2, center, left rear seat	46 not consistent w/majority; 59 bad data					
1383	2	23,24	right, left rear sill	average looks good					
1722	2	30,31	right, left rear floor	32,33 bad data					
1309	2	23,24	left, right rear sill	24 inconsistently high but no basis for elimination	0.154	lr	0.216	rr	0.062
1331	2	17,18	left, right rear sill		0.092	lr	0.111	rr	0.019
834				<i>impact attenuator</i>					
837				<i>impact attenuator</i>					
913				<i>impact attenuator</i>					
915				<i>impact attenuator</i>					
1975	4	11,12,51,52	right-2, left-2 b-pillar		0.167	l b-p	0.218	r b-p	0.051
1768	2	17,18	right, left rear seat		0.118	rr	0.152	lr	0.034
1888	3	30,31,33	right, left rear floor; trunk						
1215	2	19,20	left, right rear seat						
1702	2	19,20	right, left rear seat		0.116	rr	0.176	lr	0.060

<u>Dir</u>	<u>Test Type</u>	<u>Ovrlp %</u>	<u>Veh Type</u>	<u>Eng Or Off</u>	<u>Make</u>	<u>Model</u>	<u>Yr</u>	<u>Tst No.</u>	<u>Rep No.</u>	<u>Imp Vel</u>	<u>Crsh</u>	<u>Imp Time</u>	<u>Zero Time</u>	<u>Reb Time</u>	<u>Reb Vel</u>	ϵ	<u>Crsh Δt</u>	<u>Rest Δt</u>	<u>Crsh Acc</u>	<u>Rest Acc</u>
F	VTRB	100	PAS	T	Pontiac	Bonneville	92	1746		56.60	321	0.000	0.100	0.142	-6.75	0.119	0.100	0.042	16.03	4.55
F	VTRB	100	PAS	T	Pontiac	Grand Am	85	1229		16.09	99	0.000	0.086	0.107	-3.50	0.218	0.086	0.021	5.30	4.72
F	VTRB	100	PAS	T	Saab	900	95	2198		56.50	551	0.000	0.084	0.116	-8.30	0.147	0.084	0.032	19.05	7.35
F	VTRB	100	PAS	T	Saab	900	96	2374		47.20	465	0.000	0.078	0.112	-6.37	0.135	0.078	0.034	17.14	5.31
F	VTRB	100	PAS	T	Toyota	Camry	92	1690		56.01	nr	0.000	0.085	0.110	-5.97	0.107	0.085	0.025	18.66	6.76
F	VTRB	100	PAS	T	Toyota	Camry	92	1707		47.48	394	0.000	0.078	0.096	-7.12	0.150	0.078	0.018	17.24	11.20
F	VTRB	100	PAS	T	Toyota	Camry	95	2255		47.96	436	0.000	0.081	0.094	-2.22	0.046	0.081	0.013	16.77	4.84
F	VTRB	100	PAS	T	Toyota	Camry	95	2280		56.60	494	0.000	0.085	0.122	-9.76	0.172	0.085	0.037	18.86	7.47
F	VTRB	100	PAS	T	Toyota	Celica	86	1099		40.23	nr	0.000	0.063	0.079	-7.23	0.180	0.063	0.016	18.09	12.80
F	VTRB	100	PAS	T	Toyota	Celica	86	1100		56.97	nr	0.000	0.069	0.104	-7.26	0.127	0.069	0.035	23.39	5.88
F	VTRB	100	PAS	T	Toyota	Celica	90	1399		55.84	nr	0.000	0.076	0.103	-10.04	0.180	0.076	0.027	20.81	10.53
F	VTRB	100	PAS	T	Toyota	Celica	90	1444		47.64	nr	0.000	0.078	0.111	-4.51	0.095	0.078	0.033	17.30	3.87
F	VTRB	100	PAS	T	Toyota	Celica	90	1557		47.48	nr	0.000	0.076	0.103	-4.38	0.092	0.076	0.027	17.70	4.59
F	VTRB	100	PAS	T	Toyota	Celica	90	1828		47.15	426	0.000	0.076	0.101	-6.62	0.140	0.076	0.025	17.57	7.50
F	VTRB	100	PAS	T	Toyota	Corolla	94	2019		47.64	384	0.000	0.069	0.086	-5.81	0.122	0.069	0.017	19.56	9.68
F	VTRB	100	PAS	T	Toyota	Corolla	94	2034		56.20	492	0.000	0.074	0.109	-9.73	0.173	0.074	0.035	21.51	7.87
F	VTRB	100	PU		Ford	Ranger	96	2457			0									
F	VTRB	100	PU	I	Chevrolet	Pick-up	81	340			524									
F	VTRB	100	PU	I	Chevrolet	Pick-up	84	696		56.65	668	0.000	0.094	0.152	-9.34	0.165	0.094	0.058	17.07	4.56
F	VTRB	100	PU	I	Chevrolet	S-10	92	1667		56.33	568	0.000	0.078	0.117	-8.70	0.154	0.078	0.039	20.46	6.32
F	VTRB	100	PU	I	Chevrolet	S-10	92	1674		47.15	437	0.000	0.077	0.104	-5.40	0.115	0.077	0.027	17.34	5.66
F	VTRB	100	PU	I	Dodge	Dakota	92	1675		56.33	690	0.000	0.079	0.100	-5.93	0.105	0.079	0.021	20.20	8.00
F	VTRB	100	PU	I	Dodge	Dakota	93	1772		47.15	572	0.000	0.094	0.135	-5.88	0.125	0.094	0.041	14.21	4.06
F	VTRB	100	PU	I	Ford	F150	88	1147		56.97	nr	0.000	0.099	0.150	-9.91	0.174	0.099	0.051	16.30	5.50
F	VTRB	100	PU	I	Ford	F150	97	2437		47.10	436	0.000	0.083	0.136	-4.11	0.087	0.083	0.053	16.07	2.20
F	VTRB	100	PU	I	Nissan	Pickup	96	2412		47.50	326	0.000	0.055	0.072	-5.87	0.124	0.055	0.017	24.46	9.78
F	VTRB	100	PU	I	Nissan	Pickup	96	2414		57.00	479	0.000	0.062	0.118	-11.56	0.203	0.062	0.056	26.04	5.85
F	VTRB	100	PU	?	Ford	Ranger	83	460		47.80	376	0.000	0.093	0.153	-3.58	0.075	0.093	0.060	14.56	1.69
F	VTRB	100	SUV	I	Chevrolet	Blazer	83	576		56.65	478	0.000	0.072	0.095	-10.62	0.187	0.072	0.023	22.29	13.08
F	VTRB	100	SUV	I	Chevrolet	Blazer	83	655		47.48	113	0.000	0.061	0.122	-10.52	0.222	0.061	0.061	22.05	4.88
F	VTRB	100	SUV	I	Chevrolet	Suburban	93	1874		56.30	681	0.000	0.098	0.144	-8.71	0.155	0.098	0.046	16.27	5.36
F	VTRB	100	SUV	I	Ford	Bronco	84	670		47.64	135	0.000	0.063	0.090	-9.31	0.195	0.063	0.027	21.42	9.77
F	VTRB	100	SUV	I	Ford	Bronco	94	2004		56.20	548	0.000	0.092	0.151	-7.29	0.130	0.092	0.059	17.30	3.50
F	VTRB	100	SUV	I	Ford	Explorer	95	2211		56.20	496	0.000	0.078	0.113	-5.63	0.100	0.078	0.035	20.41	4.56

Test No.	Vehicle Crush Information						Test Lab	Eng Mass	Eng Desc	Eng Disp	Trans	Drive	Door	Length	Width	Whl-base	FAxle to		Barr Data
	C1	C2	C3	C4	C5	C6											Cg	DL'd	
1746	518	627	719				CAL	1842	S6TF	3.8	A	F	4	5118	1869	2827	1156	X	A
1229							TRC	1360	4TF	2.5	A	F	2	4493	1715	2629	533	X	
2198	486	563	569	568	551	524	TRC	1601	4TF	2.3	A	F	5	4615	1724	2604	1096	X	A
2374	429	472	470	472	475	447	TRC	1535	4TF	2.3	M	F	3	4658	1722	2601	1060	X	
1690							CAL	1632	4TF	2.2	A	F	4	4783	1770	2616	1163	X	A
1707	310	394	386	409	442	363	TRC	1585	4TF	2.2	M	F	4	4775	1778	2616	1168	X	
2255	300	445	467	475	460	368		1601						nr					
2280	464	550	550	504	445	382	MGA	1576	4TF	2.2	M	F	2	4585	1781	2615	1113	X	
1099							CAL	1225	4TF	2.0	M	F	2	4422	1676			X	A
1100							CAL	1247	4TF	2.0	M	F	2	4422	1676	2517	879	X	A
1399							CAL	1352	4TF	1.6	M	F	2	4465	1689	2527	1052	X	A
1444							CAL	1334	4TF	1.6	M	F	2	4465	1689	2532	1026	X	
1557							CAL	1352	4TF	1.6	A	F	2	4463	1704	2522	1024	X	
1828							TRC	1358	4TF	1.6	M	F	2	4483	1697	2502	1016	X	
2019	396	401	396	381	373	345	TRC	1271	4TF	1.6	M	F	4	4371	1689	2469	1064	X	
2034	464	488	498	498	513	464	MS	1344	4TF	1.8	A	F	4	4372	1685	2170	1268	X	A
2457																			
340	511	521	533	528	523	516	NTS	2064	S6IF	4.1	M	R	PU	5392	2032	3353	1506		
696	648	625	666	706	681	676	MS	2191	V8IF	5.0	A	R	PU	5540	2032	3348	1516	X	A
1667	513	559	592	599	569	531	TRC	1653	V6IF	4.3	M	R	PU	4712	1638	2743	1290	X	A
1674	391	434	450	457	439	422	TRC	1683	S6IF	4.3	A	R	PU	4775	1664	2756	1257	X	
1675	589	686	739	739	693	599	TRC	1615	4IF	2.5	M	R	PU	4803	1808	2850	1422	X	A
1772	470	577	615	620	577	472	TRC	1785	S6IF	3.9	A	R	PU	4966	1808	2850	1377	X	
1147							MS	1989	V6IF	4.9	A	R	PU	5329	1969	3378	1384	X	A
2437	408	419	478	496	412	340	MGA	2136	V6IF	4.2	M	R	PU	5714	1940	3520	1642	X	
2412	336	323	333	330	321	308	MGA	1612	4IF	2.4	M	R	PU	4562	1645	2660	1293	X	
2414	453	472	485	493	485	471	CAL	1566	4IF	2.4	M	R	PU	4422	1525	2650	1325	X	A
460	366	368	378	383	381	373	NTS	1428	-	2.3	M	R	PU	4465	1656	2743	1293	X	
576	391	452	485	506	511	483	MS	1822	V6IF	2.8	M	R	SUV	4313	1575	2563	1311	X	
655	368	381					MS	1336	S6IF	2.0	M	R	SUV	4323	1600	2560	1278	X	
1874	584	685	706	729	706	578	TRC	2849	V8IF	5.7	A	F	SUV	5595	2010	3340	1790	X	A
670	432	457					MS	1471	V6IF	2.8	M	R	SUV	4084	1588	2517	1283	X	
2004	498	568	592	567	536	460	TRC	2447	V8IF	5.0	A	F	SUV	4674	2026	2648	1385	X	A
2211	440	491	527	522	492	452	TRC	2206	V8IF	4.0	A	F	SUV	4773	1746	2835	1404	X	A

<u>Test No.</u>	<u>Acc No.</u>	<u>Trace No.</u>	<u>Location</u>	<u>Notes</u>	ϵ <u>Low</u>	<u>Loc</u>	ϵ <u>High</u>	<u>Loc</u>	ϵ <u>Diff</u>
1746	2	23,24	right, left rear sill		0.114	lr	0.125	rr	0.011
1229	2	5,6	rear deck	restitution assumed finished at 0.115					
2198	4	37,38,44,45	right-2, left-2 rear seat	redundants give about .02 restitution than primaries					
2374	2	17,18	right, left rear seat						
1690	2	25,26	right, left rear sill	uncharacteristicly low restitution					
1707	2	19,20	right, left rear seat						
2255	2	17,18	right, left rear cross	<i>inconsistently low restitution; questionable traces</i>					
2280	4	20,29,70,71	right-2, left-2 rear cross						
1099	3	45,47,49	right, center, left rear x-member	46, 48 discarded					
1100	5	46,47,48,49,50	right, center, left-3 rear x-member						
1399	1	24	right rear sill	23 bad data					
1444	2	17,18	right, left rear sill						
1557	2	17,18	right, left rear sill						
1828	2	17,18	right, left rear seat						
2019	2	31,32	right, left rear seat		0.112	rr	0.140	lr	0.028
2034	4	44,45,46,47	right-2, left-2 rear seat						
2457				<i>report not available</i>					
340				<i>no reported trace data</i>					
696	2	25,26	right front, left rear floor		0.150	rf	0.190	lr	0.040
1667	1	19	left rear seat	20 consistent but noisy					
1674	2	19,20	left, right rear seat		0.116	lr	0.120	rr	0.004
1675	1	19	left rear seat	20 bad data					
1772	2	19,20	left, right rear seat		0.116	rr	0.136	lr	0.020
1147	2	30,31	left, right rear floor		0.153	rr	0.200	lr	0.047
2437	2	24,25	left, right rear x-member		0.072	lr	0.103	rr	0.031
2412	2	23,24	left, right rear x-member		0.112	rr	0.138	lr	0.026
2414	4	39,40,46,47	left-2, right-2 rear seat		0.196	lr	0.222	rr	0.026
460	1	13	left rear floor	15,37 bad data					
576	1	18	left rear floor	17 bad data					
655	1	2	left rear floor	1 bad data; 2 high rebound velocity, but no basis for elimination					
1874	3	19,20,27	left, right-2 rear seat		0.140	lr	0.174	rr	0.034
670	2	1,2	right front, left rear floor						
2004	4	32,33,39,40	right-2, left-2 rear seat						
2211	3	45,46,53	left, right-2 rear seat						

<u>Dir</u>	<u>Test Type</u>	<u>Ovrlp %</u>	<u>Veh Type</u>	<u>Eng Or</u>	<u>Eng Off</u>	<u>Make</u>	<u>Model</u>	<u>Yr</u>	<u>Tst No.</u>	<u>Rep No.</u>	<u>Imp Vel</u>	<u>Crsh</u>	<u>Imp Time</u>	<u>Zero Time</u>	<u>Reb Time</u>	<u>Reb Vel</u>	ϵ	<u>Crsh Δt</u>	<u>Rest Δt</u>	<u>Crsh Acc</u>	<u>Rest Acc</u>	
F	VTRB	100	SUV	I		Ford	Explorer	95	2256		47.31	428	0.000	0.068	0.110	-4.40	0.093	0.068	0.042	19.71	2.97	
F	VTRB	100	SUV	I		Isuzu	Rodeo	95	2313		56.40	429	0.000	0.073	0.099	-8.45	0.150	0.073	0.026	21.88	9.21	
F	VTRB	100	SUV	I		Isuzu	Rodeo	96	2406		47.20	379	0.000	0.073	0.117	-5.04	0.107	0.073	0.044	18.31	3.24	
F	VTRB	100	SUV	I		Isuzu	Trooper II	96	2413		56.70	479	0.000	0.070	0.103	-8.77	0.155	0.070	0.033	22.94	7.53	
F	VTRB	100	SUV	I		Jeep	Cherokee	96	2430		56.30	480	0.000	0.076	0.115	-9.01	0.160	0.076	0.039	20.98	6.54	
F	VTRB	100	SUV	I		Jeep	Cherokee	96	2441		47.15	396	0.000	0.078	0.097	-4.17	0.088	0.078	0.019	17.12	6.22	
F	VTRB	100	SUV	I		Toyota	4Runner	96	2378		47.20	389	0.000	0.084	0.129	-3.98	0.084	0.084	0.045	15.92	2.51	
F	VTRB	100	SUV	I		Toyota	4Runner	96	2409		55.70	580	0.000	0.076	0.107	-7.32	0.131	0.076	0.031	20.76	6.69	
F	VTRB	100	SUV	T		Isuzu	Trooper II	96	2444		47.30	399	0.000	0.075	0.107	-5.29	0.112	0.075	0.032	17.86	4.68	
F	VTRB	100	VAN			Chevrolet	VentureVan	97	2552			0	0.000									
F	VTRB	100	VAN	I		Chevrolet	Astro	92	1677		56.33	517	0.000	0.063	0.098	-9.00	0.160	0.063	0.035	25.33	7.28	
F	VTRB	100	VAN	I		Chevrolet	Astro	92	1692		47.48	437	0.000	0.069	0.096	-6.25	0.132	0.069	0.027	19.49	6.56	
F	VTRB	100	VAN	I		Chevrolet	Sportvan	82	504		47.31	280	0.000	0.053	0.086	-2.16	0.046	0.053	0.033	25.28	1.85	
F	VTRB	100	VAN	I		Chevrolet	Sportvan	87	978		56.33	545	0.000	0.083	0.127	-7.32	0.130	0.083	0.044	19.22	4.71	
F	VTRB	100	VAN	I		Dodge	Ram Wagon	95	2142		56.60	544	0.000	0.067	0.080	-5.27	0.093	0.067	0.013	23.93	11.48	
F	VTRB	100	VAN	I		Dodge	Ram Wagon	95	2277		47.40	189	0.000	0.066	0.010	-4.96	0.105	0.066	-0.056	20.34	-2.51	
F	VTRB	100	VAN	I		Ford	Aerostar	92	1697		56.17	nr	0.000	0.065	0.091	-6.35	0.113	0.065	0.026	24.48	6.92	
F	VTRB	100	VAN	I		Ford	Club MPV	92	1694		47.15	361	0.000	0.073	0.106	-6.92	0.147	0.073	0.033	18.29	5.94	
F	VTRB	100	VAN	I		Ford	Club MPV	92	1695		56.65	463	0.000	0.070	0.102	-8.71	0.154	0.070	0.032	22.92	7.71	
F	VTRB	100	VAN	T		Dodge	Caravan	96	2279		47.15	424	0.000	0.069	0.010	-8.01	0.170	0.069	-0.059	19.36	-3.85	
F	VTRB	100	VAN	T		Dodge	Caravan	96	2335		56.20	489	0.000	0.089	0.122	-8.32	0.148	0.089	0.033	17.89	7.14	
F	VTRB	100	VAN	T		Ford	Windstar	95	2130		56.10	461	0.000	0.090	0.154	-12.77	0.228	0.090	0.064	17.66	5.65	
F	VTRB	100	VAN	T		Ford	Windstar	95	2155		47.64	327	0.000	0.096	0.152	-7.02	0.147	0.096	0.056	14.06	3.55	
F	VTRB	100	VAN	T		Plymouth	Voyager	87	1011		56.33	550	0.000	0.077	0.128	-6.62	0.118	0.077	0.051	20.72	3.68	
F	VTRB	100	VAN	T		Plymouth	Voyager	92	1662		47.64	nr	0.000	0.082	0.113	-8.10	0.170	0.082	0.031	16.46	7.40	

<u>Dir</u>	<u>Test Type</u>	<u>Ovrlp %</u>	<u>Veh Type</u>	<u>Tst No.</u>	<u>Eng Or</u>	<u>Eng Make</u>	<u>Model</u>	<u>Yr</u>	<u>Yeh</u>	<u>Imp Vel</u>	<u>Crsh</u>	<u>Imp Time</u>	<u>Zero Time</u>	<u>Reb Time</u>	<u>Reb Vel</u>	ϵ	<u>Crsh Δt</u>	<u>Rest Δt</u>	<u>Crsh Acc</u>	<u>Rest Acc</u>		
F	VTV	50	PAS	1780					COMB	118.80		0.000	0.000	0.000	0.00	0.000						
F	VTV	50	PAS	1780	T	Chevrolet	Corsica	92		59.40	789											
F	VTV	50	PAS	1780	T	Honda	Accord	90		-59.40	337											
F	VTV	50	PAS	1896					COMB	116.20		0.000	0.000	0.000	0.00	0.000						
F	VTV	50	PAS	1896	T	Chevrolet	Corsica	92		58.10	685											
F	VTV	50	PAS	1896	T	Honda	Accord	90		-58.10	356											

Test No.	Vehicle Crush Information						Test Lab	Eng Mass	Eng Desc	Eng Disp	Trans	Drive	Door	Length	Width	Whl-base	FAxle to		Barr Data
	C1	C2	C3	C4	C5	C6											Cg	DL'd	
2256	406	427	450	450	419	381	CAL	2199	V6IF	4.0	A	F	SUV	4788	1746	2840	1417	X	
2313	428	410	431	452	434	410	MGA	2075	V6IF	3.2	A	F	SUV	4448	1672	2760	1362	X	A
2406	325	378	396	396	386	348	TRC	1870	4IF	2.5	M	R	SUV	4674	1664	2764	1459	X	
2413	465	485	500	500	470	410	CAL	2227	S6IF	3.2	A	F	SUV	4535	1410	2750	1458	X	A
2430	492	523	509	468	466	376	TRC	1998	S6IF	4.0	A	F	SUV	4489	1772	2690	1291	X	A
2441	318	412	427	429	422	262	CAL	1804	V6IF	4.0	M	F	SUV	4209	1772	2565	1247	X	
2378	376	422	411	401	368	305	TRC	1840	4IF	2.7	M	R	SUV	4534	1692	2667	1364	X	
2409	467	531	654	670	558	509	CAL	2076	S6IF	3.4	A	F	SUV	4515	1730	2682	1355	X	A
2444	361	381	414	424	406	381	CAL	2286	V6TF	3.2	M	F	SUV	4544	1410	2761	1065	X	
2552																			
1677	462	536	549	544	508	434	TRC	2084	S6IF	4.3	A	R	VAN	4524	1956	2819	1313	X	A
1692	394	444	460	465	429	376	TRC	2187	S6IF	4.3	A	F	VAN	4526	1951	2819	1549	X	
504	254	264	274	285	295	305	MS	1654	S6IF	4.1	M	R	VAN	4699	2032	2807	1194	X	
978	467	536	556	569	559	539	TRC	2475	V8IF	5.7	A	R	VAN	5138	2040	3188	1534	X	A
2142	495	560	592	590	515	429	CAL	2162	V8IF	5.2	A	R	VAN	5220	1971	3241	-	X	A
2277	152	173	228	220	176	145	MGA	2165	V8IF	5.2	A	R	VAN	5044	1971	3227	1375	X	
1697							CAL	1941	V6IF	3.0	A	R	VAN	4445	1821	3023	1369	X	A
1694	323	363	378	378	363	320	TRC	2692	V8IF	5.0	A	R	VAN	5413	2019	3500	1681	X	
1695	399	450	508	503	457	394	TRC	2624	S6IF	4.9	A	R	VAN	5382	2007	3505	1720	X	A
2279	343	445	445	455	427	348	CAL	2054	V6TF	3.3	A	F	VAN	5067	1932	3040	1397	X	
2335	435	540	553	494	442	395	TRC	2003	V6TF	3.3	A	F	VAN	5060	1932	3030	1319	X	A
2130	406	448	467	470	486	463	MGA	2005	V6TF	3.8	A	F	VAN	5063	1677	3073	1279	X	A
2155	328	325	338	335	315	312	TRC	1963	S6TF	3.8	A	F	VAN	5085	1908	3073	1321	X	
1011	518	549	564	564	554	523	CAL	1660	4TF	2.2	M	F	VAN	4470	1557	2845	1245	X	A
1662							CAL	1859	4TF	2.5	A	F	VAN	4521	1829	2852	1280	X	
1780									TT										
1780	1367	1290	884	630	368	178	CAL	1297	4TF	2.2	A	F	4	4653	1732	2639	1100	X	
1780	706	594	434	244	58	0	CAL	1369	4TF	2.2	M	F	4	4697	1725	2718	1199	X	
1896									TT										
1896	991	1029	874	648	356	43	CAL	1315	4TF	2.2	A	F	4	4648	1732	2642	1085	X	
1896	551	594	495	312	102	0	CAL	1369	4TF	2.2	M	F	4	4686	1725	2718	1270	X	

<u>Test No.</u>	<u>No. Acc</u>	<u>Trace No.</u>	<u>Location</u>	<u>Notes</u>	ϵ <u>Low</u>	<u>Loc</u>	ϵ <u>High</u>	<u>Loc</u>	ϵ <u>Diff</u>
2256	2	17,18	left, right rear seat		0.083	rr	0.111	lr	0.028
2313	4	20,30,63,69	left-2, right-2 rear floor						
2406	2	39,40	left, right rear seat						
2413	2	39,40	left, right rear seat		0.151	lr	0.159	rr	0.008
2430	4	89,90,96,97	left-2, right-2 rear seat						
2441				<i>data stops at 0.1 sec</i>					
2378	2	39,40	left, right rear seat	39 reported as questionable	0.072	lr	0.098	rr	0.026
2409	3	40,46,47	left, right-2 rear seat	39 bad data					
2444	2	37,38	left rear seat; right rear sill		0.110	rr	0.121	lr	0.011
2552				<i>report not available</i>					
1677	2	19,20	left, right rear seat		0.136	rr	0.186	lr	0.050
1692	2	19,20	left, right rear seat		0.099	rr	0.165	lr	0.066
504	2	1,2	right front, left rear floor	data questionable					
978	1	21	left rear seat	22 inconsistent					
2142	4	37,38,44,45	left-2, right-2 rear seat	all traces noisy					
2277	2	14,24	right, left rear x-member		0.101	rr	0.125	lr	0.024
1697	1	23	left rear sill						
1694	2	17,18	left, right rear seat		0.138	lr	0.158	rr	0.020
1695	2	25,26	left, right rear seat		0.152	rr	0.159	lr	0.007
2279	2	17,18	left rear seat; right rear sill		0.162	lr	0.178	rr	0.016
2335	4	79,80,86,87	left-2, right-2 rear seat						
2130	3	11,12,62	left-2, right b-pillar						
2155	2	19,20	left, right rear seat		0.128	rr	0.168	lr	0.040
1011	2	25,26	right, left rear sill		0.083	rr	0.152	lr	0.069
1662	2	17,18	left, right rear sill		0.152	lr	0.192	rr	0.040
1780				<i>questionable data</i>					
1780				<i>questionable data</i>					
1780				<i>questionable data</i>					
1896				<i>questionable data</i>					
1896				<i>questionable data</i>					
1896				<i>questionable data</i>					

<u>Dir</u>	<u>Test Type</u>	<u>Ovrlp %</u>	<u>Veh Type</u>	<u>Tst No.</u>	<u>Eng Or</u>	<u>Make</u>	<u>Model</u>	<u>Yr</u>	<u>Veh</u>	<u>Imp Vel</u>	<u>Crsh</u>	<u>Imp Time</u>	<u>Zero Time</u>	<u>Reb Time</u>	<u>Reb Vel</u>	ϵ	<u>Crsh Δt</u>	<u>Rest Δt</u>	<u>Crsh Acc</u>	<u>Rest Acc</u>
F	VTV	55	PAS	865					COMB	94.48		0.000	0.164	0.200	-2.25	0.024				
F	VTV	55	PAS	865	I	Renault	Fuego	83		47.24	581									
F	VTV	55	PAS	865	T	Honda	Accord	84		-47.24	996									
F	VTV	60	PAS	1544					COMB	115.24		0.000	0.113	0.175	-5.95	0.052				
F	VTV	60	PAS	1544	T	Honda	Accord	90		57.62	409									
F	VTV	60	PAS	1544	T	Isuzu	Stylus	91		-57.62	524									
F	VTV	60	PAS	1551					COMB	103.00		0.000	0.121	0.133	-1.66	0.016				
F	VTV	60	PAS	1551	T	Ford	Taurus	86		51.50	338									
F	VTV	60	PAS	1551	T	Honda	Accord	90		-51.50	336									
F	VTV	60	PAS	1554					COMB	99.78		0.000	0.000	0.000	0.00	0.000				
F	VTV	60	PAS	1554	I	Volvo	740	91		49.89	351									
F	VTV	60	PAS	1554	T	Honda	Accord	90		-49.89	233									
F	VTV	60	PAS	1618					COMB	116.84		0.000	0.000	0.173	0.43	0.000				
F	VTV	60	PAS	1618	I	Volvo	740	91		58.42	411									
F	VTV	60	PAS	1618	T	Honda	Accord	90		-58.42	430									
F	VTV	60	PAS	1665					COMB	117.80		0.000	0.112	0.156	-6.64	0.056				
F	VTV	60	PAS	1665	T	Ford	Taurus	86		58.90	459									
F	VTV	60	PAS	1665	T	Honda	Accord	90		-58.90	607									
F	VTV	60	PAS	1666					COMB	116.60		0.000	0.126	0.174	-3.59	0.031				
F	VTV	60	PAS	1666	I	Chevrolet	Corsica	91		58.30	744									
F	VTV	60	PAS	1666	T	Honda	Accord	90		-58.30	407									
F	VTV	70	PAS	1770					COMB	117.48		0.000	0.110	0.150	-7.27	0.062				
F	VTV	70	PAS	1770	T	Chevrolet	Corsica	92		58.74	749									
F	VTV	70	PAS	1770	T	Honda	Accord	90		-58.74	424									
F	VTV	100	PAS	132					COMB	112.98		0.000	0.091	0.122	-10.12	0.090				
F	VTV	100	PAS	132	T	Chevrolet	Citation	80		56.49	106									
F	VTV	100	PAS	132	T	Plymouth	Horizon	80		-56.49	140									
F	VTV	100	PAS	214					COMB	102.04		0.000	0.112	0.150	-4.77	0.047				
F	VTV	100	PAS	214	I	Oldsmobile	Cutlass	80		51.02	700									
F	VTV	100	PAS	214	T	Volkswagen	Rabbit	80		-51.02	462									
F	VTV	100	PAS	254					COMB	102.36		0.000	0.098	0.122	-3.66	0.036				
F	VTV	100	PAS	254	I	American	Concord	80		51.18	398									
F	VTV	100	PAS	254	T	Volkswagen	Rabbit	80		-51.18	749									
F	VTV	100	PAS	285					COMB	98.16		0.000	0.110	0.147	-5.32	0.054				

Test No.	Vehicle Crush Information						Test Lab	Mass	Eng Desc	Eng Disp	Trans	Drive	Door	Length	Width	Whl-base	FAxle to		Barr Data
	C1	C2	C3	C4	C5	C6											Cg	DL'd	
865								IT											
865	663	671	612	610	483	396	TRC	1354	4IF	1.6	M	F	3	4488	1692	2441	1100	X	
865	1232	1143	1057	947	843	744	TRC	1301	4TF	1.8	M	F	4	4465	1669	2451	1128	X	
1544								TT											
1544	706	635	622	351	84	0	CAL	1365	4TF	2.2	M	F	4	4681	1725	2720	1212	X	
1544	787	770	795	495	165	0	CAL	1207	4TF	1.6	M	F	4	4181	1679	2456	1062	X	
1551								TT											
1551							CAL	1533	S6TF	3.0	A	F	4	4293	1798	2692	1085	X	
1551							CAL	1370	4TF	2.2	M	F	4	4681	1725	2720	1189	X	
1554								IT											
1554	826	643	439	262	0	0	CAL	1492	4IF	2.3	A	R	4	4712	1760	2771	1349	X	
1554	533	406	274	160	58	0	CAL	1370	4TF	2.2	M	F	4	4681	1725	2720	1171	X	
1618								IT											
1618	973	742	516	274	38	0	CAL	1487	4IF	2.3	A	R	4	4811	1760	2791	1318	X	
1618	838	820	546	292	71	0	CAL	1369	4TF	2.2	M	F	4	4679	1725	2720	1171	X	
1665								TT											
1665							CAL	1533	S6TF	3.0	A	F	4	4780	1798	2692	1052	X	
1665							CAL	1369	4TF	2.2	M	F	4	4676	1725	2718	1242	X	
1666								IT											
1666	1171	1046	1019	681	330	114	CAL	1292	4IF	2.2	A	F	4	4658	1732	2624	1031	X	
1666	701	625	605	325	130	0	CAL	1369	4TF	2.2	M	F	4	4676	1725	2718	1171	X	
1770								TT											
1770	950	965	922	879	462	81	CAL	1301	4TF	2.2	A	F	4	4661	1732	2639	1087	X	
1770	686	630	582	419	145	0	CAL	1369	4TF	2.2	M	F	4	4686	1725	2718	1204	X	
132							CAL	73	TT										
132		528					CAL	1361	4TF	2.5	M	F	2	4493	1735	2664	1102	X	
132	521	439					CAL	1288	4TF	1.7	A	F	3	4404	1676	2456	1001	X	
214							CAL	622	IT										
214	531	622	744	754	716	798	CAL	1792	V8IF	4.3	A	R	2	5113	1826	2743	1257	X	
214	412	422	467	483	490	480	CAL	1170	4TF	1.5	M	F	2	3932	1610	2413	1039	X	
254							CAL	610	IT										
254	353	361	368	396	442	495	CAL	1783	V6IF	4.2	A	R	2	4747	1803	2743	1306	X	
254	620	683	747	790	803	820	CAL	1173	4TF	1.5	M	F	2	3932	1610	2413	1039	X	
285							CAL	462	II										

<u>Test No.</u>	<u>No. Acc</u>	<u>Trace No.</u>	<u>Location</u>	<u>Notes</u>	ϵ <u>Low</u>	<u>Loc</u>	ϵ <u>High</u>	<u>Loc</u>	ϵ <u>Diff</u>
865					-0.039	rr	0.085	lr	0.124
865	5	105,107,120,124,125	left(2), right rear seat; right, left b-pillar						
865	3	42,53,55	left (2), right rear seat	56 bad data; 57 no symmetric accelerometer					
1544					-0.026	rr	0.136	lr	0.162
1544	2	67,68	right, left rear seat						
1544	2	26,27	left, right rear seat	didn't use center accelerometer					
1551					-0.044	rr	0.076	lr	0.120
1551	3	27,28	left, right rear x-member	center rear not used					
1551	2	67,68	left, right rear x-member	72 not consistent					
1554				<i>something wrong; predicts vehicles drive through one another</i>					
1554	2	26,27	<i>left, right rear seat</i>	<i>center rear not used, but matches average well</i>					
1554	2	67,68	<i>left, right rear x-member</i>	<i>72 not consistent</i>					
1618					-0.024	rr	0.017	lr	0.041
1618	2	27,28	left, right rear seat	didn't use center accelerometer					
1618	2	68,69	left, right rear x-member	73 not consistent					
1665					0.006	rr	0.108	lr	0.102
1665	2	27,28	left, right rear x-member	center rear not used					
1665	2	68,69	left, right rear x-member	73 not consistent					
1666					-0.043	rr	0.106	lr	0.149
1666	2	27,28	left, right rear seat	center trace not used					
1666	2	68,69	left, right rear seat						
1770					0.003	rr	0.121	lr	0.118
1770	2	27,28	left, right rear seat	center trace not used, although close to average					
1770	2	68,69	left, right rear seat						
132									
132	1	13	left rear floor	11 bad data; 53 noisy; subject trace also somewhat noisy					
132	1	39	left rear floor	37,52,56 noisy					
214									
214	1	27	rear cross-member	12 bad data; 25 noisy					
214	2	51,66	left frame; rear x-member	64 bad data; 68 noisy					
254									
254	2	25,27	left frame; rear x-member	13 inconsistent; 29 noisy					
254	1	51	left frame	64, 66 bad data; 68 noisy but consistent					
285									

<u>Dir</u>	<u>Test Type</u>	<u>Ovrlp %</u>	<u>Veh Type</u>	<u>Tst No.</u>	<u>Eng Or</u>	<u>Make</u>	<u>Model</u>	<u>Yr</u>	<u>Veh</u>	<u>Imp Vel</u>	<u>Crsh</u>	<u>Imp Time</u>	<u>Zero Time</u>	<u>Reb Time</u>	<u>Reb Vel</u>	ϵ	<u>Crsh Δt</u>	<u>Rest Δt</u>	<u>Crsh Acc</u>	<u>Rest Acc</u>
F	VTV	100	PAS	285	I	Chevrolet	Citation	80		49.08	68									
F	VTV	100	PAS	285	I	Chevrolet	Impala	80		-49.08	68									
F	VTV	100	PAS	286					COMB	113.94		0.000	0.091	0.132	-13.96	0.123				
F	VTV	100	PAS	286	I	Chevrolet	Chevette	80		56.97	79									
F	VTV	100	PAS	286	I	Toyota	Corolla	80		-56.97	58									
F	VTV	100	PAS	434					COMB	103.32		0.000	0.126	0.157	-5.74	0.056				
F	VTV	100	PAS	434	I	Mercury	Marquis	81		51.66	588									
F	VTV	100	PAS	434	T	Volkswagen	Rabbit	82		-51.66	536									
F	VTV	100	PAS	447					COMB	111.68		0.000	0.103	0.132	-10.22	0.092				
F	VTV	100	PAS	447	I	Volvo	DL	82		55.84	484									
F	VTV	100	PAS	447	T	Chevrolet	Citation	81		-55.84	452									
F	VTV	100	PAS	456					COMB	113.62		0.000	0.109	0.140	-6.65	0.059				
F	VTV	100	PAS	456	I	Ford	Mustang	82		56.81	133									
F	VTV	100	PAS	456	T	Plymouth	Horizon	82		-56.81	201									
F	VTV	100	PAS	472					COMB	105.90		0.000	0.111	0.144	-10.08	0.095				
F	VTV	100	PAS	472	I	Mercury	Marquis	82		52.95	131									
F	VTV	100	PAS	472	T	Fiat	Strada	82		-52.95	181									
F	VTV	100	PAS	804					COMB	96.72		0.000	0.082	0.125	-12.43	0.129				
F	VTV	100	PAS	804	I	Renault	Fuego	82		48.36	403									
F	VTV	100	PAS	804	T	Honda	Accord	84		-48.36	589									
F	VTV	100	PAS	806					COMB	88.20		0.000	0.093	0.164	-12.04	0.137				
F	VTV	100	PAS	806	T	Chevrolet	Celebrity	84		88.20	537									
F	VTV	100	PAS	806	T	Dodge	Omni	84		0.00	496									
F	VTV	100	PAS	810					COMB	60.67		0.000	0.082	0.132	-8.60	0.142				
F	VTV	100	PAS	810	T	Chevrolet	Celebrity	84		60.67	265									
F	VTV	100	PAS	810	T	Dodge	Omni	84		0.00	343									
F	VTV	100	PAS	812					COMB	89.48		0.000	0.095	0.137	-11.40	0.127				
F	VTV	100	PAS	812	T	Chevrolet	Celebrity	84		89.48	488									
F	VTV	100	PAS	812	T	Honda	Accord	84		0.00	572									
F	VTV	100	PAS	815					COMB	88.35		0.000	0.080	0.122	-12.45	0.141				
F	VTV	100	PAS	815	I	American	Concord	82		88.35	302									
F	VTV	100	PAS	815	T	Honda	Accord	84		0.00	606									
F	VTV	100	PAS	816					COMB	88.67		0.000	0.091	0.138	-10.49	0.118				
F	VTV	100	PAS	816	I	American	Concord	82		88.67	283									

Test No.	Vehicle Crush Information						Test Lab	Eng Mass	Eng Desc	Eng Disp	Trans	Drive	Door	Length	Width	Whl-base	FAxle to		Barr Data
	C1	C2	C3	C4	C5	C6											Cg	DL'd	
285	676						CAL	1384	4IF	2.5	M	F	2	4496	1737	2659	1057	X	
285	676						CAL	1846	V6IF	3.8	A	F	4	5398	1915	2944	1448	X	
286							CAL	18	II										
286	785						CAL	1193	4IF	1.6	A	R	4	4186	1570	2471	1176	X	
286	582						CAL	1211	4IF	1.8	A	R	4	4224	1610	2400	1141	X	
434							CAL	630	IT										
434	493	566	577	594	635	640	CAL	1796	V8IF	4.9	A	R	2	5425	1969	2903	1186	X	
434	663	747	790	810			CAL	1166	4TF	1.7	M	F	2	3922	1610	2413	1041	X	
447							CAL	14	IT										
447	663	660	691	737			CAL	1452	4IF	2.1	M	F	2	4851	1631	2654	1311	X	
447	561	666	686	627			CAL	1438	4TF	2.5	M	F	3	4496	1603	2667	1102	X	
456							CAL	158	IT										
456	554	386					CAL	1415	4IF	2.3	M	R	2	4554	1346	2553	1130	X	
456	673	668					CAL	1257	4TF	1.7	M	F	3	4409	1250	2451	1115	X	
472							CAL	594	IT										
472	216	549					CAL	1796	V8IF	4.2	A	R	2	5428	1930	2908	1395	X	
472	526	643					CAL	1202	4TF	1.5	M	F	5	4089	1651	2449	1026	X	
804							TRC	4	IT										
804	406	457	424	475	457		TRC	1315	4IF	1.6	M	F	2	4465	1638	2451	1344	X	
804	483	599	638	640	589	475	TRC	1311	4TF	1.8	M	F	4	4450	1664	2456	1123	X	
806							TRC	256	TT										
806	419	546	559	574	561	475	TRC	1540	4TF	2.5	A	F	4	4821	1778	2670	1097	X	
806	373	447	493	500	554	597	TRC	1284	4TF	1.6	M	F	4	4155	1664	2510	1268	X	
810							TRC	171	TT										
810	234	259	295	292	249	229	TRC	1539	4TF	2.5	A	F	4	4788	1765	2667	1135	X	
810	376	363	363	343	310	292	TRC	1368	4TF	1.6	M	F	5	4155	1689	2515	1199	X	
812							TRC	219	TT										
812	384	526	521	508	503	384	TRC	1539	4TF	2.5	A	F	4	4780	1765	2667	1110	X	
812	574	612	587	561	561	503	TRC	1320	4TF	1.8	M	R	4	4465	1651	2454	1146	X	
815							TRC	267	IT										
815	325	318	302	297	300	262	TRC	1590	S6IF	4.2	A	R	4	4623	1778	2758	1171	X	
815	549	622	620	694	605	429	TRC	1323	4TF	1.8	M	F	4	4458	1654	2451	1123	X	
816							TRC	275	IT										
816	279	282	279	282	287	290	TRC	1610	S6IF	4.2	A	R	4	4623	1819	2769	1572	X	

Test No.	No. Acc	Trace No.	Location	Notes	ϵ Low	ϵ Loc	ϵ High	ϵ Loc	ϵ Diff
285	2	37,50	right, left rear floor						
285	1	12	left rear floor	9,25 not possible					
286									
286	2	37,50	left rear, right front floor	34 noisy					
286	3	9,12,25	toe pan; left rear, right front floor						
434									
434	1	25	left b-pillar	29, 31 consistent but noisy					
434	3	64,66,68	right, left b-pillar; rear x-member	70 consistent but noisy					
447									
447	3	25,27,29	right, left b-pillar; rear bumper	31 consistent but noisy					
447	2	64,66	right, left b-pillar	68, 70 consistent but noisy					
456									
456	3	23,24,25	right front, left rear floor; cg						
456	3	66,67,68	right front, left rear floor; cg						
472									
472	3	25,27,29	right, left b-pillar; rear bumper						
472	2	62,64	right, left b-pillar	66 noisy					
804									
804	5	96,98,99,100,104	left (2), right (2) rear seat; right b-pillar						
804	5	36,38,39,55,56	left (2), right (2) rear seat; right b-pillar						
806									
806	4	108,111,112,113	right (2), left rear seat; left b-pillar						
806	4	49,52,64,69	right, left rear seat; right, left b-pillar	51, 68 bad data; 55 noisy					
810									
810	5	109,111,112,113,117	right, left (2) rear seat; right, left b-pillar						
810	6	49,51,52,64,68,69	right (2), left (2) rear seat; right, left b-pillar						
812									
812	5	109,111,112,113,117	right, left (2) rear seat; right, left b-pillar						
812	5	49,51,52,68,69	left (2), right (2) rear seat; right b-pillar	64 bad data					
815									
815	5	109,111,112,113,117	right, left (2) rear seat; right, left b-pillar						
815	4	49,64,68,69	right (2), left rear seat; left b-pillar						
816									
816	5	109,111,112,113,117	right, left (2) rear seat; right, left b-pillar						

<u>Dir</u>	<u>Test Type</u>	<u>Ovrlp %</u>	<u>Veh Type</u>	<u>Tst No.</u>	<u>Eng Or</u>	<u>Make</u>	<u>Model</u>	<u>Yr</u>	<u>Veh</u>	<u>Imp Vel</u>	<u>Imp Crsh</u>	<u>Zero Time</u>	<u>Reb Time</u>	<u>Reb Vel</u>	ϵ	<u>Crsh Δt</u>	<u>Rest Δt</u>	<u>Crsh Acc</u>	<u>Rest Acc</u>
F	VTV	100	PAS	816	T	Dodge	Omni	83		0.00	620								
F	VTV	100	PAS	824					COMB	90.93		0.000	0.097	0.136	-9.03	0.099			
F	VTV	100	PAS	824	I	Chevrolet	Celebrity	83		90.93	553								
F	VTV	100	PAS	824	I	Renault	Fuego	83		0.00	432								

<u>Dir</u>	<u>Test Type</u>	<u>Ovrlp %</u>	<u>Veh Type</u>	<u>Eng Or</u>	<u>Make</u>	<u>Model</u>	<u>Yr</u>	<u>Tst No.</u>	<u>Veh</u>	<u>Imp Vel</u>	<u>Imp Crsh</u>	<u>Zero Time</u>	<u>Reb Time</u>	<u>Reb Vel</u>	ϵ	<u>Crsh Δt</u>	<u>Rest Δt</u>	<u>Crsh Acc</u>	<u>Rest Acc</u>
F	VTV(2)	50	PAS	I	Renault	Fuego	83	864	COMB	94.78		0.000	0.152	0.187	-4.37	0.046			
F	VTV(2)	50	PAS	I	Renault	Fuego	83	864	1	47.39	612								
F	VTV(2)	50	PAS	I	Renault	Fuego	83	864	2	47.39	617								
F	VTV(2)	50	PAS	T	Dodge	Omni	83	845	COMB	96.40		0.000	0.130	0.168	-6.00	0.062			
F	VTV(2)	50	PAS	T	Dodge	Omni	83	845	1	48.20	467								
F	VTV(2)	50	PAS	T	Dodge	Omni	83	845	2	48.20	407								
F	VTV(2)	51	PAS	T	Ford	Taurus	86	2076	COMB	112.00		0.000	0.000	0.000	0.00	0.000			
F	VTV(2)	51	PAS	T	Ford	Taurus	86	2076	1	56.00	458								
F	VTV(2)	51	PAS	T	Ford	Taurus	92	2076	2	56.00	483								
F	VTV(2)	54	PAS	T	Honda	Accord	84	860	COMB	95.44		0.000	0.000	0.000	0.00	0.000			
F	VTV(2)	54	PAS	T	Honda	Accord	84	860	1	47.72	418								
F	VTV(2)	54	PAS	T	Honda	Accord	84	860	2	47.72	416								
F	VTV(2)	60	PAS	T	Honda	Accord	90	1676	COMB	112.66		0.000	0.104	0.145	-8.41	0.075			
F	VTV(2)	60	PAS	T	Honda	Accord	90	1676	1	56.33	307								
F	VTV(2)	60	PAS	T	Honda	Accord	90	1676	2	56.33	451								
F	VTV(2)	64	PAS	T	Hyundai	Excel GLS	86	1374	COMB	113.62		0.000	0.139	0.173	-2.32	0.020			
F	VTV(2)	64	PAS	T	Hyundai	Excel GLS	86	1374	1	56.81	445								
F	VTV(2)	64	PAS	T	Hyundai	Excel GLS	86	1374	2	56.81	429								
F	VTV(2)	64	PAS	T	Toyota	Celica	86	1371	1	57.13	497								
F	VTV(2)	64	PAS	T	Toyota	Celica	86	1371	2	57.13	433								
F	VTV(2)	64	PAS	T	Toyota	Celica	86	1371	COMB	165.12		0.000	0.000	0.000	0.00	0.000			
F	VTV(2)	90	PAS	T	Hyundai	Excel GLS	86	1373	COMB	110.08		0.000	0.078	0.108	-9.33	0.085			
F	VTV(2)	90	PAS	T	Hyundai	Excel GLS	86	1373	1	55.04	454								
F	VTV(2)	90	PAS	T	Hyundai	Excel GLS	86	1373	2	55.04	413								
F	VTV(2)	90	PAS	T	Toyota	Celica	86	1372	COMB	112.00		0.000	0.075	0.099	-12.37	0.110			
F	VTV(2)	90	PAS	T	Toyota	Celica	86	1372	1	56.00	450								
F	VTV(2)	90	PAS	T	Toyota	Celica	86	1372	2	56.00	439								

Test No.	Vehicle Crush Information						Test Lab	Eng Mass	Eng Desc	Eng Disp	Trans	Drive	Door	Length	Width	Whl-base	FAxle to		Barr Data
	C1	C2	C3	C4	C5	C6											Cg	DL'd	
816	579	643	643	633	594	599	TRC	1335	4TF	2.2	M	F	5	4161	1679	2512	1100	X	
824							TRC	19	II										
824	368	554	564	671	579	422	TRC	1363	V6IF	2.8	A	F	4	4785	1770	2672	1135	X	
824	417	447	437	424	424	442	TRC	1382	4IF	1.6	M	F	2	4470	1702	2438	1120	X	
864							TRC	64											
864	805	762	668	574	467	371	TRC	1293	4IF	1.6	M	F	3	4488	1692	2441	1295	X	
864	846	765	678	617	432	335	TRC	1357	4IF	1.6	M	F	3	4488	1692	2441	1351	X	
845							TRC	15											
845	864	737	582	394	173	31	TRC	1283	4TF	2.2	M	F	5	4158	1666	2515	1138	X	
845	775	643	503	343	135	46	TRC	1298	4TF	2.2	M	F	5	4168	1684	2515	1074	X	
2076							CAL	4											
2076	805	754	579	368	185	0	CAL	1573	V6TF	3.0	A	F	4	4785	1808	-	-	X	
2076	937	887	879	127	51	0	CAL	1569	V6TF	3.0	A	F	4	4785	1808	2690	-	X	
860							TRC	30											
860	813	691	587	368	132	-188	TRC	1265	4TF	1.8	M	F	4	4460	1664	2451	1133	X	
860	800	622	556	427	152	-152	TRC	1295	4TF	1.8	M	F	4	4465	1664	2451	1110	X	
1676							CAL	141											
1676	584	569	422	211	41	0	CAL	1510	4TF	2.2	A	F	WAG	4730	1725	2718	1125	X	
1676	658	658	737	432	99	0	CAL	1369	4TF	2.2	M	F	4	4676	1725	2718	1171	X	
1374							CAL	14											
1374	752	655	569	455	198	-61	CAL	1143	4TF	1.5	M	F	4	4260	1608	2377	1029	X	
1374	813	683	579	424	112	-124	CAL	1157	4TF	1.5	M	F	4	4260	1615	2377	1034	X	
1371	561	605	767	561	267	5	CAL	1243	4TF	2.0	M	F	2	4422	1697	2525	1013	X	
1371	528	574	709	455	188	-53	CAL	1252	4TF	2.0	M	F	2	4422	1697	2525	978	X	
1371							CAL	1156											
1373							CAL	5											
1373	559	483	480	483	442	206	CAL	1161	4TF	1.5	M	F	4	4260	1608	2377	1021	X	
1373	541	450	439	455	366	170	CAL	1166	4TF	1.5	M	F	4	4260	1608	2377	1036	X	
1372							CAL	14											
1372	566	505	516	505	368	150	CAL	1247	4TF	2.0	M	F	2	4422	1697	2525	1001	X	
1372	635	480	472	500	373	102	CAL	1261	4TF	2.0	M	F	2	4422	1697	2525	973	X	

<u>Test No.</u>	<u>No. Acc</u>	<u>Trace No.</u>	<u>Location</u>	<u>Notes</u>	ϵ <u>Low</u>	<u>Loc</u>	ϵ <u>High</u>	<u>Loc</u>	ϵ <u>Diff</u>
816	6	49,51,52,64,68,69	right (2), left (2) rear seat; right, left b-pillar						
824	5	109,111,112,113,117	right, left (2) rear seat; right, left b-pillar						
824	6	49,51,52,64,68,69	right (2), left (2) rear seat; right, left b-pillar						
864					-0.002	rr	0.094	lr	0.096
864	5	40,42,43,44,48	left (2), right rear seat; left, right b-pillar	ang vel trace dl'd					
864	3	92,94,112	left (2), right rear seat	ang vel trace dl'd					
845					0.062	rr	0.066	lr	0.004
845	4	36,38,54,55	left (2), right (2) rear seat						
845	3	95,97,98	left(2), right rear seat	ang vel trace dl'd					
2076				<i>bad data</i>					
2076									
2076									
860									
860	5	40,42,43,44,48	left (2), right rear seat; left, right b-pillar	<i>bad data</i>					
860									
1676					0.033	rr	0.118	lr	0.085
1676	2	27,28	left, right rear seat	center trace not used					
1676	2	68,69	left, right rear seat						
1374					-0.072	rr	0.118	lr	0.190
1374	2	31,32	left, right rear seat	center trace not used					
1374									
1371				<i>no rr accelerometer available</i>					
1371									
1371									
1373	3	31,32,33	right, left, center rear seat	34 inconsistent					
1373	3	77,78,79	right, center (2) rear seat	76 bad data					
1372									
1372	4	31,32,33,34	left, right, center (2) rear seat						
1372									

<u>Dir</u>	<u>Test Type</u>	<u>Ovrlp %</u>	<u>Veh Type</u>	<u>Eng Or</u>	<u>Make</u>	<u>Model</u>	<u>Yr</u>	<u>Tst No.</u>	<u>Yeh</u>	<u>Imp Vel</u>	<u>Crsh</u>	<u>Imp Time</u>	<u>Zero Time</u>	<u>Reb Time</u>	<u>Reb Vel</u>	<u>ε</u>	<u>Crsh Δt</u>	<u>Rest Δt</u>	<u>Crsh Acc</u>	<u>Rest Acc</u>
F	VTV(2)	94	PAS	T	Ford	Taurus	92	2075	COMB	119.00		0.000	0.000	0.000	0.00	0.000				
F	VTV(2)	94	PAS	T	Ford	Taurus	92	2075	1	59.50	510									
F	VTV(2)	94	PAS	T	Ford	Taurus	92	2075	2	59.50	514									
F	VTV(2)	100	PAS	I	Renault	Fuego	83	796	COMB	96.56		0.000	0.070	0.097	-12.18	0.126				
F	VTV(2)	100	PAS	I	Renault	Fuego	83	796	1	48.28	0									
F	VTV(2)	100	PAS	I	Renault	Fuego	83	796	2	48.28	0									
F	VTV(2)	100	PAS	T	Chevrolet	Cavalier	84	974	COMB	81.43		0.000	0.074	0.094	-8.34	0.102				
F	VTV(2)	100	PAS	T	Chevrolet	Cavalier	84	974	1	40.72	0									
F	VTV(2)	100	PAS	T	Chevrolet	Cavalier	84	974	2	40.72	0									
F	VTV(2)	100	PAS	T	Chevrolet	Cavalier	84	976	COMB	81.59		0.000	0.072	0.093	-9.52	0.117				
F	VTV(2)	100	PAS	T	Chevrolet	Cavalier	84	976	1	40.80	0									
F	VTV(2)	100	PAS	T	Chevrolet	Cavalier	84	976	2	40.80	0									
F	VTV(2)	100	PAS	T	Dodge	Omni	83	795	COMB	96.56		0.000	0.079	0.109	-12.36	0.128				
F	VTV(2)	100	PAS	T	Dodge	Omni	83	795	1	48.28	0									
F	VTV(2)	100	PAS	T	Dodge	Omni	83	795	2	48.28	0									
F	VTV(2)	100	PAS	T	Dodge	Omni	83	877	COMB	96.40		0.000	0.000	0.000	0.00	0.000				
F	VTV(2)	100	PAS	T	Dodge	Omni	83	877	1	48.20	0									
F	VTV(2)	100	PAS	T	Dodge	Omni	83	877	2	48.20	0									
F	VTV(2)	100	PAS	T	Honda	Accord	84	785	COMB	96.88		0.000	0.078	0.100	-13.13	0.136				
F	VTV(2)	100	PAS	T	Honda	Accord	84	785	1	48.44	0									
F	VTV(2)	100	PAS	T	Honda	Accord	84	785	2	48.44	0									

<u>Dir</u>	<u>Test Type</u>	<u>Ovrlp %</u>	<u>Veh Type</u>	<u>Tst No.</u>	<u>Eng Or</u>	<u>Make</u>	<u>Model</u>	<u>Yr</u>	<u>Yeh</u>	<u>Imp Vel</u>	<u>Crsh</u>	<u>Imp Time</u>	<u>Zero Time</u>	<u>Reb Time</u>	<u>Reb Vel</u>	<u>ε</u>	<u>Crsh Δt</u>	<u>Rest Δt</u>	<u>Crsh Acc</u>	<u>Rest Acc</u>
F/R	VTV	100	PAS	21	I				COMB	48.12		0.000	0.128	0.200	-4.40	0.091				
F/R	VTV	100	PAS	21	I	Chevrolet	Impala	71	F	48.12	77									
F/R	VTV	100	PAS	21	I	Ford	Pinto	71	R	0.00	359									
F/R	VTV	100	PAS	48	I				COMB	56.01		0.000	0.107	0.153	-8.26	0.147				
F/R	VTV	100	PAS	48	I	Chevrolet	Impala	71	F	56.01	129									
F/R	VTV	100	PAS	48	I	Chevrolet	Vega	71	R	0.00	333									
F/R	VTV	100	PAS	147	I				COMB	65.50		0.000	0.108	0.178	-9.97	0.152				
F/R	VTV	100	PAS	147	I	Chevrolet	Impala	71	F	65.50	270									
F/R	VTV	100	PAS	147	I	Chevrolet	Vega	71	R	0.00	409									
F/R	VTV	100	PAS	187	I				COMB	56.49		0.000	0.119	0.172	-7.79	0.138				

Test No.	Vehicle Crush Information						Test Lab	Eng Mass	Eng Desc	Eng Disp	Trans	Drive	Door	Length	Width	Whl-base	FAxle to		Barr Data
	C1	C2	C3	C4	C5	C6											Cg	DL'd	
2075							CAL	0											
2075	724	650	630	701	206	0	CAL	1574	V6TF	3.0	A	F	4	4888	1815	2693	1064	X	
2075	414	472	678	716	422	147	CAL	1574	V6TF	3.0	A	F	4	4875	1830	2695	1003	X	
796							TRC	2											
796							TRC	1327	4IF	1.6	M	F	3	4359	1687	2444	1039	X	
796							TRC	1329	4IF	1.6	M	F	3	4476	1676	2438	1039	X	
974							GM	0											
974							GM	1393	4TF	2.0	A	F	4	4369	1684	2571	993	X	
974							GM	1393	4TF	2.0	A	F	4	4369	1684	2571	986	X	
976							GM	2											
976							GM	1391	4TF	2.0	A	F	4	4369	1684	2571	983	X	
976							GM	1393	4TF	2.0	A	F	4	4369	1684	2571	983	X	
795							TRC	2											
795							TRC	1247	4TF	2.2	M	F	5	4158	1689	2515	980	X	
795							TRC	1245	4TF	2.2	M	F	5	4115	1684	2520	1041	X	
877							TRC	5											
877							TRC	1268	4TF	2.2	M	F	5	4145	1684	2525	1077	X	
877							TRC	1273	4TF	2.2	M	F	5	4155	1676	2520	1067	X	
785							TRC	5											
785							TRC	1250	4TF	1.8	M	F	4	4460	1646	2464	1123	X	
785							TRC	1245	4TF	1.8	M	F	4	4473	1661	2451	1209	X	
21							DS	900											
21	30	46	137	130	38	38	DS	1972	V8IF	5.7	A	R	4	5507	2019	3086		X	
21	355	343	350	366	366	389	DS	1072	4IF	1.6	M	R	2	4140	1763	2388		X	
48							DS	867											
48	0	76	244	244	76	10	DS	1985	V8IF	5.7	A	R	4	5507	2019	3086		X	
48	343	328	305	312	356	381	DS	1118	4IF	2.3	M	R	3	4310	1661	2464		X	
147							DS	882											
147	76	198	366	366	320	122	DS	2002	V8IF	5.7	A	R	4	5507	2019	3086		X	
147	495	434	389	381	396	396	DS	1120	4IF	2.3	M	R	3	4310	1661	2463		X	
187							DS	876											

<u>Test No.</u>	<u>No. Acc</u>	<u>Trace No.</u>	<u>Location</u>	<u>Notes</u>	ϵ <u>Low</u>	<u>Loc</u>	ϵ <u>High</u>	<u>Loc</u>	ϵ <u>Diff</u>
2075									
2075	2	61,63	left, right rear floor						
2075				bad data					
796									
796	4	24,33,39,40	left, right b-pillar; right rear seat-2	no center trace for inline engine	0.122	lb-p	0.133	rr	0.011
796	3	81,82,84	right rear seat-2; left b-pillar	78,80,86 inconsistent; no center trace for inline engine					
974									
974	1	80	left rear sill	81 bad data					
974	4	58,59,60,61	left, right rear sill; left, right rear floor		0.094	rrFl	0.117	lrSill	0.023
976									
976	2	31,32	left rear, left front sill	33 (rr) bad data	0.176	lr	0.180	lf	0.004
976	2	71,73	left front, right rear sill	72 (lr) noisy; data questionable	0.073	lf	0.095	rr	0.022
795				all data but trace 33 used to develop plot					
795	5	21,23,24,39,40	left-2, right-2 rear seat; right b-pillar	33 bad data; huge difference between right and left accel	0.076	lr avg	0.163	rr avg	0.087
795	6	78,80,81,84,82,86	left-2, right-2 rear seat; left, right b-pillar	large difference between right and left	0.100	lr avg	0.180	rr avg	0.080
877									
877				can't resolve accelerometer differences					
877				can't resolve accelerometer differences					
785									
785	5	21,24,33,39,40	left, right rear-2 seat; left, right b-pillar	23 bad data	0.118	rr avg	0.145	lr avg	0.027
785	6	78,80,81,82,84,86	left-2, right-2 rear seat; left, right b-pillar						
21									
21	2	17,18	right, left front floor						
21	2	13,16	right, left front floor						
48									
48	2	16,17	right, left front floor						
48	2	12,15	right, left front floor						
147									
147	2	17,18	right, left front floor						
147	2	13,16	right, left front floor						
187									

<u>Test Dir</u>	<u>Type</u>	<u>Ovrlp %</u>	<u>Veh Type</u>	<u>Tst No.</u>	<u>Eng Or</u>	<u>Make</u>	<u>Model</u>	<u>Yr</u>	<u>Veh</u>	<u>Imp Vel</u>	<u>Imp Crsh</u>	<u>Zero Time</u>	<u>Reb Time</u>	<u>Reb Vel</u>	ϵ	<u>Crsh Δt</u>	<u>Rest Δt</u>	<u>Crsh Acc</u>	<u>Rest Acc</u>
F/R	VTV	100	PAS	187	I	Chevrolet	Impala	71	F	56.49	251								
F/R	VTV	100	PAS	187	I	Chevrolet	Vega	71	R	0.00	287								

<u>Test Dir</u>	<u>Type</u>	<u>Ovrlp %</u>	<u>Veh Type</u>	<u>Eng Or</u>	<u>Make</u>	<u>Model</u>	<u>Yr</u>	<u>Tst No.</u>	<u>Veh</u>	<u>Imp Vel</u>	<u>Imp Crsh</u>	<u>Zero Time</u>	<u>Reb Time</u>	<u>Reb Vel</u>	ϵ	<u>Crsh Δt</u>	<u>Rest Δt</u>	<u>Crsh Acc</u>	<u>Rest Acc</u>
F/R	VTV(2)	100	PAS	I	Chevrolet	Impala	71	49	COMB	55.68		0.000	0.150	0.215	-6.75	0.121			
F/R	VTV(2)	100	PAS	I	Chevrolet	Impala	71	49	F	55.68	60								
F/R	VTV(2)	100	PAS	T	Chevrolet	Impala	71	49	R	0.00	515								
R	ITV	100	PAS		Acura	Legend	88	1278			0								
R	ITV	100	PAS		American	Concord	80	76	COMB	56.33		0.000	0.069	0.107	-5.35	0.095			
R	ITV	100	PAS		American	Concord	80	76	IMP	56.33									
R	ITV	100	PAS		American	Concord	80	76	V	0.00	0								
R	ITV	100	PAS		Chevrolet	Cavalier	81	362			615								
R	ITV	100	PAS		Chevrolet	Cavalier	88	1279			0								
R	ITV	100	PAS		Chevrolet	Chevette	78	176			0								
R	ITV	100	PAS		Chevrolet	Chevette	79	37	COMB	56.17		0.000	0.097	0.151	-8.48	0.151			
R	ITV	100	PAS		Chevrolet	Chevette	79	37	IMP	56.17									
R	ITV	100	PAS		Chevrolet	Chevette	79	37	V	0.00	0								
R	ITV	100	PAS		Chevrolet	Citation	80	28	COMB	55.49		0.000	0.095	0.168	-6.95	0.125			
R	ITV	100	PAS		Chevrolet	Citation	80	28	IMP	55.49									
R	ITV	100	PAS		Chevrolet	Citation	80	28	V	0.00	55								
R	ITV	100	PAS		Dodge	Colt	79	146	COMB	56.81		0.000	0.000	0.000	0.00	0.000			
R	ITV	100	PAS		Dodge	Colt	79	146	IMP	56.81									
R	ITV	100	PAS		Dodge	Colt	79	146	V	0.00	155								
R	ITV	100	PAS		Dodge	Colt	85	524	COMB	47.31		0.000	0.106	0.139	-3.84	0.081			
R	ITV	100	PAS		Dodge	Colt	85	524	IMP	47.31									
R	ITV	100	PAS		Dodge	Colt	85	524	V	0.00	0								
R	ITV	100	PAS		Dodge	Neon	96	2439			0								
R	ITV	100	PAS		Ford	Escort	93	1969			0								
R	ITV	100	PAS		Ford	LTD	79	101	COMB	56.33		0.000	0.000	0.000	0.00	0.000			
R	ITV	100	PAS		Ford	LTD	79	101	IMP	56.33									
R	ITV	100	PAS		Ford	LTD	79	101	V	0.00	53								
R	ITV	100	PAS		Ford	Mustang	79	210	COMB	56.81		0.000	0.104	0.156	-8.59	0.151			
R	ITV	100	PAS		Ford	Mustang	79	210	IMP	56.81									

Test No.	Vehicle Crush Information						Test Lab	Eng Mass	Eng Desc	Eng Disp	Trans	Drive	Door	Length	Width	Whl-base	FAxle to		Barr Data
	C1	C2	C3	C4	C5	C6											Cg	DL'd	
187	198	206	389	411	152	0	DS	2025	V8IF	6.6	A	R	4	5507	2019	3086		X	
187	267	305	312	282	267	267	DS	1149	4IF	2.3	M	R	3	4310	1661	2464		X	
49							DS	163											
49	0	0	152	147	0	0	DS	2175	V8IF	6.5	A	R	4	5507	2019	3086		X	
49	481	526	549	541	488	457	DS	2012	V8IF	5.7	A	R	4	5507	2019	3086		X	
1278																			
76							CAL	118											
76							CAL	1805											X
76							CAL	1687						1709					X
362	610	607	620	620	617	610	NTS	1300	4TF	1.8	M	F	2	4346	1664	2578	1026		
1279																			
176																			
37							DS	601											
37							DS	1810						3658	1524	3048			X
37							DS	1209	4IF	1.6	M	R	5	4006	1549	2477	1049		X
28							CAL	344											
28							CAL	1805						3658	1524	3048			X
28	549						CAL	1461	S6TF	2.8	A	F	5	4511	1730	2667	993		X
146							NTS	760											
146							NTS	1804											X
146	533	508					NTS	1044	4TF	1.4	M	F	3	3975	1626	2311	1016		X
524							TRC	655											
524							TRC	1791											X
524							TRC	1136	4TF	1.5	M	F	4	4267	1636	2388	1036		X
2439																			
1969																			
101							NTS	112											
101							NTS	1804											X
101	533						NTS	1916	V8IF	4.9	A	R	2	5316	1969	2896	1499		X
210							DS	366											
210							DS	1810											X

<u>Test No.</u>	<u>No. Acc</u>	<u>Trace No.</u>	<u>Location</u>	<u>Notes</u>	ϵ <u>Low</u>	ϵ <u>Loc</u>	ϵ <u>High</u>	ϵ <u>Loc</u>	ϵ <u>Diff</u>
187	2	15,16	right, left front floor						
187	2	11,14	right, left front floor						
49									
49	2	33,40	right, left front floor						
49	1	25	left front floor	28 bad data					
1278				<i>vehicle data only</i>					
76									
76	1	26	cg	NHTSA Flat					
76	2	21,23	rear cross-member; cg						
362				<i>no data available</i>					
1279				<i>vehicle data only</i>					
176				<i>vehicle data only</i>					
37									
37				NHTSA Flat					
37									
28									
28	1	26	cg	19 bad data; NHTSA Flat					
28	1	21	rear cross-member	21 bad data					
146				<i>data scaling problem--adjusted traces senseless</i>					
146				<i>NHTSA Flat</i>					
146									
524									
524	1	4	cg	NHTSA Flat					
524	1	1	cg						
2439				<i>vehicle data only</i>					
1969				<i>vehicle data only</i>					
101				<i>data scaling problem</i>					
101				<i>NHTSA Flat</i>					
101									
210									
210	1	18	?	NHTSA Flat					

<u>Dir</u>	<u>Test Type</u>	<u>Ovrlp %</u>	<u>Veh Type</u>	<u>Eng Or</u>	<u>Make</u>	<u>Model</u>	<u>Yr</u>	<u>Tst No.</u>	<u>Veh</u>	<u>Imp Vel</u>	<u>Crsh</u>	<u>Imp Time</u>	<u>Zero Time</u>	<u>Reb Time</u>	<u>Reb Vel</u>	<u>ε</u>	<u>Crsh Δt</u>	<u>Rest Δt</u>	<u>Crsh Acc</u>	<u>Rest Acc</u>
R	ITV	100	PAS		Ford	Mustang	79	210	V	0.00	0									
R	ITV	100	PAS		Ford	Taurus	86	1146	COMB	47.48		0.000	0.079	0.175	-9.00	0.190				
R	ITV	100	PAS		Ford	Taurus	86	1146	IMP	47.48										
R	ITV	100	PAS		Ford	Taurus	86	1146	V	0.00	340									
R	ITV	100	PAS		Ford	Tempo	88	1258			316									
R	ITV	100	PAS		Ford	Thunderbird	79	144	COMB	56.65		0.000	0.000	0.000	0.00	0.000				
R	ITV	100	PAS		Ford	Thunderbird	79	144	IMP	56.65										
R	ITV	100	PAS		Ford	Thunderbird	79	144	V	0.00	0									
R	ITV	100	PAS		Ford	Thunderbird	83	712	COMB	47.31		0.000	0.103	0.206	-12.36	0.261				
R	ITV	100	PAS		Ford	Thunderbird	83	712	IMP	47.31										
R	ITV	100	PAS		Ford	Thunderbird	83	712	V	0.00	0									
R	ITV	100	PAS		Honda	Accord	78	112			0									
R	ITV	100	PAS		Honda	Accord	82	421	COMB	47.80		0.000	0.133	0.168	-1.37	0.029				
R	ITV	100	PAS		Honda	Accord	82	421	IMP	47.80										
R	ITV	100	PAS		Honda	Accord	82	421	V	0.00	599									
R	ITV	100	PAS		Honda	Accord	90	1432			273									
R	ITV	100	PAS		Honda	Civic	79	185	COMB	56.33		0.000	0.093	0.127	-4.07	0.072				
R	ITV	100	PAS		Honda	Civic	79	185	IMP	56.33										
R	ITV	100	PAS		Honda	Civic	79	185	V	0.00	0									
R	ITV	100	PAS		Honda	Civic	80	142	COMB	56.33		0.000	0.082	0.127	-4.92	0.087				
R	ITV	100	PAS		Honda	Civic	80	142	IMP	56.33										
R	ITV	100	PAS		Honda	Civic	80	142	V	0.00	0									
R	ITV	100	PAS		Honda	Civic	81	293	COMB	56.33		0.000	0.087	0.128	-5.26	0.093				
R	ITV	100	PAS		Honda	Civic	81	293	IMP	56.33										
R	ITV	100	PAS		Honda	Civic	81	293	V	0.00	0									
R	ITV	100	PAS		Honda	Civic	84	923	COMB	47.48		0.000	0.099	0.120	-1.67	0.035				
R	ITV	100	PAS		Honda	Civic	84	923	IMP	47.48										
R	ITV	100	PAS		Honda	Civic	84	923	V	0.00	383									
R	ITV	100	PAS		Honda	Civic	88	1276			0									
R	ITV	100	PAS		Honda	Civic	95	2268			0									
R	ITV	100	PAS		Mitsubishi	Galant	89	1405			0									
R	ITV	100	PAS		Nissan	Sentra	87	1110	COMB	47.96		0.000	0.092	0.150	-5.35	0.112				
R	ITV	100	PAS		Nissan	Sentra	87	1110	IMP	47.96										
R	ITV	100	PAS		Nissan	Sentra	87	1110	V	0.00	451									

Test No.	Vehicle Crush Information						Test Lab	Eng Mass	Eng Desc	Eng Disp	Trans	Drive	Door	Length	Width	Whl-base	FAxle to Cg	DL'd	Barr Data
	C1	C2	C3	C4	C5	C6													
210							DS	1444						1755				X	
1146							TRC	160											
1146							TRC	1793					3526	2027	2596	762		X	
1146	340	335	338	343	343	343	TRC	1633		3.0	A	F	4	4806	1788	2692	1105		X
1258	300	343	330	305	305	292	MS	1670	4TF	2.3	M	F	2	4501	1638	2527	1201		
144							NTS	398											
144							NTS	1804											X
144							NTS	2202					2002						X
712							NTS	184											
712							NTS	1809					3526	2027	2596	762		X	
712							NTS	1625	V8IF	3.8	A	R	2	5010	1816	2649	1212		X
112																			
421							DS	624											
421							DS	1810					3658	1524	3048				X
421	594	602	605	602	597	579	DS	1186	4TF	1.8	M	F	4	4570	1621	2380	963		X
1432	226	279	290	290	279	226	MS	1445	4TF	2.2	M	F	4	4712	1725	2720	1074		
185							DS	861											
185							DS	1810											X
185							DS	949					1506						X
142							DS	797											
142							DS	1810											X
142							DS	1013					1580						X
293							NTS	722											
293							NTS	1804											X
293							NTS	1082		1.5	M	F	4	4059	1575	2311	1024		X
923							NTS	837											
923							NTS	1809											X
923	368	384	391	391	379	368	NTS	972	4TF	1.3	M	F	2	3673	1623	2200	927		X
1276																			
2268																			
1405																			
1110							TRC	689											
1110							TRC	1799					3526	2027	2596	726			X
1110	427	467	472	462	445	391	TRC	1110	4TF	1.6	M	F	2	4277	1636	2433	963		X

<u>Test No.</u>	<u>No. Acc</u>	<u>Trace No.</u>	<u>Location</u>	<u>Notes</u>	ϵ <u>Low</u>	ϵ <u>Loc</u>	ϵ <u>High</u>	ϵ <u>Loc</u>	ϵ <u>Diff</u>
210	1	10	right front floor						
1146				questionable traces					
1146				NHTSA Flat					
1146									
1258				<i>vehicle data only</i>					
144				<i>data scaling problem</i>					
144				<i>NHTSA Flat</i>					
144									
712				uncharacteristically high restitution					
712	1	1	front cross-member	NHTSA Flat					
712	1	2	cg						
112				<i>vehicle data only</i>					
421									
421	2	1,2	?	NHTSA Flat					
421	4	3,4,5,6	left rear floor (2); front cross-member (2)						
1432				<i>vehicle data only</i>					
185									
185	1	18	?	NHTSA Flat					
185	1	4	right front floor	7 bad data					
142									
142	2	5,6	?L	NHTSA Flat					
142	2	1,3	right front floor	2,4 bad data-probably in crush zone					
293									
293				NHTSA Flat					
293									
923				questionable traces					
923	1	1	front cross-member	NHTSA Flat					
923	1	2	cg						
1276				<i>vehicle data only</i>					
2268				<i>vehicle data only</i>					
1405				<i>vehicle data only</i>					
1110									
1110	1	4	cg	NHTSA Flat					
1110	1	1	cg						

<u>Dir</u>	<u>Test Type</u>	<u>Ovrlp %</u>	<u>Veh Type</u>	<u>Eng Or</u>	<u>Make</u>	<u>Model</u>	<u>Yr</u>	<u>Tst No.</u>	<u>Veh</u>	<u>Imp Vel</u>	<u>Crsh</u>	<u>Imp Time</u>	<u>Zero Time</u>	<u>Reb Time</u>	<u>Reb Vel</u>	<u>ε</u>	<u>Crsh Δt</u>	<u>Rest Δt</u>	<u>Crsh Acc</u>	<u>Rest Acc</u>
R	ITV	100	PAS		Oldsmobile	Cutlass	80	154	COMB	56.49		0.000	0.095	0.142	-7.41	0.131				
R	ITV	100	PAS		Oldsmobile	Cutlass	80	154	IMP	56.49										
R	ITV	100	PAS		Oldsmobile	Cutlass	80	154	V	0.00	0									
R	ITV	100	PAS		Plymouth	Acclaim	91	2151	COMB	49.20		0.000	0.098	0.199	-2.84	0.058				
R	ITV	100	PAS		Plymouth	Acclaim	91	2151	IMP	49.20										
R	ITV	100	PAS		Plymouth	Acclaim	91	2151	V	0.00	415									
R	ITV	100	PAS		Plymouth	Horizon	79	143	COMB	57.13		0.000	0.000	0.000	0.00	0.000				
R	ITV	100	PAS		Plymouth	Horizon	79	143	IMP	57.13										
R	ITV	100	PAS		Plymouth	Horizon	79	143	V	0.00	0									
R	ITV	100	PAS		Pontiac	Bonneville	84	931	COMB	47.15		0.000	0.096	0.146	-8.55	0.181				
R	ITV	100	PAS		Pontiac	Bonneville	84	931	IMP	47.15										
R	ITV	100	PAS		Pontiac	Bonneville	84	931	V	0.00	316									
R	ITV	100	PAS		Pontiac	Grand Prix	79	68	COMB	56.49		0.000	0.099	0.153	-9.12	0.161				
R	ITV	100	PAS		Pontiac	Grand Prix	79	68	IMP	56.49										
R	ITV	100	PAS		Pontiac	Grand Prix	79	68	V	0.00	0									
R	ITV	100	PAS		Pontiac	Sunbird	79	62	COMB	56.17		0.000	0.091	0.144	-7.46	0.133				
R	ITV	100	PAS		Pontiac	Sunbird	79	62	IMP	56.17										
R	ITV	100	PAS		Pontiac	Sunbird	79	62	V	0.00	0									
R	ITV	100	PAS		Subaru	GL	80	212	COMB	56.49		0.000	0.090	0.117	-4.02	0.071				
R	ITV	100	PAS		Subaru	GL	80	212	IMP	56.49										
R	ITV	100	PAS		Subaru	GL	80	212	V	0.00	654									
R	ITV	100	PAS		Subaru	GL	85	893	COMB	47.48		0.000	0.083	0.111	-5.22	0.110				
R	ITV	100	PAS		Subaru	GL	85	893	IMP	47.48										
R	ITV	100	PAS		Subaru	GL	85	893	V	0.00	455									
R	ITV	100	PAS		Toyota	Celica	79	23	COMB	55.84		0.000	0.095	0.155	-6.92	0.124				
R	ITV	100	PAS		Toyota	Celica	79	23	IMP	55.84										
R	ITV	100	PAS		Toyota	Celica	79	23	V	0.00	39									
R	ITV	100	PAS		Toyota	Celica	79	230	COMB	47.64		0.000	0.080	0.138	-7.55	0.158				
R	ITV	100	PAS		Toyota	Celica	79	230	IMP	47.64										
R	ITV	100	PAS		Toyota	Celica	79	230	V	0.00	191									
R	ITV	100	PAS		Toyota	Celica	86	1038	COMB	47.64		0.000	0.074	0.100	-4.23	0.089				
R	ITV	100	PAS		Toyota	Celica	86	1038	IMP	47.64										
R	ITV	100	PAS		Toyota	Celica	86	1038	V	0.00	0									
R	ITV	100	PAS		Toyota	Corolla	80	149	COMB	56.65		0.000	0.000	0.000	0.00	0.000				

Test No.	Vehicle Crush Information						Test Lab	Eng Mass	Eng Desc	Eng Disp	Trans	Drive	Door	Length	Width	Whl-base	FAxle to Cg	DL'd	Barr Data
	C1	C2	C3	C4	C5	C6													
154							NTS	3											
154							NTS	1804											X
154							NTS	1807					1816						X
2151							TRC	188											
2151							TRC	1821											X
2151	381	409	460	429	407	363	TRC	1633	4TF	2.5	A	F	4	4625	1727	2629	1082		X
143							NTS	530											
143							NTS	1804											X
143							NTS	1274					1676						X
931							NTS	124											
931							NTS	1809											X
931	267	305	320	333	335	305	NTS	1685	V6IF	3.8	A	R	4	5062	1842	2743	1280		X
68							CAL	27											
68							CAL	1805											X
68							CAL	1778	V8IF	4.9	A	R	2	5116	1847	2746	1189		X
62							CAL	344											
62							CAL	1805											X
62							CAL	1461	4IF	2.5	M	R	2	4552	1661	2464	1135		X
212							NTS	643											
212							NTS	1804						3658	1524	3048			X
212	635	638	660	663	658	671	NTS	1161		1.6	M	F	4	4232	1610	2471	1024		X
893							TRC	0											
893							TRC	1350											X
893	384	467	472	470	467	412	TRC	1350	4IF	1.8	M	F	WAG	4415	1537	2479	1113		X
23							CAL	462											
23							CAL	1805						3658	1524	3048			X
23	389						CAL	1343	4IF	2.2	M	R	3	4427	1638	2489	1143		X
230							NTS	484											
230							NTS	1804						3658	1524	3048			X
230	254	264	272	292	0	0	NTS	1320	4IF	2.2	M	R	2	4415	1638	2497	1270		X
1038							TRC	471											
1038							TRC	1793											X
1038							TRC	1322	4TF	2.0	M	F	2	4415	1689	2517	975		X
149							NTS	622											

<u>Test No.</u>	<u>No. Acc</u>	<u>Trace No.</u>	<u>Location</u>	<u>Notes</u>	ϵ <u>Low</u>	ϵ <u>Loc</u>	ϵ <u>High</u>	ϵ <u>Loc</u>	ϵ <u>Diff</u>
154				<i>data scaling problem; x, y data scaled by 2</i>					
154				<i>NHTSA Flat</i>					
154									
2151									
2151	1	8	cg	NHTSA Flat					
2151	2	1,6	cg; right rear sill	4 inconsistent					
143				<i>bad data</i>					
143				<i>NHTSA Flat</i>					
143									
931									
931	1	1	front cross-member	NHTSA Flat					
931	1	2	cg						
68									
68	1	26	front face	NHTSA Flat; 19 noisy, inconsistent					
68	2	21,23	rear cross-member; cg						
62									
62	1	26	cg	NHTSA Flat; 19 unreasonable					
62	1	21	rear cross-member	23 consistent but noisy					
212									
212	1	1	?	NHTSA Flat					
212	3	2,3,4	?; left rear, right front floor						
893									
893	1	4	cg	NHTSA Flat					
893	1	1	cg						
23									
23	1	26	cg	NHTSA Flat					
23	3	19,21,23	front, rear cross-member; cg						
230									
230	1	1	?	NHTSA Flat					
230	1	5	?						
1038									
1038				NHTSA Flat					
1038									
149				<i>data scaling problem</i>					

<u>Dir</u>	<u>Test Type</u>	<u>Ovrlp %</u>	<u>Veh Type</u>	<u>Eng Or</u>	<u>Make</u>	<u>Model</u>	<u>Yr</u>	<u>Tst No.</u>	<u>Veh</u>	<u>Imp Vel</u>	<u>Crsh</u>	<u>Imp Time</u>	<u>Zero Time</u>	<u>Reb Time</u>	<u>Reb Vel</u>	<u>ε</u>	<u>Crsh Δt</u>	<u>Rest Δt</u>	<u>Crsh Acc</u>	<u>Rest Acc</u>
R	ITV	100	PAS		Toyota	Corolla	80	149	IMP	56.65										
R	ITV	100	PAS		Toyota	Corolla	80	149	V	0.00	429									
R	ITV	100	PAS		Toyota	Corolla	80	151	COMB	56.65		0.000	0.000	0.000	0.00	0.000				
R	ITV	100	PAS		Toyota	Corolla	80	151	IMP	56.65										
R	ITV	100	PAS		Toyota	Corolla	80	151	V	0.00	428									
R	ITV	100	PAS		Toyota	Corolla	84	560	COMB	47.64		0.000	0.080	0.123	-4.05	0.085				
R	ITV	100	PAS		Toyota	Corolla	84	560	IMP	47.64										
R	ITV	100	PAS		Toyota	Corolla	84	560	V	0.00	327									
R	ITV	100	PAS		Toyota	Tercel	83	635	COMB	47.48		0.000	0.080	0.123	-4.05	0.085				
R	ITV	100	PAS		Toyota	Tercel	83	635	IMP	47.48										
R	ITV	100	PAS		Toyota	Tercel	83	635	V	0.00	0									
R	ITV	100	PAS		Volvo	244	79	74	COMB	55.68		0.000	0.000	0.000	0.00	0.000				
R	ITV	100	PAS		Volvo	244	79	74	IMP	55.68										
R	ITV	100	PAS		Volvo	244	79	74	V	0.00	0									
R	VTRB	100	PAS		Chevrolet	Vega	72	31		34.44	408	0.000	0.112	0.163	-6.99	0.203	0.112	0.051	8.71	3.88

<u>Dir</u>	<u>Test Type</u>	<u>Veh Type</u>	<u>Offset</u>	<u>Make</u>	<u>Model</u>	<u>Yr</u>	<u>Tst No.</u>	<u>Veh</u>	<u>Imp Vel</u>	<u>Crsh</u>	<u>Imp Time</u>	<u>Zero Time</u>	<u>Reb Time</u>	<u>Reb Vel</u>	<u>ε</u>	<u>Crsh Δt</u>	<u>Rest Δt</u>	<u>Crsh Acc</u>	<u>Rest Acc</u>
SL	ITV	PAS		Chevrolet	Cavalier	87	2122			0									
SL	ITV	PAS		Chevrolet	Cavalier	87	2122	IMP											
SL	ITV	PAS	?	Acura	Legend	93	1921	COMB	48.00		0.000	0.063	0.099	-7.03	0.146				
SL	ITV	PAS	?	Acura	Legend	93	1921	IMP	48.00										
SL	ITV	PAS	?	Acura	Legend	93	1921	V	0.00	0									
SL	ITV	PAS	?	Acura	Legend	93	1960	COMB	53.80		0.000	0.072	0.112	-6.72	0.125				
SL	ITV	PAS	?	Acura	Legend	93	1960	IMP	53.80										
SL	ITV	PAS	?	Acura	Legend	93	1960	V	0.00	0									
SL	ITV	PAS	?	Honda	Civic	93	1961	COMB	47.80		0.000	0.061	0.101	-7.350	0.154				
SL	ITV	PAS	?	Honda	Civic	93	1961	IMP	47.80										
SL	ITV	PAS	?	Honda	Civic	93	1961	V	0.00	0									
SL	ITV	PAS	?	Honda	Civic	93	1962	COMB	54.60		0.000	0.066	0.096	-5.000	0.092				
SL	ITV	PAS	?	Honda	Civic	93	1962	IMP	54.60										
SL	ITV	PAS	?	Honda	Civic	93	1962	V	0.00	0									
SL	ITV	PAS	?	Mitsubishi	Galant	94	2096	COMB	47.15		0.000	0.067	0.105	-2.54	0.054				
SL	ITV	PAS	?	Mitsubishi	Galant	94	2096	IMP	47.15										

Test No.	Vehicle Crush Information						Test Lab	Eng Mass	Eng Desc	Eng Disp	Trans	Drive	Door	Length	Width	Whl-base	FAxle to		Barr Data
	C1	C2	C3	C4	C5	C6											Cg	DL'd	
149							NTS	1804					3658	1524	3048			X	
149	429	437	434	434	419	409	NTS	1182	41F	1.8	M	R	4	4229	1588	2405	1138	X	
151							NTS	733											
151							NTS	1804					3658	1524	3048			X	
151	424	424	442	439	422	399	NTS	1071	41F	1.5	M	F	2	4064	1560	2497	1052	X	
560							NTS	587											
560							NTS	1809					3658	1524	3048			X	
560	315	325	335	335	325	310	NTS	1222	4TF	1.6	A	F	4	4224	1636	2431	1003	X	
635							NTS	598											
635							NTS	1809										X	
635							NTS	1211	41F	1.5	M	F	WAG	4318	1610	2438	1194	X	
74							CAL	267											
74							CAL	1805										X	
74							CAL	1538	41F	2.1	A	R	2	4872	1704	2649	1234	X	
31	427	396	404	419	411	396	DS	1262	41F	2.3	A	R	3	4310	1661	2464		X	
2122																			
2122																			
1921							MGA	377											
1921							MGA	1363										X	
1921							MGA	1740					1640	2905	1268			X	
1960							MGA	379											
1960							MGA	1363										X	
1960							MGA	1742					1640	2905	1268			X	
1961								219											
1961								1363										X	
1961								1144					1692	2616	1150			X	
1962								213											
1962								1363										X	
1962								1150					1692	2616	1177			X	
2096							MGA	1469											
2096							MGA											X	

<u>Test No.</u>	<u>No. Acc</u>	<u>Trace No.</u>	<u>Location</u>	<u>Notes</u>	ϵ <u>Low</u>	ϵ <u>Loc</u>	ϵ <u>High</u>	ϵ <u>Loc</u>	ϵ <u>Diff</u>
149				NHTSA Flat					
149									
151				data scaling problem					
151				NHTSA Flat					
151									
560									
560	1	1	front cross-member	NHTSA Flat					
560	1	2	cg						
635									
635				NHTSA Flat					
635									
74									
74				NHTSA Flat; bad data					
74									
31	2	12,15	left, right front floor						
2122				not available					
2122									
1921				214 compliance					
1921	1	2	cg	NHTSA Deformable Impactor					
1921	2	30,36	right rear sill, seat						
1960				214 compliance					
1960	1	2	cg	NHTSA Deformable Impactor					
1960	2	30,36	right rear sill, seat						
1961				214 compliance					
1961	1	2	cg	NHTSA Deformable Impactor					
1961	2	30,36	right rear sill, seat						
1962				214 compliance					
1962	1	2	cg	NHTSA Deformable Impactor					
1962	2	30,36	right rear sill, seat						
2096				214 compliance					
2096	1	2	cg	NHTSA Deformable Impactor					

<u>Test</u>		<u>Veh</u>				<u>Tst</u>		<u>Imp</u>		<u>Imp</u>	<u>Zero</u>	<u>Reb</u>	<u>Reb</u>		<u>Crsh</u>	<u>Rest</u>	<u>Crsh</u>	<u>Rest</u>	
<u>Dir</u>	<u>Type</u>	<u>Type</u>	<u>Offset</u>	<u>Make</u>	<u>Model</u>	<u>Yr</u>	<u>No.</u>	<u>Veh</u>	<u>Vel</u>	<u>Crsh</u>	<u>Time</u>	<u>Time</u>	<u>Time</u>	<u>Vel</u>	ϵ	<u>Δt</u>	<u>Δt</u>	<u>Acc</u>	<u>Acc</u>
SL	ITV	PAS	?	Mitsubishi	Galant	94	2096	V	0.00	0									
SL	ITV	PAS	-488	Nissan	Sentra	85	1346	COMB	42.49		0.000	0.000	0.000	0.00	0.000				
SL	ITV	PAS	-488	Nissan	Sentra	85	1346	IMP	42.49										
SL	ITV	PAS	-488	Nissan	Sentra	85	1346	V	0.00	0									
SL	ITV	PAS	-445	Nissan	Sentra	85	1344	COMB	28.32		0.000	0.057	0.102	-3.16	0.112				
SL	ITV	PAS	-445	Nissan	Sentra	85	1344	IMP	28.32										
SL	ITV	PAS	-445	Nissan	Sentra	85	1344	V	0.00	0									
SL	ITV	PAS	-348	Chevrolet	Celebrity	85	1347	COMB	32.67		0.000	0.052	0.073	-3.72	0.114				
SL	ITV	PAS	-348	Chevrolet	Celebrity	85	1347	IMP	32.67										
SL	ITV	PAS	-348	Chevrolet	Celebrity	85	1347	V	0.00	143									
SL	ITV	PAS	-348	Chevrolet	Celebrity	85	1349	COMB	48.76		0.000	0.085	0.085	0.00	0.000				
SL	ITV	PAS	-348	Chevrolet	Celebrity	85	1349	IMP	48.76										
SL	ITV	PAS	-348	Chevrolet	Celebrity	85	1349	V	0.00	0									
SL	ITV	PAS	-277	Nissan	Sentra	85	1345	COMB	42.49		0.000	0.061	0.093	-2.91	0.068				
SL	ITV	PAS	-277	Nissan	Sentra	85	1345	IMP	42.49										
SL	ITV	PAS	-277	Nissan	Sentra	85	1345	V	0.00	0									
SL	ITV	PAS	-236	Chevrolet	Celebrity	85	1119	COMB	47.96		0.000	0.060	0.099	-2.94	0.061				
SL	ITV	PAS	-236	Chevrolet	Celebrity	85	1119	IMP	47.96										
SL	ITV	PAS	-236	Chevrolet	Celebrity	85	1119	V	0.00	350									
SL	ITV	PAS	-236	Chevrolet	Lumina	92	1865	COMB	47.04		0.000	0.062	0.079	-3.63	0.077				
SL	ITV	PAS	-236	Chevrolet	Lumina	92	1865	IMP	47.04										
SL	ITV	PAS	-236	Chevrolet	Lumina	92	1865	V	0.00	0									
SL	ITV	PAS	-231	Chevrolet	Lumina	92	1866	COMB	54.92		0.000	0.000	0.000	0.00	0.000				
SL	ITV	PAS	-231	Chevrolet	Lumina	92	1866	IMP	54.92										
SL	ITV	PAS	-231	Chevrolet	Lumina	92	1866	V	0.00	0									
SL	ITV	PAS	-185	Cadillac	De Ville	94	2073			185	0.000								
SL	ITV	PAS	-183	Toyota	Avalon	95	2226	COMB	53.00		0.000	0.080	0.080	0.00	0.000				
SL	ITV	PAS	-183	Toyota	Avalon	95	2226	IMP	53.00										
SL	ITV	PAS	-183	Toyota	Avalon	95	2226	V	0.00	225									
SL	ITV	PAS	-165	Chevrolet	Citation	82	548	COMB	56.49		0.000	0.077	0.105	-5.51	0.098				
SL	ITV	PAS	-165	Chevrolet	Citation	82	548	IMP	56.49										
SL	ITV	PAS	-165	Chevrolet	Citation	82	548	V	0.00	393									
SL	ITV	PAS	-132	Chevrolet	Citation	82	549	COMB	41.52		0.000	0.061	0.093	-5.78	0.139				
SL	ITV	PAS	-132	Chevrolet	Citation	82	549	IMP	41.52										

Test No.	Vehicle Crush Information						Test Lab	Mass	Eng Desc	Eng Disp	Trans	Drive	Door	Length	Width	Whl-base	FAxle to Cg	DL'd	Barr Data
	C1	C2	C3	C4	C5	C6													
2096							MGA	1469						1722	2639	1102	X		
1346							TRC	298											
1346							TRC	1203										X	
1346							TRC	905					1626	2400	889		X		
1344							TRC	298											
1344							TRC	1203					3526	1981	2591	848	X		
1344							TRC	905	4IF	-	M	F	2	4196	1626	2400	889	X	
1347							TRC	6											
1347							TRC	1264					3526	1981	2591	765	X		
1347	0	178	191	191	157	0	TRC	1258	S6TF	2.8	A	F	4	4775	1753	2654	947	X	
1349							TRC	6											
1349							TRC	1264										X	
1349							TRC	1258					1753	2654	947		X		
1345							TRC	298											
1345							TRC	1203										X	
1345							TRC	905					1626	2400	889		X		
1119							TRC	67											
1119							TRC	1359					4077	2235	2489	1036	X		
1119	46	340	394	394	404	391	TRC	1292	4TF	2.5	A	F	4	4775	1722	2662	1044	X	
1865							MS	354											
1865							MS	1342										X	
1865							MS	1696					1816	2731	1029		X		
1866							MS	348											
1866							MS	1342										X	
1866							MS	1690					1816	2731	1130		X		
2073	0	216	262	277	168	0	MGA	1930	V8IF	4.9	A	F	4	5207	1885	2819	1209		
2226							MGA	72											
2226							MGA	1356					4115	2014	2591	1102	X		
2226	0	268	322	314	220	0	MGA	1284	V6TF	3.0	A	F	4	4830	1781	2720	1075	X	
548							DS	23											
548							DS	1369					4115	1829				X	
548	147	462	450	432	412	274	DS	1392	4TF	2.5	M	F	5	4496	1717	2662	1087	X	
549							DS	18											
549							DS	1366					4115	1829				X	

<u>Test No.</u>	<u>No. Acc</u>	<u>Trace No.</u>	<u>Location</u>	<u>Notes</u>	ϵ <u>Low</u>	ϵ <u>Loc</u>	ϵ <u>High</u>	ϵ <u>Loc</u>	ϵ <u>Diff</u>
2096	2	45,50	right rear sill, seat	<i>non-compliance; PDOF = 270; can't reconcile data NHTSA Deformable Impactor</i>					
1346									
1346									
1346									
1344	1	3	cg	270 deg - non-compliance NHTSA Deformable Impactor					
1344	1	1	right front sill	right rear sill trace (preferred trace) has offset in it					
1347									
1347	1	3	cg	270 deg - non-compliance NHTSA deformable					
1347	2	1,2	right front, right rear sill						
1349									
1349	1	3	cg	PDOF = 270; noisy vehicle traces; looks like vehicles locked NHTSA Deformable Impactor					
1349	2	1,2	right front, right rear sill						
1345									
1345	1	3	cg	non-compliance; PDOF = 270 NHTSA Deformable Impactor					
1345	1	2	right rear sill						
1119									
1119	1	24	cg	214 compliance NHTSA deformable					
1119	1	4	right rear sill						
1865									
1865	1	46	cg	214 compliance NHTSA Deformable Impactor					
1865	1	33	right rear sill						
1866									
1866				<i>214 compliance; no common velocity NHTSA Deformable Impactor</i>					
1866									
2073				vehicle data only					
2226				non-compliance					
2226				NHTSA Deformable Impactor					
2226									
548				compliance					
548	1	55	cg	26.5 deg crab					
548	1	47	right rear sill						
549				looks like compliance					
549	1	55	cg	26.5 deg crab					

<u>Dir</u>	<u>Test Type</u>	<u>Veh Type</u>	<u>Offset</u>	<u>Make</u>	<u>Model</u>	<u>Yr</u>	<u>Tst No.</u>	<u>Veh</u>	<u>Imp Vel</u>	<u>Crsh</u>	<u>Imp Time</u>	<u>Zero Time</u>	<u>Reb Time</u>	<u>Reb Vel</u>	ϵ	<u>Crsh Δt</u>	<u>Rest Δt</u>	<u>Crsh Acc</u>	<u>Rest Acc</u>
SL	ITV	PAS	-132	Chevrolet	Citation	82	549	V	0.00	262									
SL	ITV	PAS	-132	Nissan	Sentra	87	1485	COMB	48.44		0.000	0.066	0.095	-3.92	0.081				
SL	ITV	PAS	-132	Nissan	Sentra	87	1485	IMP	48.44										
SL	ITV	PAS	-132	Nissan	Sentra	87	1485	V	0.00	0									
SL	ITV	PAS	-122	Honda	Accord	92	1864	COMB	47.46		0.000	0.080	0.090	-0.69	0.015				
SL	ITV	PAS	-122	Honda	Accord	92	1864	IMP	47.46										
SL	ITV	PAS	-122	Honda	Accord	92	1864	V	0.00	0									
SL	ITV	PAS	-92	Nissan	Sentra	96	2365	COMB	47.76		0.000	0.052	0.075	-6.47	0.135				
SL	ITV	PAS	-92	Nissan	Sentra	96	2365	IMP	47.76										
SL	ITV	PAS	-92	Nissan	Sentra	96	2365	V	0.00	186									
SL	ITV	PAS	-76	Nissan	Sentra	92	1862	COMB	53.11		0.000	0.000	0.000	0.00	0.000				
SL	ITV	PAS	-76	Nissan	Sentra	92	1862	IMP	53.11										
SL	ITV	PAS	-76	Nissan	Sentra	92	1862	V	0.00	0									
SL	ITV	PAS	-51	Lincoln	Town Car	94	2097			0									
SL	ITV	PAS	-51	Toyota	Camry	94	2094	COMB	47.48		0.000	0.059	0.114	-4.69	0.099				
SL	ITV	PAS	-51	Toyota	Camry	94	2094	IMP	47.48										
SL	ITV	PAS	-51	Toyota	Camry	94	2094	V	0.00	0									
SL	ITV	PAS	-48	Dodge	Intrepid	93	1913	COMB	51.00		0.000	0.099	0.111	-0.63	0.012				
SL	ITV	PAS	-48	Dodge	Intrepid	93	1913	IMP	51.00										
SL	ITV	PAS	-48	Dodge	Intrepid	93	1913	V	0.00	0									
SL	ITV	PAS	-48	Dodge	Intrepid	93	1919	COMB	54.44		0.000	0.080	0.135	-5.33	0.098				
SL	ITV	PAS	-48	Dodge	Intrepid	93	1919	IMP	54.44										
SL	ITV	PAS	-48	Dodge	Intrepid	93	1919	V	0.00	0									
SL	ITV	PAS	-10	Nissan	Sentra	87	1145	COMB	48.44		0.000	0.071	0.094	-4.31	0.089				
SL	ITV	PAS	-10	Nissan	Sentra	87	1145	IMP	48.44										
SL	ITV	PAS	-10	Nissan	Sentra	87	1145	V	0.00	0									
SL	ITV	PAS	0	Ford	Escort	86	1652	COMB	24.14		0.000	0.093	0.130	-3.10	0.128				
SL	ITV	PAS	0	Ford	Escort	86	1652	IMP	24.14										
SL	ITV	PAS	0	Ford	Escort	86	1652	V	0.00	99									
SL	ITV	PAS	10	Nissan	Sentra	83	856	COMB	48.31		0.000	0.063	0.096	-9.72	0.201				
SL	ITV	PAS	10	Nissan	Sentra	83	856	IMP	48.31										
SL	ITV	PAS	10	Nissan	Sentra	83	856	V	0.00	0									
SL	ITV	PAS	23	Hyundai	Excel	88	1264	COMB	49.03		0.000	0.081	0.107	-1.88	0.038				
SL	ITV	PAS	23	Hyundai	Excel	88	1264	IMP	49.03										

Test No.	Vehicle Crush Information						Test Lab	Mass	Eng Desc	Eng Disp	Trans	Drive	Door	Length	Width	Whl-base	FAxle to Cg	DL'd	Barr Data	
	C1	C2	C3	C4	C5	C6														
549	69	300	307	297	272	203	DS	1384	4TF	2.5	M	F	5	4496	1717	2672	1087	X		
1485							TRC	210												
1485							TRC	1366											X	
1485							TRC	1156						1641	2426		1080		X	
1864							MS	162												
1864							MS	1342											X	
1864							MS	1504						1704	2731		1128		X	
2365							MGA	128												
2365							MGA	1356					4115	2014	2591		1102		X	
2365	0	168	207	307	250	0	MGA	1228	4TF	1.6	M	F	4	4296	1690	2536	1074		X	
1862							MS	67												
1862							MS	1342					4115	1829	2591		1130		X	
1862							MS	1275	4TF	1.6	M	F	4	4326	1669	2431	1039		X	
2097							MGA													
2094							MGA	1325												
2094							MGA	?											X	
2094							MGA	1325						1768	2604		1158		X	
1913							MGA	341												
1913							MGA	1363											X	
1913							MGA	1704						1745	2883		1218		X	
1919							MGA	351												
1919							MGA	1363											X	
1919							MGA	1714						1745	2883		1183		X	
1145							TRC	226												
1145							TRC	1365											X	
1145							TRC	1139						1649	2426		1201		X	
1652							TRC	857												
1652							TRC	1828					5207	1702	2593		2537		X	
1652	0	61	124	239	71	0	TRC	971	4TF	1.9	M	F	3	4272	1626	2375	833		X	
856							TRC	276												
856							TRC	1357											X	
856							TRC	1081					4229	1626	2400		1097		X	
1264							CAL	95												
1264							CAL	1320					4115	1676	2596		1072		X	

<u>Test No.</u>	<u>No. Acc</u>	<u>Trace No.</u>	<u>Location</u>	<u>Notes</u>	ϵ <u>Low</u>	ϵ <u>Loc</u>	ϵ <u>High</u>	ϵ <u>Loc</u>	ϵ <u>Diff</u>
549	1	47	right rear sill						
1485				214 compliance					
1485	1	64	cg	NHTSA Deformable Impactor					
1485	1	73	right rear sill						
1864				214 compliance					
1864	1	46	cg	NHTSA Deformable Impactor					
1864	1	33	right rear sill						
2365				214 compliance					
2365	1	2	cg	NHTSA Deformable Impactor					
2365	1	35	right rear sill						
1862									
1862				<i>NHTSA Deformable Impactor</i>					
1862				<i>no right side data</i>					
2097				vehicle data only					
2094				214 compliance					
2094	1	2	cg	NHTSA Deformable Impactor					
2094	2	45,50	right rear sill, seat						
1913				214 compliance					
1913	1	2	cg	NHTSA Deformable Impactor					
1913	2	29,35	right rear sill, seat						
1919				214 compliance					
1919	1	2	cg	NHTSA Deformable Impactor					
1919	2	30,36	right rear sill, seat						
1145				214 compliance					
1145	1	57	cg	NHTSA Deformable Impactor					
1145	1	43	right rear sill						
1652				non-compliance					
1652	1	7	cg	NHTSA contoured impactor					
1652	1	2,4	right front, right rear sill						
856				214 compliance					
856	1	56	cg	NHTSA Deformable Impactor					
856	1	44	right rear sill						
1264				334 deg - non-compliance;					
1264	1	42	cg	NHTSA Deformable Impactor					

<u>Test</u>		<u>Veh</u>					<u>Tst</u>		<u>Imp</u>		<u>Imp</u>	<u>Zero</u>	<u>Reb</u>	<u>Reb</u>	ϵ	<u>Crsh</u>	<u>Rest</u>	<u>Crsh</u>	<u>Rest</u>
<u>Dir</u>	<u>Type</u>	<u>Type</u>	<u>Offset</u>	<u>Make</u>	<u>Model</u>	<u>Yr</u>	<u>No.</u>	<u>Veh</u>	<u>Vel</u>	<u>Crsh</u>	<u>Time</u>	<u>Time</u>	<u>Time</u>	<u>Vel</u>		<u>Δt</u>	<u>Δt</u>	<u>Acc</u>	<u>Acc</u>
SL	ITV	PAS	23	Hyundai	Excel	88	1264	V	0.00	395									
SL	ITV	PAS	33	Toyota	Corolla	93	1869	COMB	48.29		0.000	0.000	0.000	0.00	0.000				
SL	ITV	PAS	33	Toyota	Corolla	93	1869	IMP	48.29										
SL	ITV	PAS	33	Toyota	Corolla	93	1869	V	0.00	0									
SL	ITV	PAS	35	Toyota	Corolla	93	1870	COMB	54.30		0.000	0.000	0.000	0.00	0.000				
SL	ITV	PAS	35	Toyota	Corolla	93	1870	IMP	54.30										
SL	ITV	PAS	35	Toyota	Corolla	93	1870	V	0.00	0									
SL	ITV	PAS	36	Nissan	Sentra	82	704	COMB	48.46		0.000	0.062	0.105	-9.33	0.193				
SL	ITV	PAS	36	Nissan	Sentra	82	704	IMP	48.46										
SL	ITV	PAS	36	Nissan	Sentra	82	704	V	0.00	0									
SL	ITV	PAS	41	Nissan	Sentra	82	820	COMB	48.31		0.000	0.069	0.102	-6.63	0.137				
SL	ITV	PAS	41	Nissan	Sentra	82	820	IMP	48.31										
SL	ITV	PAS	41	Nissan	Sentra	82	820	V	0.00	0									
SL	ITV	PAS	57	Subaru	Legacy	95	2210	COMB	46.42		0.000	0.053	0.097	-9.21	0.198				
SL	ITV	PAS	57	Subaru	Legacy	95	2210	IMP	46.42										
SL	ITV	PAS	57	Subaru	Legacy	95	2210	V	0.00	147									
SL	ITV	PAS	91	Nissan	Sentra	92	1863	COMB	60.99		0.000	0.000	0.000	0.00	0.000				
SL	ITV	PAS	91	Nissan	Sentra	92	1863	IMP	60.99										
SL	ITV	PAS	91	Nissan	Sentra	92	1863	V	0.00	0									
SL	ITV	PAS	102	Honda	Accord	94	2087	COMB	47.48		0.000	0.060	0.098	-5.68	0.120				
SL	ITV	PAS	102	Honda	Accord	94	2087	IMP	47.48										
SL	ITV	PAS	102	Honda	Accord	94	2087	V	0.00	258									
SL	ITV	PAS	135	Honda	Accord	92	1867	COMB	54.92		0.000	0.072	0.101	-4.14	0.075				
SL	ITV	PAS	135	Honda	Accord	92	1867	IMP	54.92										
SL	ITV	PAS	135	Honda	Accord	92	1867	V	0.00	343									
SL	ITV	PAS	426	Geo	Metro	95	2228	COMB	47.76		0.000	0.059	0.064	-0.58	0.012				
SL	ITV	PAS	426	Geo	Metro	95	2228	IMP	47.76										
SL	ITV	PAS	426	Geo	Metro	95	2228	V	0.00	177									
SL	ITV	PAS	927	Ford	Taurus	90	1498	COMB	48.44		0.000	0.068	0.114	-8.65	0.179				
SL	ITV	PAS	927	Ford	Taurus	90	1498	IMP	48.44										
SL	ITV	PAS	927	Ford	Taurus	90	1498	V	0.00	248									
SL	ITV	PAS	963	Ford	Taurus	90	1497	COMB	54.06		0.000	0.000	0.000	0.00	0.000				
SL	ITV	PAS	963	Ford	Taurus	90	1497	IMP	54.06										
SL	ITV	PAS	963	Ford	Taurus	90	1497	V	0.00	258									

Test No.	Vehicle Crush Information						Test Lab	Eng Mass	Eng Desc	Eng Disp	Trans	Drive	Door	Length	Width	Whl-base	FAxle to Cg	DL'd	Barr Data	
	C1	C2	C3	C4	C5	C6														
1264	404	422	437	429	442	89	CAL	1225	4IF	1.4	M	F	4	4255	1618	2377	1110	X		
1869							TRC	109												
1869							TRC	1343					4115	2014	2591	1102	X			
1869							TRC	1234	4TF	1.6	M	F	4	4374	1684	2464	1096	X		
1870							TRC	109												
1870							TRC	1343					4115	2014	2591	1102	X			
1870							TRC	1234	4TF	1.6	M	F	4	4380	1684	2471	1099	X		
704							TRC	295												
704							TRC	1356											X	
704							TRC	1061					4244	1623	2403	1130	X			
820							TRC	275												
820							TRC	1353											X	
820							TRC	1078					4242	1638	2413	1146	X			
2210							MGA	113												
2210							MGA	1356					4115	2014	2591	1102	X			
2210	0	150	200	294	90	0	MGA	1469	4TF	2.2	M	F	WAG	4692	1691	2629	1270	X		
1863							MS	84												
1863							MS	1342					4115	1829	2591	1130	X			
1863							MS	1258	4TF	1.6	M	F	4	4331	1669	2431	1024	X		
2087							MGA	1452												
2087							MGA												X	
2087	0	287	333	358	312	0	MGA	1452	4IF	2.2	A	F	4	4666	1783	2718	1163	X		
1867							MS	163												
1867	91	33	23	18	18	36	MS	1342					4115	1829	2591	1130	X			
1867	0	358	457	513	389	0	MS	1505	4TF	2.2	A	F	4	4694	1704	2731	1128	X		
2228							MGA	256												
2228							MGA	1356					4115	2014	2590	1102	X			
2228	0	225	211	232	216	0	MGA	1100	4TF	1.3	M	F	4	4202	1570	2372	1091	X		
1498							FORD	1593												
1498							FORD												X	
1498	13	102	318	356	404	102	FORD	1593	V6TF	3.0	A	F	4					X		
1497							FORD	1599												
1497							FORD												X	
1497	13	203	318	356	368	76	FORD	1599	V6TF	3.0	A	F	4					X		

<u>Test No.</u>	<u>No. Acc</u>	<u>Trace No.</u>	<u>Location</u>	<u>Notes</u>	<u>ε Low</u>	<u>ε Loc</u>	<u>ε High</u>	<u>ε Loc</u>	<u>ε Diff</u>
1264	1	29	right rear sill						
1869				<i>no rr sill data - no common velocity</i>					
1869				<i>NHTSA Deformable Impactor</i>					
1869									
1870				<i>no common velocity</i>					
1870				<i>NHTSA Deformable Impactor</i>					
1870									
704				214 compliance					
704	2	55,58	cg; front cross member	NHTSA Deformable Impactor					
704	1	43	right rear sill						
820				214 compliance					
820	1	56	cg	NHTSA Deformable Impactor					
820	1	44	right rear sill						
2210				214 compliance					
2210	1	2	cg	NHTSA Deformable Impactor					
2210	2	46,51	right rear sill; right rear seat						
1863									
1863				<i>NHTSA Deformable Impactor</i>					
1863				<i>not enough right side data</i>					
2087				214 compliance					
2087	1	2	cg	NHTSA Deformable Impactor					
2087	2	43,48	right rear sill; right rear seat						
1867				214 compliance					
1867				NHTSA Deformable Impactor					
1867									
2228				214 compliance; questionable traces					
2228	1	2	cg	NHTSA 214 Deformable Impactor					
2228	1	46	right rear sill						
1498				possible compliance angles; estimated rebound					
1498	1	62	cg	EEVC Deformable Impactor					
1498	1	103	floor (?)						
1497				<i>no details on angle; unreasonable data for expected angles</i>					
1497				<i>EEVC Deformable Impactor</i>					
1497									

<u>Test</u>	<u>Veh</u>					<u>Tst</u>		<u>Imp</u>	<u>Imp</u>	<u>Zero</u>	<u>Reb</u>	<u>Reb</u>		<u>Crsh</u>	<u>Rest</u>	<u>Crsh</u>	<u>Rest</u>	
<u>Dir</u>	<u>Type</u>	<u>Offset</u>	<u>Make</u>	<u>Model</u>	<u>Yr</u>	<u>No.</u>	<u>Veh</u>	<u>Vel</u>	<u>Crsh</u>	<u>Time</u>	<u>Time</u>	<u>Time</u>	<u>Vel</u>	<u>ε</u>	<u>Δt</u>	<u>Δt</u>	<u>Acc</u>	<u>Acc</u>
SL	RITV	PAS	-282	Chevrolet	Citation	80	964	IMP										
SR	ITV	PAS		Chevrolet	Cavalier	97	2485		0									
SR	ITV	PAS		Chevrolet	Cavalier	97	2485	IMP										
SR	ITV	PAS		Dodge	Intrepid	97	2484		0									
SR	ITV	PAS		Dodge	Intrepid	97	2484	IMP										
SR	ITV	PAS		Ford	Escort	97	2482		0									
SR	ITV	PAS		Ford	Escort	97	2482	IMP										
SR	ITV	PAS		Ford	Escort	97	2501		0									
SR	ITV	PAS		Ford	Escort	97	2501	IMP										
SR	ITV	PAS		Honda	Accord	97	2479		0									
SR	ITV	PAS		Honda	Accord	97	2479	IMP										
SR	ITV	PAS		Honda	Civic	97	2477		0									
SR	ITV	PAS		Honda	Civic	97	2477	IMP										
SR	ITV	PAS		Honda	Civic	97	2538		0									
SR	ITV	PAS		Honda	Civic	97	2538	IMP										
SR	ITV	PAS		Toyota	Camry	97	2516		0									
SR	ITV	PAS		Toyota	Camry	97	2516	IMP										
SR	ITV	PAS	-122	Mitsubishi	Galant	95	2217	COMB	53.30	0.000	0.000	0.000	0.00	0.000				
SR	ITV	PAS	-122	Mitsubishi	Galant	95	2217	IMP	53.30									
SR	ITV	PAS	-122	Mitsubishi	Galant	95	2217	V	0.00	0								
SR	ITV	PAS	-114	Hyundai	Sonata	96	2410	COMB	47.31	0.000	0.060	0.099	-8.86	0.187				
SR	ITV	PAS	-114	Hyundai	Sonata	96	2410	IMP	47.31									
SR	ITV	PAS	-114	Hyundai	Sonata	96	2410	V	0.00	0								
SR	ITV	PAS	-102	Honda	Accord	96	2389	COMB	47.49	0.000	0.059	0.090	-10.62	0.224				
SR	ITV	PAS	-102	Honda	Accord	96	2389	IMP	47.49									
SR	ITV	PAS	-102	Honda	Accord	96	2389	V	0.00	0								

Test No.	Vehicle Crush Information						Test Lab	Eng Mass	Eng Desc	Eng Disp	Trans	Drive	Door	Length	Width	Whl-base	FAxle to		Barr Data
	C1	C2	C3	C4	C5	C6											Cg	DL'd	
964							TRC	1465											
2485																			
2485																			
2484																			
2484																			
2482																			
2482																			
2501																			
2501																			
2479																			
2479																			
2477																			
2477																			
2538																			
2538																			
2516																			
2516																			
2217							MGA	94											
2217							MGA	1356	-	-	-	-	-	4115	2014	2591	1102	X	
2217							MGA	1450	4TF	2.4	M	F	4	4770	1720	2636	1095	X	
2410							MGA	201											
2410							MGA	1356	-	-	-	-	-	4115	2014	2591	1102	X	
2410							MGA	1557	4TF	2.0	A	F	4	4555	1759	2700	1133	X	
2389							MGA	142											
2389							MGA	1356	-	-	-	-	-	4115	2014	2591	1102	X	
2389							MGA	1498	4TF	2.2	M	F	2	4541	1773	2710	1151	X	

<u>Test No.</u>	<u>No. Acc</u>	<u>Trace No.</u>	<u>Location</u>	<u>Notes</u>	ϵ <u>Low</u>	ϵ <u>Loc</u>	ϵ <u>High</u>	ϵ <u>Loc</u>	ϵ <u>Diff</u>
964				<i>NHTSA Flat Impactor; impactor data only</i>					
2485				<i>report not posted</i>					
2485									
2484				<i>report not posted</i>					
2484									
2482				<i>report not posted</i>					
2482									
2501				<i>report not posted</i>					
2501									
2479									
2479				<i>report not posted</i>					
2477									
2477				<i>report not posted</i>					
2538									
2538				<i>report not posted</i>					
2516				<i>report not posted</i>					
2516									
2217									
2217				<i>NHTSA Deformable Impactor</i>					
2217				<i>bad data</i>					
2410				214 compliance					
2410	1	2	cg	NHTSA Deformable Impactor					
2410	1	9	floor pan	very similar to first part of lr sill trace, which lost validity later					
2389				214 compliance					
2389	1	2	cg	NHTSA Deformable Impactor					
2389	1	9	floor pan						

Appendix B

Integration Program Listing - VelCalc

```

/*-----
VelCalc.c

This file generates velocity-time data from acceleration-time data.

Programmed by: Ken Monson    23 Apr 1997
Revised:      23 Apr 1997
-----*/
/*-----
Include files
-----*/
#include<stdio.h>
#include<stdlib.h>
#include<string.h>
#include<math.h>

/*-----
Defined Constants
-----*/
#define MAXTIME 0.2
#define GRAV 9.807
#define MPS_TO_KPH 3.6

main()
{
    int numPts, i, zeroFlg = 0;
    char response[80], filename[80], outName[80];
    double timeStep, startVel, dum1, dum2, dum3, minVel, minVelTime, zeroTime;
    double *timePtr, *accPtr, *velPtr;
    FILE *inFPtr, *outVelFPtr;

/* Get input file name. */
    printf("\nEnter the name of the input file:\t");
    fgets(response, 79, stdin);
    sscanf(response, "%s", filename);

/* Open file to calculate time step. */
    if((inFPtr = fopen(filename,"r")) == NULL)
    {
        printf("The entered file is not readable!\n\n");
        exit(EXIT_FAILURE);
    }

/* Calculate time step. */
    fscanf(inFPtr, "%lf%lf", &dum1, &dum2);
    fscanf(inFPtr, "%lf%lf", &dum2, &dum3);
    timeStep = dum2 - dum1;
    numPts = MAXTIME / timeStep;
    fclose(inFPtr);

```

```

/* Dynamically allocate arrays. */
timePtr = (double *)malloc(sizeof(double) * (numPts + 1));
accPtr = (double *)malloc(sizeof(double) * (numPts + 1));
velPtr = (double *)malloc(sizeof(double) * (numPts + 1));
if((timePtr == NULL) || (accPtr == NULL))
{
    printf("\nERROR: malloc failed!\n");
    free(timePtr);
    free(accPtr);
    free(velPtr);
    return;
}

/* Get pre-impact velocity. */
printf("\nEnter the vehicle's pre-impact velocity (kph):t");
scanf("%lf", &startVel);

/* Open velocity output file. */
sprintf(outName, "%s.vel", filename);
if((outVelFPtr = fopen(outName,"w")) == NULL)
{
    printf("The entered file is not writeable!\n\n");
    exit(EXIT_FAILURE);
}

/* Re-open file to read data. */
if((inFPtr = fopen(filename,"r")) == NULL)
{
    printf("The entered file is not readable!\n\n");
    exit(EXIT_FAILURE);
}

/* Don't read in data until time zero. */
do
{
    fscanf(inFPtr, "%lf%lf", &dum1, &dum2);
} while(dum1 < (-1 * timeStep));

/* Read in data, convert acceleration from g's to m/s^2, and
integrate to get velocity profile. */
for(i = 0; i <= numPts; i++)
{
    fscanf(inFPtr, "%lf%lf", &timePtr[i], &accPtr[i]);
    accPtr[i] *= GRAV;

    if(i < 1)
    {
        velPtr[i] = startVel;
        minVel = startVel;
    }
    else
    {
        velPtr[i] = velPtr[i-1] + (accPtr[i] + accPtr[i-1])

```

```

        / 2 * timeStep * MPS_TO_KPH;          /* kph */
    timePtr[i] -= timeStep / 2;
}

if(velPtr[i] < minVel) /* record time and magnitude of max. neg. vel. */
{
    minVel = velPtr[i];
    minVelTime = timePtr[i];
}

if(velPtr[i] < 0 && zeroFlg == 0)
{
    zeroTime = timePtr[i];
    zeroFlg = 1;
}
}
fclose(inFPtr);

/* Output calculated parameters.          */
printf("\nTime at zero velocity:\t\t%f sec", zeroTime);
printf("\nMax. Negative Velocity:\t\t%f kph @ %f sec", minVel, minVelTime);
printf("\nCoeff. of Restitution:\t\t%f\n", -minVel/startVel);

/* Write velocity-time file.          */
for(i = 0; i <= numPts; i++)
    fprintf(outVelFPtr, "%f\t%f\n", timePtr[i], velPtr[i]);

fclose(outVelFPtr);
}

```

Integration Program Listing - FCFCalc

```

/*-----
FCFCalc.c

This file creates barrier force v. time data, dynamic crush data, and
force v. vehicle crush data. The force v. time data includes total force,
force as a function of lateral position, and force as a function of
area, all as a function of time. Dynamic crush is determined by
integrating an applicable velocity trace. The force v. crush data
gives only total barrier force v. vehicle crush.

Programmed by: Ken Monson    23 May 1997
Revised:      2 Jun 1997
-----*/

/*-----
Include files
-----*/

#include<stdio.h>
#include<stdlib.h>
#include<string.h>
#include<math.h>

```



```

/*-----
  Defined Constants
  -----*/
#define MAXTIME 0.2
#define MPS_TO_KPH 3.6

main()
{
  int numPts, i, j, n, frame;
  char response[80], filename[80], filenameFor[80], outName[80];
  double timeStep, dum1, dum2, dum3, timeInc, lastTime, sum, sum2;
  double *timeForPtr, **forcePtr;
  double firstStep, sepTime, maxCrsh=0, maxCrshTime, resCrsh, newDef;
  double *timeDefPtr, *velPtr, *defPtr;
  FILE *inFPtr, *outFPtr2, *inDatFPtr, *outFPtr;

/*-----FORCE V TIME PORTION OF CODE-----*/

/* Get filename for file holding input file names. */
printf("\nBeginning force v time portion of the program . . .");
printf("\nEnter the name of the file that lists the 36 input files.\n"
      "(Files should be arranged in order from A1-D9):\t");
fgets(response, 79, stdin);
fflush(stdin);
sscanf(response, "%s", filename);

/* Open file to read input files. */
if((inFPtr = fopen(filename, "r")) == NULL)
{
  printf("The entered file is not readable!\n\n");
  exit(EXIT_FAILURE);
}

/* Read input file names and open and read the files. */
for(i = 0; i < 36; i++)
{
  fgets(response, 79, inFPtr);
  sscanf(response, "%s", filename);

  if((inDatFPtr = fopen(filename, "r")) == NULL)
  {
    printf("The entered file is not readable!\n\n");
    exit(EXIT_FAILURE);
  }

  if(i == 0)
  {
/* Calculate time step (assuming same for all files). */
fscanf(inDatFPtr, "%lf%lf", &dum1, &dum2);
fscanf(inDatFPtr, "%lf%lf", &dum1, &dum2);
fscanf(inDatFPtr, "%lf%lf", &dum2, &dum3);
timeStep = dum2 - dum1;
numPts = MAXTIME / timeStep + 1;

```

```

fclose(inDatFPtr);
inDatFPtr = fopen(filename, "r");

/*   Dynamically allocate arrays, matrices.   */
timeForPtr = (double *)malloc(sizeof(double) * numPts);
forcePtr = (double **)malloc(sizeof(double) * 36);
if((timeForPtr == NULL) || (forcePtr == NULL))
{
    printf("\nERROR: malloc failed!\n");
    free(timeForPtr);
    free(forcePtr);
    return;
}
for(j = 0; j < 36; j++)
{
    forcePtr[j] = (double *)malloc(sizeof(double) * numPts);

    if(forcePtr[j] == NULL)
    {
        printf("\nERROR: malloc failed!\n");
        free(forcePtr[j]);
        return;
    }
}

/*   Don't read in data until time zero.   */
do
{
    fscanf(inDatFPtr, "%lf%lf", &dum1, &dum2);
} while(dum1 < (-1 * timeStep));

/*   Read in data.   */
for(j = 0; j <= (numPts - 1); j++)
{
    fscanf(inDatFPtr, "%lf%lf", &timeForPtr[j], &forcePtr[i][j]);

    if(j < 1) forcePtr[i][j] = 0;
}
fclose(inDatFPtr);
fclose(inFPtr);

printf("\nEnter the crash test number (with desired output files path):\t");
fgets(response, 79, stdin);
fflush(stdin);
sscanf(response, "%s", filenameFor);

/*   Create files for 9X4 movie.   */
frame = 1;

sprintf(outName, "%s.%d.mov", filenameFor, frame);
if((outFPtr = fopen(outName, "w")) == NULL)

```

```

{
    printf("The entered file is not writeable!\n\n");
    exit(EXIT_FAILURE);
}

printf("\nEnter the time increment for the 9X4 movie:\t");
scanf("%lf", &timeInc);

fprintf(outFPtr, "%lf", timeForPtr[0]);
fprintf(outFPtr, "\n\t1\t2\t3\t4\t5\t6\t7\t8\t9");
for(j = 0; j < 4; j++)
{
    fprintf(outFPtr, "\n%d\t", (j + 1));
    for(i = 0; i < 9; i++)
    {
        fprintf(outFPtr, "%lf\t", forcePtr[(j * 9) + i][0]);
    }
}
fclose(outFPtr);

lastTime = 0;
for(n = 1; n <= (numPts - 1); n++)
{
    if(timeForPtr[n] - lastTime > timeInc)
    {
        lastTime = timeForPtr[n];
        frame++;

        sprintf(outName, "%s.%d.mov", filenameFor, frame);
        if((outFPtr = fopen(outName, "w")) == NULL)
        {
            printf("The entered file is not writeable!\n\n");
            exit(EXIT_FAILURE);
        }

        fprintf(outFPtr, "%lf", timeForPtr[n]);
        fprintf(outFPtr, "\n\t1\t2\t3\t4\t5\t6\t7\t8\t9");
        for(j = 0; j < 4; j++)
        {
            fprintf(outFPtr, "\n%d\t", (j + 1));
            for(i = 0; i < 9; i++)
            {
                fprintf(outFPtr, "%lf\t", forcePtr[(j * 9) + i][n]);
            }
        }
        fclose(outFPtr);
    }
}

/* Create barrier force surface v time (3-D surface). */
sprintf(outName, "%s.fvtsurf", filenameFor);
if((outFPtr = fopen(outName, "w")) == NULL)
{
    printf("The entered file is not writeable!\n\n");
}

```

```

    exit(EXIT_FAILURE);
}

printf("\nEnter the time increment for the force v time surface:\t");
scanf("%lf", &timeInc);

fprintf(outFPtr, "\t1\t2\t3\t4\t5\t6\t7\t8\t9\n");
fprintf(outFPtr, "%lf", timeForPtr[0]);
for(i = 0; i < 9; i++)
{
    sum = forcePtr[i][0] + forcePtr[i + 9][0] + forcePtr[i + 18][0]
        + forcePtr[i + 27][0];
    fprintf(outFPtr, "\t%lf", sum);
}
fprintf(outFPtr, "\n");

lastTime = 0;
for(n = 1; n <= (numPts - 1); n++)
{
    if(timeForPtr[n] - lastTime > timeInc)
    {
        lastTime = timeForPtr[n];

        fprintf(outFPtr, "%lf", timeForPtr[n]);
        for(i = 0; i < 9; i++)
        {
            sum = forcePtr[i][n] + forcePtr[i + 9][n] + forcePtr[i + 18][n]
                + forcePtr[i + 27][n];
            fprintf(outFPtr, "\t%lf", sum);
        }
        fprintf(outFPtr, "\n");
    }
}
fclose(outFPtr);

/* Create total barrier force v time. */
sprintf(outName, "%s.fvt", filenameFor);
if((outFPtr = fopen(outName, "w")) == NULL)
{
    printf("The entered file is not writeable!\n\n");
    exit(EXIT_FAILURE);
}

for(n = 0; n <= (numPts - 1); n++)
{
    sum = 0;
    for(i = 0; i < 36; i++)
    {
        sum += forcePtr[i][n];
    }
    fprintf(outFPtr, "%lf\t%lf\n", timeForPtr[n], sum);
}
fclose(outFPtr);

```

```

/*-----DYNAMIC CRUSH PORTION OF CODE-----*/

/* Get input file name. */
printf("\n\nBeginning dynamic crush portion of the program . . .");
printf("\nEnter the name of the velocity input file:\t");
fflush(stdin);
fgets(response, 79, stdin);
fflush(stdin);
sscanf(response, "%s", filename);

/* Open file to calculate time step. */
if((inFPtr = fopen(filename, "r")) == NULL)
{
    printf("The entered file is not readable!\n\n");
    exit(EXIT_FAILURE);
}

/* Get time for barrier-vehicle separation. */
printf("\nEnter the time when the vehicle separates from the barrier (sec):\t");
scanf("%lf", &sepTime);

/* Calculate time step (first and repeated). */
fscanf(inFPtr, "%lf%lf", &dum1, &dum2);
fscanf(inFPtr, "%lf%lf", &dum2, &dum3);
firstStep = dum2 - dum1;
fscanf(inFPtr, "%lf%lf", &dum1, &dum3);
timeStep = dum1 - dum2;
numPts = sepTime / timeStep + 1;
fclose(inFPtr);

/* Dynamically allocate arrays. */
timeDefPtr = (double *)malloc(sizeof(double) * (numPts + 1));
velPtr = (double *)malloc(sizeof(double) * (numPts + 1));
defPtr = (double *)malloc(sizeof(double) * (numPts + 1));
if((timeDefPtr == NULL) || (velPtr == NULL) || (defPtr == NULL))
{
    printf("\nERROR: malloc failed!\n");
    free(timeDefPtr);
    free(velPtr);
    free(defPtr);
    return;
}

/* Open deformation output file for writing. */
sprintf(outName, "%s.def", filename);
if((outFPtr = fopen(outName, "w")) == NULL)
{
    printf("The entered file is not writeable!\n\n");
    exit(EXIT_FAILURE);
}

/* Re-open input velocity file to read data. */
if((inFPtr = fopen(filename, "r")) == NULL)
{

```

```

    printf("The entered file is not readable!\n\n");
    exit(EXIT_FAILURE);
}

/* Read in data and integrate to get dynamic crush.    */
for(i = 0; i <= numPts; i++)
{
    fscanf(inFPtr, "%lf%lf", &timeDefPtr[i], &velPtr[i]);
    velPtr[i] /= MPS_TO_KPH;

    if(i < 1) defPtr[i] = 0;
    else
    {
        if(i == 1)
        {
            defPtr[i] = defPtr[i-1] + (velPtr[i] + velPtr[i-1])
                / 2 * firstStep * 1000;          /* mm */
            timeDefPtr[i] -= firstStep / 2;
        }
        else
        {
            defPtr[i] = defPtr[i-1] + (velPtr[i] + velPtr[i-1])
                / 2 * timeStep * 1000;          /* mm */
            timeDefPtr[i] -= timeStep / 2;
        }
    }
}
if(defPtr[i] > maxCrsh) /* record time and magnitude of max. crush */
{
    maxCrsh = defPtr[i];
    maxCrshTime = timeDefPtr[i];
}

resCrsh = defPtr[i];
}
fclose(inFPtr);

/* Output calculated parameters.    */
printf("\nMax. Dynamic Crush:\t\t%lf mm @ %lf sec", maxCrsh, maxCrshTime);
printf("\nCalculated Residual Crush:\t\t%lf sec\n", resCrsh);

/* Write crush-time file.    */
for(i = 0; i <= numPts; i++)
    fprintf(outFPtr, "%lf\t%lf\n", timeDefPtr[i], defPtr[i]);

fclose(outFPtr);

/*-----FORCE V CRUSH PORTION OF CODE-----*/

/* Create barrier force surface v crush (3-D surface) file
and total barrier force v crush file.    */

sprintf(outName, "%s.fvcsurf", filenameFor);
if((outFPtr = fopen(outName, "w")) == NULL)
{

```

```

printf("The entered file is not writeable!\n\n");
exit(EXIT_FAILURE);
}

sprintf(outName, "%s.fvc", filenameFor);
if((outFPtr2 = fopen(outName, "w")) == NULL)
{
printf("The entered file is not writeable!\n\n");
exit(EXIT_FAILURE);
}

fprintf(outFPtr, "\t1\t2\t3\t4\t5\t6\t7\t8\t9\n");
for(n = 0; n <= numPts; n++)
{
if(timeForPtr[n] == timeDefPtr[n])
{
fprintf(outFPtr, "%lf\t", defPtr[n]);
sum = 0;
sum2 = 0;
for(i = 0; i < 9; i++)
{
sum = forcePtr[i][0] + forcePtr[i + 9][0] + forcePtr[i + 18][0]
+ forcePtr[i + 27][0];
fprintf(outFPtr, "\t%lf", sum);
sum2 += sum;
}
fprintf(outFPtr, "\n");
fprintf(outFPtr2, "%lf\t%lf\n", defPtr[n], sum2);
}
else
{
i = 0;
if(timeForPtr[n] > timeDefPtr[n])
{
do{
i++;
} while(timeForPtr[n] - timeDefPtr[n+i] > 0);
newDef = defPtr[n+i-1] + (defPtr[n+i] - defPtr[n+i-1])
* ((timeForPtr[n] - timeDefPtr[n+i-1])
/ (timeDefPtr[n+i] - timeDefPtr[n+i-1]));
}
else
{
do{
i++;
} while(timeForPtr[n] - timeDefPtr[n-i] < 0);
newDef = defPtr[n-i] + (defPtr[n-i+1] - defPtr[n-i])
* ((timeForPtr[n] - timeDefPtr[n-i])
/ (timeDefPtr[n-i+1] - timeDefPtr[n-i]));
}
fprintf(outFPtr, "%lf\t", newDef);
sum = 0;
sum2 = 0;
for(i = 0; i < 9; i++)

```

```
{
    sum = forcePtr[i][n] + forcePtr[i + 9][n] + forcePtr[i + 18][n]
        + forcePtr[i + 27][n];
    fprintf(outFPtr, "\t%f", sum);
    sum2 += sum;
}
fprintf(outFPtr, "\n");
fprintf(outFPtr2, "%f\t%f\n", newDef, sum2);
}
}
fclose(outFPtr);
fclose(outFPtr2);
}
```


Appendix C

MOMEX settings and outputs associated with the analysis of NHTSA Test 820 are included in the following graphics page.

